The Stability of Flows in Channels with Small Wall Curvature.

by

George Afxentiou Georgiou.

Submitted for the degree of Ph.d.

The City University
London
Department of Mathematics.

July 1982.

TABLE OF CONTENTS.

TABLES.

TABLE 1. Jeffery-Hamel profiles at $\eta = 0$, evaluated by Elliptic functions and the present perturbation scheme, for various v.

TABLE 2. Results of G_0 and some derivatives at $\eta = 0.5$, G_0' at the wall, showing convergence to 4 sig-fig. for 64 perturbation terms, with $v = 5$ for a straight walled channel.

TABLE 3. Results of G_0 and some derivatives at $\eta = 0.6$, G_0' at the wall, showing convergence to 5 sig-fig. for 80 η steps, with $v = 5$ for a straight walled channel.

TABLE 4. Results of H_0 and some derivatives at $\eta = 0.6$, H_0' at the wall, showing convergence to 4 sig-fig. for 80 η steps, with $v = 5$ for a curved walled channel (i.e positive curvature)

TABLE 5. The steady state velocity profile with and without the $0(\varepsilon)$ correction for different straight walled channels.

TABLE 6. Values of R-crit for a range of v in a straight walled channel, with and without the $0(\varepsilon)$ correction.

TABLE 7. Values of R-crit for a range of v in a straight walled channel, and a curved walled channel (i.e. positive curvature), at $\sigma_1 = 0$.

TABLE 8. Values of R-crit for a range of v at $\sigma_1 = 0.0$ and $\sigma_1 = 0.4$, for the curved walled channel (i.e. positive curvature).

TABLES 9a,9b. R-crit for a range of v, at various σ_1 planes including and excluding the $0(\varepsilon)$ correction.

TABLE 10. The overall R-crit (R^*-crit) for a range of v including and excluding the $0(\varepsilon)$ correction.

ILLUSTRATIONS

FIG-1 A curved walled channel given by $\alpha(\tau)=\varepsilon^{1/2}+\varepsilon^{1/2}m\tau$, for m=1 and $\varepsilon^{1/2} = 0.4$.

FIG-2a,2b The approximate eigenvalue compared with the correct one, for v = 4.093, R = 100, β = 1.5

FIG-3 The steady state stream function in the downstream direction at different orders, for v = 3.572, R = 30, m = 1, η = 0.5

FIGS-4a,4b The steady state stream function in the transverse direction at different orders, for v = 4.71, R = 30, m = 1.0, at σ_1 = 0.0, and σ_1 = 1.6.

FIG-5 The effect of the $0(\varepsilon)$ correction to the steady state velocity profile in the straight walled channel for v = 4.71, R = 10.5.

FIGS-6a,6b The general behaviour of the eigenvalue with the intrinsic frequency in the straight walled channel for v = 3.572.

FIG-7 The imaginary part of the eigenvalue with the intrinsic frequency in the straight walled channel for v = 4.71 and R = 30.

FIGS-8a,8b The eigenfunction in the transverse direction, showing slight dependence with increased Reynolds number, and some non-parallel dependence for the straight walled channel, with v = 4.093.

FIGS-9a,9b,9c The downstream development of the amplitude function A_0 for the straight walled channel, with R = 30 and β=0.2.

FIGS-10a,10b, The downstream development of the transverse behaviour of f_1, and the changes in f_1 associated with increased Reynolds number for the straight walled channel, with v = 3.572, and β = 0.2.

FIGS-11a,11b,11c The downstream development of the amplitude function A_1, for the straight walled channel, with v = 3.572, R = 30, and β = 0.2.

FIG-12 The downstream behaviour of the relative kinetic energy in the straight walled channel with v = 3.572, R = 30, and β = 0.2.

FIGS-13,14 The downstream behaviour of the relative kinetic energy in the straight walled channel with v = 4.71, β = 0.12, for the cases R = 20, and R = 10 respectively.

FIG-15 The behaviour of the relative kinetic energy vs. β_I intrinsic frequency in a straight walled channel, for increasing Reynolds number, when v = 3.572.

FIGS-16,17,18 Neutral stability curves at different orders for the straight walled channel, with v = 3.572, v = 4.093, and v = 4.71 respectively.

FIG-19 Boundary curves separating stable and unstable flow at different orders for the straight walled channel.

FIGS-20,21,22 The transverse behaviour of the steady state profile for the curved walled channel, at different positions downstream, for the cases v = 4.093 (positive curvature, m=1), v = 4.71 (positive curvature, m=1) and v = 3.572 (negative curvature, m=-1) respectively.

FIGS-23a,23b,23c The downstream development of the amplitude function A_0 for the curved walled channel (positive curvature, m=1) with v = 4.093, R = 30, and β = 0.2.

FIGS-24a,24b,24c The downstream development of the amplitude function A_1 for the curved walled channel (positive curvature, m=1) with v = 4.093, R = 30, and β = 0.2.

FIGS-25a,25b The downstream development of f_1 (with fixed η) for the curved walled channel (positive curvature, m=1), with v = 3.572, R = 30, and β = 0.2.

FIGS-26,27 The downstream development of the relative kinetic energy for the curved walled channel (positive curvature, m=1), where R = 30, β = 0.2, with v = 3.572 and v = 4.093 respectively.

FIG-28 The downstream development of the relative kinetic energy for the curved walled channel (positive curvature, m=1), with v = 4.71, R = 20, and β = 0.12.

FIG-29a,29b The behaviour of the relative kinetic energy with the frequency and Reynolds number, for the curved walled channel (positive curvature, m=1) at σ_1=0 with v=3.572.

FIGS-30,31	Neutral stability curves for the curved walled channel (positive curvature, m=1), at $\sigma_1 = 0$, for the cases v = 3.572 and v = 4.093 respectively.
FIG-32	THe relationship between R-crit and curvature at $\sigma_1 = 0$, with v = 3.572.
FIG-33	The boundary curves separating stable and unstable flow for the curved walled channel (positive curvature, m=1) at different σ_1 planes.
FIG-34	A Fraenkel-type channel given by $\alpha(\tau) = \varepsilon^{1/2} m_1 \operatorname{sech}^2(\tau)$ with $\varepsilon^{1/2} = 0.4$ and $m_1 = 1$.
FIFS-35a,35b	The downstream behaviour of R-crit for different v's in a Fraenkel-type channel at different orders.
FIG-36	Boundary curves separating stable and unstable flow for a Fraenkel-type channel at different orders.
FIG-37	Another Fraenkel-type channel, $\alpha(\tau) = \varepsilon^{1/2} m_2 \tau/(1+\tau^2)$.
FIG 38a,38b,38c	Neutral stability curves for "temporally growing" , "spatially growing" waves, and the complex mapping of α (the complex wavenumber) with β (the complex frequency) respectively.
FIG-39	The neutral stability curve for the disturbance function Φ, at the centre of the straight walled channel with v = 3.572.
FIG-40a,40b	The behaviour of the disturbance downstream (at time t=0), evaluated for different incremental steps of the frequency β, with v = 3.572 and R = 70.
FIG-41	The travelling wave packet at different times with v = 3.572 and R = 70.
FIGS-42,43	The travelling wave packet at different times for R=70, and the cases v = 4.093 and v = 4.71 respectively.

ACKNOWLEDGEMENTS

Firstly, I should like to extend my sincere gratitude to my supervisor Dr P.M.Eagles for his numerous helpful suggestions over the years, and the general way in which the problem was tackled.

Secondly, I should like to express my appreciation to [redacted] for the many hours of tuition in numerical methods and general discussions about fluids.

Finally, I dedicate this thesis to my loving mother Anastasia, and thank her for the years of encouragement throughout my education.

DECLARATION

The author of this thesis grants powers of discretion to the University Librarian to allow the thesis to be copied in whole or in part without further reference to the author. This permission covers only single copies made for study purposes, subject to normal conditions of acknowledgement.

ABSTRACT.

This investigation was initiated with the view of studying the stability of flows in symmetric curved walled channels, by essentially combining Fraenkel's small wall curvature theory, with the multiple scaling (or WKB) method.

The overall scheme is designed so that the straight walled channel problem can be retrieved to any relevant order of accuracy. In this way the higher order and curvature effects can be described separately or together. We rewrite the Navier-Stokes equations for an incompressible fluid in terms of Fraenkel's generalized orthogonal coordinates (ξ,η), allowing for wall curvature. Then, by assuming a steady state slowly varying basic flow in the ξ (downstream) direction, and posing an asymptotic expansion in powers of $\varepsilon^{1/2}$ for the steady state stream function $\Omega(\xi,\eta)$, we ensure the leading term is characterised by the non-linear Jeffery-Hamel profiles. These non-linear profiles are linearized by perturbing about v (the parameter defining the profiles), and then solving the resulting set of linear differential equations. These equations, and the linear higher order equations necessary to make the asymptotic expansion plausible, are solved directly by using central difference formulae to express and solve the equations in matrix form.

We are now able to develop the stability analysis by superimposing an infinitesimal disturbance $\Phi(\xi,\eta,t)$ to the basic flow, and to obtain the linearized disturbance equation. The coefficients of this equation are slowly varying with ξ and independent of the time t, so constant frequency disturbances with wave number slowly varying with ξ are appropriate. An asymptotic expansion for $\Phi(\xi,\eta,t)$ in powers of $\varepsilon^{1/2}$ yields the well known Orr-Sommerfeld problem at lowest order. The coefficients here however, are functions of the slow variable $\sigma_1 = \varepsilon^{1/2}\xi$. By constructing an analytical approximation to the eigenrelation, a good initial guess is predicted by which a modified Newton Raphson is used to converge to the correct eigenvalue. The eigenfunction and higher order disturbance equations can now be solved using Runga-Kutta methods.

Spatially dependent growth rates are defined, and the "true" measure of the growth of the disturbance is taken to be the mean kinetic energy density of the disturbance relative to the mean kinetic energy density of the basic flow. Different flow quantities are found to have different growth rates, where the quasi-parallel prediction appears at lowest order, and is common to all flow quantities. By considering neutral stability curves of the relative energy growth rates, we are able to consider the separate effects of higher order corrections and curvature.

The higher order corrections to the straight walled channel do produce shifts in the stability curves, but these shifts are small. However, a constant positive curvature, produces a marked stabilizing effect, whereas a constant negative curvature produces a marked destabilizing effect, at a position in the channel where the angle of divergence is the same as the straight walled case.

A related problem in which curvature is allowed to vary in sign is also considered. This particular channel exhibits a bottle-neck effect, and the flow becomes more like Pois euille far upstream and downstream. R-crits are found at different positions in the streamwise direction, and these R-crits decrease or increase according to whether the angle of divergence is increasinging or decreasing respectively. Thus, minimum R-crits can be found for different channels. This type of channel may be more suitable for experimentation than the previous idealised constant curvature channel. A further channel problem with varying curvature is suggested, which would also exibit Pois ueille flow far upstream and downstream.

Finally, the divergent straight walled channel is considered once more and a model of a wave maker producing an impulsive type disturbance at some suitable position is constructed. This isolated disturbance is shown to produce a wave packet type disturbance, which, according to quasi-parallel theory will grow or decay downstream, depending on whether $R > R\text{-crit}$ or $R < R\text{-crit}$ respectively. This idea is extended to the non-parallel case by superposing slowly varying, fixed frequency modes, which satisfy the linear disturbance equations. In this case, the isolated disturbance still produces a wave packet type disturbance, but any growth that appears is limited in the streamwise direction, and is restricted to some interval of time. All the cases considered show that the disturbance eventually decays downstream according to this linearized slowly varying approximation. Nevertheless, the results do suggest that when the dominant terms measuring the growth of the disturbance grow, (even if only for a very small range downstream, and a very small time interval) for some $R > R\text{-crit}$, then the disturbance might also be expected to grow for this $R > R\text{-crit}$.

LIST OF SYMBOLS.

a_1, a_2	General orthogonal coordinates.
$A_0(\sigma_1), A_1(\sigma_1), A_2(\sigma_1)$	Amplitude functions for the disturbance stream functions Φ_0, Φ_1, Φ_2 respectively.
b	A length scale approximately equal to half the throat width.
C_1, C_2	Constants of integration defining z scales and origin respectively.
$C_1(\sigma_1)$-$C_{25}(\sigma_1)$	Integrals appearing in the amplitude equations.
D^2	The operator $\frac{\partial^2}{\partial\eta^2} + \frac{\partial^2}{\partial\xi^2}$.
D_1^2, D_2	The operators $\frac{\partial^2}{\partial\eta^2}$, $\frac{d}{dy}$ respectively.
E	The kinetic energy density of the disturbance.
E_0	The kinetic energy density of the steady state.
$\hat{E}$	The relative kinetic energy density E/E_0.
$E_{00}(\eta)$	A term in the $O(\varepsilon^{3/2})$ steady state stream function.
$f, f_0, \tilde{f}_0$	The eigenfunctions (f, f_0), and the adjoint eigenfunction.
f_1, f_2	Solutions to the $O(\varepsilon^{1/2})$ and $O(\varepsilon)$ disturbance equations respectively.
$F_0(\eta), F_1(\eta), F_2(\eta)$	Terms in the $O(\varepsilon^{1/2}), O(\varepsilon)$, and $O(\varepsilon^{3/2})$ steady state stream function respectively.
$F(\sigma_1)$	Coefficient in the amplitude equation for $A_1(\sigma_1)$.
$G_0(\eta), G_1(\eta), G_2(\eta), G_3(\eta)$	Terms in the $O(1), O(\varepsilon^{1/2}), O(\varepsilon)$, and $O(\varepsilon^{3/2})$ steady state stream function respectively.
GR_ξ	Function used to define a spatial growth rate.
$h(\xi,\eta)$	Non-dimensional scaling factor.
h_1, h_2	General orthogonal dimensionalised scaling factors.
$H(\xi,\eta)$	Dimensionalised scaling factor.
$H(\sigma_1)$	Coefficient in the amplitude equation for $A_0(\sigma_1)$.
$k(\sigma_1)$	Complex wave number.
K_1, K_2	Constants of integration like C_1 and C_2 respectively.
l	A transformation parameter.
L	Operator in the $O(1)$ disturbance equation.
L_1, L_2, L_3, L_4	Operators in the $O(\varepsilon^{1/2})$ disturbance equation.
m, m_1, m_2	Curvature parameters.

M	Half the volumetric flow rate.
$M_1, M_2, M_3, M_4, M_5, M_6, M_7$	Operators in the $O(\varepsilon)$ disturbance equation.
P	Dimensionalised pressure.
$P(\sigma_1)$	Integral appearing in $GR_\xi(\hat{E})$.
Q	The volumetric flow rate.
R	The Reynolds number M/ν.
R-crit	The critical Reynolds number.
R^*-crit	The overall critical Reynolds number.
$S_1(\sigma_1)$	Integral appearing in $GR_\xi(\hat{E})$.
t	Non-dimensional time.
T	Dimensional time.
$u_1(\eta), u_2(\eta)$	Solutions to the $O(1)$ disturbance equations.
$u_3(\eta), u_4(\eta)$	Solutions to the $O(\varepsilon^{1/2})$, and $O(\varepsilon)$ disturbance equations.
u_ξ, u_η	Velocities of the disturbance in the ξ and η direction respectively.
$\overline{u_\xi^2}, \overline{u_\eta^2}$	Mean square velocities in the ξ and η direction respectively.
$\underset{\sim}{U}$	Dimensional velocity vector.
v	Parameter defining the Jeffery-Hamel profiles.
v_ξ, v_η	Velocities of the steady state flow in the ξ and η directions respectively.
$w(y)$	A parallel steady state velocity profile.
$\underset{\sim}{W}$	curl $\underset{\sim}{U}$.
W_I, W_F	Initial and final throat widths of the channel.
x, x_Q	Non-dimensionalised x-cartesian coordinates of the channel, and the channel wall respectively.
X	Dimensionalised x-cartesian coordinate.
y, y_Q	Non-dimensionalised y-cartesian coordinates of the channel, and the channel wall respectively.
Y	Dimensionalised y-cartesian coordinate.
Z	$X + iY$.

$\alpha(\sigma_1)$	Like the semi-divergence angle of the channel walls.
β	A real frequency.
β_I	The intrinsic real frequency.
$\Gamma_1(v,\sigma_1),\Gamma_2(v,\sigma_1)$	Integrals appearing in the expression for $GR_\xi(\hat{E})$.
$\Gamma(v,\sigma_1)$	$\Gamma_1+\varepsilon^{1/2}\Gamma_2$.
δ	The small parameter = $R\varepsilon \ll 1$.
ε	The parameter characterising the slow variation.
ζ	The non-dimensional complex variable (= $\xi + i\eta$).
η	The non-dimensional transverse coordinate.
θ	The polar angle.
$\vartheta(\xi,\eta),\Theta(\xi)$	The angle between corresponding line elements in the z, ζ plane, and the phase angle respectively.
κ, λ	Like the curvatures of the lines in the z plane.
$\mu(\zeta)$	The complex function generating symmetric channels.
ν	The kinematic viscosity.
ξ	The non-dimensional downstream coordinate.
ρ	The density of an incompressible fluid.
σ	The slow downstream variable (= $\varepsilon\xi$).
σ_1	The slow downstream variable (= $\varepsilon^{1/2}\xi$).
σ_0	A constant downstream coordinate.
τ	The slow complex variable (= $\varepsilon\zeta$).
$\Phi(\sigma_1,\eta)$	The time-independent disturbance stream function.
$\Phi_0(\sigma_1,\eta),\Phi_1(\sigma_1,\eta),\Phi_2(\sigma_1,\eta)$	The time-independent disturbance stream functions of $O(1),O(\varepsilon^{1/2})$, and $O(\varepsilon)$ respectively.
$\Phi(\xi,\eta,t)$	The time-dependent disturbance stream function.
$\chi(\sigma_1,\eta),\chi(\sigma_1,\eta),\chi(\sigma_1,\eta)$	The steady state stream functions of $O(1),O(\varepsilon^{1/2})$, and $O(\varepsilon)$ respectively.
$\Psi(\xi,\eta,t)$	The non-dimensional total stream function = $\Omega + \Phi$.
$\hat{\Psi}(\xi,\eta,t)$	The dimensional total stream function.
$\Omega(\xi,\eta)$	The steady state stream function.
$\Omega_0,\Omega_1,\Omega_2,\Omega_3$	The $O(1),O(\varepsilon^{1/2}),O(\varepsilon)$, and $O(\varepsilon^{3/2})$ steady state stream functions respectively.

1.INTRODUCTION.

It is the intention that this chapter will provide a general picture of the important developements in Hydrodynamic Stability theory of parallel and non-parallel flows over the last century.

The steady state case will be considered first,followed by the stability of essentially steady-state, basic or mean flows. The case of Shen's (1961) unsteady mean flow will also be discussed as his findings are relevant to non-parallel flows. A section is devoted to the more recent developements in the past two decades of non-parallel flows. In the great majority of the investigations cited, an attempt has been made to give a résumé of the problems and their relevance to other investigations. Some important issues will be reviewed at greater length, in particular, the cases which are relevant to this present work directly or indirectly.

The last section will be concerned with describing the overall layout, propositions, methods of solution, and a brief account of the results in the present thesis.

1.1 A HISTORICAL RÉSUMÉ OF SOME IMPORTANT INVESTIGATIONS IN PARALLEL AND NON-PARALLEL FLOWS.

1.1.1 The Steady-State Problem.

Laminar flow of a viscous fluid in symmetric channels of slowly varying width was first studied by Blasius(1910). He proposed a theory for channels with walls given by

$y = \pm f(\varepsilon x)$ (Blasius 1910 p226) where x and y are the usual cartesian coordinates and ε is a small parameter independent of the Reynolds number.

In this theory Blasius considered a perturbation solution of the Navier Stokes equations and calculated the first two terms of his expansion with Pois euille flow at O(1). His aim was to provide a solution valid at separation, that is , the position on the channel walls where the increase in pressure due to a decrease in the velocity of the fluid retards the already slowly moving fluid particles, such that they cease to continue moving forward against these combined viscous and pressure forces, consequently they separate from the wall and a dividing line of particles with zero velocity (originally along the wall) is visualised in which two regions of fluid motion exist. The region nearer the wall is one of reversed flow,and the other is forward flow. This explanation of separation was originally given by Prandtl (1904) and an account of it with simplified illustrations can also be found in Goldstein (1938 vol.1. p57). Blasius's theory does in fact provide a solution which exhibits the separation phenomenon.

Patterson , (1934,1935) devised experiments and constructed Blasius's exponential channel to test the theory. A comprehensive summary of Blasius's work is given by Patterson (1935, pp676-677) which analyses the criterion for separation in more detail and shows that Blasius's numerical criterion was far too high. Nevertheless,Patterson's experiments do support

Blasius's work for a limited range of low Reynolds numbers and more important, demonstrated that two-dimensional velocity profiles with reversed flow at each wall could be achieved under laboratory conditions.

Direct extensions of Blasius's work was carried out some years later by Abramowitz (1949) who calculated an additional term to the Blasius solution. Though this did lead to a numerical criterion closer to the experimental one given by Patterson it was still too large.

A significant advance in the solution of two dimensional viscous flow between non-parallel plane walls came a few years after Blasius when Jeffery (1915), and then Hamel (1917) showed that the flow was purely radial. The physical parameters of this problem ν (the kinematic viscosity) and Q (the total flux of the fluid outwards from the origin) are linearly related, where the coefficients in this relationship are expressed in terms of elliptic integrals.

Jeffery's approach was to show that the streamlines of this motion were straight lines passing through the origin, while Hamel showed these streamlines were a special case of a more general flow in which the streamlines were equiangular spirals. Even though this solution was known since 1915, it was not till Rosenhead's (1940) paper that a general treatment of the Elliptic Integrals was given. This paper was in response to a statement made by Goldstein (1938 pp106-107) on the behaviour of the velocity distributions in convergent and divergent flows as the Reynolds number (R) was increased.

The usual definition of R ($l|U_{max}|/\nu$, where l is a representative length scale, ν the kinematic viscosity and $|U_{max}|$ the magnitude of the velocity in the flow) was inadequate for the flows to be considered in Rosenhead's paper, as it did not distinguish between the cases when $|U_{max.outwards}|$ and $|U_{max.inwards}|$ were equal. He chose to use $Q/2\nu$ (here Q is still the flux, but more specifically it is the volume of fluid passing from the narrower end of the channel to the wider end, in unit time, between two planes which are at unit distance apart and are perpendicular to both walls, and which may be positive or negative) thus a positive value of R will now correspond to average outflow and a negative value of R to average inflow.

Rosenhead analysed the velocity profile by deriving a fundamental cubic equation from which the principal results could be deduced. (A more detailed account is found in Rosenhead 1940 ch.4).

If 2α is the angle between the channel walls then for every $v = \alpha R$ an infinity of mathematical possibilities exist. We summarise them here as cases (i),(ii) and (iii).

CASE (i)

Symmetrical velocity profiles with pure outflow along the centre line, and as α is increased the flow pattern becomes progressively structured with outflow always along the centre line.

CASE (ii)

Symmetrical velocity profiles with pure inflow along the centre line, and as α is increased, the flow pattern becomes progressively structured with inflow along the centre line.

CASE (iii)

Non-symmetrical velocity profiles where inflow always appears at one wall (either), and as α is increased, the flow pattern becomes progressively structured.
(Illustrations of these cases can be found in Rosenhead (1940) pp448-450).

Rosenhead clearly emphasizes that the mathematical analysis only predicts the types of possible flows but says nothing about which flow pattern will be adopted for a given R and α in a real fluid.

In a normal experiment the pressure conditions over the inlet and outlet ends are of paramount importance. In fact, imposed pressure conditions in experiment are closer to those implied by pure outflow or pure inflow than those implied by the other more complicated types previously mentioned. Rosenhead thus felt justified in speculating that pure inflow/outflow are more likely to occur. He was led to conclude that stability considerations were necessary in order to determine which type of flow pattern the fluid will assume.

An important assumption was made by Rosenhead about the distribution of pressure in order to classify the sequences of changes that occur in pure inflow/outflow for a fixed channel with increasing R. We shall describe this as it will be relevant in later discussions, and it is fundamental in deducing the flow patterns.

If we assume that the pressure distribution across the channel is not rigidly imposed, that is if it is "loosely self adjusting" then the velocity profiles will be the simplest ones. Thus, by assuming this pressure condition and ignoring the non-symmetrical profiles (case (iii)), along with those having inflow at the centre together with regions of outflow (structured cases of (ii)), Rosenhead deduces that for inflow, an increase in R produces a flattening of the profile in the centre of the channel, and the drop in velocity to zero at the walls takes place over a narrower layer (i.e. the classic boundary layer behaviour). On the other hand, in outflow, an increase in R concentrates the flow in the centre of the channel until regions of inflow appear at each wall. More regions of outflow and inflow appear with further increases in R.

Rosenhead finally considers a numerical example in which he discusses the transition from pure outflow, to outflow at the centre with regions of inflow near the walls, followed by progressively more regions of outflow and inflow. Rosenhead goes on to argue that since this transition occurs for a small increase in R, this is an indication of the instability in this type of flow.

This infinite set of mathematical possible profiles appears to be the first complete solution to a non-parallel flow problem.

Fraenkel (1962 I) was later able to show, that these profiles could be regarded, as providing the first term of a series solution for a family of symmetric channels with slightly curved walls.

In the first part of the investigation Fraenkel, (1962 I) demonstrated that within the limitations of his theory, (if a wedge of semi-divergence angle α and a curvature parameter ε were sufficiently small) analytic separation and reattachment ($\alpha \sim \alpha_2$) could occur even at high Reynolds number. These solutions were shown to be unique by limiting the channels and Reynolds numbers such that $\alpha_2(R) < \alpha < \alpha_3(R)$, where α_2 and α_3 are the bounding curves in the $R\alpha$-plane. The Jeffery-Hamel profiles in this range are always symmetrical, and even in the extreme case, only exhibit one region of reversed flow at each wall. In Fraenkel's work $\alpha = \alpha_2$ corresponded to separation and $\alpha = \alpha_3$ corresponded to a singularity.

The classic result of the singularity associated with separation was first shown mathematically by Goldstein (1948b), following the suggestion by Hartree (1939a). The validity of Goldstein's solution depended on inherent integral conditions which he could not satisfy at the time. The problem was not really resolved until Stewartson (1958) showed that by adding on logarithmic terms to the velocities already obtained, the integral conditions could be satisfied. Terrill (1960) extended Stewartson's work and also showed that logarithmic terms were necessary.

It is important to realise that Fraenkel's solution was not in disagreement with these results, when we consider the assumptions that were made for Goldstein's singularity to appear at separation. In fact the pressure distribution assumed by Goldstein, Stewartson, and Terrill do suggest the appearance of the singularity, but they do not claim that it must occur. Other writers have chosen pressure distributions which avoid the singularity.(Meksyn (1956), and Dean (1950)).

Stewartson (1958) and later Brown & Stewartson (1969) suggested that two types of boundary-layer separation may exist in practice. The singularity type, which is appropriate to the "break-away" of the boundary layer from the surface, and the regular type, in which the boundary layer persists downstream with reversed flow past separation. Fraenkel speculated that $\alpha \sim \alpha_3$ could be likened to the singular type of separation and $\alpha \sim \alpha_2$ could be likened to the regular type. Fraenkel was thus able to modify Blasius's perturbation of Pois euille flow in the light of the Jeffery-Hamel profiles. (Fraenkel 1963 II).

More recently Lucas (1972) showed that if the Blasius perturbation expansion was taken to enough terms a very good degree of accuracy could be obtained for the Jeffery-Hamel profiles. In one case he computed thirteen terms to obtain good agreement. (Lucas 1972 p.47).

Fraenkel's generalized coordinate system considers a class of symmetric channels with small wall curvature. Thus, by fitting conformal coordinates to Patterson's (1934,1935) exponential channel he was able to make comparisons with experiments and the work of Blasius. He showed that the numerical criterion for separation using his theory ($\gamma = \varepsilon R$) was equal to 4.7 and this compared more favourably with Patterson's experimental value, (somewhere between 3 and 4.3) than that found by Blasius which was as high as 8.75.

A general practical difficulty when considering experimental verification of Fraenkel's theory is the enormity of the final throat width of the channel that can exist at and beyond separation, compared with the initial throat width. This is implied by the imposed limitations of the theory. It is possible however, to choose the parameters defining this ratio of the throat widths so that it is not enormous. Fraenkel suggested that his hyperbolic-tangent channel (Fraenkel 1963 II p.409) could be tested experimentally. This suggestion does not appear to have been considered yet.

1.1.2 The Stability Problem.

The study of the transition from laminar flow to turbulent flow has been one of the major issues of hydrodynamics for the last century. It was generally accepted that if the disturbance to the laminar flow ultimately decayed then the flow was stable, but if the disturbance was permanently growing then the flow was unstable. It does not follow that instability is sufficient for turbulent motion. However, the initial problem was to solve for stability of laminar flows to small disturbances.

The first mathematical investigation of two dimensional hydrodynamic instability seems to have been made by Helmholtz (1868). He considered two parallel streams at different velocities and proved the instability of wavy disturbances over the surface of discontinuity. Later, Lord Rayleigh (1880) extended this idea by considering velocity profiles approximated by broken straight lines for an inviscid fluid in a parallel channel. An important result from this study was that in unstable motion the velocity profile approximated by straight lines has a shape consistent with a point of inflexion, indicating that a point of inflexion is a necessary condition for instability in inviscid fluids.

Osborne Reynolds (1883) showed experimentally that if water passed through a circular straight pipe, and the flow conditions were disturbed at entry, then this disturbance would eventually die downstream if the value of his now famous Reynolds number R, was small enough. If R was then increased, a critical value of R was reached (R-crit) such that if R > R-crit the flow in the pipe becomes turbulent. Reynolds also explained that viscosity played a dual role in this question of stability. In one way it had a damping effect, and at the same time a destabilizing effect, through the no-slip condition at the walls of the pipe.

In a later paper Reynolds (1895) suggested that the physical mechanism responsible for the transition of laminar flow to turbulent flow was the transfer of energy between the basic laminar flow and the superimposed disturbance. If the disturbance grows , it implies that energy is being absorbed from the basic flow faster than it is dissipated by viscosity. On the other hand , if the disturbance decays then viscosity is the dominant factor. This view was generally accepted and many early stability investigations were based on energy principles.

Some notable investigators of the time include Lorentz (1896b), Orr (1907), and Sommerfeld (1908). They considered the conditions under which the energy of a disturbance increased or decreased with time by assuming a convenient disturbance at some instance, and then finding out whether the energy associated with this disturbance increased or decreased immediately afterwards. The assumed disturbances were chosen to satisfy the boundary conditions but not the equations of motion, the R-crits found were not satisfactory. They were in fact much lower than those observed experimentally. (see Lin (1955) p.59, Rosenhead (1963) pp516-518).

A significant advance in the study of real fluids was made possible when Prandtl (1922) showed that the viscous forces induce a modified stress (Reynolds) which is absent in this form in the inviscid case. These Reynolds stresses were shown to be the physical mechanism for transfering the energy from the basic laminar flow to the disturbance. In this way the presence of viscosity could lead to instability.

One of the existing classical problems of hydrodynamic stability was that of plane Pois euille flow. The implications of this problem are extremely important in the development of non-parallel flows and in particular to this present investigation. We now consider some of these ideas and important investigations leading up to its solution.

Heis enberg (1924) was probably the initiator of modern day stability theory. He formulated the mathematical problem by considering a given steady-state solution of the Navier-Stokes equations, and by adding to it a suitable disturbance function, derived the non-linear disturbance equations. Even though Heis enberg did not actually solve the complicated non-linear problem he did solve the Orr-Sommerfeld problem and concluded that plane Pois euille flow was unstable for a sufficiently high Reynolds number.

The controversy that ensued as a consequence of Heis enberg's theory discouraged many investigators in pursuing the problem along his lines. Nevertheless, the general difficulties as a result of Heis enberg's work were taken up by Tietjens (1925), and then Tollmien (1929). They considered two dimensional

infinitesimal wave like disturbances of the form $\phi(y).\exp(i(kx-\beta t))$. The x and y are the usual cartesian coordinates, and t is the time. The values k and β can both be complex in general, where the real part of k (k_r) is the wave-number, and the real part of β (β_r) is the frequency. The imaginary parts k_i and β_i are the amplification rates in space and time respectively. This assumed wave like disturbance was substituted into the equations of motion this time, and by neglecting non-linear terms in ϕ in the disturbance equation, they obtained the well known Orr-Sommerfeld problem (4.30). This equation formed the basis of linearized stability theory.

Tietjens (1925) applied the theory to the velocity profiles consisting of broken lines in the manner of Rayleigh (1880), but now taking viscosity into account, and found instability in many cases. Tollmien (1929) applied the theory to the case of the boundary layer of constant thickness with Blasius's velocity profile. The same problem was also considered by Schlichting (1933). The R-crits found by Tollmien and Schlichting were found to be 420 and 475 respectively. This application of parallel flow theory to the boundary layer received some criticism by Taylor (1938), as it was well known that the boundary layer increased in thickness downstream no matter how thin it was. However, the parallel theory applied to the boundary layer seemed to have been completely vindicated by the experiments of Schubauer & Skramstad (1947).

Tollmien (1935) extended Tietjens (1925) problem to continuous velocity profiles and proved the converse of Lord Rayleigh's theorem for viscous fluids. That is, a point of inflexion in the velocity profile is a sufficient condition for instability in flow between parallel walls or along a wall. This condition is not necessarily sufficient for other velocity profiles. (see Lin 1945 II p.222).

The linearized theory with infinitesimal disturbances was not convincingly applied to the plane Pois euille case until Lin (1945 I) calculated an R-crit of 5,300. Other notable workers around the same time applied this theory essentially along the lines of Heis enberg and Tollmien, and found R-crits of similar magnitude. Among them, Meksyn (1946a) found 6,800, Shen (1954) calculated coordinates of the neutral stability curve by perturbing Lin's neutral curve and confirmed Lin's results. Thomas (1953) solved the Orr-Sommerfeld equation numerically on a high speed computer for both damped and amplified disturbances and found 5,780. This value could be regarded as the most accurate. Lock (1954) found 6,000 by improving the analytical method of solving the Orr-Sommerfeld equation. All these theoretical results were however substantially higher than the experimental results of Davies & White (1928), who found R-crit to be as low as 1000.

It was suggested by Meksyn & Stuart (1951), (see also Stuart (1951)) that considerations of finite disturbances including non-linear effects of the mean flow could resolve the discrepancy. They solved the Orr-Sommerfeld problem simultaneously with a non-linear mean flow and obtained after some approximations an R-crit as low as 3,000. Even though this

did not completely remedy the situation it did at least give support to this approach. This controversial state of affairs motivated many investigations into the non-linear aspects of plane Poisseuille flow.

An important contribution was made by later by Stuart (1960) and Watson (1960).They followed on from Landau (1946b) and others, by considering the evolution of disturbances of the form $A(t)\,\phi(y)\,\exp(i(kx-\beta t))$, both for plane Pois euille flow and plane Couette flow. These disturbances with time dependent amplitudes were conveniently considered for real k and complex β.

A non-linear theory was also developed by Watson (1962) on disturbances of the form $A(x)\,\phi(y)\,\exp(i(kx-\beta t))$, with β real. These disturbances with spatially dependent amplitudes were felt to be more closely related to the disturbances investigated experimentally.

Gaster (1962) showed formally how the amplification rates β_i and k_i, for these "time-dependent" and "spatially-dependent" flows respectively,were related through the group velocity $(\partial\beta_r/\partial k_r)$. These relatonships hold only when the wave number k_r is common, and when the amplification rates are small. The same relationship was in fact used earlier by Schlichting (1933) to compute the spatial amplification rate (k_i) from considerations of a "time-dependent" flow, but apparently without any formal justification.

It has since been demonstrated that linearized stability only provides a sufficiency condition for instability, but this condition is not a necessary one as non-linear considerations may imply instability at a lower R-crit (see Stewartson & Stuart (1971)).

This seems an appropriate point at which to leave the non-linear development of plane Pois euille flow and consider the implications of the linearized theory to essentially

non-parallel flows.

1.1.3. Recent Developments in the Stability non-parallel flows.

The mean or basic flows above , have always naturally been assumed parallel and steady. When the basic flow is neither of these but is slowly varying with respect to the variable concerned it seems reasonable to assume that the stability at some point depends only on the local physical properties of the flow, such as the velocity profile and the Reynolds number.

In these flows the mean or basic flow is still taken to be steady and parallel but the growth rate is recognized to vary with space and/or time. This is in contrast to the parallel flow theory in which the growth rate is constant in space or time. This extension describes the "quasi-parallel" or "quasi-steady" theory. In the case of the boundary layer we have seen that the quasi-parallel approach was experimentally verified. (Schubauer & Skramstad (1947)).

Lanchon & Eckhaus (1964) have shown that by considering a formal local expansion of the slowly varying coefficients about some point downstream, and studying the asymptotic behaviour at high Reynolds number, that the steady, quasi-parallel assumption is good as a first approximation to the boundary layer flows, but that in more rapidly varying flows such as jets, the non-parallel dependence has to be included in the solution of the Orr-Sommerfeld problem.

The need to introduce a theory which took account of the change in the basic flow with time and/or space, was becoming increasingly apparent.

A general treatment for spatially-varying and time dependent flows was given by Benney & Rosenblat (1964).They considered basic flows as local approximations to true flows. Thus, if these basic flows were slowly varying with a particular variable (x,y,z,t), to then formally introduce slow variables ($X = \mu x$; $Y = \mu y$; $Z = \mu z$; $T = \mu t$), rather than assume complete independence of them, as in the quasi-parallel or the quasi- steady assumption. They suggested that the linearized disturbance to the basic flow should also exhibit these slow variations with respect to the variable concerned, and that the resulting equations should be solved by a WKB (Wentzel-Kramers-Brillouin) approximation. This approximation is applicable to situations in which the wave equation (in this case the Orr-Sommerfeld problem) can be separated into one or more total differential equations, each of which involves a single independent variable. The method is also known as the "ray" or "multiple scaling" method, and was used to approximate the solution to Schrödingers wave equation. (see Wentzel (1926), Kramers (1926), Brillouin (1926)). In fact the mathematical technique was even used earlier by Liouville (1837),Rayleigh (1912), and Jeffreys (1923).

This suggestion by Benney & Rosenblat (1964) was not in fact considered until six years later when Rosenblat & Herbert (1970), applied the method to thermal convection in which the temperature of one boundary was slowly oscillating with time.

In the multiple-scaling method the quasi-parallel solution appears at the lowest order.

Prior to this , parallel and unsteady basic flow was already considered by Shen (1961). His aim was to extend the theoretical attempts (Karman & Lin (1955)) to explain vortex creation by deceleration. This phenomenon was demonstrated experimentally by Fales (1955), by gradually stopping a moving flat plate in a water tank. The slowing down of the boundary layer caused transverse vorticity to appear. Coles (1958), demonstrated vortex creation between coaxial circular cylinders. A start stop mechanism on the outer cylinder generated vortices with axes parallel to the cylinders.

Shen introduced the concept of "momentary stability" for unsteady basic flows. He argued that since the basic flow is changing, the growth or decay of a disturbance must be measured relative to the base flow. Since , if the disturbance is increasing but the basic flow is increasing at a faster rate, the disturbance relative to the basic flow would appear to decay at a later instant. The converse argument for decaying disturbances and decaying basic flows equally holds. Thus the disturbance may only be seen to decay or grow momentarily. If the flow sustains the "momentary instability" after a certain instant, it may be concluded that transition to turbulence must occur sooner or later.

Shen found that the quasi-parallel solution was only acceptable for small accelerations or decelarations, and that deceleration was found to have an "overwhelming" destabilizing influence irrespective of the velocity profile considered. Shen's suggestion then, was that the experiments of Fales (1955) and Coles (1958) could be explained on the basis of an inflexion point mechanism and a parallel but unsteady basic flow.

At this stage the quasi-parallel/quasi-steady theory, the local expansion theory due to Lanchon & Eckhaus (1964), and the slowly varying theory suggested by Benney & Rosenblat (1964), formed a trilogy of theories from which many problems in hydrodynamic stability could be tackled.

Eagles (1966), considered the stability of the Jeffery-Hamel profiles in a straight walled channel of divergence 2α. He adopted the usual quasi-parallel theory and solved the classic Orr-Sommerfeld problem for basic flows, which are characterized by the Jeffery-Hamel profiles, rather than the plane Poisseuille profiles. Here k is real and β is complex. The parameter αR (γ in Eagles paper) defines the Jeffery-Hamel profile. The neutral stability curves ($\beta_i = 0$) were obtained for various values of γ up to 5.45,(the singularity in the velocity profile occurs at $\gamma = 5.46$), where $\gamma = 0$ corresponds to plane Poisseuille flow.

The Jeffery-Hamel profiles were shown to be drastically more unstable than the plane Poisseuille profiles. Thomas's (1953) calculations of R-crit, (5,780) becomes 3910 (based on $R = Q/2\nu$) and Eagles's R-crit was about 215, for a channel whose semi-divergence angle was as small as 0.01.

Ling & Reynolds (1973) considered infinitesimal amplitude disturbances to a steady but non-parallel basic flow. This basic flow was assumed to be slowly varying with the downstream coordinate x, and an expansion of the parallel solution was posed about some point x_0, where the Orr-Sommerfeld appeared at lowest order. This approach was essentially along the lines of Lanchon & Eckhaus (1964). They applied this local expansion to the Blasius boundary layer and the two dimensional jet.

In the former case they found that the neutral stability curve was virtually unchanged by their non-parallel correction. (R-crit was reduced by 0.1% at most). In the latter case ,there was a distinct destabilizing effect due to the non-parallel correction, analogous to Shen's (1961) destabilizing effect due to the unsteady base flow correction. However, the small R-crits involved in such flows makes the expansion dubious, as the expansion is essentially in powers of 1/R. These non-parallel effects become less significant at higher Reynolds number.

Around this time there had been experimental evidence (Ross et al (1970), Mattingley & Criminale (1972), Scotti & Corcos (1972)), demonstrating the deficiencies of the quasi-parallel theory in a quantitative way. Even from a theoretical point of view, the quasi-parallel approach is questionable. It does recognize that the growth of the disturbance is a function of space, but it cannot determine this function in terms of the downstream coordinate, it can only predict whether a wave is growing or decaying at a point. In addition, it cannot predict the effect that the change in the basic flow will have on the disturbance.

The local expansion theory has also been shown to be incomplete. It does take into account the variation of the basic flow, and consequently its effect on the growth of the disturbance, but since the solutions take the form of a series in powers of $(x-x_0)$, it cannot be considered as a complete solution of the downstream variable x, but is only useful near x_0.

Local expansion solutions have only been developed for temporally growing disturbances and thus cannot compare with experiments

involving spatially growing modes. (see Saric & Nafeh (1975)). The zeroth-order approximation of the solution of Ling & Reynolds (1973) for the two dimensional jet,(which is really the quasi-parallel solution) has been shown by Joseph (1974) to be not uniformly valid. Thus for these experimental and theoretical reasons, other investigators have chosen to adopt the multiple-scaling (WKB) approach for non-parallel flows. In particular, Bouthier (1972,1973) applied this method to the Blasius boundary layer and achieved very good agreement with the experimental data of Ross et al (1970). Unfortunately he was not specific about whether the local kinetic energy he used to obtain the corrected neutral stability curve, was the same as that observed in experiment.

In a detailed description of the three theories mentioned, Bouthier showed that the local expansion was really a Taylor series expansion of the multiple scaling solution about x_o. In addition he showed the surprising result that different flow quantities (streamfunction, energy, velocity, etc) have different neutral curves. Thus, comparisons of theoretical and experimental results have to be carried out with definite flow quantities in mind.

Gaster (1974) comments on Bouthier's expansion, and in particular, discusses an important theoretical point concerning the ordering of the terms in the expansion. The small parameter (ε say), used in the scaling of the coordinates and in the formal expansion procedure is $O(1/R)$. There is in fact a formal relationship between ε and R in the basic flow problem. This relationship was ignored in the disturbance equation, and ε and R were treated as independent parameters. Ling & Reynolds (1973) adopted a similar approach. This means that the viscous term $(1/R)\nabla^4\Psi$ is retained at lowest order, even though it is

formally smaller than the other terms. Gaster argues that artificially separating these parameters does not take into account the vertical structure of the Orr-Sommerfeld solutions in ordering the terms of the expansion. He recognizes however, that this is necessary to do this if one wants to avoid a singular perturbation problem, where the expansion procedure has to be carried out separately in the various layers (i.e. regions where viscous terms dominate, and regions where non-viscous terms dominate). Eagles & Weissman (1975) argue that as 1/R multiplies the highest derivative, the term $(1/R)\nabla^4\Psi$ will be important somewhere in the flow field. Thus, numerical techniques to solve for the vertical structure (which are appropriate here since R is large), require the viscous term to be kept at lowest order. The formal relationship between ε and R is returned to when numerical values are required for ε and R. In fact by treating ε and R as independent parameters, one obtains a more general solution at lowest order than necessary. If this relationship between ε and R is retained throughout, a singular perturbation problem is obtained where matched inner and outer solutions can be found. This has recently been considered by Smith (1979), who applied the problem to the lower branch of the neutral curve for the boundary layer, and obtained good agreement with Bouthier and Gaster. Gaster in fact uses a different formalism to Bouthier, so as to account for the vertical structure in ordering the terms of the expansion. His theoretical results did not compare as well as Bouthier's, but this was probably due to the way he defined the flow quantity to obtain the neutral stability curves.

Another contribution to this general theory was made by Nayfeh, Mook, & Saric (1974), who also considered the stability of the boundary layer. Eagles & Weissman (1975), have commented that the solutions of Nayfeh et al did not include the downstream dependence of the eigenfunction, (a solution of the Orr-Sommerfeld problem) in their expressions for the corrected growth rate and wave number.(see equations (27) & (38) in Eagles & Weissman (1975)). However, as Nayfeh et al obtain very good agreement with the experiment of Schubauer & Skramstad (1947), and Ross et al (1970), it may be that the downstream dependence of the eigenfunction is insignificant for large Reynolds numbers in the case of the boundary layer.

The investigation of Eagles & Weissman (1975),(on which this thesis is partly based) could be considered as forming the second part of the investigation by Eagles (1966), and receives an extended summary here.

In the usual way, the linearized disturbance equation based on an assumed basic state flow, (in this case the steady two-dimensional symmetric Jeffery-Hamel profiles) was found. The coefficients of this disturbance are independent of time, and slowly varying with ξ , ($\xi=(1/\alpha)\ \ln(\alpha r)$, α is the semi-divergence angle and r is the polar displacement) hence constant frequency (β) solutions are appropriate.

The fundamental difference between quasi-parallel theory and the multiple scaling method (WKB) is exemplified here. The latter method recognizes that the eigenfunction and wavenumber are slowly varying with ξ , whereas the quasi-parallel theory would now completely ignore this variation. Thus the disturbance takes the form $\Psi(\eta,X)\ \exp(i(\Theta(\xi)-\beta t))$ + c.c, where c.c represents the complex conjugate of the preceding terms. The modified polar angle $\eta = \phi/\alpha$, and $X = \alpha\xi$ is the slow variable. The phase function $\Theta(\xi)$, describes the

fast variation of the wave, while the wave number $K(X) = d\Theta/d\xi$ (K_r, the real part of K, is no longer the physical wavenumber) is slowly varying. For spatially growing waves, K is complex, and β is real.

The trial disturbance was substituted into the disturbance equations in the usual way, and by expanding Ψ in powers of α, a sequence of problems was obtained at different orders of α. As already explained, α and R were considered as independent parameters in the disturbance equations, and their formal relationship ($\gamma = \alpha R$ in this case) is returned to in the final analysis.

The lowest order equation obtained was the Orr-Sommerfeld problem. The difference here being, that where the physical frequency and the physical wavenumber normally appear, we see the slowly varying functions $\beta \exp(2X)$ and $K(X)$ respectively. This partial differential eigenvalue problem, becomes amenable to solution since X appears parametrically. Thus a solution of the form $A(X)\, f(\eta;X)$ can be found. Here, A(X) is a complex amplitude function, and it can be interpreted as the amplitude of the streamfunction along the centre of the channel. The function $f(\eta;X)$ is a solution of the Orr-Sommerfeld equation for fixed X.

Drazin (1974), considered the two-dimensional jet flow problem using the multiple scaling method, but did not include the amplitude function in any equivalent form, and consequently could not obtain higher order corrections to the growth of the disturbance. He did show however that the quasi-parallel flow is invalid in practical terms even as a first order approximation for long waves.

The amplitude function A(X) above, was solved for, by finding the equation satisfied by the next order stream function. The resulting inhomogeneous equation has a solution only if a certain solvability condition is satisfied. This condition yields the equation for A(X) at

this order, and this process is necessarily repeated to obtain higher order amplitude functions.

As already shown by Bouthier (1972,1973) not all flow quantities have the same growth rate. The choice of the flow quantity usually depends on the one chosen in experiment to define the neutral stability curve. In the absence of experimental data, Eagles & Weissman chose to use a mean kinetic energy density averaged over time and integrated across the channel. This defined the absolute energy E. Shen's (1961) arguments on the growth or decay of the basic flow were adapted here for spatially growing waves. A relative kinetic energy density was also defined ($\hat{E}$), such that $\hat{E} = E/E_0$ where E_0 is the kinetic energy density of the base flow.

In comparing the growth rates of different flow quantities, Eagles & Weissman found a consistently destabilizing effect. (Recall Shen's (1961) result for unsteady mean flows). The quasi-parallel growth rate $-K_i$ (imaginary part of K(X)) appears at first order, and as the corrected term is of $0(\alpha)$, the quasi-parallel solution can only be thought of as providing a good first approximation, if $|K_i|$ is much larger than α numerically. It was suggested that a useful parameter could be $\alpha/|K_i|$, and that if it was small, the variation of the basic state on the growth could be ignored.

No experimental evidence existed in which to compare their theoretical results, and Eagles & Weissman acknowledged that their assumed steady-state solution may not actually exist in experiment. They referred to the results of Briggs (1964) and Gaster (1965), who both considered an initial value problem where the wave maker is suddenly turned on. These investigators found that in parallel flows, if the real part of the group velocity is positive for unstable modes, then a transient disturbance would propagate downstream,leaving a steady-state wave behind. It seemed reasonable to assume that the same criterion would hold for unstable slowly varying flows, as the solutions investigated by Eagles & Weissman showed that the real part of the group velocity was positive for all frequencies.

Waves of all frequencies were found eventually to decay downstream, and in the unstable regions, the waves did not grow very much before they started to decay.

The stability of the above analysis was based on a linearized theory for infinitesimal disturbances. It may be argued that the amplitude of the wave may become large enough for non-linear terms to become important. The paper of Eagles (1973) considered this problem for the Jeffery-Hamel profiles, and applied the non-linear theory of Stuart (1960) and Watson (1960). The downstream variation of the disturbance was ignored here (as in the quasi-parallel approach), and the calculations were for temporally growing disturbances, not for spatially growing ones. Eagles found that the non-linear effects were stabilizing. The same stabilizing effect might be expected for slowly varying spatial disturbances, but of course this is purely speculative as this analysis does not appear to have been attempted in full. On this basis then, we might expect small and finite amplitude waves to pass through regions of growth, but to eventually decay as they travelled downstream.

The investigations discussed so far have flows characterized by large Reynolds numbers. Di Prima & Stuart (1972) applied a multiple scales method to flows between eccentric rotating cylinders, with flows characterized by O(1) Reynolds number. They found that the effects of the non-parallel flow, increased the critical Taylor number predicted by quasi-parallel theory.

The multiple scaling method can equally be applied to basic flows which change slowly with time rather than space. Hall & Parker (1976) have applied the method to the linear stability of laminar flow in a suddenly blocked channel. They found that the quasi-steady approximation, was only uniformly valid if the Reynolds number was large.

Eagles, (1977) has also applied the theory to the linear stability of slowly varying flows between concentric cylinders. Here, Eagles considered the outer cylinder fixed, and the speed of the inner

cylinder, slowly increasing with time. The Taylor number T, was now considered as a function of the slow variable in time, t^*, where $t^* = \varepsilon T$ By varying the Taylor number close to T , (the critical Taylor number of steady flow) he was able to examine this effect on the instantaneous Taylor number, at which vortices first appear. Axisymmetric disturbances, to the axisymmetric basic flow were considered. They were in fact the typical WKB modifications of the quasi-steady disturbances, and the expansions posed for the basic and disturbed flow, yielded the steady state eigenvalue problem at lowest order with the eigenvalue now dependent on t^*. The growth of the disturbance was based on Shen's (1961) relative growth rate, and Eagles found that the inclusion of higher order corrections, predicted a somewhat surprising stabilizing effect. The critical Taylor number was found to increase by as much as 24% in one case.

More recent applications of the multiple scaling method to non-parallel flows, have been made by Zollars & Krantz, (1980) as an extension to their steady state solution. (Zollars & Krantz (1976)). The sequel paper considered non-parallel effects to the stability of film flows down a right circular cone. This investigation was carried out because of the same deficiencies already discussed in quasi-parallel theory. Zollars's & Krantz's findings bear a strong resemblance to those of Eagles & Weissman. They found that all disturbances eventually decay far enough from the apex of the cone, but disturbances can become amplified locally near the apex, both in an absolute and relative sense. (i.e. relative to the base flow).

By considering expressions for their spatially growing amplitude factors, both for absolute and relative growth,(4.2 and 4.4 respectively in their paper) they were able to compare the sizes

of terms characterizing (i) frequency of the disturbance, (ii) the dynamics of the flow, and (iii) the physical properties of the fluid, as functions of the axial distance. They found that the principle stabilizing effects in these non-parallel flows were the viscous forces. These forces became more dominant with the progressive thinning of the film (i.e. far from the apex). This was in contrast to the parallel case in which the principal stabilizing effect was the increase in surface tension, (associated with increases in frequency) and this accounted for the stability of high frequency disturbances. In fact an increase in surface tension has a destabilizing effect in non-parallel film flows.

In an attempt to construct a model which might test the multiple scaling method for steady, non-parallel flows experimentally, Eagles & Smith, (1980) recently considered symmetric two-dimensional channels with slowly varying widths. They used cartesian coordinates (x,y) where the channel walls were given by $y = \pm H(X)$; $X = \varepsilon x$, ε is a small parameter, thus X is the slow variable. The particular channel they considered for experimental testing was $H(X) = 1 + \tanh X / 2$ so that as $X \longrightarrow \pm \infty$ Pois euille flow is expected.

The channel walls were chosen to vary slowly, and the degree of this slow variation was achieved by considering axial length scales of $O(R)$. This implied that the slope of the walls were of $O(1/R)$. the small parameter was then necessarily of $O(1/R)$. In fact $R\varepsilon = \lambda$, where λ is a constant of $O(1)$. This choice yielded the classic boundary layer equations for the slowly varying flow. The pressure was not assumed in this problem and thus separation, if it occured would be regular, in the manner of Fraenkel's (1962 I) analysis, and not like the singular type suggested by Goldstein's (1948b), Stewartson,s (1958), and Terrill's (1960) investigations.

The problem was theoretically tested for the special case when $H(X) = X$, and the steady state flow then becomes the Jeffery-Hamel one which is independent of X. The stability problem they considered was for fixed frequency distributions to the basic flow, in the manner of Eagles & Weissman (1975). In the expansion that followed, the Orr-Sommerfeld problem appeared at lowest order. One important difference was that the downstream dependence was not just in the frequency term, and the local wave number, but also in the basic flow. The general scheme that followed has already been described earlier in some detail, for the investigation of Eagles & Weissman (1975).

The basic flow varies with X, and different neutral stability curves can be obtained for each X as well as for each λ . In the straight walled case, neutral curves were plotted for intrinsic frequency $\beta_I = \beta \exp(2X)$ vs. R. If R > some R-crit, growing disturbances could be expected at all X stations, since random disturbances of the steady state flow would contain components of the fixed frequency waves considered. In this curved walled case however, neutral curves need to be plotted for w ($w \equiv \beta$ here) against R for each X and for each λ . From these three-dimensional neutral stability boundaries, plots of R vs. X can be extracted for each λ . This would show that if R > some R-crit, disturbances grow for a limited range of X, and this would only be possible for a corresponding range of frequencies.

Both the problems of Eagles & Weissman (1975) and Eagles & Smith (1980), have been considered by Allmen (1980). He tackled them by a direct numerical approach on the partial differential equations governing the motions. The close agreement between Allmen and both the above investigations , serve to support the theoretical ideas discussed in the expansion procedure.

1.2 The Present Thesis.

The general dimensional Navier-Stokes equations for two-dimensional, incompressible flow will be rewritten in terms of Fraenkel's generalized non-dimensionalized coordinate system (2.16). This equation, which governs the total stream function Ψ , will be considered by superimposing infinitesimal disturbances ($\Phi(\xi,\eta,t)$) to the basic flow ($\Omega(\xi,\eta)$). The non-linear equation for the steady state basic flow will be considered first, and the disturbance equation for $\Phi(\xi,\eta,t)$ will be determined by neglecting the non-linear terms.

The class of symmetric channels will be generated by choosing a slowly varying complex function $\alpha(\tau)$, which we will show behaves like the slope of the channel walls. This function will be used to determine the physical coordinates of the channel. This can be done numerically or analytically in the first case given by (3.7). We will express the coordinates of the channel walls in ascending powers of a small parameter $\varepsilon^{1/2}$, (which is a measure of the divergence angle) and we will see that the modified polar coordinates used by Eagles & Weissman (1975), emerge as a special case of Fraenkel's generalized cordinates, in the limit as $\varepsilon^{1/2} \to 0$.

Before considering the asymptotic development of the equation governing $\Omega(\xi,\eta)$ and $\Phi(\xi,\eta,t)$, we shall introduce a slow streamwise variable $\sigma_1 = \varepsilon^{1/2}\xi$. In Fraenkel's (1963 II) asymptotic development of the steady state solution, the original slow variable $\sigma = \varepsilon\xi$ was used. The variable σ_1 is seen to be necessary when we consider the disturbance equation, and in particular the unboundedness of the term $h^2\frac{\partial}{\partial\eta}$ in (2.19a). This term is not bounded in the limit $\varepsilon^{1/2} \to 0$, σ fixed, but it is for $\varepsilon^{1/2} \to 0$, σ_1 fixed.

We shall initially develop the asymptotic analysis for $\Omega(\xi,\eta)$ in terms of σ. ($\Omega = \Omega_0(\sigma,\eta) + \varepsilon^{1/2}\Omega_1(\sigma,\eta) + \varepsilon\Omega_2(\sigma,\eta) + \ldots$). Ω_0 represents a set of Jeffery-Hamel solutions for some fixed σ .

In order to avoid the problem of unboundedness in the disturbance equation, we shall develop a further asymptotic expansion of Ω_0, Ω_1, and Ω_2 in terms of G_0, G_1, G_2, F_0, F_1, and H_0, for $\varepsilon^{1/2} \to 0, \sigma_1$ fixed. This really corresponds to a Taylor series expansion of Ω_0, Ω_1, and Ω_2 about $\sigma = 0$. This way we shall have a consistent asymptotic analysis for both $\Omega(\xi,\eta)$ and $\Phi(\xi,\eta,t)$. (i.e. $\varepsilon^{1/2} \to 0, \sigma_1, \eta$ fixed).

The two essential conditions necessary to apply Fraenkel's small wall curvature theory, are given by (3.3) and (3.4). This implies a relationship between R and $\varepsilon^{1/2}$ (4.3). It also ensures that the non-linear, streamwise independent, Jeffery-Hamel profiles appear at O(1), thus providing the required first approximation for channels with slightly curved walls. The simplest ones will be considered, that is, the symmetric ones with at most one region of reversed flow at each wall.

We will consider three convincing checks on the validity of this double expansion. The first will be obtained through the curvature parameter m, in (3.7). The equations governing the staight walled case are conveniently retrieved by setting $m = 0$, and then letting $\varepsilon^{1/2} \to 0$. We shall see that the term ommited by Eagles & Weissman (1975) (see equations (2) and (3) of their paper) is equivalent to $\varepsilon\, dH_0/d\eta$ in this analysis. The second check will be obtained through a direct expansion of $\Omega(\xi,\eta)$ in terms of functions of σ_1. The resulting ordered set of partial differential equations are shown to be satisfied by the corresponding ordered functions in the former double expansion. The third check takes the double expansion to the next order, $(O(\varepsilon^{3/2}))$ and we will show that when dealing with the numerical results, the solution of the basic flow up to and including the $O(\varepsilon)$ terms is sufficiently accurate for the purposes of this investigation.

We will begin the asymptotic development of the disturbance stream function Φ by considering (2.19a). The coefficients of this equation are independent of time, but slowly varying with ξ . The most appropriate form of Φ will be the usual WKB modification of the quasi-parallel approach. (i.e. $\Phi(\sigma_1, \eta, t) = \Phi(\sigma_1, \eta) \exp(i(\Theta(\xi)-\beta t)) + c.c$). We shall forego any detailed discussion on the artificial separating of the relationship between R and $\varepsilon^{1/2}$ in the disturbance equation here, and refer this to previous arguments.

The important problem in the unboundedness of h, will be clearly seen now in (4.26), where the need for σ_1 as the slow variable (as opposed to σ) is necessary. The usefulness of Fraenkel's generating function is seen in (4.27), where $\alpha(\sigma)$ represents the semi-divergence of the channel walls. ($\eta = \pm 1$).

The asymptotic expansion of $\Phi(\sigma_1, \eta)$ in ascending powers of $\varepsilon^{1/2}$ ($\Phi = \Phi_0 + \varepsilon^{1/2}\Phi_1 + \varepsilon \Phi_2 + \ldots$) yields a sequence of problems with the Orr-Sommerfeld problem at lowest order, where now, the coefficients and the eigenvalue (k) are functions of the slow variable σ_1. This eigenvalue problem will be solved by means of an approximation to the eigenrelation, defined by the essential characteristic equation (4.56), which ensures non-trivial solutions to (4.46). We will then utilize the theory of homogeneous linear differential equations, to solve for Φ_0 and Φ_1. We look for solutions in the form $\Phi_0(\sigma_1, \eta) = A_0(\sigma_1) f_0(\sigma_1, \eta)$, and $\Phi_1(\sigma_1, \eta) = f_1(\sigma_1, \eta) + A_1(\sigma_1) f_0(\sigma_1, \eta)$ where A_0 and A_1 are interpreted as the amplitudes of Φ_0, Φ_1 respectively along the centre of the channel. Thus f_0 , f_1 , which satisfy (4.29a) and (4.32a) respectively for fixed σ_1, can be normalized arbitrarily. The equations for A_0 , and A_1, are found by appealing to solvability conditions for Φ_1 and $\Phi_2 = f_2(\sigma_1, \eta) + A_2(\sigma_1) f_0(\sigma_1, \eta)$ respectively. It will be necessary to solve (4.37a) for fixed σ_1 as a further check on A_1, but we wont solve for $A_2(\sigma_1)$.

In establishing higher order expressions for the growth rates of various flow quantities, we shall use the "yardstick" suggested by Shen (1961) as a measure of the growth or the decay of a disturbance. That is, the relative mean kinetic energy density, averaged over time , and integrated across the channel. These expressions will show that all growth rates are the same at lowest order, (as predicted by the quasi-parallel theory) but they will be different however for different flow quantities with the higher order corrections. They are given in convenient forms suitable for computing purposes, aswell as comparing with the corresponding expressions for the straight walled case of Eagles & Weissman (1975).

The theoretical scheme briefly described above, is first applied to a channel whose curvature is constant in sign λ but may be positive or negative. This channel can theoretically be extended to $\pm \infty$, but we must imagine our channel for analysis, to be representative of some portion of the theoretical infinite channel (see FIG-1). In the second instant it will be applied to the case of a more realistic channel given by (7.1). This channel is called a Fraenkel-type channel as it satisfies the conditions required by Fraenkel (1963 II p403). Here we will introduce a facility to enable commencement of the stability analysis anywhere in the given channel. We will thus be able to give a complete picture of the flow as we travel upstream or downstream. This facility is not really necessary in the constant signed λ curvature channel, even though we will follow the growth or decay of a disturbance downstream for a limited range of σ_1.

The equations obtained describing the steady state functions, will at first appear different from the former constant curvature case, but a transformation will be considered which makes the two problems equivalent,with the exception of some additional terms. These additional terms, which appear in the Fraenkel-type channel analysis, can be shown to stem directly from the fact that the curvature is varying in a more general way.

The problems associated with choosing parameters in order to avoid the difficulty of a large final and initial throat width ratio, will be discussed analytically, and a reference will be made to a particular channel for experimental purposes.

Finally, the straight walled channel is recalled once more in order to consider a more general disturbance to the base flow. This general disturbance will be constructed by adding slowly varying fixed frequency modes of the form $\Phi(\sigma_1,\eta)\ \exp(i(\Theta(\xi)-\beta t))$. Boundary conditions will be defined in order to make this general disturbance a δ-type function in t, at $\sigma_1 = 0$. This impulsive disturbance will be shown to produce a wave packet type disturbance. The object will be to consider whether this resulting disturbance develops into a growing or decaying packet downstream, and whether this is dependent on R > R-crit or R < R-crit respectively.

2. The Governing Equations.

Consider the dimensionalized, non-linear, incompressible, two-dimensional Navier-Stokes equations in vector form.

$$\frac{\partial \underset{\sim}{U}}{\partial T} - \underset{\sim}{U}\times\underset{\sim}{W} = -\nabla\left\{\frac{P}{\rho}+\frac{1}{2}\underset{\sim}{U}^2\right\} - \nu\nabla\times\underset{\sim}{W}\,, \tag{2.1}$$

$$\nabla\cdot\underset{\sim}{U} = 0\,, \tag{2.2}$$

where
$$\underset{\sim}{W} = \nabla\times\underset{\sim}{U}\,. \tag{2.3}$$

The continuity equation (2.2), implies the existence of a stream function $\hat{\Psi}$, which is defined here in terms of general orthogonal coordinates, (a_1, a_2), and the velocity components are

$$U_{a_2} = \frac{1}{h_2}\frac{\partial\hat{\Psi}}{\partial a_1}\,, \tag{2.4}$$

$$U_{a_1} = -\frac{1}{h_1}\frac{\partial\hat{\Psi}}{\partial a_2}\,. \tag{2.5}$$

Here, h_1 and h_2 are the scale factors.

Using (2.2), (2.4), (2.5) and the general orthogonal coordinates the third component of (2.1), yields the required equation in terms of $\hat{\Psi}$. (Goldstein (1938) p114 Vol.1)

$$\frac{\partial(\nabla^2\hat{\Psi})}{\partial T} + \frac{1}{h_1h_2}\left[\frac{\partial\hat{\Psi}}{\partial a_2}\frac{\partial(\nabla^2\hat{\Psi})}{\partial a_1} - \frac{\partial\hat{\Psi}}{\partial a_1}\frac{\partial(\nabla^2\hat{\Psi})}{\partial a_2}\right] = \nu\nabla^4\hat{\Psi} \tag{2.6}$$

where $\nabla^2 = \frac{1}{h_1h_2}\left[\frac{\partial}{\partial\alpha}\left(\frac{h_2}{h_1}\frac{\partial}{\partial\alpha}\right) + \frac{\partial}{\partial\beta}\left(\frac{h_1}{h_2}\frac{\partial}{\partial\beta}\right)\right]$

The coordinate system to be used here is due to Fraenkel (1963 II). This system is recalled and amplified.

Let (X,Y) denote the dimensional cartesian coordinates. The following conformal transformation is used.

$$Z = Z(\zeta) \text{ where } Z = X + iY \text{ and } \zeta = \xi + i\eta.$$

Also we define H and ϑ by

$$\frac{dZ}{d\zeta} = H(\xi,\eta)\exp(i\vartheta(\xi,\eta)) \qquad .(2.7)$$

Here, H is a dimensional scaling factor, (i.e. an arc length dS_1 in the Z plane is H times the corresponding arc length in the ζ plane, $|dZ| = H|d\zeta|$); ϑ is the angle between corresponding line elements ($\arg(dZ) - \arg(d\zeta) = \vartheta$).

Let $$\frac{d}{d\zeta}\left(\ln\frac{dZ}{d\zeta}\right) = \kappa(\xi,\eta) - i\lambda(\xi,\eta) = \mu(\zeta) \qquad .(2.8)$$

Using (2.7) and (2.8), the Cauchy-Riemann equations yield

$$\kappa = \frac{1}{H}\frac{\partial H}{\partial \xi} = \frac{\partial \vartheta}{\partial \eta} \qquad ,(2.9)$$

$$\lambda = \frac{1}{H}\frac{\partial H}{\partial \eta} = -\frac{\partial \vartheta}{\partial \xi} \qquad ,(2.10)$$

where κ/H and λ/H are the curvatures in the Z-plane of the coordinate lines corresponding to ξ = constant, and η = constant respectively. A closer examination will be given in Ch.3 dealing with a particular

curved walled channel. The walls will be defined by $\eta = \pm 1$, and symmetry will be imposed about $\eta = 0$.

Now that the coordinate system to be used has been introduced, the form of Navier-Stokes equations can be derived in terms of Fraenkel's coordinates using (2.4), (2.5), (2.6), and noting that the scaling factors are now given by $h_1 = h_2 = H$, hence equation (2.6) becomes

$$\left\{\nu D^2 - \left(\frac{\partial\hat{\Psi}}{\partial\eta}\frac{\partial}{\partial\xi} - \frac{\partial\hat{\Psi}}{\partial\xi}\frac{\partial}{\partial\eta}\right) - H^2\frac{\partial}{\partial T}\right\}\left(\frac{1}{H^2}D^2\hat{\Psi}\right) = 0 \qquad ,(2.11)$$

where
$$D^2 = \frac{\partial^2}{\partial\xi^2} + \frac{\partial^2}{\partial\eta^2} \qquad .(2.12)$$

Equation (2.11) can now be non-dimensionalized by setting

$$\hat{\Psi} = M\Psi, \quad H = bh, \quad T = b^2 t/M \quad \text{yielding}$$

$$\left\{\frac{1}{R}D^2 - \left(\frac{\partial\Psi}{\partial\eta}\frac{\partial}{\partial\xi} - \frac{\partial\Psi}{\partial\xi}\frac{\partial}{\partial\eta}\right) - h^2\frac{\partial}{\partial t}\right\}\left(\frac{1}{h^2}D^2\Psi\right) = 0 \qquad ,(2.13)$$

where the Reynolds number R has been defined by $R = M/\nu$.

We note that R is defined in this way , so that it will not vary from station to station in a curved walled channel, and that M is defined to be half the volumetric flow rate per unit thickness.
(Rosenhead (1940))

It can be shown that 2H, is approximately the width of the channel for some constant ξ line, (Fraenkel 1963 II p.408) and at the throat of the channel (ξ=0) the width is approximately given by b.

The boundary conditions to (2.13) are

$$\Psi = \pm 1 \quad \text{at} \quad \eta = \pm 1 \qquad ,(2.14)$$

$$\frac{\partial \Psi}{\partial \eta} = \pm 1 \quad \text{at} \quad \eta = \pm 1 \qquad .(2.15)$$

Equation (2.14) follows from the definition of Ψ and M, and (2.15) is the no-slip condition at the wall for a viscous fluid. Note that even though (2.14) and (2.15) do not assume a symmetric velocity profile, they are consistent with that assumption.

A more convenient form of (2.13) is one which separates h^2 from $1/h^2 (D^2\Psi)$. This is done by using (2.9) and (2.10) when operating on $1/h^2 (D^2\Psi)$. A term appears in the analysis which is of the form $D^2 h$, and it is quite straight forward to show with the use of the Cauchy-Riemann equations, ((2.9) and (2.10)) that $D^2 h = h(\kappa^2 + \lambda^2)$. Hence (2.13) becomes

$$\left\{ \frac{1}{R} \left(D^2 - 4\left\{ \kappa \frac{\partial}{\partial \xi} + \lambda \frac{\partial}{\partial \eta} \right\} + 4\{\kappa^2 + \lambda^2\} \right) - h^2 \frac{\partial}{\partial t} - \left(\frac{\partial \Psi}{\partial \eta}\frac{\partial}{\partial \xi} - \frac{\partial \Psi}{\partial \xi}\frac{\partial}{\partial \eta} - 2\kappa \frac{\partial \Psi}{\partial \eta} + 2\lambda \frac{\partial \Psi}{\partial \xi} \right) \right\} D^2\Psi = 0 \,. \quad (2.16)$$

It will be assumed that Ψ, the total stream function is given by

$$\Psi(\xi,\eta,t) = \Omega(\xi,\eta) + \Phi(\xi,\eta,t) \qquad (2.17)$$

where $\Omega(\xi,\eta)$ is called the steady state stream function, and $\Phi(\xi,\eta,t)$ is called the time-dependent stream function. In fact Ω and Φ will later be chosen to be odd and even respectively. Their equations will form the basis in solving for Ψ.

2.1 The Steady State and Time-dependent Equations.

The equation satisfied by $\Omega(\xi,\eta)$ can be stated now, using (2.16). The term $h^2\partial/\partial t$ disappears, and Ψ is replaced by Ω, yielding

$$\left\{\frac{1}{R}\left(D^2-4\left\{\kappa\frac{\partial}{\partial\xi}+\lambda\frac{\partial}{\partial\eta}\right\}+4\{\kappa^2+\lambda^2\}\right)-\left(\frac{\partial\Omega}{\partial\eta}\frac{\partial}{\partial\xi}-\frac{\partial\Omega}{\partial\xi}\frac{\partial}{\partial\eta}-2\kappa\frac{\partial\Omega}{\partial\eta}+2\lambda\frac{\partial\Omega}{\partial\xi}\right)\right\}D^2\Omega=0 \quad ,(2.18a)$$

$$\Omega = \pm 1 \text{ at } \eta=\pm 1 \; ; \; \frac{\partial\Omega}{\partial\eta}=0 \text{ at } \eta=\pm 1 \quad .(2.18b)$$

Note that this equation is non-linear.

The equation for $\Phi(\xi,\eta,t)$ can be found by using (2.16) and replacing Ψ by $\Omega+\Phi$. We are going to consider infinitesimal disturbances to the base flow, so we assume non-linear terms are small enough to be neglected. Therefore, upon substituting and linearizing we obtain

$$\left\{\frac{1}{R}\left(D^2-4\left\{\kappa\frac{\partial}{\partial\xi}+\lambda\frac{\partial}{\partial\eta}\right\}+4\{\kappa^2+\lambda^2\}\right)-h^2\frac{\partial}{\partial t}-\left(\frac{\partial\Omega}{\partial\eta}\frac{\partial}{\partial\xi}-\frac{\partial\Omega}{\partial\xi}\frac{\partial}{\partial\eta}-2\kappa\frac{\partial\Omega}{\partial\eta}+2\lambda\frac{\partial\Omega}{\partial\xi}\right)\right\}D^2\Phi$$

$$-\left(\frac{\partial\Phi}{\partial\eta}\frac{\partial}{\partial\xi}-\frac{\partial\Phi}{\partial\xi}\frac{\partial}{\partial\eta}-2\kappa\frac{\partial\Phi}{\partial\eta}+2\lambda\frac{\partial\Phi}{\partial\xi}\right)D^2\Omega=0 \quad ,(2.19a)$$

$$\Phi = \pm 1 \text{ at } \eta=\pm 1 \; ; \; \frac{\partial\Phi}{\partial\eta}=0 \text{ at } \eta=\pm 1 \quad .(2.19b)$$

The equation for Ω needs to be solved before Φ can be considered.

3. A Symmetric Curved Walled Channel.

The notation used in (2.7) and (2.8), is recalled here for the purpose of establishing the channel walls. The non-dimensional form of (2.7) remains the same ($Z=bz$; $H=bh$). Thus we use (2.7) and (2.8) as dimensionless forms.

The details of how $\mu(\zeta)$ was made to be approximately equal to the semi-divergence angle of the walls were originally given by Fraenkel (1963 II pp407-408). He introduced a small constant ε such that

$$\varepsilon\zeta = \tau \; ; \quad \varepsilon\xi = \sigma \; ; \quad \tau = \sigma + \varepsilon i\eta \qquad ,(3.1)$$

and posed

$$\mu(\zeta) = \alpha(\tau) \qquad .(3.2) \quad *$$

This ensured that μ varied slowly with ζ and was nearly real. The choice of $\alpha(\tau)$ depends crucially on conditions imposed on other parameters, namely R and ε. The details of these conditions, and why they were necessary were discussed by Fraenkel (1963 II pp410-411). They will simply be stated here.

Fraenkel's asymptotic development of the solution to (2.18a) depends on the constant ε. It is in fact based on $\varepsilon \to 0$ with σ (not ξ) and η fixed. He justified this development very clearly and posed an asymptotic expansion in powers of ε for the steady state case with the Jeffery-Hamel profile as leading term. An alternative method which he used for computing the problem was in terms of a double series expansion in powers of $1/R^{-2}$ and δ where $\delta = R\varepsilon$. In each case

* $\alpha(\tau)$ is a slowly-varying complex function which is like the local semi divergence of the channel walls.

however, two essential conditions had to be satisfied, namely

$$R\alpha = O(1) \qquad ,(3.3)$$

and

$$R\varepsilon < O(1) \qquad .(3.4)$$

In the present analysis for the solution to (2.18a), the conditions (3.3) and (3.4) will be satisfied in the following way

$$\alpha = O(\varepsilon^{1/2}) \qquad ,(3.5)$$

and

$$R = O(1/\varepsilon^{1/2}) \qquad .(3.6)$$

The first channel chosen for consideration is given by

$$\alpha(\tau) = \varepsilon^{1/2} + \varepsilon^{1/2} m\tau \qquad .(3.7)$$

The curvature parameter m gives an additional degree of freedom, to study a family of channels with a common initial angle of divergence at $\sigma = 0$. A positive value of m corresponds to positive curvature, and a negative one, to negative curvature. It is worth noting that (3.7) does satisfy the conditions given by (3.3) and (3.4), but it does not satisfy the conditions described by Fraenkel (1963 II p408), thus α is not real as $\sigma \to \pm\infty$, but it is real on $\eta = 0$. We shall not be attempting to analyse the flow in this channel far upstream or far downstream, but imagine we are considering a portion of the channel between two finite, positive, and convenient values of σ, but ignore some problems associated with boundary conditions.

The special case m = 0, yields a straight walled channel. The constant $\varepsilon^{1/2}$ corresponds to the real constant α as defined in Eagles & Weissman (1975).

With this choice of $\alpha(\tau)$ it was found necessary to introduce another slow variable like σ . The main reason for this being, that under the asymptotic development $\varepsilon \to 0$, σ fixed, problems of unboundedness were encountered in the time-dependent anlysis. In fact h, the scaling factor which appears in (2.19a) was unbounded under this limit for this particular channel. The slow variable necessary to ensure the boundeness of h was

$$\sigma_1 = \varepsilon^{1/2}\xi \qquad ,(3.8)$$

hence

$$\sigma = \varepsilon^{1/2}\sigma_1 \qquad .(3.9)$$

The variable σ_1 will be used in evaluating the channel given by (3.7), and the asymptotic development will now be based on $\varepsilon^{1/2} \to 0$, with σ_1 and η fixed.

The channel walls can be found from (2.8), and on using (3.1),(3.2), and (3.7) we get

$$\frac{d}{d\zeta}\left[\ln\left(\frac{dz}{d\zeta}\right)\right] = \varepsilon^{1/2} + \varepsilon^{3/2} m\zeta$$

$$\frac{dz}{d\zeta} = C_1 \exp(\varepsilon^{1/2}\zeta + \frac{\varepsilon^{3/2} m \zeta^2}{2})$$

$$z = C_1 \int \exp(\varepsilon^{1/2}\zeta + \varepsilon^{3/2} m \zeta^2).d\zeta + C_2 \qquad .(3.10)$$

Here, C_1 and C_2 are real constants of integration, they correspond to different z scales and different origins respectively. The shape of the channel as $\varepsilon^{1/2} \to 0$, with σ_1 fixed, depends on the choice of C_1 and C_2.

The evaluation of (3.10) is rather lengthy, and it will suffice to describe the method and state the final results.

A reduction formula was found for the integral and after applying the formula repeatedly, the following general result was obtained.

$$z = C_1\left\{\frac{e^{\varepsilon^{1/2}\zeta}}{\varepsilon^{1/2}}\left[1 + \sum_{s=1}^{\infty}\sum_{t=1}^{2s} m^s \varepsilon^{\frac{(s+t)}{2}} (-1)^t \frac{(2s)!\,\zeta^t}{2^s\, s!\, t!} + \sum_{s=1}^{\infty} \frac{m\,(2s)!\,\varepsilon^{5/2}}{2^s s!}\right]\right\} + C_2 \quad ,(3.11)$$

and with the conditions

$$\zeta = 0 \; ; \; \frac{dz}{d\zeta} = 1 \text{ and } z = \frac{1}{\varepsilon^{1/2}}, \; C_1 \text{ and } C_2$$

become

$$C_1 = 1 \; ; \; C_2 = -\frac{1}{\varepsilon^{1/2}} \sum_{s=1}^{\infty} m^s . (2s)! \qquad .(3.12)$$

On substituting (3.12) back into (3.11) and rewriting (3.11) in modulus, argument form up to $O(\varepsilon)$, we obtain

$$|z| = r = \frac{e^{\sigma_1}}{\varepsilon^{1/2}}\left[1 + \varepsilon^{1/2}(m - me^{-\sigma_1} - m\sigma_1 + \frac{m\sigma_1^2}{2}) + \varepsilon(3m^2 - 3m^2e^{-\sigma_1} - 3m^2\sigma_1 + \frac{3m^2\sigma_1^2}{2} - \frac{m^2\sigma_1^3}{2} + \frac{m^2\sigma_1^4}{8})\right] ,(3.13)$$

$$\arg(z) = \theta = \varepsilon^{1/2}\eta + \varepsilon(m\eta\sigma_1 + m\eta e^{-\sigma_1} - m\eta) \qquad .(3.14)$$

Consider now the behaviour of (3.13) and (3.14) under the limit $\varepsilon^{1/2} \to 0$, σ_1, η, m fixed, then

$$|z| \simeq \frac{e^{\sigma_1}}{\varepsilon^{1/2}}; \quad \arg(z) \simeq \varepsilon^{1/2}\eta.$$

These in fact are the modified polar coordinates of Eagles (1966) and (1973), Eagles & Weissman (1975), where σ_1 corresponds to $\alpha\xi$, $\varepsilon^{1/2}$ to α. We can see how (3.14) demonstrates the usefulness of $\alpha(\tau)$ since θ is approximately $\alpha(\sigma)\eta$. The channel walls are defined by $\eta = \pm 1$, and symmetry is imposed about $\eta = 0$. Note also that irrespective of m and $\varepsilon^{1/2}$ if $\sigma_1 = 0$

$$|z| = \frac{1}{\varepsilon^{1/2}}; \quad \arg(z) = \varepsilon^{1/2}\eta.$$

The curved walled channel has the same angle of divergence at $\sigma_1 = 0$, as the straight walled channel defined by $\varepsilon^{1/2}$. A plot is given for the curved walled channel, for the particular case m = 1.0, and $\varepsilon^{1/2} = 0.4$, using (3.13) and (3.14) to compute the coordinates (see Fig-1). In physical space the initial throat width is approximately 2b, and the walls are defined by $\eta = \pm 1$.

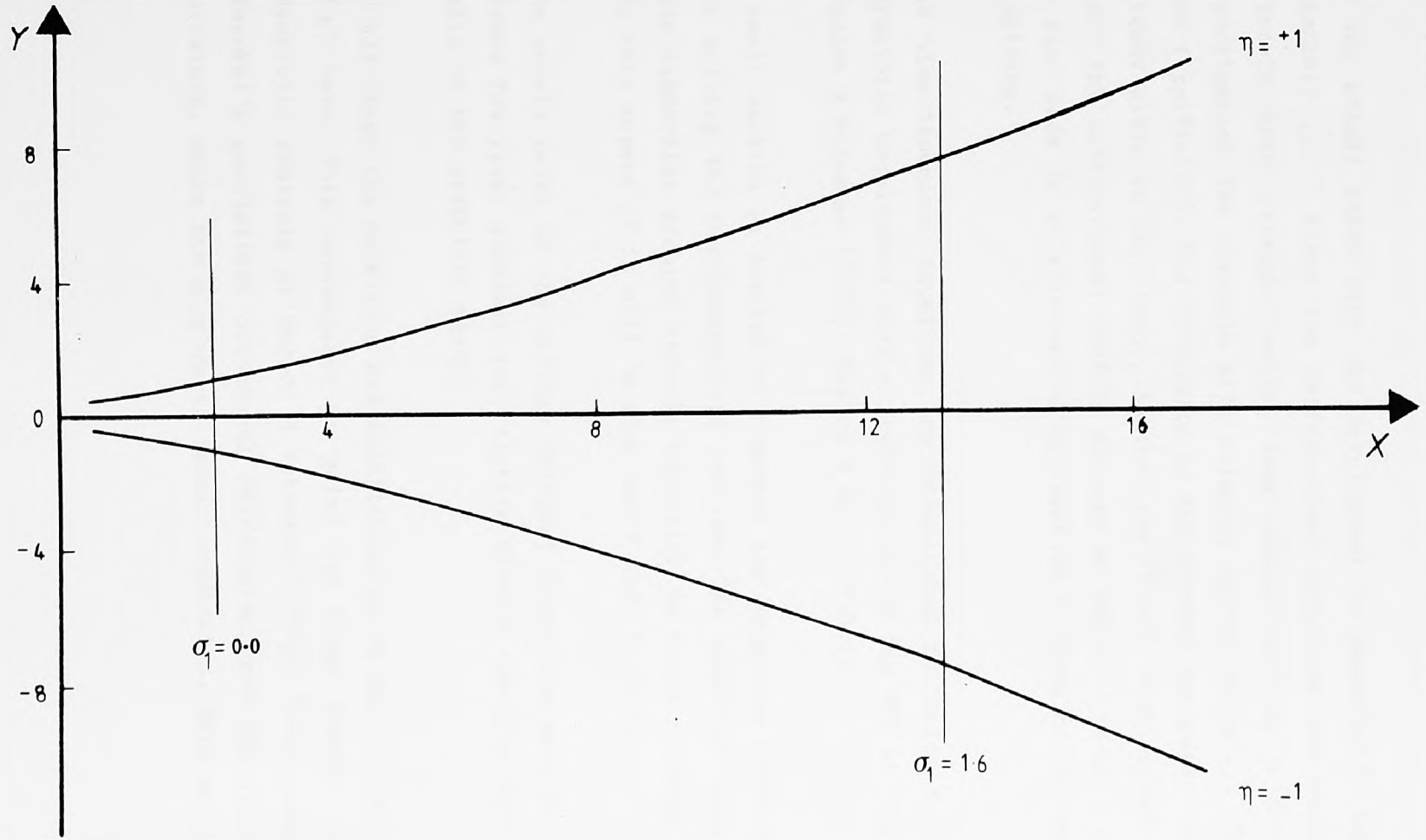

A curved walled channel given by $\alpha\varpi = \varepsilon^{1/2} + \varepsilon^{1/2} m\tau$ *for* $m=1$ *and* $\varepsilon^{1/2}=0{\cdot}4$.

FIG-1

4. The Asymptotic Development.

This chapter will be solely concerned with establishing the equations to be solved in the form derived from the asymptotic development.

In the steady state case the development is essentially that of Fraenkel; ... " Since the Jeffery-Hamel solutions are exact for channels with straight walls, they should provide a first approximation for channels with slightly curved walls"... (Fraenkel 1962 I pp121-122). The difference in the present analysis, for reasons already given in Ch.3 (p56), is that now $\varepsilon^{1/2} \to 0$, with σ_1 and η fixed, where the Jeffery-Hamel profile appears as the O(1) term. A reference is also made to an alternative approach as a check on the resulting equations.

The time-dependent equations are established following a similar asymptotic development with a modification to the WKB or "ray" method (Eagles & Weissman (1975), Eagles & Smith (1980)).

A small section is devoted to a method for obtaining starting values for solving the Orr-Sommmerfeld problem. The numerical solution to this eigenvalue problem depends crucially on these starting values, and this aspect of it will be also dealt with in Ch.5.

The growth rates of the various physical quantities such as velocity, stream function, absolute and relative kinetic energies will form the basis of the stability study.

In all cases the equations are established up to and including the $O(\varepsilon)$ term. This corresponds to going one stage further in the asymptotic analysis of Eagles & Weissman (1975). This, coupled with Fraenkel's generalized orthogonal coordinates, and the inclusion of curvature, makes the algebra extremely complicated. More so in the

unsteady case, and in particular, equation (4.37), which is necessary in order to check the amplitude function A_1.

An attempt has been made to represent the equations in such a way, so as to see the extra effects resulting from curvature, the $O(\varepsilon)$ terms, and to be easily comparable with those of Eagles & Weissman (1975).

4.1 The Steady State Equations.

In recalling the vorticity equation (2.18a), it is necessary to find expressions for κ , λ in terms of $\varepsilon^{1/2}$. This is easily done by using (2.8) and comparing real and imaginary parts. This yields exact relationships for κ and λ in the case of $\alpha(\tau) = \varepsilon^{1/2} + \varepsilon^{1/2} m \tau$, namely

$$\kappa = \varepsilon^{1/2} + m\varepsilon^{1/2}\sigma \qquad ,(4.1)$$

$$\lambda = -\varepsilon^{3/2} m \eta \qquad .(4.2)$$

The condition on R, α given in (3.3) defines a parameter v in the following way

$$R = \frac{v}{\varepsilon^{1/2}} \qquad .(4.3)$$

This ensures that the term $R\varepsilon^{1/2} = v$ will appear in the $O(1)$ equation for the steady state case.

The asymptotic expansion of $\Omega(\xi,\eta)$ is assumed to be of the form (following Fraenkel for our special case)

$$\Omega(\xi,\eta;v,m) = \Omega_0(\sigma,\eta;v,m) + \varepsilon^{1/2}\Omega_1(\sigma,\eta;v,m) + \varepsilon\,\Omega_2(\sigma,\eta;v,m)+\ldots \qquad .(4.4)$$

The variable σ_1 is not introduced yet, therefore on substituting (4.1), (4.2), (4.3), and (4.4) into (2.18a), with $\frac{\partial}{\partial \xi} = \frac{\varepsilon \partial}{\partial \sigma}$ (from (3.1)) it is possible to obtain the equations for Ω_0, Ω_1, Ω_2, by comparing coefficients of powers of $\varepsilon^{1/2}$. We obtain

$\underline{O(1)}$

$$\frac{\partial^4 \Omega_0}{\partial \eta^4} + 2v(1+m\sigma)\frac{\partial \Omega_0}{\partial \eta}\frac{\partial^2 \Omega_0}{\partial \eta^2} = 0 \qquad ,(4.5a)$$

and $$\Omega_0(\sigma, \pm 1) = \pm 1 \; ; \; \frac{\partial \Omega_0}{\partial \eta}(\sigma, \pm 1) = 0 \qquad ,(4.5b)$$

$\underline{O(\varepsilon^{1/2})}$

$$\frac{\partial^4 \Omega_1}{\partial \eta^4} + 2v(1+m\sigma)\frac{\partial}{\partial \eta}\left\{\frac{\partial \Omega_0}{\partial \eta}\frac{\partial \Omega_1}{\partial \eta}\right\} = v\left(\frac{\partial \Omega}{\partial \eta}_0\frac{\partial^3 \Omega}{\partial \sigma \partial \eta^2}_0 - \frac{\partial \Omega}{\partial \sigma}_0\frac{\partial^3 \Omega}{\partial \eta^3}_0\right) \qquad ,(4.6a)$$

and $$\Omega_1(\sigma, \pm 1) = 0 \; ; \quad \frac{\partial \Omega}{\partial \eta}_1(\sigma, \pm 1) = 0 \qquad ,(4.6b)$$

$\underline{O(\varepsilon)}$

$$\frac{\partial^4 \Omega_2}{\partial \eta^4} + 2v(1+m\sigma)\frac{\partial}{\partial \eta}\left\{\frac{\partial \Omega_0}{\partial \eta}\frac{\partial \Omega_2}{\partial \eta}\right\} = v\left(\frac{\partial \Omega}{\partial \eta}_0\frac{\partial^3 \Omega}{\partial \sigma \partial \eta^2}_1 + \frac{\partial \Omega}{\partial \eta}_1\frac{\partial^3 \Omega}{\partial \sigma \partial \eta^2}_0 - \frac{\partial \Omega_0}{\partial \sigma}\frac{\partial^3 \Omega_1}{\partial \eta^3} - \frac{\partial \Omega_1}{\partial \sigma}\frac{\partial^3 \Omega_0}{\partial \eta^3} - 2(1+m\sigma)\frac{\partial \Omega}{\partial \eta}_1\frac{\partial^2 \Omega}{\partial \eta^2}_1\right)$$

$$-4(1+m\sigma)^2\frac{\partial^2 \Omega_0}{\partial \eta^2} \qquad ,(4.7a)$$

and $$\Omega_2(\sigma, \pm 1) = 0 \; ; \quad \frac{\partial \Omega}{\partial \eta}_2(\sigma, \pm 1) = 0 \qquad ,(4.7b)$$

Even though Ω_0 is not the ξ independent Jeffery-Hamel profile for a wedge, (4.5a) still describes Jeffery-Hamel profiles for fixed values of σ, and given values of v and m.

At this stage the variable σ_1 is introduced, and $\Omega_0, \Omega_1, \Omega_2$, are all expanded in a Taylor series about $\sigma = 0$, in the form

$$\Omega_0(\sigma,\eta) = \Omega_0(0,\eta) + \sigma\frac{\partial\Omega_0}{\partial\sigma}(0,\eta) + \frac{\sigma^2}{2!}\frac{\partial^2\Omega_0}{\partial\sigma^2}(0,\eta) + \ldots \qquad .(4.8)$$

It can be seen that $\sigma = 0$ coverts (4.5a) into the wedge flow problem. The scheme exemplified by (4.8) would correspond to perturbing the steady state solution about the wedge flow problem, thus providing the required Jeffery-Hamel profile as a first approximation for channels with slightly curved walls.

Equation (4.8) and the corresponding ones for Ω_1 and Ω_2 can be written in more appropriate forms using (3.9).

$$\Omega_0(\sigma,\eta;v,m) = G_0(\eta;v) + \varepsilon^{1/2}\sigma_1 G_1(\eta;v,m) + \varepsilon\sigma_1^2 G_2(\eta;v,m) + \ldots \qquad ,(4.9)$$

$$\Omega_1(\sigma,\eta;v,m) = F_0(\eta;v) + \varepsilon^{1/2}\sigma_1 F_1(\eta;v,m) + \varepsilon\sigma_1^2 F_2(\eta;v,m) + \ldots \qquad ,(4.10)$$

$$\Omega_2(\sigma,\eta;v,m) = H_0(\eta;v) + \varepsilon^{1/2}\sigma_1 H_1(\eta;v,m) + \varepsilon\sigma_1^2 H_2(\eta;v,m) + \ldots \qquad .(4.11)$$

The equations (4.9), (4.10), and (4,11) are substituted into (4.5a), (4.6a), and (4.7a) respectively, and coefficients of powers of $\varepsilon^{1/2}$ are compared.

It is only necessary to obtain the equations for G_0, G_1, G_2, F_0, F_1, and H_0, since the other functions correspond to at least $O(\varepsilon^{3/2})$ terms. The solution for $\Omega(\xi,\eta;v,m)$ the total steady state stream function takes the form

$$\Omega(\xi,\eta;v,m) = G_0 + \varepsilon^{1/2}(F_0 + \sigma_1 G_1) + \varepsilon(H_0 + \sigma_1 F_1 + \sigma_1^2 G_2) + \ldots \quad .(4.12)$$

The equations for $G_0, G_1, G_2, F_0, F_1, H_0$ are stated here mainly for the purpose of deriving the equations describing the stream function for a wedge, up to and including $O(\varepsilon)$ terms. The equations are as follows

$$\frac{d^4 G_0}{d\eta^4} + 2v \frac{dG_0}{d\eta}\frac{d^2 G_0}{d\eta^2} = 0 \quad ,(4.13a)$$

$$G_0 = \pm 1 \; ; \; \frac{dG_0}{d\eta} = 0 \text{ at } \eta = \pm 1 \quad ,(4.13b)$$

$$\frac{d^4 G_1}{d\eta^4} + 2v \frac{d}{d\eta}\left[\frac{dG_0}{d\eta}\frac{dG_1}{d\eta}\right] = -2vm \frac{dG_0}{d\eta}\frac{d^2 G_0}{d\eta^2} \quad ,(4.14a)$$

$$G_1 = 0 \; ; \; \frac{dG_1}{d\eta} = 0 \text{ at } \eta = \pm 1 \quad ,(4.14b)$$

$$\frac{d^4 G_2}{d\eta^4} + 2v \frac{d}{d\eta}\left[\frac{dG_0}{d\eta}\frac{dG_2}{d\eta}\right] = -2v \frac{dG_1}{d\eta}\frac{d^2 G_1}{d\eta^2} - 2vm \frac{dG_0}{d\eta}\frac{d^2 G_1}{d\eta^2} - 2vm \frac{dG_1}{d\eta}\frac{d^2 G_0}{d\eta^2} \quad ,(4.15a)$$

$$G_2 = 0 \; ; \; \frac{dG_2}{d\eta} = 0 \text{ at } \eta = \pm 1 \quad ,(4.15b)$$

$$\frac{d^4F_0}{d\eta^4} + 2v \frac{d}{d\eta}\left[\frac{dG_0}{d\eta}\frac{dF_0}{d\eta}\right] = v\left(\frac{dG_0}{d\eta}\frac{d^2G_1}{d\eta^2} - G_1\frac{d^3G_0}{d\eta^3}\right) \qquad ,(4.16a)$$

$$F_0 = 0 \; ; \quad \frac{dF_0}{d\eta} = 0 \text{ at } \eta = \pm 1 \qquad ,(4.16b)$$

$$\frac{d^4F_1}{d\eta^4} + 2v \frac{d}{d\eta}\left[\frac{dG_0}{d\eta}\frac{dF_1}{d\eta}\right] = v\left(2\frac{dG_0}{d\eta}\frac{d^2G_2}{d\eta^2} + \frac{dG_1}{d\eta}\frac{d^2G_1}{d\eta^2} - G_1\frac{d^3G_1}{d\eta^3} - 2G_2\frac{d^3G_0}{d\eta^3}\right.$$
$$- 2\frac{dF_0}{d\eta}\frac{d^2G_1}{d\eta^2} - \frac{dG_1}{d\eta}\frac{d^2F_0}{d\eta^2} - 2m\frac{dG_0}{d\eta}\frac{d^2F}{d\eta^2}$$
$$\left. - 2m\frac{dF_0}{d\eta}\frac{d^2G_0}{d\eta^2}\right) \qquad ,(4.17a)$$

$$F_1 = 0 \; ; \quad \frac{dF_1}{d\eta} = 0 \text{ at } \eta = \pm 1 \qquad ,(4.17b)$$

$$\frac{d^4H_0}{d\eta^4} + 2v \frac{d}{d\eta}\left[\frac{dG_0}{d\eta}\frac{dH_0}{d\eta}\right] = v\left(\frac{dG_0}{d\eta}\frac{d^2F_1}{d\eta^2} + \frac{dF_0}{d\eta}\frac{d^2G_1}{d\eta^2} - G_1\frac{d^3F_0}{d\eta^3}\right.$$
$$\left. - F_1\frac{d^3G_0}{d\eta^3} - 2\frac{dF_0}{d\eta}\frac{d^2F_0}{d\eta^2}\right) - 4\frac{d^2G_0}{d\eta^2} \qquad ,(4.18a)$$

$$H_0 = 0 \; ; \quad \frac{dH_0}{d\eta} = 0 \text{ at } \eta = \pm 1 \qquad .(4.18b)$$

This scheme can readily describe the wedge-flow problem, simply by assigning m = 0. Thus we can see $G_1 = G_2 = F_0 = F_1 = 0$, satisfy (4.14a), (4.15a), (4.16a), (4,17a) respectively. The resulting equations are given by (4.13a) and

$$\frac{d^4H_0}{d\eta^4} + 2v \frac{d}{d\eta}\left[\frac{dG_0}{d\eta}\frac{dH_0}{d\eta}\right] = -4\frac{d^2G_0}{d\eta^2} \qquad ,(4.19a)$$

$$H_0 = 0 \; ; \quad \frac{dH_0}{d\eta} = 0 \text{ at } \eta = \pm 1 \qquad ,(4.19b)$$

Hence $\varepsilon dH_0/d\eta$ can be thought of as the $O(\varepsilon)$ correction to the velocity profile, and it represents the $O(\alpha^2)$ term not included by Eagles & Weissman (1975).

4.2 An Alternative Approach.

The final form of (4.12) suggests that as opposed to the asymptotic scheme given by (4.4) and (4.9) to (4.11), it should be possible to expand $\Omega(\xi,\eta;v,m)$, the total steady state stream function initially in the following way.

$$\Omega(\xi,\eta;v,m) = \chi_0(\sigma_1,\eta;v) + \varepsilon^{1/2}\chi_1(\sigma_1,\eta;v,m) + \varepsilon\chi_2(\sigma_1,\eta;v,m) + \ldots \quad .(4.20)$$

We can now substitute (4.20) into (2.18a) as before, but with a slight modification to (4.1), (i.e. $\kappa = \varepsilon^{1/2} + m\varepsilon\sigma_1$, and $\frac{\partial}{\partial\xi} = \varepsilon^{1/2}\frac{\partial}{\partial\sigma_1}$) thus by comparing the coefficients of powers of $\varepsilon^{1/2}$ the following equations are obtained.

O(1)

$$\frac{\partial^4\chi_0}{\partial\eta^4} + 2v\frac{\partial\chi_0}{\partial\eta}\frac{\partial^2\chi_0}{\partial\eta^2} = v\left(\frac{\partial\chi_0}{\partial\eta}\frac{\partial^3\chi_0}{\partial\sigma_1\partial\eta^2} - \frac{\partial\chi_0}{\partial\sigma_1}\frac{\partial^3\chi_0}{\partial\eta^3}\right) \quad ,(4.21a)$$

$$\chi_0 = \pm 1 \; ; \; \frac{\partial\chi_0}{\partial\eta} = 0 \quad \text{at } \eta = \pm 1 \quad ,(4.21b)$$

$O(\varepsilon^{1/2})$

$$\frac{\partial^4 \chi_1}{\partial \eta} + 2\nu \frac{\partial}{\partial \eta}\left[\frac{\partial \chi_0}{\partial \eta}\frac{\partial \chi_1}{\partial \eta}\right] = \nu\left(\frac{\partial \chi_0}{\partial \eta}\frac{\partial^3 \chi_1}{\partial \sigma_1 \partial \eta^2} + \frac{\partial \chi_1}{\partial \eta}\frac{\partial^3 \chi_0}{\partial \sigma_1 \partial \eta^2} - \frac{\partial \chi_0}{\partial \sigma_1}\frac{\partial^3 \chi_1}{\partial \eta^3}\right.$$

$$\left. - \frac{\partial \chi_1}{\partial \sigma_1}\frac{\partial^3 \chi_0}{\partial \eta^3} - 2m\sigma_1 \frac{\partial \chi_0}{\partial \eta}\frac{\partial^2 \chi_0}{\partial \eta^2}\right) \qquad ,(4.22a)$$

$$\chi_1 = 0 \; ; \; \frac{\partial \chi_1}{\partial \eta} = 0 \quad \text{at } \eta = \pm 1 \qquad ,(4.22b)$$

$O(\varepsilon)$

$$\frac{\partial \chi_2}{\partial \eta} + 2\nu \frac{\partial}{\partial \eta}\left[\frac{\partial \chi_0}{\partial \eta}\frac{\partial \chi_2}{\partial \eta}\right] = \nu\left(\frac{\partial \chi_0}{\partial \eta}\frac{\partial^3 \chi_2}{\partial \sigma_1 \partial \eta^2} + \frac{\partial \chi_1}{\partial \eta}\frac{\partial^3 \chi_1}{\partial \sigma_1 \partial \eta^2} + \frac{\partial \chi_2}{\partial \eta}\frac{\partial^3 \chi_0}{\partial \sigma_1 \partial \eta^2}\right.$$

$$- \frac{\partial \chi_0}{\partial \sigma_1}\frac{\partial^3 \chi_2}{\partial \eta^3} - \frac{\partial \chi_1}{\partial \sigma_1}\frac{\partial^3 \chi_1}{\partial \eta^3} - \frac{\partial \chi_2}{\partial \sigma_1}\frac{\partial^3 \chi_0}{\partial \eta^3}$$

$$\left. -2\frac{\partial \chi_1}{\partial \eta}\frac{\partial^2 \chi_1}{\partial \eta^2} - 2\sigma_1 \frac{\partial}{\partial \eta}\left[\frac{\partial \chi_0}{\partial \eta}\frac{\partial \chi_1}{\partial \eta}\right]\right) - 4\frac{\partial^2 \chi_0}{\partial \eta^2}$$

$$+4\frac{\partial^3 \chi_0}{\partial \sigma_1 \partial \eta^2} \qquad ,(4.23a)$$

$$\chi_2 = 0 \; ; \; \frac{\partial \chi_2}{\partial \eta} = 0 \quad \text{at } \eta = \pm 1 \qquad ,(4.23b)$$

The two schemes defined by (4.12) and (4.20), are obviously not identical when comparing corresponding order terms, but the value of Ω for prescribed $\varepsilon^{1/2}$, v, m with fixed σ_1 and η should be the same. The additional non-linear terms in (4.21a) clearly makes this latter scheme less appealing from a numerical point of view. It can be shown that G_0, $(F_0 + \sigma_1 G_1)$, and $(H_0 + \sigma_1 F_1 + \sigma^2 G_2)$ satisfy (4.21a), (4.22a), and (4.23a) respectively. On the basis of this check, the steady state stream function Ω was computed using the original scheme (4.13a) to (4.18a).

Rosenhead, (1940) showed that for a given v (i.e. for every pair of $\varepsilon^{1/2}$ and R) there exists an infinity of solutions for G_0. These solutions become progressively more complex with increasing R for the case of "outflow" in a divergent channel. Some of the well known mathematical characteristics with increasing R for this case, are progressively more regions of "outflow" bounded by regions of "inflow". This has clearly been shown by Patterson's (1934,1935) experiments.

We take G_0 to be the simplest of the possible Jeffery-Hamel profiles in such a way that for fixed σ_1 and η, G_0 is a continuous function of v such that G_0, with v=0, reduces to the Poisseuille flow case. Fraenkel's theory shows that we can obtain separation and reattachment without singularities when our v is just greater or just less than 4.7 respectively. The theory is restricted in fact to certain combinations of $\varepsilon^{1/2}$ and R which exibit the simpler symmetric velocity profiles, with at most one region of reversed flow near the walls. For this reason our values of v do not extend far beyond 4.7 (Fraenkel 1962 I p133).

4.3 The Time-dependent Equations.

Assuming the solution for Ω is known, (2.19a) is recalled and the asymptotic development can commence.

In the steady state case a certain condition was imposed on R and $\varepsilon^{1/2}$ (4.3). This condition is relaxed for the time-dependent analysis, where R and $\varepsilon^{1/2}$ are treated as independent parameters in the asymptotic development, but (4.3) is returned to in the final analysis of the results. This technique has already been used extensively by other authors, (Eagles & Weissman (1975), Gaster (1974), Bouthier (1972,1973), Ling & Reynolds (1973), Lanchon & Eckhaus (1964), Eagles & Smith (1980)) where substantial arguments are given in its support.

Formally, the viscous terms in (2.19a) which are given by $\frac{1}{R}\left[D^2 - 4\left(\kappa\frac{\partial}{\partial\xi} + \lambda\frac{\partial}{\partial\eta}\right) + 4(\kappa^2 + \lambda^2)\right] D^2\Phi$, appear to be smaller than the inertia terms. However these terms which are $O(1/R^{1/3})$ (Lin 1955) over some of the flow field, may be dominant enough to be retained in the O(1) terms. We formally allow these viscous terms to appear in the O(1) terms by artificially separating R and $\varepsilon^{1/2}$. A more accurate representation of the exact solution to (2.19a) is thus contained in the O(1) solution on returning to the relationship (4.3).
The coefficients of (2.19a) are independent of time and slowly varying with ξ, therefore the stream function of the disturbance for constant frequencies is chosen to be of the form

$$\Phi(\xi,\eta,t) = \Phi(\sigma_1,\eta)\exp(i(\Theta(\xi) - \beta t)) + \text{c.c.} \qquad ,(4.24)$$

where c.c. represents the complex conjugate of the preceeding term, and where β is chosen to be real.

The slow variation of the coefficients in the ξ direction, is allowed for by the complex wave number $k(\sigma_1)$, which is defined in terms of the complex phase function $\Theta(\xi)$ by

$$\frac{d\Theta}{d\xi} = k(\sigma_1) \qquad .(4.25)$$

A negative imaginary part of Θ, hence a negative imaginary part of k (k_i) will correspond to "growth" of the disturbance function. This growth may or may not persist downstream. If k_i assumes a negative value, it will not necessarily follow that the flow is unstable, but it will be termed " locally unstable " if the disturbance ultimately decays (i.e. if k_i resumes a positive value). This idea of "growth" will be dealt with in more detail in a later subsection, and also in Ch.6 when analysing the results.

The values of h, and ϑ can be determined for this particular channel using (2.7), (2.8), and $dz/d\zeta = 1$, when $\zeta = 0$. Even though ϑ is never used directly in the expansion, it can still be used to describe the local semi-divergence angle of the channel, which in this case is exact.

$$h = \exp\left[\sigma_1 + \frac{\varepsilon^{1/2} m \sigma_1^2}{2} - \frac{m \varepsilon^{3/2} \eta^2}{2}\right] \qquad ,(4.26)$$

$$\vartheta = \eta(\varepsilon^{1/2} + \varepsilon m \sigma_1) = \eta\alpha(\sigma) \qquad .(4.27)$$

When $\eta = \pm 1$, ϑ is the local angle of the channel walls with the x-axis.

The aim is to obtain a solution to (2.19a) in terms of an ascending series in powers of $\varepsilon^{1/2}$, and we therefore take

$$\Phi(\sigma_1,\eta;R,v,m) = \Phi_0(\sigma_1,\eta;R,v,m)+\varepsilon^{1/2}\Phi_1(\sigma_1,\eta;R,v,m)+ \varepsilon\Phi_2(\sigma_1,\eta;R,v,m)+.. \quad .(4.28)$$

Now (4.24) to (4.28) are substituted into (2.19a) and powers of $\varepsilon^{1/2}$ are compared. Even though the equation for Φ_2 is extremely long, it is quoted here so that the contributions from curvature and extra terms $(O(\varepsilon))$ can be seen. A particular integral to the equation for Φ_2 will eventually be found. We obtain

O(1)

$$L\,\Phi_0 = 0 \qquad ,(4.29a)$$

$$\Phi_0(\sigma_1,\pm1) = 0 \; ; \quad \frac{\partial\Phi_0}{\partial\eta}(\sigma_1,\pm1) = 0 \qquad ,(4.29b)$$

$$L \equiv \frac{1}{R}(D_1^2-k^2)^2 + i\left\{\beta_I - kd\frac{G_0}{d\eta}\right\}(D_1^2-k^2) + ikd^3\frac{G_0}{d\eta^3} \qquad ,(4.30)$$

where $$\beta_I = \beta e^{2\sigma_1} \qquad ,(4.31)$$

and $$D_1^2 = \frac{\partial^2}{\partial\eta^2}.$$

In place of the frequency and wavenumber, (4.30) contains functions of the slow variable, but (4.29a) is still the well known Orr-Sommerfeld problem, and β_I is called the intrinsic frequency. For a given β(real) (4.29a) is an eigenvalue problem in k.

Further equations are

$\underline{O(\varepsilon^{1/2})}$

$$L\Phi_1 \equiv L\frac{\partial\Phi_0}{\partial\sigma_1} + \frac{dk}{d\sigma_1}L_2\Phi_0 + (L_3 + L_4)\Phi_0 \qquad ,(4.32a)$$

$$\Phi_1(\sigma_1,\pm1) = 0 \; ; \; \frac{\partial\Phi_1}{\partial\eta}(\sigma_1,\pm1) = 0 \qquad ,(4.32b)$$

where $$L_1 \equiv -\frac{4ik}{R}(D_1^2-k^2) + 2k\beta_I + \frac{dG_0}{d\eta}(D_1^2-3k^2) - \frac{d^3G_0}{d\eta^3} \qquad ,(4.33)$$

$$L_2 \equiv -\frac{2i}{R}(D_1^2-3k^2) + \beta_I - \frac{3kdG_0}{d\eta} \qquad ,(4.34)$$

$$L_3 \equiv \frac{4ik}{R}(D_1^2-k^2) - \left\{\frac{2dG_0}{d\eta} + \beta_I im\sigma_1^2\right\}(D_1^2-k^2) - \frac{2d^2G_0}{d\eta^2}D_1, \qquad (4.35)$$

$$L_4 \equiv ik\left[\frac{dF_0}{d\eta} + \sigma_1\frac{dG_1}{d\eta}\right](D_1^2-k^2) - ik\left[\frac{d^3F_0}{d\eta^3} + \sigma_1\frac{d^3G_1}{d\eta^3}\right] \qquad .(4.36)$$

It is worth noting so far, that the system defined by (4.29a) to (4.30), and (4.32a) to (4.36), can easily be compared with the Eagles & Weissman case for a straight walled channel. The equations (4,29a) to (4.30) are identical in form to those given by Eagles & Weissman at O(1), but equations (4.32a) to (4.36) differ in the operators L_3 and L_4. The additional term $\beta_I im\sigma_1^2$ in L_3 and the introduction of L_4 are both a direct consequence of the curvature of the channel, and would disappear on setting $m = 0$.

Continuing we obtain

$\underline{O(\varepsilon)}$

$$L\Phi_2 = L_1\frac{\partial\Phi_1}{\partial\sigma_1} + \frac{dk}{d\sigma_1}L_2\Phi_1 + (L_3 + L_4)\Phi_1$$

$$+(M_1 + M_2)\frac{\partial\Phi_0}{\partial\sigma_1} + \frac{dk}{d\sigma_1}(M_3 + M_4)\Phi_0 + \frac{dk}{d\sigma_1}M_5\frac{\partial\Phi_0}{\partial\sigma_1}$$

$$+\left(M_6 + M_7 + M_8 + \frac{d^2k}{d\sigma_1^2}\left\{\frac{4k}{R} + i\frac{dG_0}{d\eta}\right\} + \frac{3}{R}\left[\frac{dk}{d\sigma_1}\right]^2\right)\Phi_0$$

$$-iL\frac{\partial^2\Phi_0}{\partial\sigma_1^2} \qquad ,(4.37a)$$

$$\Phi_2(\sigma_1,\pm1) = 0 \; ; \; \frac{\partial\Phi_2}{\partial\eta}(\sigma_1,\pm1) = 0 \qquad ,(4.37b)$$

The first line of (4.37a) is identical in form to (4.32a), the additional terms M_1, M_2, M_3, M_4, M_5, M_6, M_7, M_8 are a consequence of curvature, and the fact that the steady state case was taken up to and including $O(\varepsilon)$. Some of these will simplify a great deal upon setting $m = 0$, and others will vanish completely, thus reducing to the case of the straight walled channel. These new operators are defined for reference.

$$M_1 \equiv \frac{4}{R}(D_1^2 - 3k^2) - \left\{4ik\frac{dG_0}{d\eta} - 2\beta_I km\sigma_1^2\right\} \qquad ,(4.38)$$

$$M_2 \equiv \left\{\frac{dF_0}{d\eta} + \sigma_1\frac{dG_1}{d\eta}\right\}(D_1^2 - 3k^2) - \left\{\frac{d^3F_0}{d\eta^3} + \sigma_1\frac{d^3G_1}{d\eta^3}\right\} \qquad ,(4.39)$$

$$M_3 \equiv -\frac{12k}{R} - i\left\{2\frac{dG_0}{d\eta} + i\beta_I m\sigma_1^2\right\} \qquad ,(4.40)$$

$$M_4 \equiv -3k\left\{\frac{dF_0}{d\eta} + \sigma_1\frac{dG_1}{d\eta}\right\} \qquad ,(4.41)$$

$$M_5 \equiv \frac{12k}{R} + 3i\frac{dG_0}{d\eta} \qquad ,(4.42)$$

$$M_6 \equiv \frac{-4(D_1^2-k^2)}{R} + \left(\frac{4m\sigma_1 ik}{R} - 2m\sigma_1\frac{dG_0}{d\eta} - i\beta_I\frac{m\sigma_1^2}{2}\right)(D_1^2-k^2) - 2m\sigma_1\frac{d^2G_0}{d\eta^2}D_1 \qquad ,(4.43)$$

$$M_7 \equiv -\left(2\left[\frac{dF_0}{d\eta} + \sigma_1\frac{dG_1}{d\eta}\right] + G_1 D_1\right)(D_1^2-k^2) + \left[\frac{d^2G_1}{d\eta^2} - 2\frac{d^2F_0}{d\eta^2} + \sigma_1\frac{d^2G_0}{d\eta^2}\right]D_1 \qquad ,(4.44)$$

$$M_8 \equiv ik\left(\frac{dH_0}{d\eta} + \sigma_1\frac{dF_1}{d\eta} + \sigma_1^2\frac{dG_2}{d\eta}\right)(D_1^2-k^2) - ik\left(\frac{d^3H_0}{d\eta^3} + \sigma_1\frac{d^3F_1}{d\eta^3} + \sigma_1^2\frac{d^3G_2}{d\eta^3}\right) \qquad ,(4.45)$$

The terms M_2, M_4, M_7 disappear when m = 0. However, M_8 does not disappear since H_0 is the $O(\varepsilon)$ correction to the steady state case.

4.4 The Orr-Sommerfeld Problem.

In the expanded form (4.29a) becomes

$$\frac{1}{R}\left[\frac{\partial^4\Phi_0}{\partial\eta^4} - 2k^2\frac{\partial^2\Phi}{\partial\eta^2} + k^4\Phi_0\right] - \frac{dG_0}{d\eta}\left[ik\frac{\partial^2\Phi_0}{\partial\eta^2} - ik^3\Phi_0\right]$$

$$+ ie^{2\sigma_1\beta}\left[\frac{\partial^2\Phi_0}{\partial\eta^2} - k^2\Phi_0\right] + ik\Phi_0\frac{d^3G_0}{d\eta^3} = 0 \qquad ,(4.46)$$

and the boundary conditions are given by (4.29b).

Since σ_1 appears only as a parameter, a solution may be found of the form

$$\Phi_0(\sigma_1,\eta) = A_0(\sigma_1)\, f_0(\sigma_1,\eta) \qquad ,(4.47)$$

The amplitude function A_0 will be considered later. Here, f_0 is a solution to (4.46) for some fixed σ_1. It is normalised arbitrarily,

The function Φ_0 is assumed to be even in η, as this yields the most unstable eigenvalue k (see Lin (1945 I), Lin (1955), and Thomas (1953).

The solution to (4.46) will be based on a "marching scheme", and the details will be considered in Ch.5 when dealing with the numerical techniques.

Defining a real frequency β and fixed σ_1, (4.46) is an eigenvalue in k. It is well known from the theory of homogeneous equations, that a certain characteristic equation must hold for the existence of a non-trivial solution to (4.46). This equation defines an eigen-relation ($k(\sigma_1) = F(\beta_I, R, v)$). There is no known analytic form of this relation, and an approximation is made in which this relation appears as a quartic in k. The roots of this quartic will be found, and the root with the positive real part, (i.e. corresponding to a physical wavenumber) will be chosen as a starting value to solve (4.46) numerically.

Since f_0 is an even function in η, it follows from the general properties of even functions that the boundary conditions of (4.29a) could be replaced by more convenient conditions for all σ_1.

$$\frac{\partial f_0}{\partial \eta} = 0 \; ; \quad \frac{\partial^3 f_0}{\partial \eta^3} = 0 \text{ at } \eta = 0 \qquad ,(4,48a)$$

$$f_0 = 0 \; ; \quad \frac{\partial f_0}{\partial \eta} = 0 \text{ at } \eta = 1 \qquad .(4.48b)$$

For the numerical solution of f_0, let $u_1(\eta)$ and $u_2(\eta)$ be solutions to (4.46) for fixed σ_1, thus

$$f_0(\sigma_1, \eta) = A\, u_1 + B\, u_2 \qquad ,(4.49)$$

where A,B, are arbitrary constants for fixed σ_1.

We define the following boundary conditions for u_1, u_2

$$u_1(0) = 0 \qquad u_2(0) = 1 \qquad ,(4.50a)$$

$$\frac{du_1}{d\eta}(0) = 0 \qquad \frac{du_2}{d\eta}(0) = 0 \qquad ,(4.50b)$$

$$\frac{d^2u_1}{d\eta^2}(0) = 1 \qquad \frac{d^2u_2}{d\eta^2}(0) = 0 \qquad ,(4.50c)$$

$$\frac{d^3u_1}{d\eta^3}(0) = 0 \qquad \frac{d^3u_2}{d\eta^3}(0) = 0 \qquad .(4.50d)$$

The above conditions ensure that u_1, u_2, satisfy the boundary conditions at the centre of the channel. We now expand $u_1(\eta)$, and $u_2(\eta)$ about $\eta = 0$.

$$u_1(\eta) = u_1(0) + \frac{du_1}{d\eta}(0)\frac{\eta}{1!} + \frac{d^2u_1}{d\eta^2}(0)\frac{\eta^2}{2!} + \frac{d^3u_1}{d\eta^3}(0)\frac{\eta^3}{3!} + \frac{d^4u_1}{d\eta^4}(0)\frac{\eta^4}{4!} + \ldots \quad ,(4.51a)$$

$$u_2(\eta) = u_2(0) + \frac{du_2}{d\eta}(0)\frac{\eta}{1!} + \frac{d^2u_2}{d\eta^2}(0)\frac{\eta^2}{2!} + \frac{d^3u_2}{d\eta^3}(0)\frac{\eta^3}{3!} + \frac{d^4u_2}{d\eta^4}(0)\frac{\eta^4}{4!} + \ldots \quad .(4.51b)$$

By substituting u_1 and u_2 into (4.46), the fourth derivatives $\frac{d^4u_1}{d\eta^4}(0)$ and $\frac{d^4u_2}{d\eta^4}(0)$ can be determined by evaluating (4.46) at $\eta = 0$ and

using (4.50a), (4.50b), (4.50c), and (4.50d). Thus

$$\frac{d^4u_1}{d\eta^4}(0) = ikR\frac{dG_0}{d\eta}(0) - iRe^{2\sigma_1}\beta + 2k^2 \qquad ,(4.52)$$

$$\frac{d^4u_2}{d\eta^4}(0) = ik^2Re^{2\sigma_1}\beta - ikR\frac{d^3G_0}{d\eta^3}(0) - ik^3R\frac{dG_0}{d\eta}(0) - k^4 \qquad .(4.53)$$

Hence substituting (4.52), (4.53), into (4.51a) and (4.51b) respectively, we obtain

$$u_1(\eta) = \frac{\eta^2}{2} + \left[ikRdG_0(0) - iR\beta e^{2\sigma_1} + 2k^2\right]\frac{\eta^2}{24} + \ldots \quad ,(4.54)$$

$$u_2(\eta) = 1 + \frac{\eta^4}{24}\left[ik^2R\beta e^{2\sigma_1} - ikRd^3G_0(0) - ik^3RdG_0(0) - k^4\right] + \ldots \quad .(4.55)$$

Now, on substituting the boundary conditions given by (4.48a) and (4.48b) into (4.49) we obtain for fixed σ_1

$$f_0(\sigma_1,1) = A\,u_1(1) + B\,u_2(1) = 0$$

$$\frac{\partial f_0}{\partial \eta}(\sigma_1,1) = A\,\frac{du_1}{d\eta}(1) + B\,\frac{du_2}{d\eta}(1) = 0$$

and for non-trivial values for A and B

$$u_1(1)\,\frac{du_2}{d\eta}(1) - u_2(1)\,\frac{du_1}{d\eta}(1) = 0 \quad .(4.56)$$

Equation (4.56) is the characteristic equation defining the eigen-relation. The approximation is made now when (4.54) and (4.55) are used in (4.56). The method may be criticised fundamentally, since $\eta = 1$ in (4.56), and the original expansions of $u_1(\eta)$ and $u_2(\eta)$ were about $\eta = 0$. Nevertheless, on proceeding, the following quartic in k is obtained.

$$\frac{k^4}{24} + \frac{iRdG_0}{24\,d\eta}k^3 + \left\{\frac{1}{3} - \frac{iR\beta_I}{24}\right\}k^2 + \frac{iR}{6}\left[\frac{1}{4}\frac{d^3G_0}{d\eta^3}(0) + \frac{dG_0}{d\eta}(0)\right]k + 1 - \frac{iR\beta_I}{6} = 0 \quad .(4.57)$$

There is some justification in not expecting (4.57) to be of any practical use, as the approximation is rather severe. It was found however, that the four complex roots predicted by (4.57), gave a rather interesting consistency. In every case considered, there were always three roots with a negative real part, and one root with a positive real part. We were thus able to dismiss the three physically unrealistic roots. In addition, the agreement between the real part of k, (k_r) predicted by the approximation, and correct values of k_r (Eagles 1978) were very good. Many cases were considered and compared before it was felt justified in using this approximation to predict a starting value. The imaginary part of k, (k_i) was not in as good agreement with known values, as k_r, but it appeared that the agreement between the real parts was sufficient to give convergence to the correct eigenvalue. Other methods were in fact tried to estimate a starting value, but often took more iterations and sometimes even converged to the wrong eigenvalue. Graphs of k_r vs. σ_1 and k_i vs. σ_1 will be discussed in Ch.5, and they will illustrate the agreement between the predicted k_r value, by this approximation, and the correct k_r.

4.5 The Amplitude Functions.

The amplitude function A_0 has already been introduced, and in the context of(4.47), it can be interpreted as the amplitude of the stream function along the centre of the channel. To solve for A_0 it is necessary to go to the $O(\varepsilon^{1/2})$ disturbance equation, and use a solvability condition on Φ_1. From the theory of homogeneous linear differential equations a solution for the inhomogeneous stream functions Φ_1 and Φ_2 may be put in the form

$$\Phi_1(\sigma_1,\eta) = f_1(\sigma_1,\eta) + A_1(\sigma_1)\, f_0(\sigma_1,\eta) \qquad ,(4.58)$$

$$\Phi_2(\sigma_1,\eta) = f_2(\sigma_1,\eta) + A_2(\sigma_1)\, f_0(\sigma_1,\eta) \qquad .(4.59)$$

(Ince 1956 pp114-115)

To solve for A_1 it is necessary to got to the $0(\varepsilon)$ disturbance equation, and use a solvability condition on Φ_2, and so on. The convenient normalisation chosen for Φ was

$$\Phi(\sigma_1,0) = 1 \qquad ,(4.60)$$

and this can be equivalently expressed by

$$\Phi_0(\sigma_1,0) = 1 \; ; \; \Phi_1(\sigma_1,0) = 0 \; ; \; \Phi_2(\sigma_1,0) = 0 \qquad .(4.61)$$

If it is desired to interpret A_1, A_2, as being the amplitudes of Φ_1, Φ_2 along the centre of the channel, the normalisations on f_1, and f_2 are obvious. Different normalisations on f_0, f_1, and f_2, merely correspond to different A_0, A_1, and A_2 respectively, but with all physical quantities such as "growth rates", (to be defined later) unaffected by this normalisation (Eagles 1977).

Thus to solve for A_0 (4.47) is substituted into (4.32a) yielding

$$L\Phi_1 = A_0 L_1 \frac{\partial f_0}{\partial \eta} + \frac{dA_0}{d\eta}(L_1 f_0) + A_0 \frac{dk}{d\eta}(L_2 f_0) + A_0(L_3 + L_4) f_0 \qquad .(4.62)$$

To solve (4.32a), it is necessary to consider the adjoint system. Let $\tilde{L}$ be the adjoint operator to L, and let $\tilde{f}_0$ be the adjoint eigenfunction to f_0 . Then it follows that

$$\tilde{L} \equiv \frac{1}{R}(D_1^2 - k^2) + i\left\{\beta_I - \frac{dG_0}{d\eta}k\right\}(D_1^2 - k^2) - 2ikd^2\frac{G_0}{d\eta^2}D_1 \qquad ,(4.63)$$

and

$$\tilde{L}\,\tilde{f}_0 = 0 \qquad ,(4.64a)$$

$$f_0 = \frac{\partial f_0}{\partial \eta} = 0 \text{ on } \eta = \pm 1 \qquad .(4.64b)$$

(c.f.Ince 1956 pp210-214)

It can be shown that, $\int_{-1}^{1} \tilde{f}_0 L\Phi_1 \, d\eta = 0$. Therefore, on multiplying (4.62) by $\tilde{f}_0$ and integrating, the following differential equation in A_0 is obtained

$$\frac{dA_0}{d\sigma_1} + H(\sigma_1)\,A_0 = 0 \qquad ,(4.65a)$$

$$A_0(0) = 1 \qquad .(4.65b)$$

From the normalisation (4.61), (4.65b) follows directly from choosing $f_0(\sigma_1,0) = 1$. The equation for $H(\sigma_1)$ is given by

$$H(\sigma_1) = \frac{(C_2 + C_3 + C_4 + C_5)}{C_1} \qquad ,(4.66)$$

where

$$C_1(\sigma_1) = \int_{-1}^{1} \tilde{f}_0 L_1 f_0 \, d\eta \qquad ,(4.67a)$$

$$C_2(\sigma_1) = \int_{-1}^{1} \tilde{f}_0 L_1 \frac{\partial f_0}{\partial \eta} \, d\eta \qquad ,(4.67b)$$

$$C_3(\sigma_1) = \frac{dk}{d\sigma_1}\int_{-1}^{1} \tilde{f}_0 L_2 f_0 \, d\eta \qquad ,(4.67c)$$

$$C_4(\sigma_1) = \int_{-1}^{1} \tilde{f}_0 L_3 f_0 \, d\eta \qquad ,(4.67d)$$

$$C_5(\sigma_1) = \int_{-1}^{1} \tilde{f}_0 L_4 f_0 \, d\eta \qquad .(4.67e)$$

Thus, (4.65a) can be integrated provided that C_1 does not vanish, which is the case under consideration.
(c.f. Eagles & Weissman 1975)

In the same fashion, A_1 can be found by insisting on a similar solvability condition, i.e. $\int_{-1}^{1} \tilde{f}_0 L \Phi_2 d\eta = 0$. The form of (4.37a) naturally yields a number of further C_i's . By choosing $f_1(\sigma_1, 0) = 0$, then $A_1(0) = 0$. its equation is given by

$$\frac{dA_1}{d\sigma} + H(\sigma_1) A_1 = F(\sigma_1) \qquad ,(4.68a)$$

$$A_1(0) = 0 \qquad ,(4.68b)$$

where

$$\begin{aligned} F(\sigma_1) = {} & i\frac{d^2 A_0}{d\sigma_1^2} C_{25} - \frac{dA_0}{d\sigma_1}(C_{10} + C_{11} + C_{16} - 2iC_{24}) \\ & - A_0(C_{12} + C_{13} + C_{14} + C_{15} + C_{17} + C_{18} + C_{19} \\ & + C_{20} + C_{21} + C_{22} - iC_{23}) \\ & - (C_6 + C_7 + C_8 + C_9) / C_1 \end{aligned} \qquad ,(4.69)$$

and

$$C_6(\sigma_1) = \int_{-1}^{1} \tilde{f}_0 L_1 \frac{\partial f_1}{\partial \sigma_1} \, d\eta \qquad ,(4.70)$$

$$C_7(\sigma_1) = \frac{dk}{d\sigma_1} \int_{-1}^{1} \tilde{f}_0 L_2 f_1 \, d\eta \qquad ,(4.70b)$$

$$C_8(\sigma_1) = \int_{-1}^{1} \tilde{f}_0 L_3 f_1 \, d\eta \qquad ,(4.70c)$$

$$C_9(\sigma_1) = \int_{-1}^{1} \tilde{f}_0 L_4 f_1 \, d\eta \qquad ,(4.70d)$$

$$C_{10}(\sigma_1) = \int_{-1}^{1} \tilde{f}_0 M_1 f_1 \, d\eta \qquad ,(4.70e)$$

$$C_{11}(\sigma_1) = \int_{-1}^{1} \tilde{f}_0 M_2 f_0 \, d\eta \qquad ,(4.70f)$$

$$C_{12}(\sigma_1) = \int_{-1}^{1} \tilde{f}_0 M_1 \frac{\partial f_0}{\partial \sigma_1} \, d\eta \qquad ,(4.70g)$$

$$C_{13}(\sigma_1) = \int_{-1}^{1} \tilde{f}_0 M_2 \frac{\partial f_0}{\partial \sigma_1} \, d\eta \qquad ,(4.70h)$$

$$C_{14}(\sigma_1) = \frac{dk}{d\sigma_1} \int_{-1}^{1} \tilde{f}_0 M_3 f_0 \, d\eta \qquad ,(4.70i)$$

$$C_{15}(\sigma_1) = \frac{dk}{d\sigma_1} \int_{-1}^{1} \tilde{f}_0 M_4 f_0 \, d\eta \qquad ,(4.70j)$$

$$C_{16}(\sigma_1) = \frac{dk}{d\sigma_1} \int_{-1}^{1} \tilde{f}_0 M_5 f_0 \, d\eta \qquad ,(4.70k)$$

$$C_{17}(\sigma_1) = \frac{dk}{d\sigma_1} \int_{-1}^{1} \tilde{f}_0 M_5 \frac{\partial f_0}{\partial \sigma_1} \, d\eta \qquad ,(4.70l)$$

$$C_{18}(\sigma_1) = \int_{-1}^{1} \tilde{f}_0 M_6 f_0 \, d\eta \qquad ,(4.70m)$$

$$C_{19}(\sigma_1) = \int_{-1}^{1} \tilde{f}_0 M_7 f_0 \, d\eta \qquad ,(4.70n)$$

$$C_{20}(\sigma_1) = \int_{-1}^{1} \tilde{f}_0 M_8 f_0 \, d\eta \qquad ,(4.70o)$$

$$C_{21}(\sigma_1) = \int_{-1}^{1} \tilde{f}_0 \left[\frac{d^2 k}{d\sigma_1^2} \left[\frac{4k}{R} + i \frac{dG_0}{d\eta} \right] \right] f_0 \, d\eta \qquad ,(4.70p)$$

$$C_{22}(\sigma_1) = \int_{-1}^{1} \tilde{f}_0 \frac{3}{R} \left[\frac{dk}{d\sigma_1} \right]^2 f_0 \, d\eta \qquad ,(4.70q)$$

$$C_{23}(\sigma_1) = \int_{-1}^{1} \tilde{f}_0 L_2 \frac{\partial^2 f_0}{\partial \sigma_1^2} \, d\eta \qquad ,(4.70r)$$

$$C_{24}(\sigma_1) = \int_{-1}^{1} \tilde{f}_0 L_2 \frac{\partial f_0}{\partial \sigma_1} d\eta \qquad ,(4.70s)$$

$$C_{25}(\sigma_1) = \int_{-1}^{1} \tilde{f}_0 L_2 f_0 \, d\eta \qquad ,(4.70t)$$

The equation for $A_2(\sigma_1)$ can be obtained in the same way. To do this however, would involve going to the $O(\varepsilon^{3/2})$ equation and insisting on the solvability condition $\int_{-1}^{1} f_0 L \Phi_3 d\eta = 0$. Fortunately, it is not necessary to do this to obtain the $O(\varepsilon)$ correction to the "growth rates", which is the next subsection to be dealt with.

4.6 The Growth Rates.

A discussion on the deficiencies of the quasi-parallel approach in determining the "growth-rates" is given by Eagles & Weissman (1975). Quasi-parallel theory only determines whether a wave can grow or decay at a particular point, and not as a function of the downstream variable. Also, it does not deal with the effect that the change in the steady state has on the local "growth". Shen, (1961) gives an intuitive argument as to what "yardstick" could be used to measure the growth or decay of a disturbance. A disturbance which appears to be increasing, might well be decaying, if it is measured relative to a steady state flow which is increasing at a faster rate and vice-versa. (see also Lin (1951)). This intuitive argument suggests, that in the case of measuring the growth of a wave based on a mean kinetic energy density E, a more appropriate measurement, would be based on a relative mean kinetic energy density $\hat{E} = E/E_0$, where E_0 is the

mean kinetic energy density of the steady state flow.

According to quasi-parallel theory, the imaginary part of k (k_i) is small in the unstable region, and may therefore be comparable to $\varepsilon^{1/2}$ or even ε, hence the need to take into account higher order terms.

These terms show how the "growth-rates" also depend on the transverse variable η. They also show that different flow quantities have different flow rates, and the effect of curvature is only realised in higher order terms.

The total physical amplitude of the wave is in terms of the total time-dependent stream function Φ. It can be shown to be

$$\text{amp}\,\Phi = 2\left|\Phi\exp(i(\Theta - \beta t))\right| = 2|\Phi|e^{-\Theta_i} \qquad ,(4.71)$$

where Θ_i is the imaginary part of Θ.

Following Eagles & Weissman, a "growth-rate" based on Φ in the ξ-space is given by

$$GR_\xi(\Phi) = (\text{amp}\Phi)^{-1}\frac{\partial}{\partial\xi}(\text{amp}\Phi) \qquad ,(4.72)$$

and this becomes

$$GR_\xi(\Phi) = -k_i + \varepsilon^{1/2}\frac{\partial}{\partial\sigma_1}(|\Phi|) \qquad .(4.73)$$
$$\frac{}{|\Phi|}$$

It is possible to rewrite (4.73) explicitly in powers of $\varepsilon^{1/2}$, by putting Φ in modulus argument form, ($\Phi = \rho e^{i\delta}$) and using $\frac{\partial}{\partial\sigma_1}(|\Phi|) = \text{Re}\left(\frac{\partial\Phi}{\partial\sigma_1}\right)$
$\frac{}{|\Phi|}$ Φ

where Re(X) is the real part of X, and this yields

$$GR_{\xi}(\Phi) = -k_i + \varepsilon^{1/2}\mathrm{Re}\left(\frac{\partial\Phi_0}{\partial\sigma_1}\Big/\Phi_0\right) + \varepsilon\,\mathrm{Re}\left(\frac{\partial}{\partial\sigma_1}\left(\frac{\Phi_1}{\Phi_0}\right)\right) + \ldots \qquad .(4.74)$$

The total streamwise and transverse disturbance velocities u_ξ, u_η are defined by (2.4) and (2.5) respectively, Here they become

$$u_\xi = \frac{1}{h}\frac{\partial\Phi}{\partial\eta} \qquad ,(4.75a)$$

$$u_\eta = \frac{-1}{h}\frac{\partial\Phi}{\partial\xi} \qquad .(4.75b)$$

Using (4.26) as h, the velocities u_ξ, u_η can be expressed in powers of $\varepsilon^{1/2}$

$$u_\xi = \bar{e}^{\sigma_1}\left(1 - \frac{m\varepsilon^{1/2}\sigma_1^2}{2} + \frac{m^2\varepsilon\,\sigma_1^4}{8} + \ldots\right)\left[e^{i(\Theta-\beta t)}\frac{\partial\Phi}{\partial\eta} + c.c\right] + O(\varepsilon^{3/2}) \qquad ,(4.75c)$$

$$u_\eta = -e^{-\sigma_1}\left(1 - \frac{m\varepsilon^{1/2}\sigma_1^2}{2} + \frac{m^2\varepsilon\,\sigma_1^4}{8} + \ldots\right)\left[e^{i(\Theta-\beta t)}\left\{ik\Phi + \varepsilon^{1/2}\frac{\partial\Phi}{\partial\sigma_1}\right\} + c.c\right] + O(\varepsilon^{3/2}). \qquad (4.75d)$$

The physical amplitudes of these functions can be found, and using (4.72) to define the growth rates

$$GR_\xi(u_\xi) = -k_i + \varepsilon^{1/2}\left[-1 + \mathrm{Re}\left(\frac{\partial^2\Phi}{\partial\sigma_1\partial\eta}\Big/\frac{\partial\Phi}{\partial\eta}\right)\right] - \varepsilon m\sigma_1 + \ldots \qquad ,(4.76a)$$

$$GR_\xi(u_\eta) = -k_i + \varepsilon^{1/2}\left[-1 + \mathrm{Re}\left(\frac{\partial}{\partial\sigma_1}(ik\Phi + \varepsilon^{1/2}\frac{\partial\Phi}{\partial\sigma_1})\Big/(ik\Phi + \varepsilon^{1/2}\frac{\partial\Phi}{\partial\sigma_1})\right)\right] - \varepsilon m\sigma_1 + \ldots \qquad ,(4.76b)$$

Note that (4.76a) and (4.76b) are not strictly in ascending powers of $\varepsilon^{1/2}$ since $\Phi = \Phi_0 + \varepsilon^{1/2}\Phi_1 + \varepsilon\Phi_2 + \ldots$. It is not necessary to quote the explicit forms here. These explicit forms have been established with the purpose of comparing with Eagles and Weissman, and in order to see the extra terms introduced by higher order effects and curvature. It is sufficient and somewhat easier to use (4.76a) and (4.76b) to compute $GR_\xi(u_\xi)$ and $GR_\xi(u_\eta)$ respectively.

We can see that the effect of curvature is implicitly contained in the $O(\varepsilon^{1/2})$ terms by virtue of the fact that all the time-dependent flow quantities for the curved walled case, are different than those for the straight walled case. Comparisons of energy growth rates have also been made, but only the forms derived for computational purposes will be given here.

Following Eagles & Weissman a mean kinetic energy density averaged over time and integrated across the channel is used as a measure for the growth of a wave.

It is necessary to determine the mean square velocities in the streamwise directions, $\overline{u_\xi^2}$ and $\overline{u_\eta^2}$ respectively. We can show from the expressions (4.75c) and (4.75d) that

$$\overline{u_\xi^2} = 2e^{-2\sigma_1}\left(1-m\varepsilon^{1/2}\sigma_1^2+\frac{m^2\varepsilon\sigma_1^4}{2}\right)\left|\frac{\partial\Phi}{\partial\eta}\right|^2 e^{-2\Theta_i} + O(\varepsilon^{3/2}) \qquad ,(4.77a)$$

$$\overline{u_\eta^2} = 2e^{-2\sigma_1}\left(1-m\varepsilon^{1/2}\sigma_1^2+\frac{m^2\varepsilon\sigma_1^4}{2}\right)\left|ik\Phi+\varepsilon^{1/2}\frac{\partial\Phi}{\partial\sigma_1}\right|^2 e^{-2\Theta_i} + O(\varepsilon^{3/2}) \qquad ,(4.77b)$$

thus the mean kinetic energy density (mean kinetic energy density per unit width in the streamwise sense) is given by

$$E = \frac{1}{2}\int_{-1}^{1} h\left(\overline{u_\xi^2} + \overline{u_\eta^2}\right) d\eta \qquad .(4.78)$$

To enable comparison with other growth rates, $GR_\xi(E)$ is defined by

$$GR_\xi(E) = \frac{1}{2}E^{-1}\frac{dE}{d\xi} \qquad .(4.79)$$

From (4.78) we obtain

$$E = e^{-\sigma_1}\, e^{2\Theta_i}\, \left(1 - \frac{m\varepsilon^{1/2}\sigma^2}{2} + \frac{m^2\varepsilon\sigma_1^4}{8}\right) S_1 \qquad ,(4.80)$$

where

$$S_1 = \int_{-1}^{1} \left(\left| \frac{\partial \Phi}{\partial \eta} \right|^2 + \left| ik\Phi + \varepsilon^{1/2} \frac{\partial \Phi}{\partial \sigma_1} \right|^2 \right) d\eta \qquad ,(4.81)$$

thus

$$GR_\xi(E) = -k_i + \varepsilon^{1/2} \left(\frac{-1}{2} + \frac{dS_1}{d\sigma_1} \right) - \frac{\varepsilon m \sigma_1}{2} \qquad .(4.82)$$

Since S_1 contains terms of $O(\varepsilon^{1/2})$ (4.82) is not strictly in ascending powers of $\varepsilon^{1/2}$.

The relative energy is defined by

$$\hat{E} = E/E_0 \qquad ,(4.83)$$

where E_0 is the kinetic energy of the steady state.

$$E_0 = \frac{1}{2} \int_{-1}^{1} h(v_\xi^2 + v_\eta^2)\, d\eta \qquad .(4.84)$$

Here

$$v_\xi = \frac{1}{h} \frac{\partial \Omega}{\partial \eta} \qquad ,(4.85a)$$

and

$$v_\eta = \frac{-1}{h} \frac{\partial \Omega}{\partial \xi} \qquad ,(4.85b)$$

where v_ξ and v_η are the total steady state streamwise and transverse velocities respectively.

By expressing v_ξ and v_η up to $O(\varepsilon)$ we obtain

$$E_0 = e^{-\sigma_1} \left[1 - \frac{m\varepsilon^{1/2}\sigma_1^2}{2} + \frac{m^2\varepsilon\sigma_1^4}{8} \right] \Gamma \qquad ,(4.86)$$

where

$$\Gamma(v, \sigma_1) = \frac{1}{2}\int_{-1}^{1}\left[\left(\frac{dG_0}{d\eta}\right)^2 + \varepsilon^{1/2}2\frac{dG_0}{d\eta}\left(\frac{dF_0}{d\eta} + \sigma_1\frac{dG_1}{d\eta}\right)\right] d\eta \qquad ,(4.87)$$

hence $$\hat{E} = \Gamma^{-1}e^{-2\Theta_i} S_1 \qquad .(4.88)$$

We now define

$$GR_\xi(\hat{E}) = \frac{1}{2}\hat{E}^{-1}\frac{d\hat{E}}{d\xi} \qquad .(4.89)$$

The expression for $GR_\xi(\hat{E})$ can be written as

$$GR_\xi(\hat{E}) = -k_i + \varepsilon^{1/2}\left(\frac{\frac{dS_1}{d\sigma_1}}{2S_1}\right) - \varepsilon\left(\frac{\frac{d\Gamma_2}{d\sigma_1}}{2\Gamma_1}\right) + \ldots \qquad ,(4.90)$$

where

$$\frac{d\Gamma_2}{d\sigma_1} = \int_{-1}^{1}\frac{dG_0}{d\eta}\frac{dG_1}{d\eta}\,d\eta \qquad ,(4.91a)$$

and

$$\Gamma_1 = \frac{1}{2}\int_{-1}^{1}\left(\frac{dG_0}{d\eta}\right)^2 d\eta \qquad .(4.91b)$$

5. Numerical Techniques and Checks.

The inclusion of higher order terms and curvature in the asymptotic development, made most of the programming lengthy and laborious. Nevertheless, in the main it was fairly straight forward. Some difficulties were encountered in the cases of :

(i) The non-linear Jeffery-Hamel equation (4.13a), where an independent numerical solution was attempted.

(ii) The eigenvalue problem, where a routine was written to compute the roots to (4.57), and the appropriate one was chosen as a starting value, to solve the Orr-Sommerfeld problem (4.46).

The techniques and checks carried out, will be discussed in the order they were carried out, so as to give a general picture of the methods employed. Attention will only be given to detail when it is felt necessary.

The following subsections are devoted to the main program and the important subroutines.

5.1. The Main Program.

The main program (CHANNEL) was used to compute the steady state flow quantities $G_0, G_1, G_2, F_0, F_1, H_0$ and hence the total steady state stream function $\Omega(\xi,\eta)$.

An overall programming check was carried out periodically by including a subroutine PINT 2. This merely served to check the amplitude function A_1 directly, and consequently other results involving A_1.

PINT 2 was a lengthy and time consuming program, it was not felt necessary to include it all the time.

Since the stream function $\Omega(\xi,\eta)$ was assumed to be an odd function about $\eta = 0$, it was only necessary to solve (4.13a), and all subsequent computations for $0 \leqslant \eta \leqslant 1$.

The independent scheme used to determine G_0 was to expand G_0 as a Taylor series in powers of v.

$$G_0(\eta) = w_0(\eta) + w_1(\eta)v + \frac{w_2(\eta)v^2}{2!}+\ldots \qquad ,(5.1)$$

w_0, w_1, w_2, etc were called the perturbation functions.

Since G_0 was chosen to be an odd function, the boundary conditions in (4.13a) can be rewritten as

$$\left.\begin{aligned} &G_0(0) = 0 \;;\quad G_0(1) = 1 \\ &\frac{d^2G_0(0)}{d\eta^2} = 0 \;;\quad \frac{dG_0(0)}{d\eta} = 0 \end{aligned}\right\} \qquad .(5.2)$$

Substituting (5.1) into (4.13a) and comparing powers of v, the following formula was obtained for each perturbation function w_r

$$\frac{d^4w_r}{d\eta^4} = \sum_{s=0}^{r}\left[\frac{r!}{(r-s-1)!s!}\,\frac{dw_s}{d\eta}\,\frac{d^2w_{r-s-1}}{d\eta^2}\right] \qquad ,(5.3)$$

which describes a finite set of linear equations . They were expressed

in matrix form using central difference formulae of $O(h^4)$ for each perturbation function.

$$\underset{\sim}{A}.\underset{\sim}{w_m} = \underset{\sim}{B} \qquad (0 \leqslant m \leqslant r) \quad ,(5.4)$$

The construction of the constant band structured matrix $\underset{\sim}{A}$, presented some initial difficulties. These difficulties were typically near, or on the boundary. In expressing the fourth derivatives of various w_r's near, or on the boundary, three extra points are introduced because of the central finite difference formulae. Backward differences may be used as an alternative, but it was found the perturbation scheme defined by (5.1), did not converge when this was done. The extra points could however be expressed in terms of points on or inside the boundary. A way of doing this is to introduce some additional known conditions on the boundary, namely

$$\frac{dw_m}{d\eta} = 0 \; ; \; \frac{d^4w_m}{d\eta^4} = 0 \; ; \; \frac{d^5w_m}{d\eta^5} = 0 \qquad .(5.5)$$

The dilemma of (5.5) was that, if difference formulae of $O(h^4)$ were used, a fourth point was introduced. In fact it is possible to use central difference formulae of different orders of accuracy near, or on the boundary, so long as they are derived from the same polynomial (Croll 1978). This was in fact done, and by using a standard Harwell

subroutine (MA07BD) for solving systems of linear equations , the perturbation functions $\underset{\sim}{w}_m$ were computed. They were found to agree to four significant figures with a number of correct results computed by Eagles (1978) in the range of v used. Part of a table is reproduced in TABLE 1 below, of some exact results using Elliptic functions, (Fraenkel 1963 II) against this present scheme for a modest range of v. They represent the Jeffery-Hamel profiles evaluated at the centre of the channel (η=0). Although other methods are available, this was found convenient to use, and in fact can be extended to solve other flow quantities (G_1, G_2, F_0, F_1, H_0) for the straight walled, and curved walled channel.

v	Elliptic	Perturbation
3.15	1.810	1.808
3.572	1.856	1.856
3.904	1.926	1.926
4.093	1.973	1.973
4.295	2.031	2.031
4.712	2.188	2.188
5.102	2.429	2.429

Jeffery-Hamel profiles at η =0, by Elliptic functions, and the present perturbation scheme, for various v.

TABLE 1.

In order to solve for G_1, G_2, F_0, F_1, H_0 it was necessary to construct a new L.H.S involving known derivatives of G_0, and applying the same technique at the boundary as before. The same matrix routine was utilised to solve the new set of equations. Thus the steady state stream function $\Omega(\xi, \eta)$ was computed.

5.2 The Eigenvalue Problem.

In order to solve the Orr-Sommerfeld problem it was necessary to solve (4.57). This quartic in k with complex coefficients yielded four complex roots. Three of these always had a negative k_r and one always had a positive k_r . The quartic was reduced to a quadratic in two stages. At each stage a Newton-Raphson technique applied to polynomials with complex coefficients was used (Ralston 1965). The initial guess to start the Newton-Raphson technique was the same in all cases. The root chosen to act as an initial guess in the Orr-Sommerfeld problem however, was that root with positive k_r.

The agreement between this latter root and a known eigenvalue became closer further in the streamwise direction. The graphs in FIGS-2a,2b show how close this was for a particular case. In fact the scheme to solve the Orr-Sommerfeld problem was started off at a value of σ_1 corresponding to decay. This value of σ_1 was always predetermined from the parameters v and β , which define the Jeffery-Hamel profile and frequency respectively.

With this initial guess for some fixed σ_1, it was possible to consider a "marching scheme" in which u_1, u_2, defined by (4.49) were computed. This "marching scheme" was really a Runga-Kutta method of order four.

The initial conditions for u_1, u_2, were defined explicitly by (4.50a) to (4.50d), and these were consistent with (4.48a). The final values at $\eta=1$, of f_0 and $\tilde{f}_0$ were invariant to changes in (4.50a) and (4.50c) as long as (4.50b) and (4.50d) were not violated.

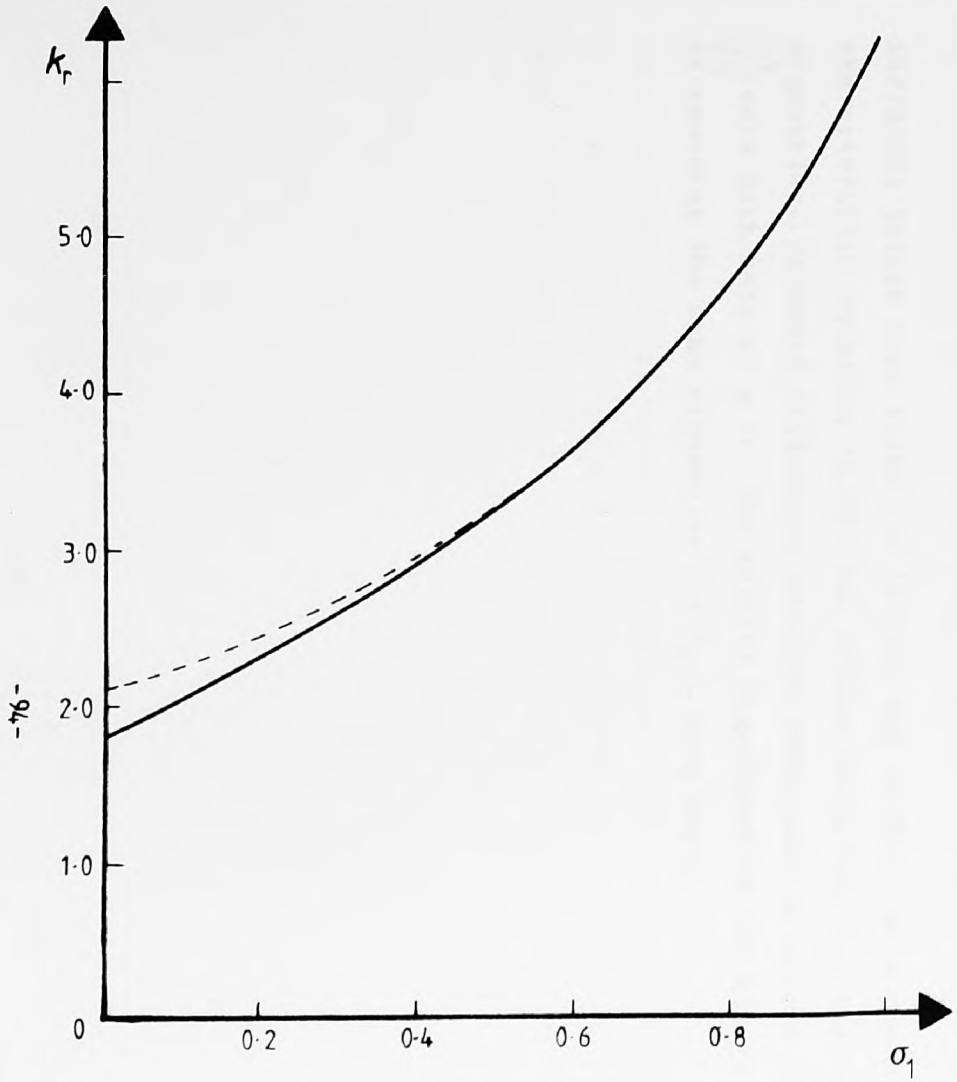

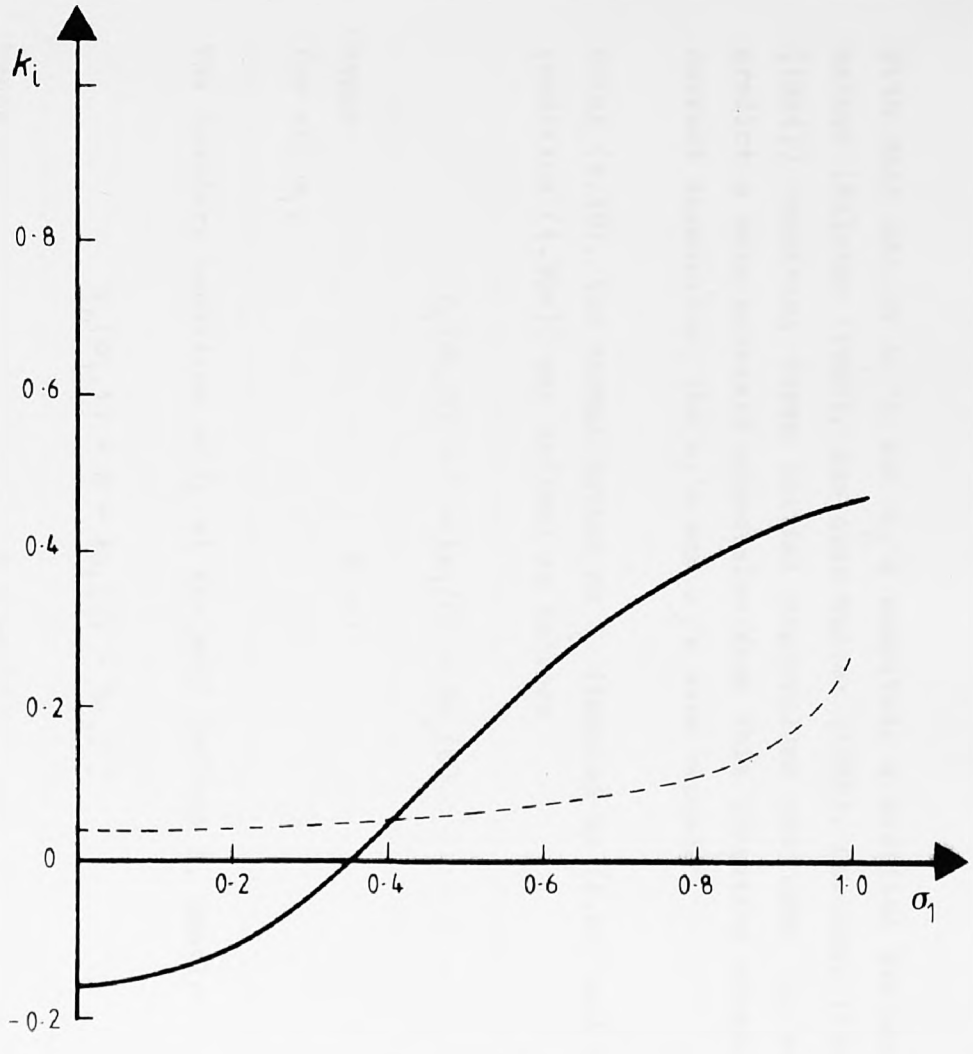

The approximate eigenvalue compared with the correct one, for v=4·093; R=100; β=1·5.
——— Eagles , ------ present analysis.

FIG-2a

FIG-2b

With each set of u_1's and u_2's computed, a modified Newton-Raphson method (Ralston (1965), see also Muller (1956), Ostrowski (1960), Traub (1964)) requiring three initial eigenvalues was used in order to predict a more accurate eigenvalue. When this iterative scheme gave the correct eigenvalue, the u_1's and u_2's were recorded.

Using (4.49), the normalisation on f_0 (imposed by (4.60) and the initial condition (4.50a)) was defined as follows

$$f_0(\sigma_1, 0) = 1 = Au_1(0) + Bu_2(0) \qquad ,(5.6a)$$

hence

$$B = 1 \qquad ,(5.6b)$$

for all σ_1.

The boundary condition on f_0 at the wall defines A, namely

$$f_0(\sigma_1, 1) = 0 = Au_1(1) + Bu_2(1) \qquad ,(5.6c)$$

hence

$$A = \frac{-u_2(1)}{u_1(1)} \qquad .(5.6d)$$

Different values were tried for (4.50a) and (4.50c) as a check, and the characteristic equation (4.56) was always satisfied for the recorded eigenvalue. Backward difference formulae were used to ensure that $\frac{\partial f_0}{\partial \eta}$, $\frac{\partial \tilde{f}_0}{\partial \eta}$ were both zero at $\eta = 1$. The adjoint eigenfunction was always computed by assuming the same eigenvalue for f_0. As a check,

the adjoint problem, ((4.46a),(4.46b)) was solved first, and the resulting eigenvalue used as an alternative method for computing f_0 . These two schemes always agreed for the cases considered. All these checks and comparisons so far were made with numerous correct results supplied by Eagles (1978), and this validated the work.

5.3 The Amplitude Function A_0.

To determine the amplitude function A_0 , the C_i's defined by (4.67a) to (4.67e) were computed. The assumed symmetric properties of $f_0(\eta)$, made it possible for the integration to be carried out from $\eta = 0$ to $\eta = 1$ using a marching Simpson's rule.

From (4.65a) it is possible to write $A_0(\sigma_1)$ as an exact integral.

$$A_0(\sigma_1) = \exp\left[-\int_0^{\sigma_1} H(s)\, ds\right] \qquad .(5.7)$$

Since σ_1 appears in the limit, it was not possible to use Simpson's rule immediately until $A_0(\sigma_1)$ was defined for at least two values of σ_1 ($\sigma_1 = 0$ and $\sigma_1 = h$, where h is the step). As we already know $A_0(0)$ from (4.65b), it remains to determine $A_0(h)$. A formula was used in terms of H(s), namely

$$A_0(h) = \exp\left[-\int_0^h H(s)\, ds\right] = \exp\left[\frac{-h}{24}\left(9H(0)+19H(1)-5H(2)+H(3)\right)\right] \qquad .(5.8)$$

For subsequent values of σ_1 , Simpson's rule was used, and the results were checked against Eagles's (1978) results for the straight walled channel. They were found to agree to at least four significant figures.

Following Eagles & Weissman (1975), an alternative method was used to compute C_1, C_2, and C_3 by taking the derivative of the equation $Lf_0=0$. It is possible to show

$$L\left(\frac{\partial f_0}{\partial \sigma_1}\right) = \frac{idkL_1 f_0}{d\sigma_1} - \frac{id\beta_I}{d\sigma_1}(D_1^2-k^2)f_0 \qquad ,(5.9)$$

and by using the solvability condition $\int_{-1}^{1} \tilde{f}_0 L\left(\frac{\partial f_0}{\partial \sigma_1}\right) d\eta = 0$ it follows that

$$0 = \frac{idk}{d\sigma_1}\int_{-1}^{1} \tilde{f}_0 L_1 f_0 \, d\eta - \frac{id\beta_I}{d\sigma_1}\int_{-1}^{1} \tilde{f}_0 (D_1^2-k^2) f_0 \, d\eta$$

Hence using (4.67a) and (4.31)

$$C_1(\sigma_1) = \left[2\beta_I \int_{-1}^{1} \tilde{f}_0 (D_1^2-k^2) f_0 \, d\eta\right] \Big/ \frac{dk}{d\sigma_1} \qquad .(5.10)$$

Thus $C_1(\sigma_1)$ was computed using (5.10) and checked with $C_1(\sigma_1)$ given by (4.67a).

On taking the total derivative of (5.9) w.r.t σ_1, and using the solvability condition $\int_{1}^{1} \tilde{f}_0 L \frac{\partial^2 f_0}{\partial \sigma_1^2} d\eta = 0$, it is possible to show after a little manipulation

$$C_2(\sigma_1) + C_3(\sigma_1) = \left[2\beta_I\left(\int_{-1}^{1} \tilde{f}_0 (D_1^2-k^2)\frac{\partial f_0}{\partial \sigma_1} d\eta - 2k\frac{dk}{d\sigma_1}\int_{-1}^{1} \tilde{f}_0 f_0 \, d\eta\right)\right] \Big/ \frac{dk}{d\sigma_1}$$

$$+ C_1\left[\frac{2dk}{d\sigma_1} - \frac{d^2k}{d\sigma_1^2}\right] \Big/ \frac{2dk}{d\sigma_1} \qquad .(5.11)$$

Thus $C_2(\sigma_1) + C_3(\sigma_1)$ were computed using (5.11) and were checked against (4.67b) and (4.67c). The results obtained using (5.10) and (5.11) agreed with the previous set, and hence A_0 was identical by both schemes. This provided another useful check on the work so far.

5.4 The Particular Integral f_1.

Having now solved for A_0 and f_0 it was possible to rewrite (4.32a), by substituting $\Phi_0 = A_0 f_0$. The resulting equation has already been given in abbreviated form by (4.62).

An identical Runga-Kutta scheme already used in the eigenvalue problem was employed, and this inhomogeneous system was solved by formulating the problem in the following way.

It is possible to write the solution for f_1, with fixed σ_1, as

$$f_1(\sigma_1,\eta) = A\, u_1(\eta) + B\, u_2(\eta) + u_3(\eta) \qquad ,(5.12)$$

(Ince 1956 pp114-115) where u_1, u_2, are the solutions to the homogeneous problem (4.46) as before, and u_3 is a particular integral to (4.62). The conditions on the wall of the channel for f_1 yield

$$f_1(\sigma_1,1) = 0 = A' u_1(1) + B' u_2(1) + u_3(1) \qquad ,(5.13a)$$

$$\frac{\partial f_1}{\partial \eta}(\sigma_1,1) = 0 = A' \frac{du_1}{d\eta}(1) + B' \frac{du_2}{d\eta}(1) + \frac{du_3}{d\eta}(1) \qquad ,(5.13b)$$

and a unique solution for A', B' only exist if and only if

$$u_1(1) \frac{du_2}{d\eta}(1) - u_2(1) \frac{du_1}{d\eta}(1) \neq 0.$$

On the other hand, to ensure a non-trivial solution for f_0, (4.56) was a necessary condition. Therefore (5.13a) and (5.13b) are not independent. In fact an infinity of solutions exists. To find a particular solution, B was chosen to be zero and therefore

$$A' = \frac{-u_3(1)}{u_1(1)} = \frac{-\frac{du_3(1)}{d\eta}}{\frac{du_1(1)}{d\eta}} \qquad ,(5.14)$$

which is an essential condition. If (5.14) is satisfied, it does provide not only a check on f_1, but moreover it ensures that A_0 is correct.

In using the Runga-Kutta scheme to find f_1, similar conditions were imposed on u_1 and u_3, as those given by (4.50a) to (4.50d). The scheme had to be modified for this inhomogeneous system, but on the whole the subroutine PINT 1 was written along the same lines as that routine (EIGEN) which solved f_0 and $\tilde{f}_0$.

At this stage it was felt necessary to thoroughly test PINT 1. There are no known values of f_1 to compare with, as Eagles & Weissman (1975) did not compute f_1 for their straight walled problem.

Extensive variations in the parameters were tested to ensure (5.14) was always satisfied. Checks were also carried out to ensure that $\frac{\partial f_1}{\partial \eta} = 0$ at $\eta = 1$ for various values of σ_1 . These tests proved to be conclusive in validating the work so far.

5.5 The Amplitude Function A_1.

The scheme to compute A_1 was identical to that of A_0. The numerous C_i's defined by (4.70a) to (4.70t), were computed first in order to define $F(\sigma_1)$ (see (4.68a). It can be shown that (4.68a) yields

$$A_1(\sigma_1) = A_0(\sigma_1)\int_0^1 \frac{F(s)ds}{A_0(s)} \qquad .(5.15)$$

This simple exact form made the computation of $A_1(\sigma_1)$ fairly straight forward, once $F(\sigma_1)$ was computed and stored.

One possible way of checking A_1 is to recall our original interpretation of it. It was thought of as the amplitude of Φ_1 along the centre of the channel. We assume $f_0(\sigma_1,0) = 1$, (i.e. the arbitrary normalisation for f_0) and note that from (4.58) and (4.61)

$$0 = f_1(\sigma_1,0) + A_1(\sigma_1) \qquad .(5.16)$$

The explicit dependence of A_1 on f_1 appears here and also in the equation of A_1. We can see that different normalisations of $f_1(\sigma_1,0)$ would correspond to a different $f_1(\sigma_1,\eta)$ and hence a different $A_1(\sigma_1)$.

Since this normalisation (previously $f_1(\sigma_1,0) = 0$, hence $A_1(0)\neq 0$)is also arbitrary, one check on $A_1(\sigma_1)$ would be to compare Φ_1's for different normalisations on $f_1(\sigma_1,0)$. Another independent check and just as conclusive, would be to compute f_2 and satisfy the essential condition

at the wall (similar to that defined by (5.14)). The latter check was in fact the one undertaken, and it is briefly described below.

5.6 The Particular Integral f_2.

The equation of f_2 in abbreviated form, is given by (4.37a). The explicit form which was used to compute f_2 was obtained by substituting $\Phi_0 = A_0 f_0$ and $\Phi_1 = f_1 + A_1 f_0$. Its length prohibits its inclusion here. The experience of computing f_1, and the difficulties encountered made it easier to formulate the computing problem for f_2.

The essential condition required to validate f_2, and moreover A_1, is obtained as before, namely

$$\frac{-u_4(1)}{-u_1(1)} = \frac{-\frac{du_4(1)}{d\eta}}{\frac{du_1(1)}{d\eta}} \qquad ,(5.17)$$

where $u_4(\eta)$ is a particular integral to the equation satisfied by f_2. Once again, extensive variations to the parameters were tested to ensure (5.17) was always satisfied

The number of η values that f_2 was computed for here, were half those computed for f_0 and f_1. In order to compute f_2 for the same number of η values, it would have been necessary to interpolate the values of a great number of functions at their midpoints, whereas it was simpler to halve the steps in the Runga-Kutta routine for the case of f_2. We do not need f_2 for the growth rates.

The checks carried out , (characterised by (5.17)) proved conclusive in all cases, and once more, backward difference formulae were used to check further that the condition $\frac{\partial f_2}{\partial \eta} = 0$ at $\eta = 1$, was satisfied.

5.7 The Growth Rates.

The growth rate terms computed, include $GR_\xi(\Phi)$, $GR_\xi(E)$, and two measures of $GR_\xi(\hat{E})$. One measure was that already given by (4.89), and the other excluded the effect of $O(\varepsilon)$, but included curvature implicitly.

It can be shown that (4.90) reduces to

$$GR_\xi(\hat{E}) = -k_i + \varepsilon^{1/2}\left[\mathrm{Re}\left(\frac{dA_0}{d\sigma_1}\right)_{A_0} + \frac{dP}{d\sigma_1}\frac{}{2P}\right] \qquad ,(5.18)$$

where

$$P(\sigma_1) = \int_{-1}^{1}\left(\left|\frac{\partial f_o}{\partial \eta}\right|^2 + |k|^2|f_o|^2\right)d\eta \qquad .(5.19)$$

Here (5.18) compares directly with Eagles & Weissman (1975 p253), but includes the effect of curvature from which the straight walled case can easily be retrieved.

In order to compute $GR_\xi(\Phi)$ and $GR_\xi(E)$ using (4.73) and (4.82), it was necessary to define and store Φ. Thus, once S_1 had been computed it was an easy task to compute $GR_\xi(\Phi)$, $GR_\xi(E)$, and $GR_\xi(\hat{E})$. All these were compared with $-k_i$, the quasi-parallel prediction for the growth rates. All integrals were determined by using Simpson's rule.

5.8 Parametric Studies for the Steady State Problem.

This part of the work was initiated with a view to answering the following questions :

(i) How accurate is the perturbation analysis given by equation (5.1) which solves for G_0 ? In particular, how many perturbation functions (w_r) were necessary for convergence ? How many η steps were necessary to ensure convergence for the functions G_1, G_2, F_0, F_1, H_0?

(ii) How far can we go in the streamwise direction so that that the asymptotic development given by (4.12) can be applied with confidence ?

The answers to case (i) were obtained by using four significant figures as a criterion for convergence. Some results have already been compared to four significant figures in TABLE 1.

We took v = 5 in case (i), fixed the number of η steps, and varied the number of perturbation functions to be computed. We can consider the results given in TABLE 2 to be the worst possible cases, and reference to it shows convergence to four significant at 64 perturbation terms for $G_0(.5)$ and $G_0'(.5)$, but not for $G_0''(.5)$ or $G_0'''(.5)$. The criterion of convergence was not too difficult to satisfy near the centre, or near the walls of the channel for a smaller number of perturbation terms. Thus η = 0.5 was chosen for evaluation. Note that G_0 does not depend on curvature, also the no slip condition is satisfied everywhere.

v = 5.0	80 steps of η				
Perturbation Terms	$G_0(.5)$	$G_0'(.5)$	$G_0''(.5)$	$G_0'''(.5)$	$G_0'(1)$
8	0.856785	0.892198	-3.505546	4.112094	0.0
16	0.873550	0.859079	-3.664425	5.208263	0.0
32	0.878250	0.849729	-3.707526	5.510530	0.0
40	0.876610	0.849011	-3.710787	5.533522	0.0
48	0.878742	0.848749	-3.711974	5.541906	0.0
56	0.878792	0.848648	-3.712430	5.545129	0.0
64	0.878813	0.848607	-3.712612	5.546515	0.0

Results of G_0 and some derivatives at $\eta=.5$, G_0' at the wall, showing convergence to 4 sig.fig. for 64 perturbation terms and for 80 η steps, with v=5.0, in a straight walled channel.

TABLE 2.

In fact 64 perturbation terms were chosen, and this number was used to determine the optimum number of η steps required for convergence.

The case of G_0 is given for various η steps in TABLE 3., where clearly 40η steps are sufficient for convergence. Nevertheless, the other functions G_1, G_2, F_0, F_1, H_0 required progressivly more η steps to achieve convergence. The no-slip condition was also becoming more difficult to satisfy with each function. The worst case is given in TABLE 4. Where H_0 converges for 70 η steps. It was covenient to consider $\eta=.6$. All the subsequent work was run on the basis of 64 perturbation terms and 80 steps. Thus, once G_0, G_1, G_2, F_0, F_1, and H_0 were computed, it was possible, and sufficient to store the values of these functions and their derivatives for just half the number of η steps in the rest of the program, using each alternate value.

v = 5.0, 64 perturbation terms					
Number of η steps	$G_0(.6)$	$G_0'(.6)$	$G_0''(.6)$	$G_0'''(.6)$	$G_0'(1)$
20	0.946175	0.509933	-3.030069	7.844196	-0.000012
30	0.946156	0.509661	-3.029546	7.848162	0.0
40	0.946152	0.509614	-3.029455	7.848649	0.0
50	0.946151	0.509602	-3.029430	7.848763	0.0
60	0.946151	0.509597	-3.029421	7.848800	0.0
70	0.946151	0.509595	-3.029417	7.848815	0.0
80	0.946151	0.509594	-3.029415	7.848822	0.0

Results of G_0 and some derivatives at η=.6, G_0' at the wall, showing convergence to 5 sig.fig. for 80 η steps and 64 perturbation terms, with v=5, for a straight walled channel.

TABLE 3.

v = 5.0, 64 perturbation terms m = 1.0					
Number of η steps	$H_0(.6)$	$H_0'(.6)$	$H_0''(.6)$	$H_0'''(.6)$	$H_0'(1)$
20	3.041040	-9.745376	-16.160815	212.483875	0.015304
30	3.011692	-9.642115	-16.079510	209.804742	0.002996
40	3.006590	-9.624146	-16.065167	209.333534	0.000946
50	3.005175	-9.619519	-16.061159	209.202239	0.000387
60	3.004662	-9.617354	-16.059703	209.154608	0.000187
70	3.004442	-9.616576	-16.059074	209.134069	0.000101
80	3.004334	-9.616197	-16.058766	209.124049	0.000059

Results of H_0 and some derivatives at η=.6, H_0' at the wall, showing convergence to 4 sig.fig. for 80 η steps and 64 perturbation terms, with v=5, for a curved walled channel.

TABLE 4.

We now come to the case (ii). Here an attempt is made to estimate the magnitude of the ommited $O(\varepsilon^{3/2})$ term in the steady state case. The most direct way to do this is to obtain the equation for $\Omega(\sigma,\eta;v,m)$, where

$$\Omega(\sigma,\eta;v,m)=\Omega_0(\sigma,\eta;v,m)+\varepsilon^{1/2}\Omega_1(\sigma,\eta;v,m)+\varepsilon\,\Omega_2(\sigma,\eta;v,m)$$
$$+\varepsilon^{3/2}\Omega_3(\sigma,\eta;v,m)+\ldots \qquad .(5.20)$$

Recalling the original scheme, we substitute (5.20) into (2.18a) and compare coefficients of powers of $\varepsilon^{1/2}$. We obtain

$$\frac{\partial^4\Omega_3}{\partial\eta^4}+2v(1+m\sigma)\frac{\partial}{\partial\eta}\left(\frac{\partial\Omega_0}{\partial\eta}\frac{\partial\Omega_3}{\partial\eta}\right)=v\left(\frac{\partial\Omega_0}{\partial\eta}\frac{\partial^3\Omega_2}{\partial\sigma\partial\eta^2}+\frac{\partial\Omega_1}{\partial\eta}\frac{\partial^3\Omega_1}{\partial\sigma\partial\eta^2}+\frac{\partial\Omega_2}{\partial\eta}\frac{\partial^3\Omega_0}{\partial\sigma\partial\eta^2}\right.$$
$$-\frac{\partial\Omega_0}{\partial\sigma}\frac{\partial^3\Omega_2}{\partial\eta^3}-\frac{\partial\Omega_1}{\partial\sigma}\frac{\partial^3\Omega_1}{\partial\eta^3}-\frac{\partial\Omega_2}{\partial\sigma}\frac{\partial^3\Omega_0}{\partial\eta^3}$$
$$\left.-2(1+m\sigma)\left(\frac{\partial\Omega_1}{\partial\eta}\frac{\partial^2\Omega_2}{\partial\eta^2}+\frac{\partial\Omega_2}{\partial\eta}\frac{\partial^2\Omega_1}{\partial\eta^2}\right)\right)$$
$$-4(1+m\sigma)^2\frac{\partial^2\Omega_1}{\partial\eta^2}+4(1+m\sigma)\frac{\partial^3\Omega_0}{\partial\sigma\partial\eta^2}$$
$$-m\eta\frac{\partial^3\Omega_0}{\partial\eta^3} \qquad ,(5.21a)$$

and
$$\Omega_3(\sigma,\pm1)=0=\frac{\partial\Omega_3}{\partial\eta}(\sigma,\pm1) \qquad .(5.21b)$$

Continuing, $\Omega_0,\Omega_1,\Omega_2$, and Ω_3 are written in a more suitable form with Ω_1 and Ω_2 as before, and Ω_0 and Ω_3 given by

$$\Omega_0(\sigma,\eta;v,m)=G_0(\eta;v)+\varepsilon^{1/2}\sigma_1G_1(\eta;v,m)+\varepsilon\,\sigma_1^2G_2(\eta;v,m)$$
$$+\varepsilon^{3/2}\sigma_1^3G_3(\eta;v,m)+\ldots \qquad ,(5.22)$$

and
$$\Omega_3(\sigma,\eta;v,m)=E_{00}(\eta;v,m)+\ldots \qquad ,(5.23)$$

thus the total steady state stream function $\Omega(\xi,\eta;v,m)$ becomes

$$\Omega(\xi,\eta;v,m) = G_0+\varepsilon^{1/2}(F_0+\sigma_1 G_1) + \varepsilon(H_0+\sigma_1 F_1+\sigma_1^2 G_2) + \varepsilon^{3/2}(E_{00}+\sigma_1 H_1+\sigma_1^2 F_2+\sigma_1^3 G_3)+\ldots \quad .(5.24)$$

The equations for G_3, F_2, H_1, and E_{oo} are obtained as before, and their equations are given here for reference.

$$\frac{d^4G_3}{d\eta^4} + 2vd\frac{d}{d\eta}\left(\frac{dG_0}{d\eta}\frac{dG_3}{d\eta}\right) = -2vd\frac{dG_1}{d\eta}\frac{d^2G_2}{d\eta^2} - 2vd\frac{dG_2}{d\eta}\frac{d^2G_1}{d\eta^2} - 2vmd\frac{dG_0}{d\eta}\frac{d^2G_2}{d\eta^2} - 2vmd\frac{dG_1}{d\eta}\frac{d^2G_1}{d\eta^2} - 2vmd\frac{dG_2}{d\eta}\frac{d^2G_0}{d\eta^2} \quad ,(5.25a)$$

$$G_3 = 0 \; ; \; \frac{dG_3}{d\eta} = 0 \text{ at } \eta = \pm 1 \quad .(5.25b)$$

$$\frac{d^4F_2}{d\eta^4} + 2vd\frac{d}{d\eta}\left(\frac{dG_0}{d\eta}\frac{dF_2}{d\eta}\right) = v\left(3d\frac{dG_0}{d\eta}\frac{d^2G_3}{d\eta^2} + 2d\frac{dG_1}{d\eta}\frac{d^2G_2}{d\eta^2} + d\frac{dG_2}{d\eta}\frac{d^2G_1}{d\eta^2} - 3G_3\frac{d^3G_0}{d\eta^3} - 2G_2\frac{d^3G_1}{d\eta^3} - G_1\frac{d^3G_2}{d\eta^3} - 2d\frac{dG_1}{d\eta}\frac{d^2F_1}{d\eta^2} - 2d\frac{d^2G_1}{d\eta^2}\frac{dF_1}{d\eta} - 2d\frac{dG_2}{d\eta}\frac{d^2F_0}{d\eta^2} - 2d\frac{d^2G_2}{d\eta^2}\frac{dF_0}{d\eta} - 2md\frac{dG_0}{d\eta}\frac{d^2F_1}{d\eta^2} - 2md\frac{d^2G_0}{d\eta^2}\frac{dF_1}{d\eta} - 2md\frac{dG_1}{d\eta}\frac{d^2F_0}{d\eta^2} - 2md\frac{d^2G_1}{d\eta^2}\frac{dF_0}{d\eta}\right) \quad ,(5.26a)$$

$$F_2 = 0 \; ; \; \frac{dF_2}{d\eta} = 0 \text{ at } \eta = \pm 1 \quad ,(5.26b)$$

$$\frac{d^4H_1}{d\eta^4} + 2vd\frac{}{d\eta}\left(\frac{dG_0}{d\eta}\frac{dH_1}{d\eta}\right) = v\left(2d\frac{dG_0}{d\eta}\frac{d^2F_2}{d\eta^2} + d\frac{dG_1}{d\eta}\frac{d^2F_1}{d\eta^2} + 2d\frac{dF_0}{d\eta}\frac{d^2G_2}{d\eta^2} + d\frac{dF_1}{d\eta}\frac{d^2G_2}{d\eta^2}\right.$$

$$- 2G_2\frac{d^3F_0}{d\eta^3} - G_1\frac{d^3F_1}{d\eta^3} - 2F_2\frac{d^3G_0}{d\eta^3} - F_1\frac{d^3G_1}{d\eta^3}$$

$$- 2d\frac{dG_1}{d\eta}\frac{d^2H_0}{d\eta^2} - 2d\frac{d^2G_1}{d\eta^2}\frac{dH_0}{d\eta} - 2d\frac{dF_0}{d\eta}\frac{d^2F_1}{d\eta^2} - 2d\frac{dF_1}{d\eta}\frac{d^2F_0}{d\eta^2}$$

$$\left. - 2md\frac{dG_0}{d\eta}\frac{d^2H_0}{d\eta^2} - 2md\frac{d^2G_0}{d\eta^2}\frac{dH_0}{d\eta} - 2md\frac{dF_0}{d\eta}\frac{d^2F_0}{d\eta^2}\right)$$

$$- 4d\frac{d^2G_1}{d\eta^2} - 8md\frac{d^2G_0}{d\eta^2} \qquad ,(5.27)$$

$$H_1 = 0 \; ; \; \frac{dH_1}{d\eta} = 0 \quad \text{at } \eta = \pm 1 \qquad ,(5.27b)$$

$$\frac{d^4E_{00}}{d\eta^4} + 2vd\frac{}{d\eta}\left(\frac{dG_0}{d\eta}\frac{dE_{00}}{d\eta}\right) = v\left(\frac{dG_0}{d\eta}\frac{d^2H_1}{d\eta^2} + \frac{dF_0}{d\eta}\frac{d^2F_1}{d\eta^2} + \frac{dH_0}{d\eta}\frac{d^2G_1}{d\eta^2} - G_1\frac{d^2H_0}{d\eta^2} - F_1\frac{d^2F_0}{d\eta^2}\right.$$

$$\left. - H_1\frac{d^3G_0}{d\eta^3} - 2d\frac{dF_0}{d\eta}\frac{d^2H_0}{d\eta^2} - 2d\frac{dH_0}{d\eta}\frac{d^2F_0}{d\eta^2}\right)$$

$$+ 4d\frac{d^2F_0}{d\eta^2} + 4d\frac{d^2G_1}{d\eta^2} - m\eta d\frac{d^3G_0}{d\eta^3} \qquad ,(5.28a)$$

$$E_{00} = 0 \; ; \; \frac{dE_{00}}{d\eta} = 0 \quad \text{at } \eta = \pm 1 \qquad .(5.28b)$$

In anticipation of the problem of satisfying the no-slip condition for the previous functions G_0 to H_0, it was found necessary to increase the number of η steps. Consequently 120 η steps were used to compute these additional functions. After computing these functions it was possible

to determine the total steady state stream function Ω up to and including the $0(\varepsilon^{3/2})$ term, and hence a measure of the magnitude of this term.

We would like to know how far in the streamwise direction we can go before the $0(\varepsilon^{3/2})$ terms become large enough to be included in the analysis. A plot is given in FIG-3 which clearly justifies the original asymptotic development. Even up to $\sigma_1 = 2.0$, the maximum observed differences amount to 1%.

The $0(\varepsilon^{3/2})$ terms increase with larger values of v and the worst possible case of $v = 4.71$ is given in FIG-4a and FIG-4b. The maximum observed differences amount to approximately 4% and 7% at $\sigma_1 = 0.0$ and $\sigma_1 = 1.6$ respectively.

The work on the whole verified the asymptotic analysis and justified the exclusion of the $0(\varepsilon^{3/2})$ terms, since the range of v was always $\leqslant 4.71$ and that the distance gone in the streamwise direction was invariably characterised by $\sigma_1 \leqslant 1.6$.

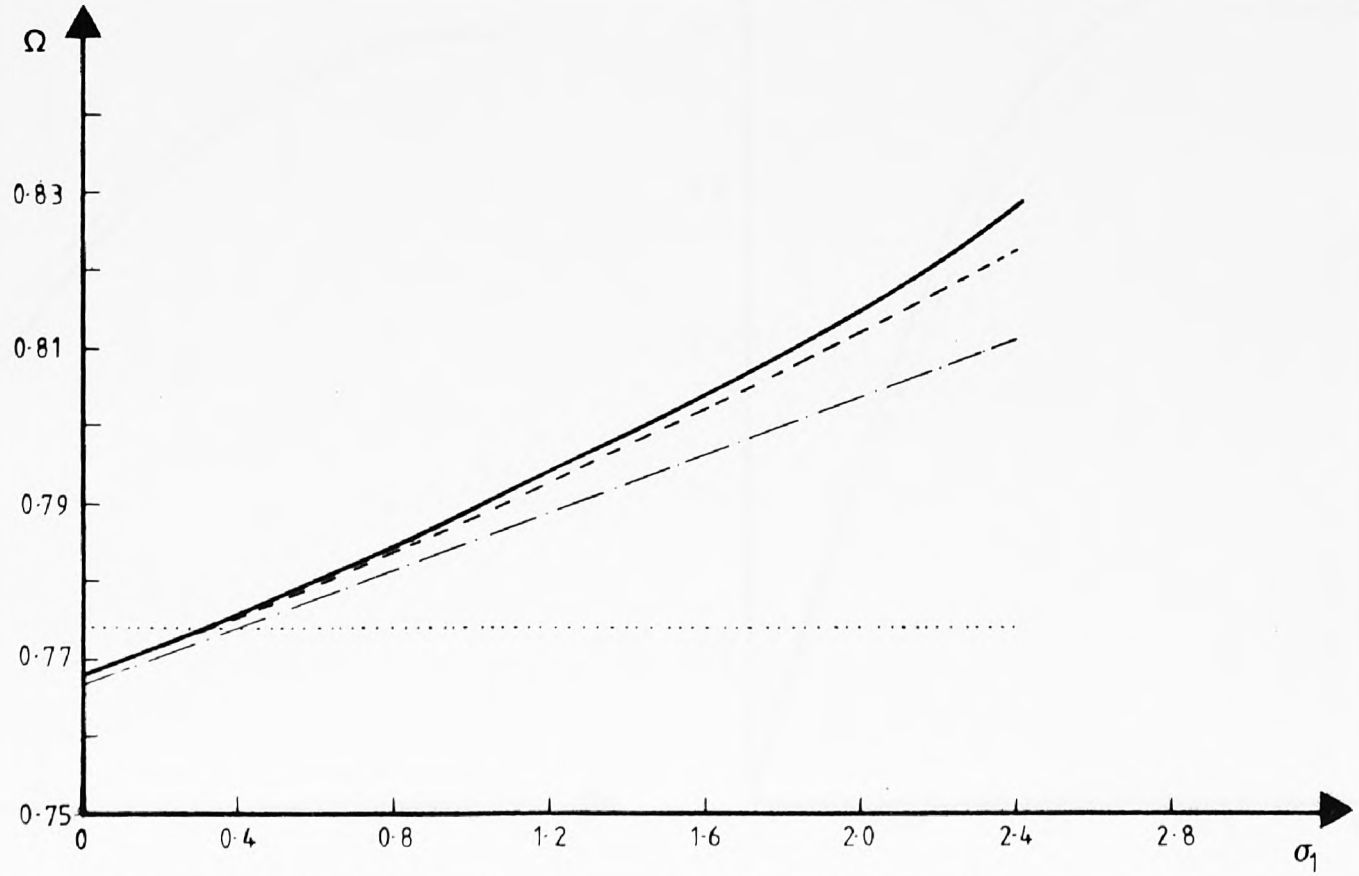

The steady state stream function in the downstream direction at different orders for,
$v = 3{\cdot}572$; $R = 30$; $m = 1{\cdot}0$; $\eta = 0{\cdot}5$. ····· $O(1)$, — — $O(\varepsilon^{1/2})$, -----$O(\varepsilon)$, ——— $O(\varepsilon^{3/2})$.

FIG-3

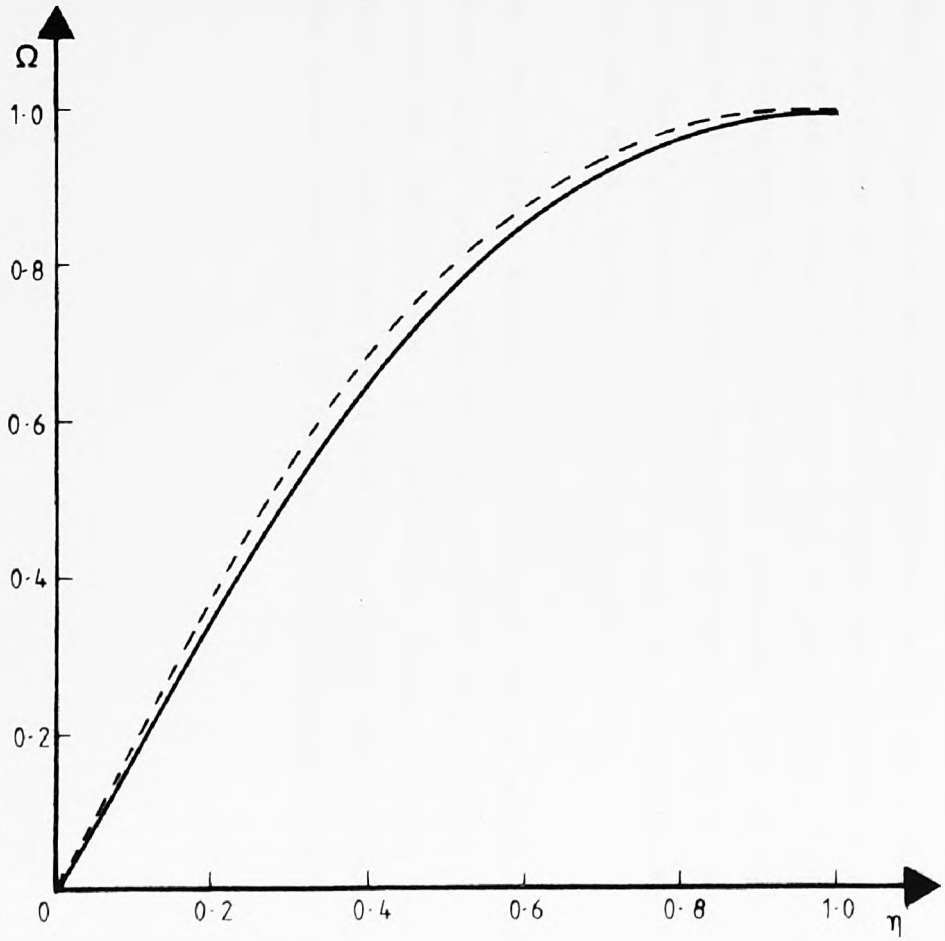

FIG-4a

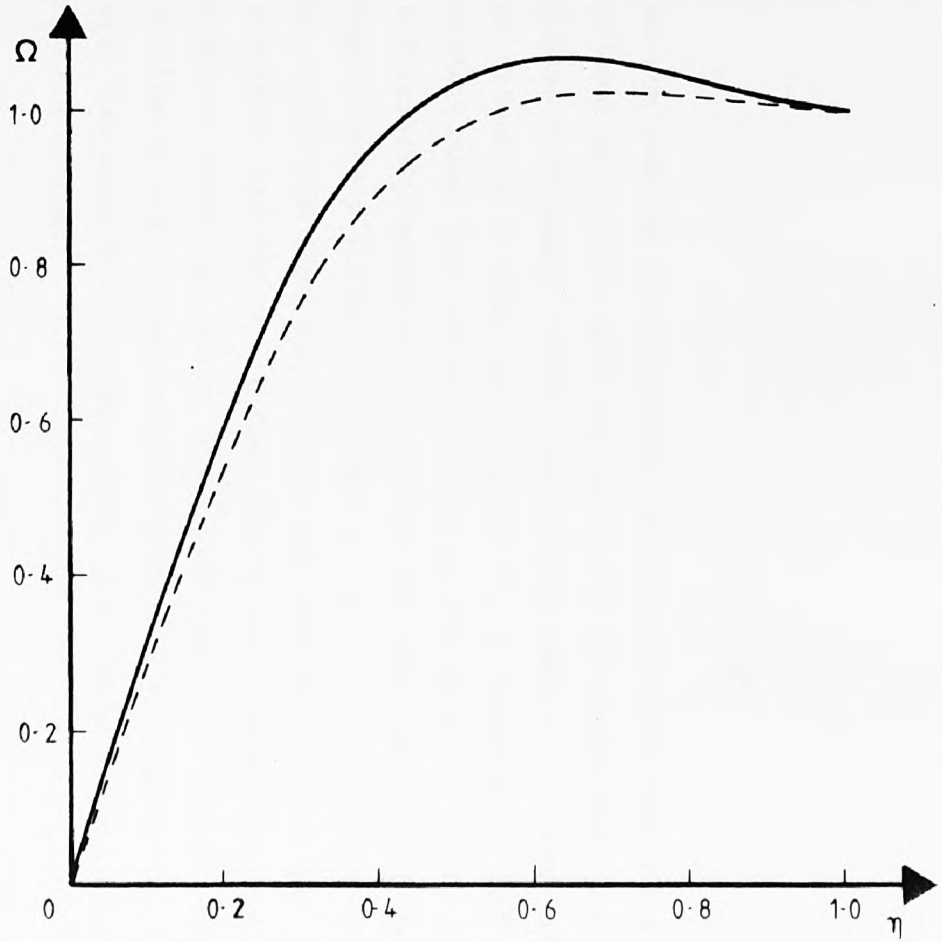

FIG-4b

The steady state stream function in transverse direction at different orders for $v = 4{\cdot}71$; $R = 30$; $m = 1{\cdot}0$; *at* $\sigma_1 = 0{\cdot}0$ *and* $\sigma_1 = 1{\cdot}6$. ----- $O(\varepsilon)$; ——— $O(\varepsilon^{3/2})$.

6 The Results.

We now come to the numerical results and interpretations. Firstly, the present work (with m=0) represents an extension and check on the work of Eagles & Weissman (1975), (henceforth E&W), to the next order term. Such an extension is important, because k_i is numerically small and it is not certain that the series for the growth rates to $O(\varepsilon^{1/2})$ (as in E&W) is sufficiently accurate. It turned out that the next order terms made comparitively little difference to the stability properties, but it must be emphasized that this result was uncertain before the calculation was complete, and it is in fact fairly surprising when one considers the comparitively high values of $\varepsilon^{1/2}$ used (up to $\varepsilon^{1/2} = 0.46$ see TABLE 6). The results of this comparison are presented in FIGS-16 to 18, and together with the results of Allmen (1980) contribute a convincing check on the results of E&W.

Next we come to the effects of curvature, which is characterised by m. When interpreting and using the results of the present curved walled calculations, we must try to imagine the physical situation, where our curved walled channel is part of a longer channel, and whereas the angle of divergence varies from point to point, the curvature is in fact constant in sign in this first case. The general theory of such channels is described by Fraenkel (1963 II), and in particular we will consider a channel with curvature varying in sign in ch. 7.

By the present analysis, our results, in a larger context, are essentially local results, but they do take account of the local curvature through the "m" parameter. These results are much more realistic than those predicted by a purely local quasi-parallel theory. The overall stability of flow in a curved walled channel would be

determined by finding the critical Reynolds number at each local point, and using the minimum of these as the overall R-crit. By the local R-crit we mean that the local growth of disturbances in the streamwise direction can occur for some values of β when R > R-crit, local, but no growth can occur for any β when R < R-crit, local.

If the channel is straight walled this R-crit is the same at all stations, and has been found as a function of $R\alpha$ by E&W. It is very strongly influenced by the nature of the steady state (Jeffery-Hamel) flow appropriate to the wedge. A question we can ask then is, if the curved walled has the same local angle of divergence as a wedge, is the flow locally more or less stable than the wedge flow ? Is the wedge approximation reasonable for a curved walled channel ? These questions can be answered by choosing v and taking $\sigma_1 = 0$ in our curved walled channel. We consider the growth rates at $\sigma_1 = 0$. We emphasize that these results are influenced both by the modification of the steady state flow, by the curvature, and by the $\frac{\partial}{\partial\sigma_1}$ terms appearing in (2.19a).

We may also follow the growth and decay of a fixed frequency disturbance in the curved walled channel in a streamwise direction, but this is of less physical interest because other frequencies will probably occur as the most unstable ones as we progress further down a divergent curved walled channel. Nevertheless, some such results are included for completeness.

6.1 The Effect of Higher-order Terms in the Straight Walled Channel.

6.1.1 The Steady State Case.

The asymptotic development of the general equation defining (2.18a) the steady state stream function, gave us the equations for G_0, G_1, G_2, F_0, F_1

and H_0 . These equations reduce to the straight walled case on setting $m = 0$. This simlified system has already been briefly described (Ch.4.1). In fact

$$\Omega(\xi,\eta;v) = G_0 + \varepsilon H_0 + \ldots \qquad ,(6.1)$$

and the equations for G_0, and H_0 are given by (4.13a), and (4.19a) respectively.

The effect of including the higher order term εH_0, is probably best described with reference to the changes suffered by the velocity profile $\frac{d\Omega}{d\eta}$.

The results in TABLE 5 clearly shows the effect for typical cases. The pattern of increased velocity at the centre and decreased velocity at the walls was common to all cases considered, and the worst case of $v = 4.71$, and $R = 10.5$ is given in FIG-5. For any fixed v, increasing R merely defines a smaller $\varepsilon^{1/2}$ and hence the effect of adding on higher order terms is less noticable, even though it persists in the way described above.

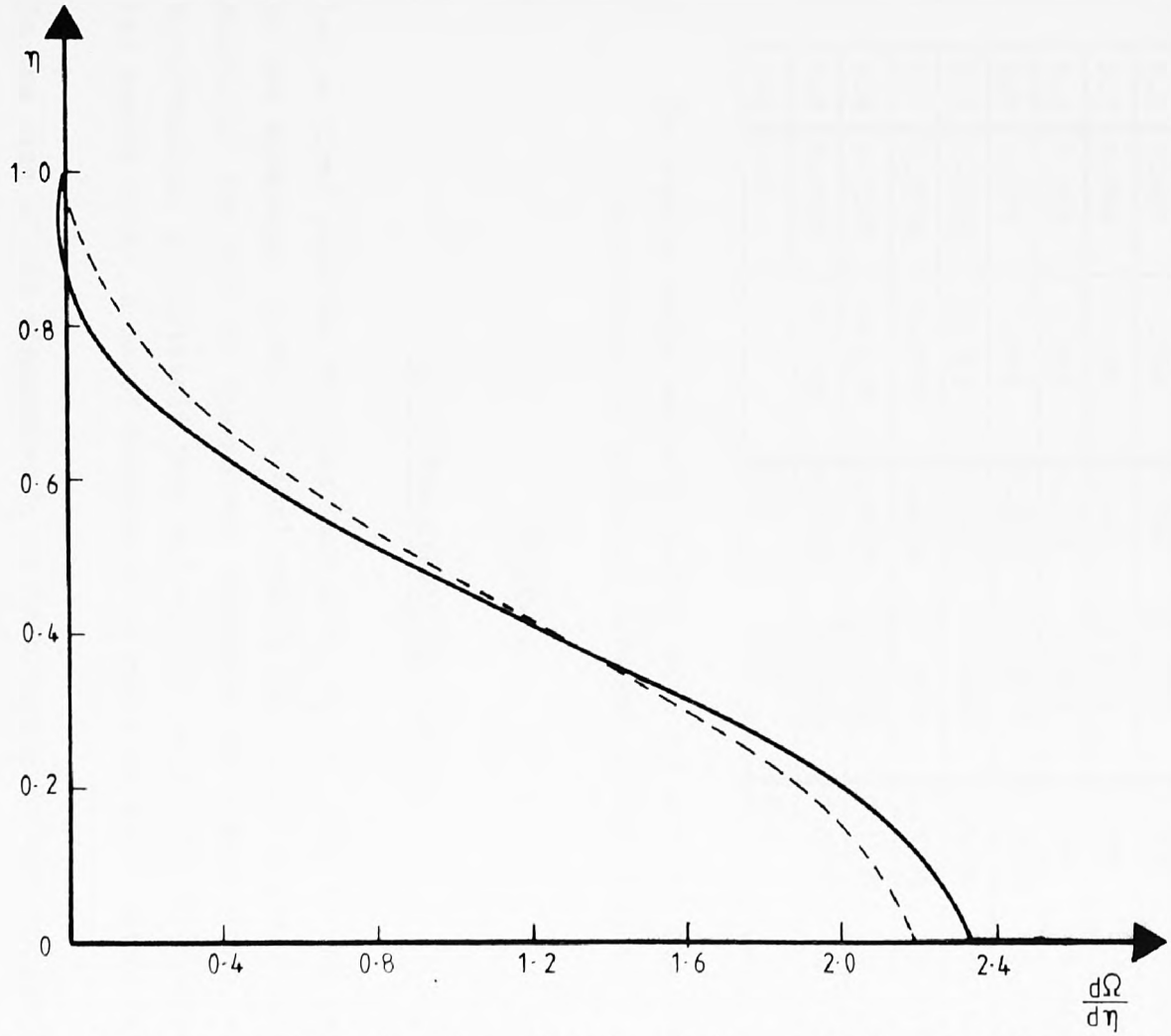

The effect of the O(ε) correction to the steady state velocity profile in the straight walled channel for $v = 4{\cdot}71$; $R = 10{\cdot}5$. ----- O(1) ; —— O(ε) .

FIG-5

	v = 3.572 ; R = 30		v = 4.093 ; R = 25		v = 4.71 ; R = 10.5	
η	$\frac{dG_0}{d\eta}$	$\frac{dG_0}{d\eta} + \varepsilon \frac{dH_0}{d\eta}$	$\frac{dG_o}{d\eta}$	$\frac{dG_o}{d\eta} + \varepsilon \frac{dH_o}{d\eta}$	$\frac{dG_o}{d\eta}$	$\frac{dG_o}{d\eta} + \varepsilon \frac{dH_o}{d\eta}$
0.0	1.856	1.860	1.973	1.985	2.187	2.339
0.1	1.813	1.817	1.920	1.931	2.113	2.251
0.2	1.691	1.694	1.768	1.777	1.906	2.005
0.3	1.504	1.505	1.542	1.546	1.604	1.650
0.4	1.273	1.273	1.269	1.269	1.256	1.248
0.5	1.021	1.019	0.9815	0.9777	0.9069	0.8555
0.6	0.7682	0.7657	0.7057	0.6993	0.5934	0.5143
0.7	0.5309	0.5279	0.4604	0.4530	0.3375	0.2494
0.8	0.3200	0.3172	0.2576	0.2508	0.1509	0.0729
0.9	0.1420	0.1402	0.1033	0.0990	0.0379	-0.0106
1.0	0.0	0.0	0.0	0.0	0.0	0.0

The steady state velocity profile with and without the $O(\varepsilon)$ correction for different straight walled channels

TABLE-5.

6.1.2 The Stability Problem.

Let us first consider the behaviour of k, f_0, A_0, and f_1. An examination of the equations (4.46), (4.65a) and (4.32a) clearly shows that these functions are not in themselves dependent on higher order terms. Nevertheless, collectively they all contribute to the $O(\varepsilon)$ correction to the growth rates. A brief discussion is given on their behaviour.

In the case of the eigenvalue k, it is uniquely defined by specifying v, R and β along with the condition (4.56), defining the eigenrelation. Its general behaviour is clear from FIGS-6a,6b and FIG-7. In FIGS-6a,and 6b, v=3.572, β =0.2, where k_l and k_r are plotted against β_I for two values of R. From FIG-6 we can see that in the case of R=57, k_l becomes negative for some β_I. Plotting k against β_I gives us the freedom of

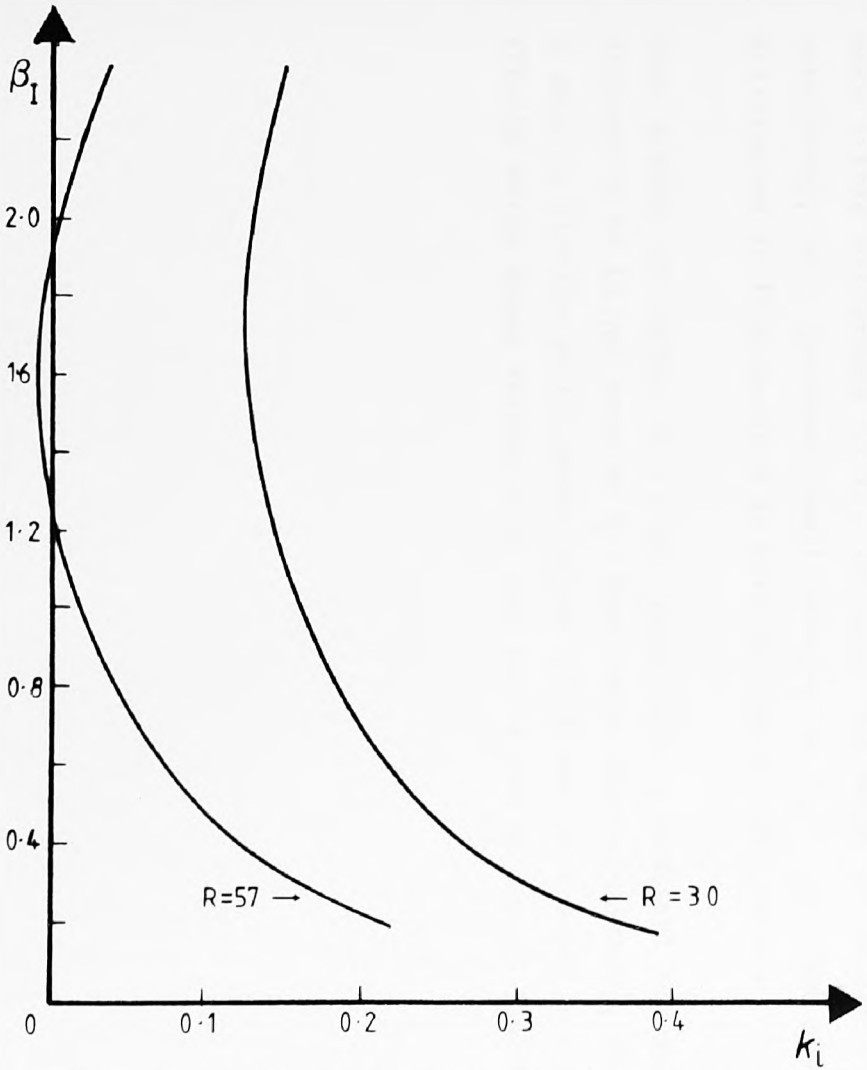

FIG-6a

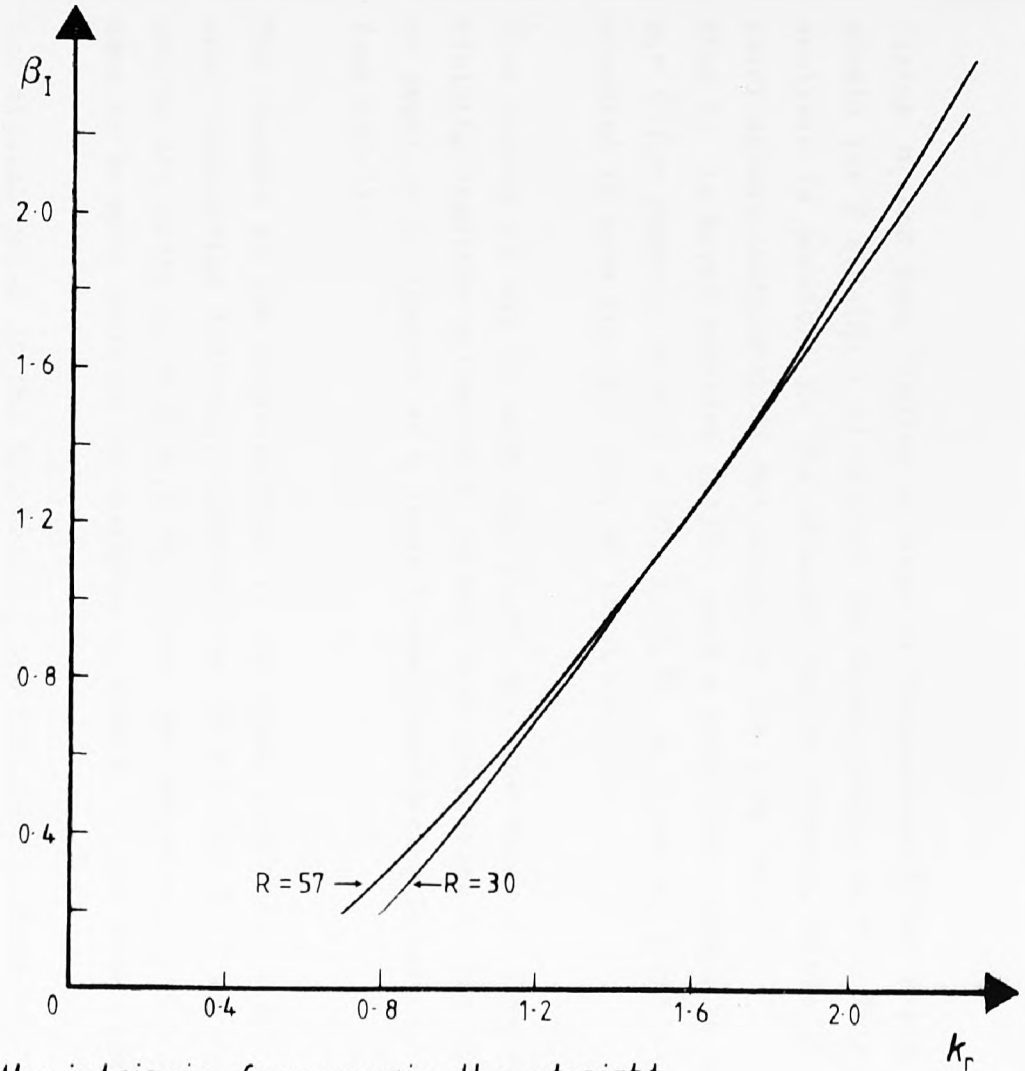

FIG-6b

The general behaviour of the eigenvalue with the intrinsic frequency in the straight walled channel ; for $v = 3 \cdot 572$.

fixing σ_1 and thus finding a range of frequencies β that might cause growth for $\hat{E}$ ($GR_\xi(\hat{E}) > 0$) through the relationship (4.31). This type of analysis is possible in the straight walled channel, since β and σ_1 never appear independently but always in the form (4.31).
When k_i is never negative (R=30), such a prediction cannot be made. At $\sigma_1 = 0$ for example, with R = 57, E, $\hat{E}$, Φ, u_ξ, and u_η might all be expected to grow for β = 1.5, at least at O(1).

From FIG-6a it can be seen for fixed σ_1, the range of frequences yielding negative values of k_i widens with increasing R. The phenomenon of negative k_i appears at a lower R when considering larger values of v (see FIG-7).

The changes in the eigenfunction f_0 for some eigenvalue k are modest when considering different combinations of v,R and β_I. Two typical graphs are given in FIGS-8a,& 8b, where the non-parallel effects are seen to be more dominant in changing f_0 than R for some fixed v.

Two typical cases of the function A_0 are compared in FIGS-9a, 9b,& 9c. Here, R = 30 and β = 0.2, and the effect of varying v is observed to make little difference to A_0. In fact, the range of values of v, R, β considered, only produced small changes in A_0, and the observed differences in FIGS-9a,9b,& 9c were typical of many cases.

Some graphs are given of f_1 to simply show a dominant non-parallel dependence as in the case of f_0. Many cases were considered, and we give a case in FIG-10a which shows values of f_1 at $\sigma_1 = 0$ and $\sigma_1 = 0.96$, and FIG-10b which shows values of f_1 for two values of R with fixed v and β.

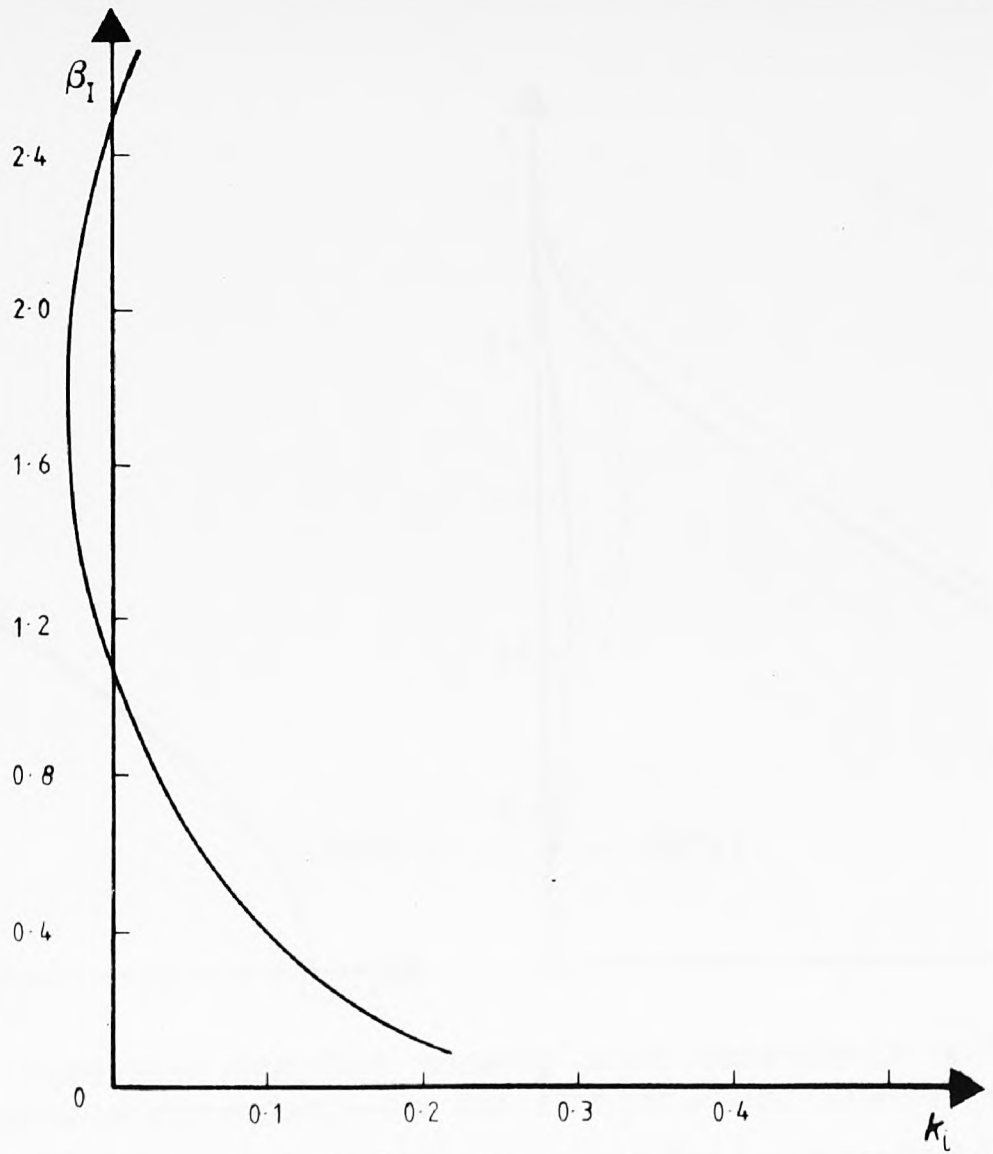

The imaginary part of the eigenvalue with the intrinsic frequency, in the straight walled channel; for v = 4·71 and R = 30.

FIG-7

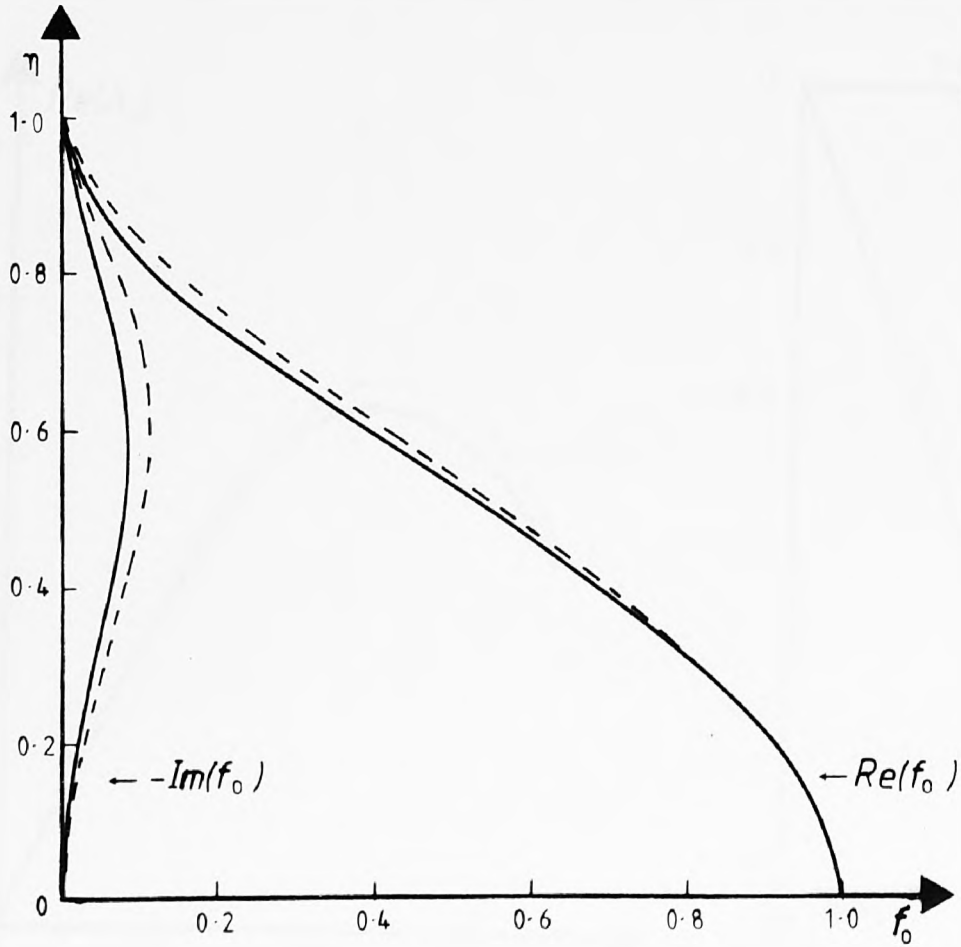

The eigenfunction in the transverse direction showing slight dependence with increased Reynolds number, and some non-parallel dependence for the straight walled channel, with $v = 4{\cdot}093$.

$\beta_1 = 2{\cdot}59$; ——— $R = 25$; - - - - - $R = 45$

FIG-8a

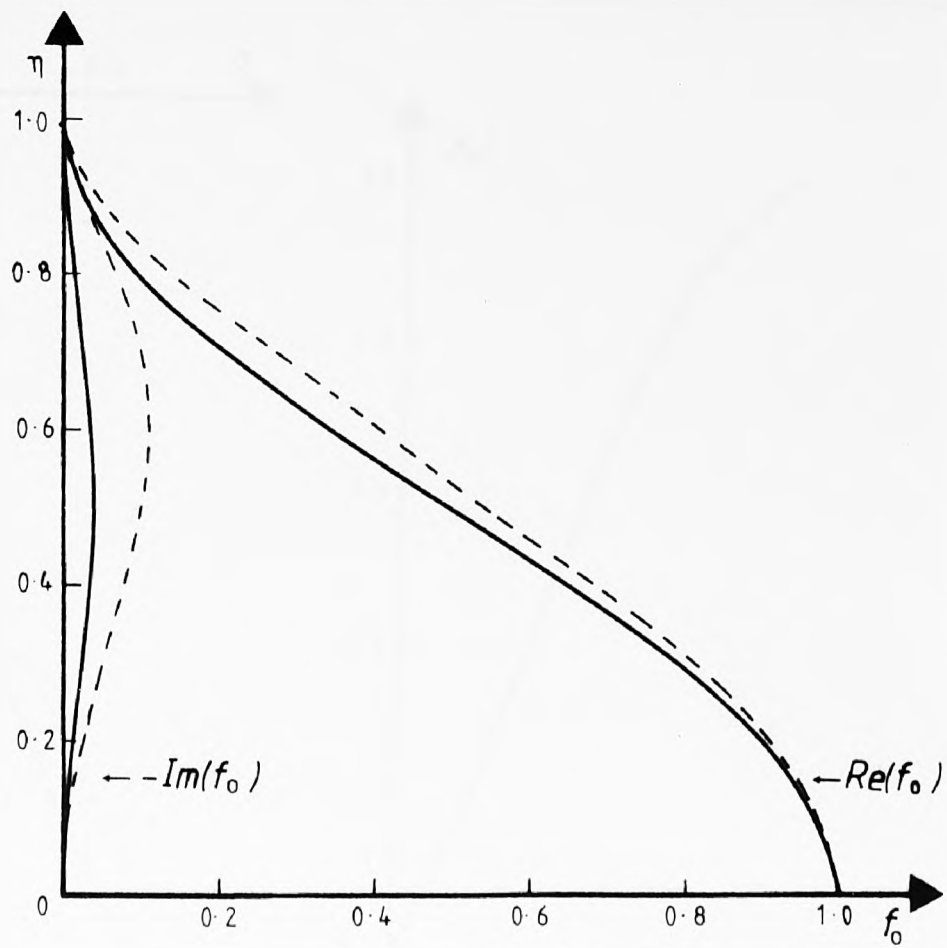

$R = 45$; ——— $\beta_1 = 0{\cdot}2$; - - - - - $\beta_1 = 2{\cdot}59$

FIG-8b

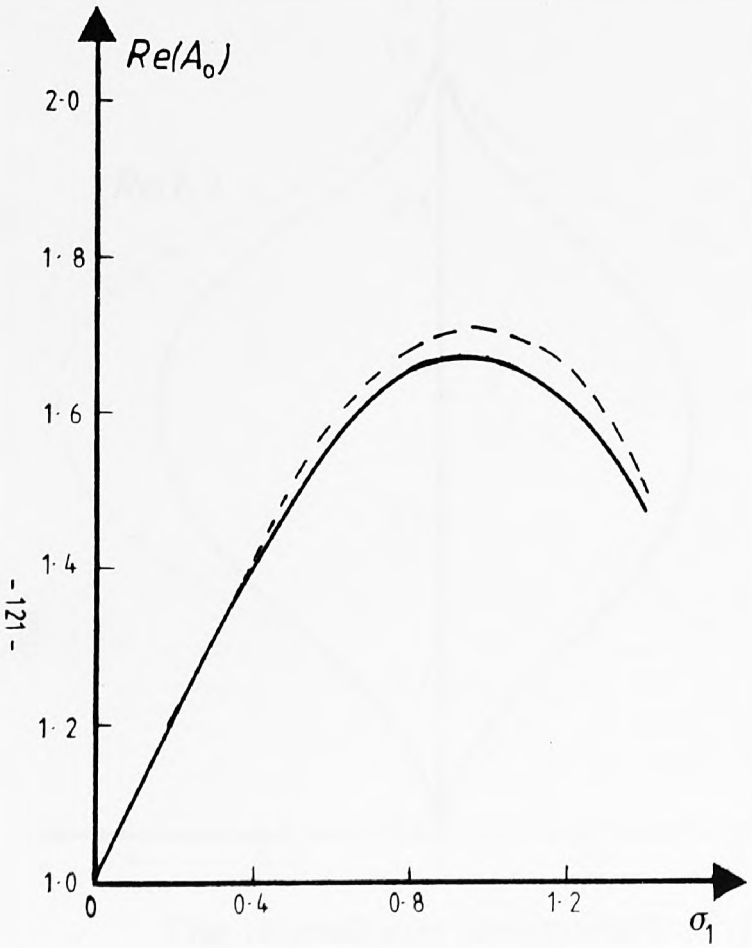

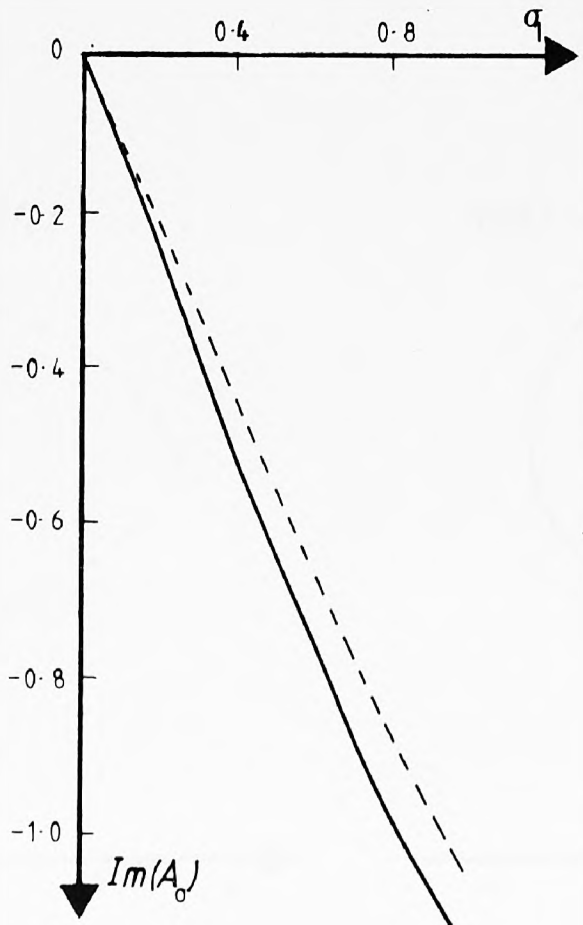

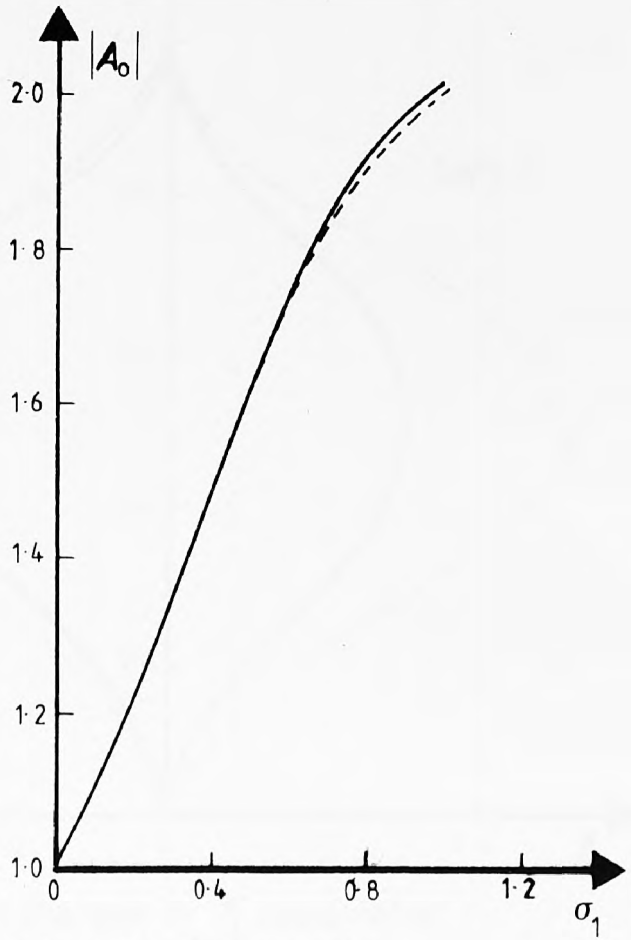

The downstream development of the amplitude function A_0 for the straight walled channel, with $R = 30$ and $\beta = 0{\cdot}2$.
——— $v = 3{\cdot}572$, - - - - - $v = 4{\cdot}093$.

FIG-9a FIG-9b FIG-9c

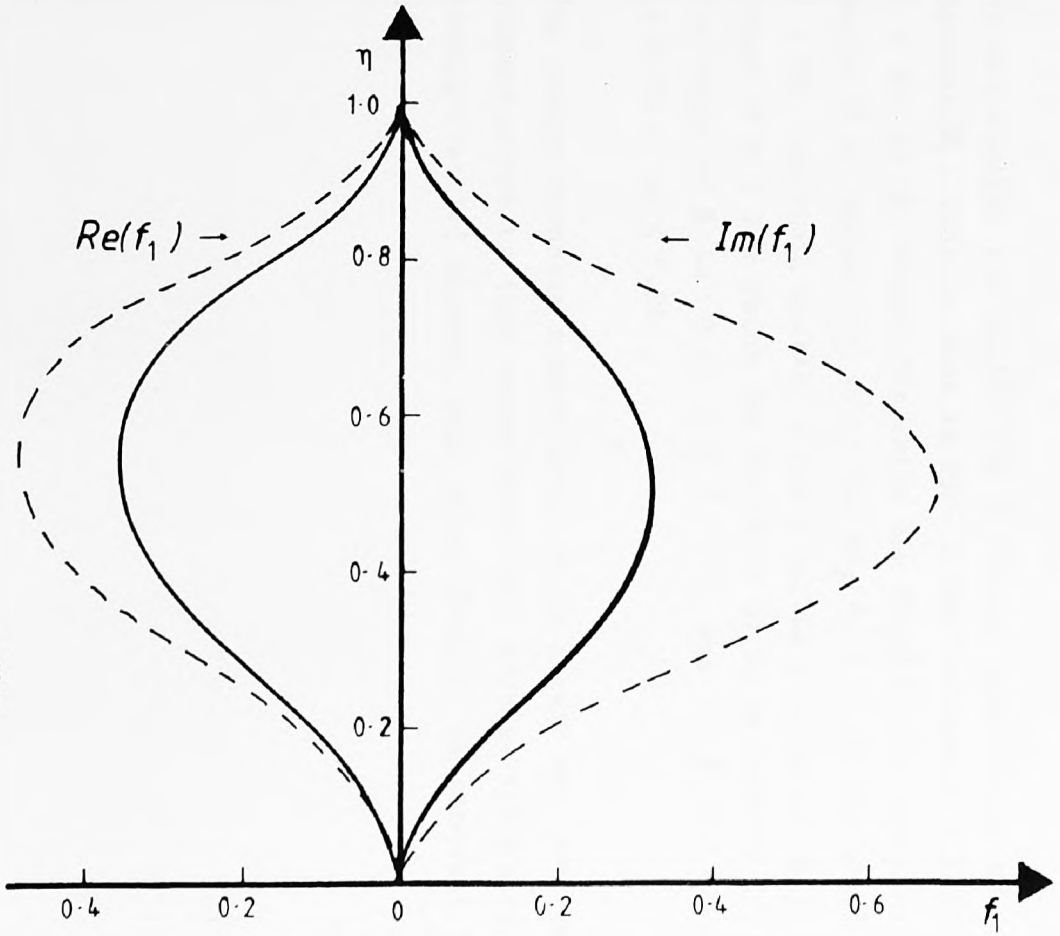

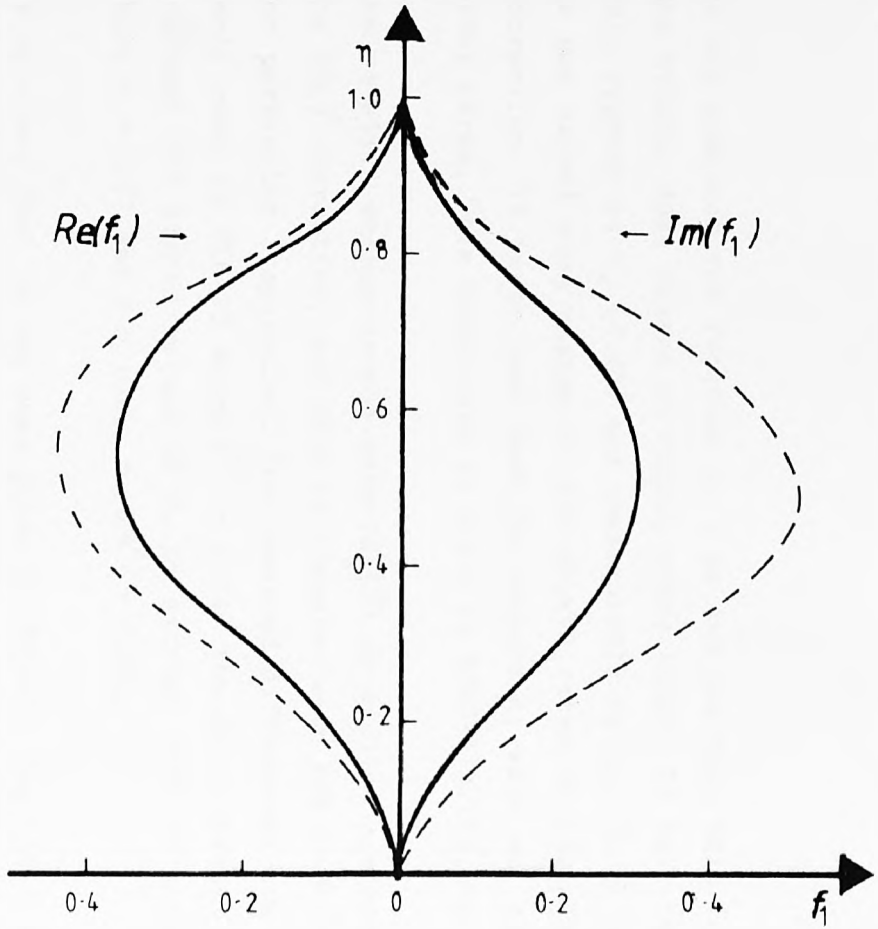

The downstream development of the transverse behaviour of f_1, also, the changes in f_1 associated with increased Reynolds number for the straight walled channel, with $v = 3{\cdot}572$ and $\beta = 0{\cdot}2$.

$R = 30$; —— $\sigma_1 = 0{\cdot}0$, ----- $\sigma_1 = 0{\cdot}96$

FIG-10a

$\sigma_1 = 0{\cdot}0$; —— $R = 30$, ----- $R = 50$

FIG-10b

We now consider the function A_1 . We can see that this function unlike the others, does depend on higher order terms. In fact this dependence only appears in M_8 (4.45) and consequently in C_{20} (4.70). Neverthless, we can expect some change in the growth rates by including the $O(\varepsilon)$ correction. It is an easy task to compute A_1 with and without higher order terms. This comparison is given in FIGS-11a,11b,and 11c.

The relative energy growth rate $GR_\xi(\hat{E})$ is plotted against σ_1 including the $O(\varepsilon)$ correction, and this is compared with E&W in FIG-12 and FIG-13 for particular frequencies. The observed differences are comparitively small even in FIG-13 where $\varepsilon^{1/2} = 0.24$. The $O(\varepsilon)$ correction is more dominant for higher values of v. An extreme case is given in FIG-14 where v = 4.71 and R = 10.5, here $\varepsilon^{1/2} = 0.45$.

It is clear that in the case given by FIG-12, the addition of the $O(\varepsilon)$ term tends to "stabilize" the $GR_\xi(\hat{E})$. This is in contrast to FIG-13 in which the addition of the $O(\varepsilon)$ term tends to "destabilize" the $GR_\xi(\hat{E})$.

We can analyse the $GR_\xi(\hat{E})$ for different frequencies by plotting $GR_\xi(\hat{E})$ against β_I . This is seen in FIG-15 for the case v = 3.572. Clearly, for R = 30, no β_I exists for which the $GR_\xi(\hat{E}) > 0$, hence no frequency or value of σ_1 exists for which the $GR_\xi(\hat{E}) > 0$. On the other hand when R = 50, "critical points" A and B define a range of β_I (and a range of σ_1) for which the $GR_\xi(\hat{E}) > 0$. In particular if $\sigma_1 = 0.4$, then the range of β is $0.44 < \beta < 1.12$, and if $\beta = 0.2$ then the range of σ_1 is $0.79 < \sigma_1 < 1.26$.

The lowest Reynolds number about which growth may just be expected, is characterised by that curve which just touches the β_I axis in FIG-15. In the straight walled channel this value (R-crit) is constant for all values of σ_1 .

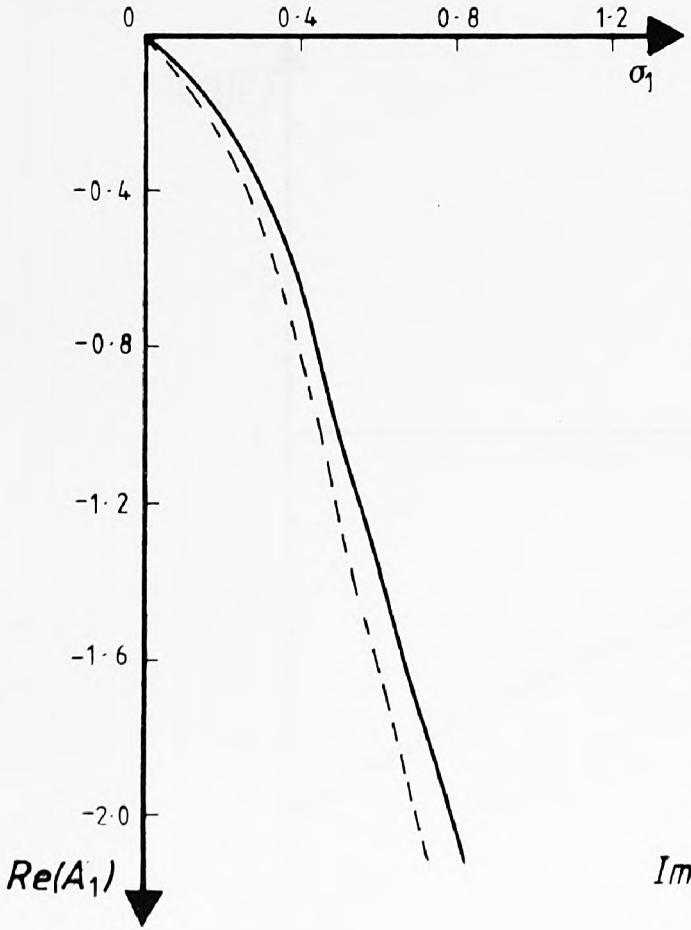

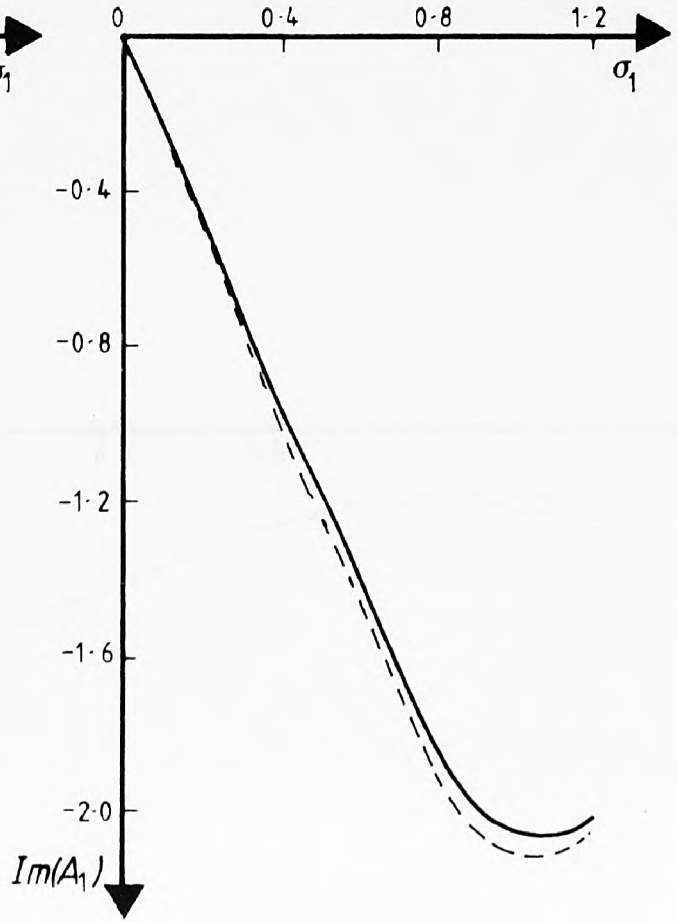

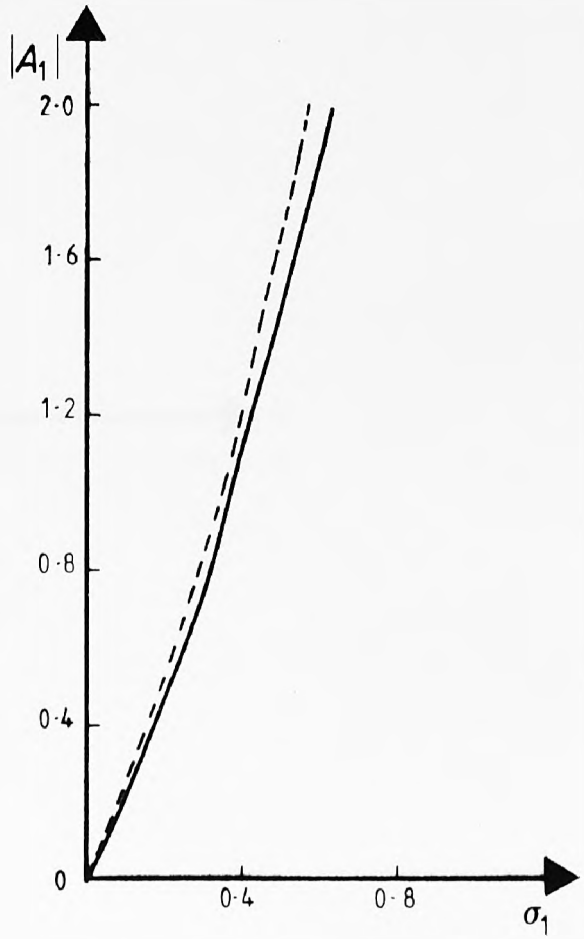

The downstream development of the amplitude function A_1, for the straight walled channel, with $v = 3572$; $R = 30$; $\beta = 0{\cdot}2$; ---- up to $O(\varepsilon^{1/2})$, —— up to $O(\varepsilon)$.

FIG-11a FIG-11b FIG-11c

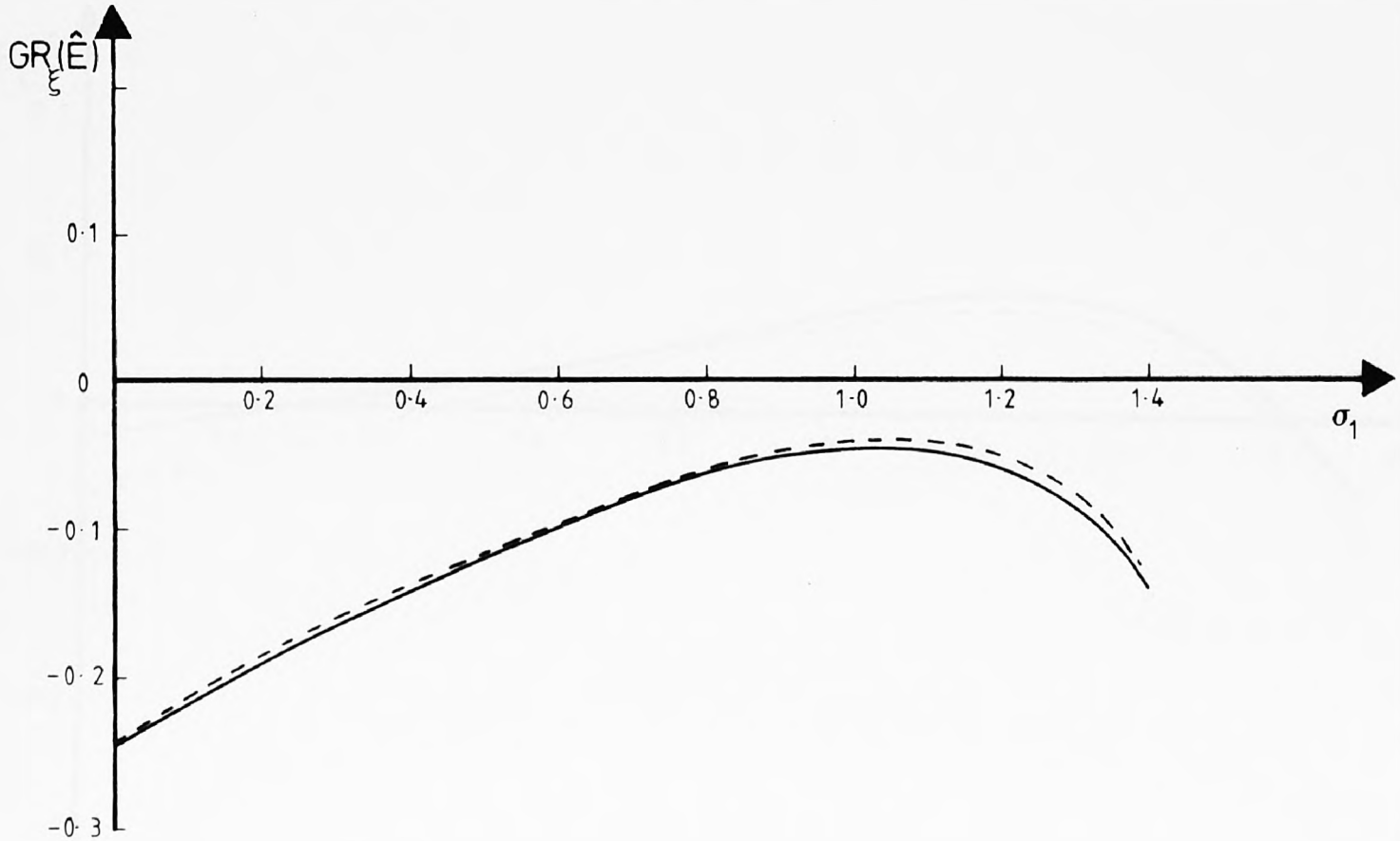

The downstream behaviour of the relative kinetic energy in the straight walled channel with $v = 3{\cdot}572$; $R = 30$ *and* $\beta = 0{\cdot}2$. ---- E&W , —— $O(\varepsilon)$ *correction.*

FIG-12

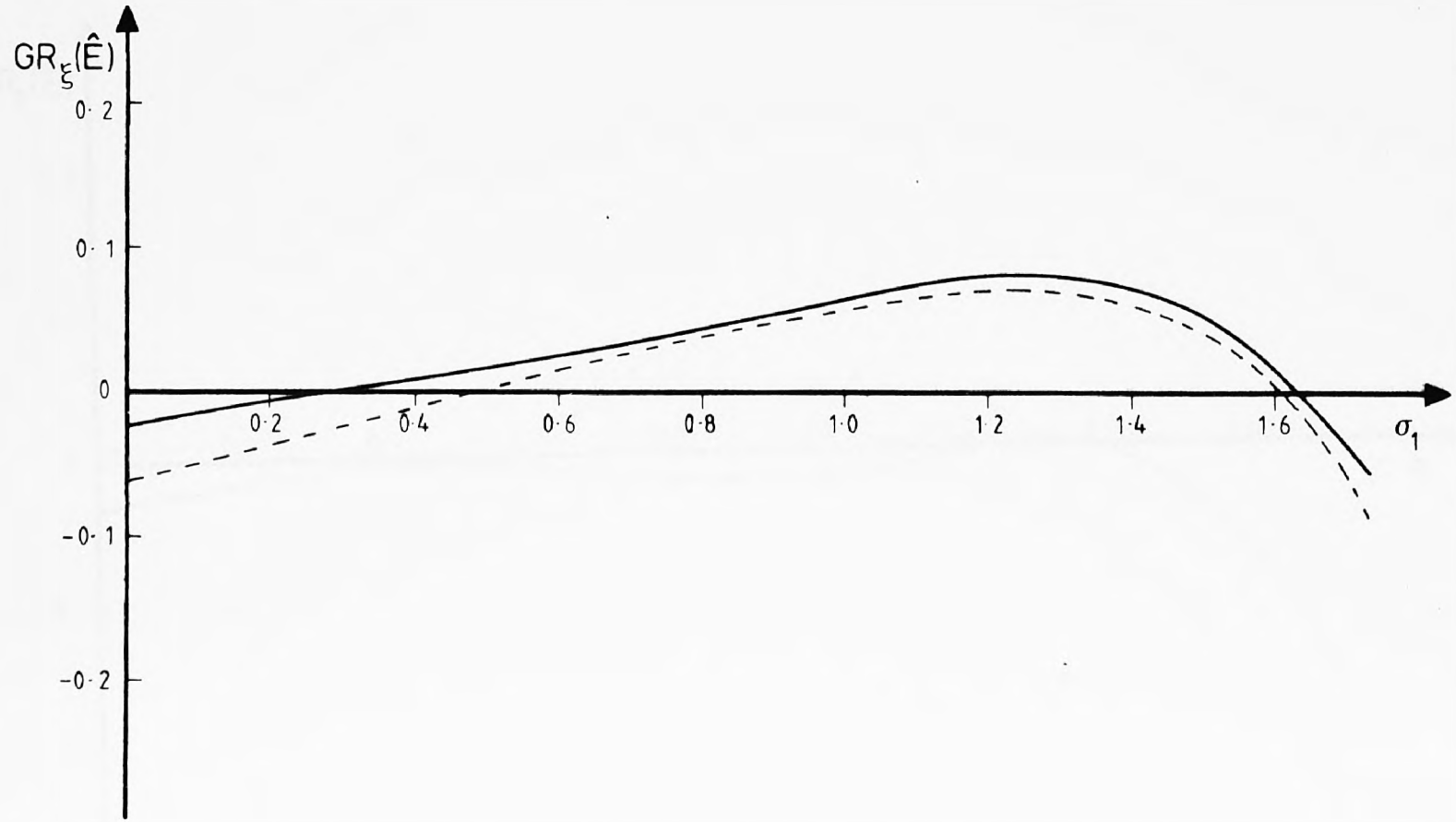

The downstream development of the relative kinetic energy in the straight walled channel ; with $v = 4{\cdot}71$; $R = 20$ and $\beta = 0{\cdot}12$. ----- E&W , ——— $O(\varepsilon)$ correction.

FIG-13

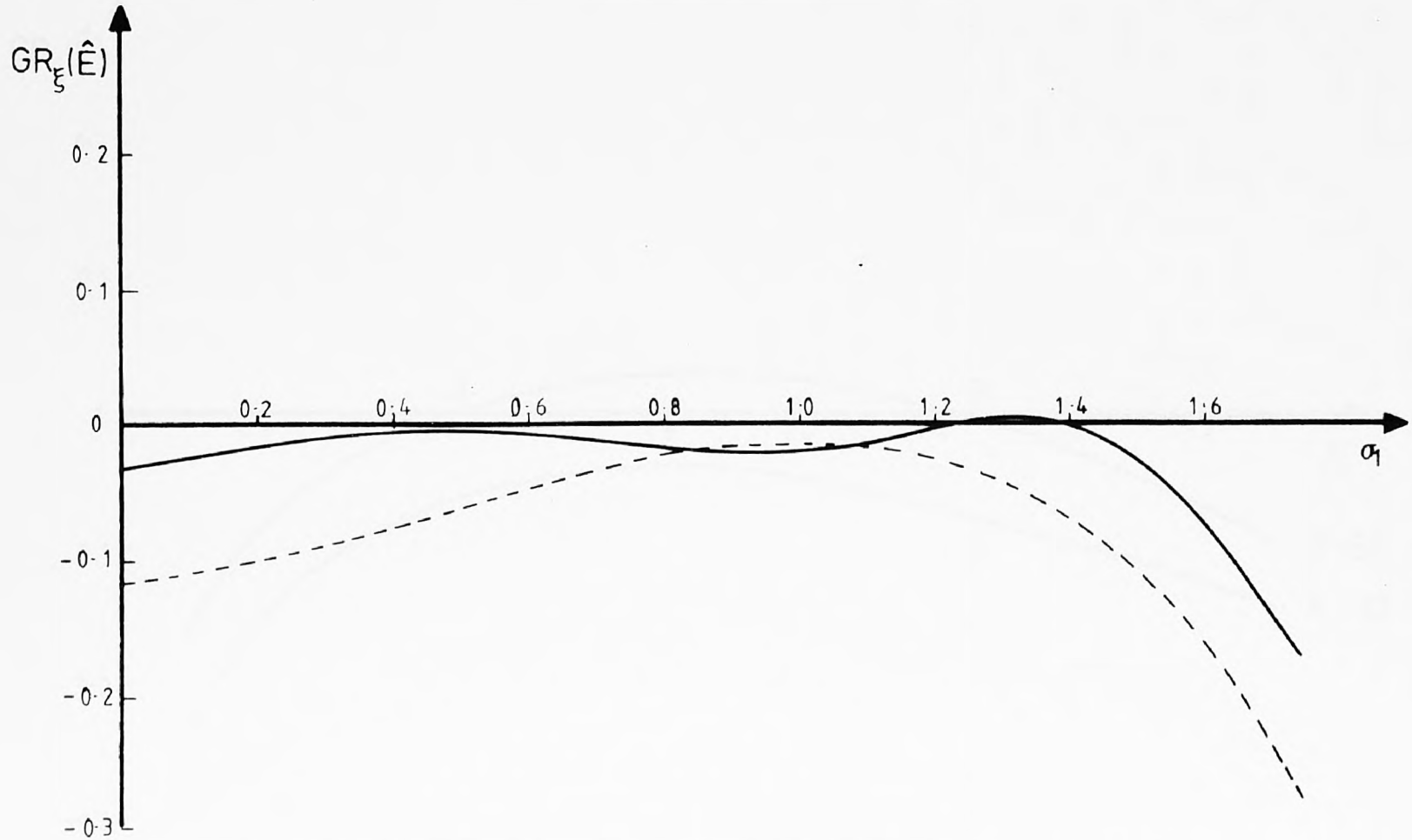

The downstream development of the relative kinetic energy in the straight walled channel; with $v = 4 \cdot 71$; $R = 10$ *and* $\beta = 0 \cdot 12$. ----- *E & W ,* —— $O(\varepsilon)$ *correction.*

FIG-14

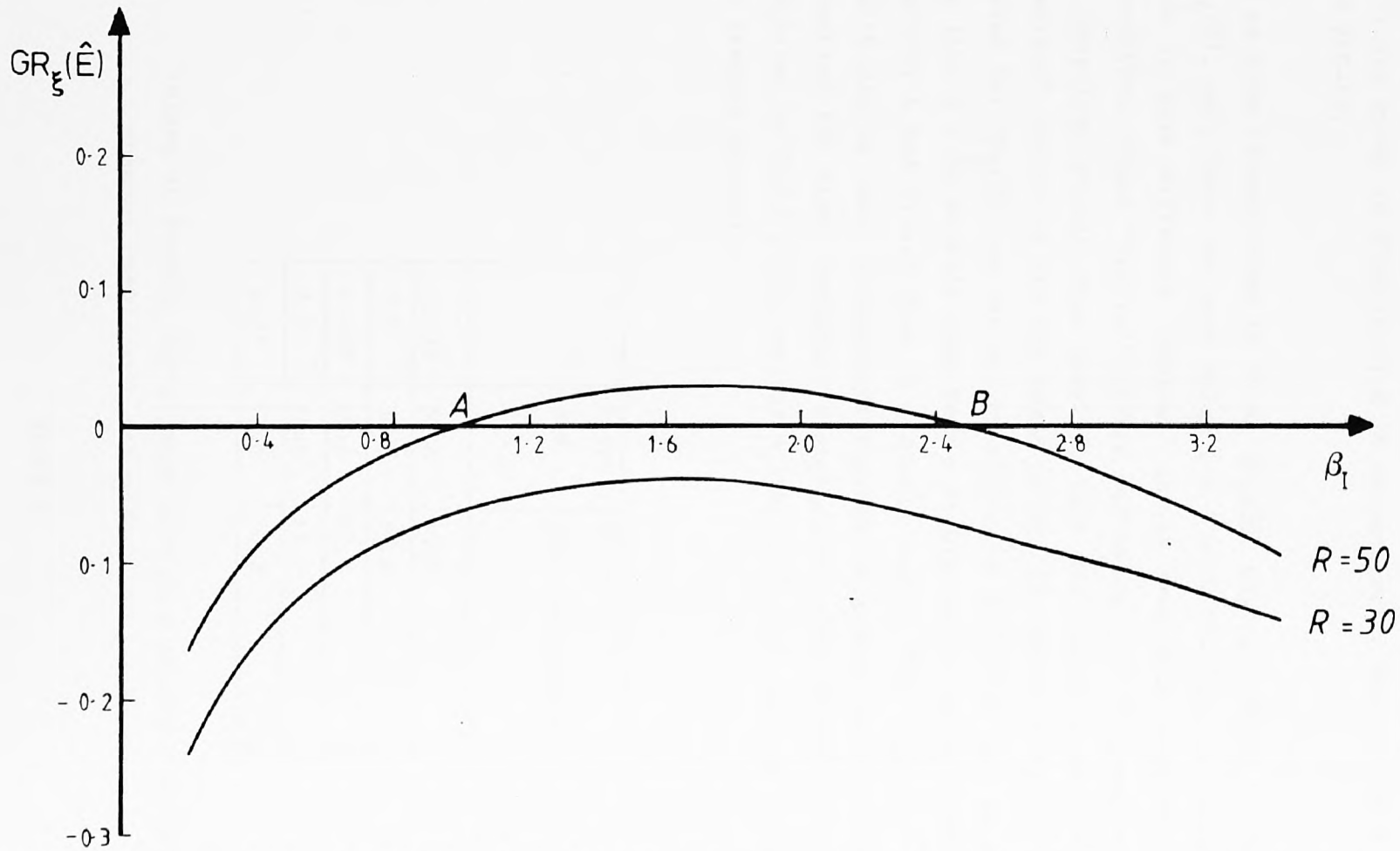

The general behaviour of the relative kinetic energy with the intrinsic frequency in a straight walled channel, for increased Reynolds number, with $v = 3 \cdot 572$.

FIG-15

By fixing v, we can establish different "critical" points for different R. These "critical" points contribute to form "neutral" curves of β_I vs. R. The "neutral" curves based on $GR_\xi(\hat{E})$ for v = 3.572, 4.093, and 4.71 are given in FIGS-16,17,& 18 respectively. Note A and B on FIG-15 and FIG-16.

As we have already seen in Ch.4, $GR_\xi(\Phi)$, $GR_\xi(u_\xi)$, $GR_\xi(u_\eta)$, $GR_\xi(E)$, and $GR_\xi(\hat{E})$, only have the same value $(-k_l)$ at O(1). Thus we expect all of them to have different "neutral" curves even with just the $O(\varepsilon^{1/2})$ correction. These "neutral" curves define regions of growth and decay. We establish R-crit from them. In fact the lowest R-crit from all "neutral" curves is the one based on $GR_\xi(\hat{E})$. Based on these "neutral" curves for $GR_\xi(\hat{E})$, we can see by referring to FIG-16 that as we move on the line R = 50 we will pass from a stable region to an unstable region (between A and B) and back to a stable region. The "neutral" curve in FIG-16 can be used to evaluate regions of growth in the streamwise direction for fixed frequency disturbances. Some values of R-crit are tabulated in TABLE 6 for various v, where the E&W case is compared with the present analysis.

v	R-crit; E&W	R-crit; $O(\varepsilon)$ correction
3.572	38.6	40.5
3.8	32.3	33.4
4.093	25.4	25.5
4.5	16.6	15.2
4.71	12.6	10.2

Values of R-crit, for a range of v in a straight walled channel (m=0), with and without $O(\varepsilon)$ correction

TABLE 6.

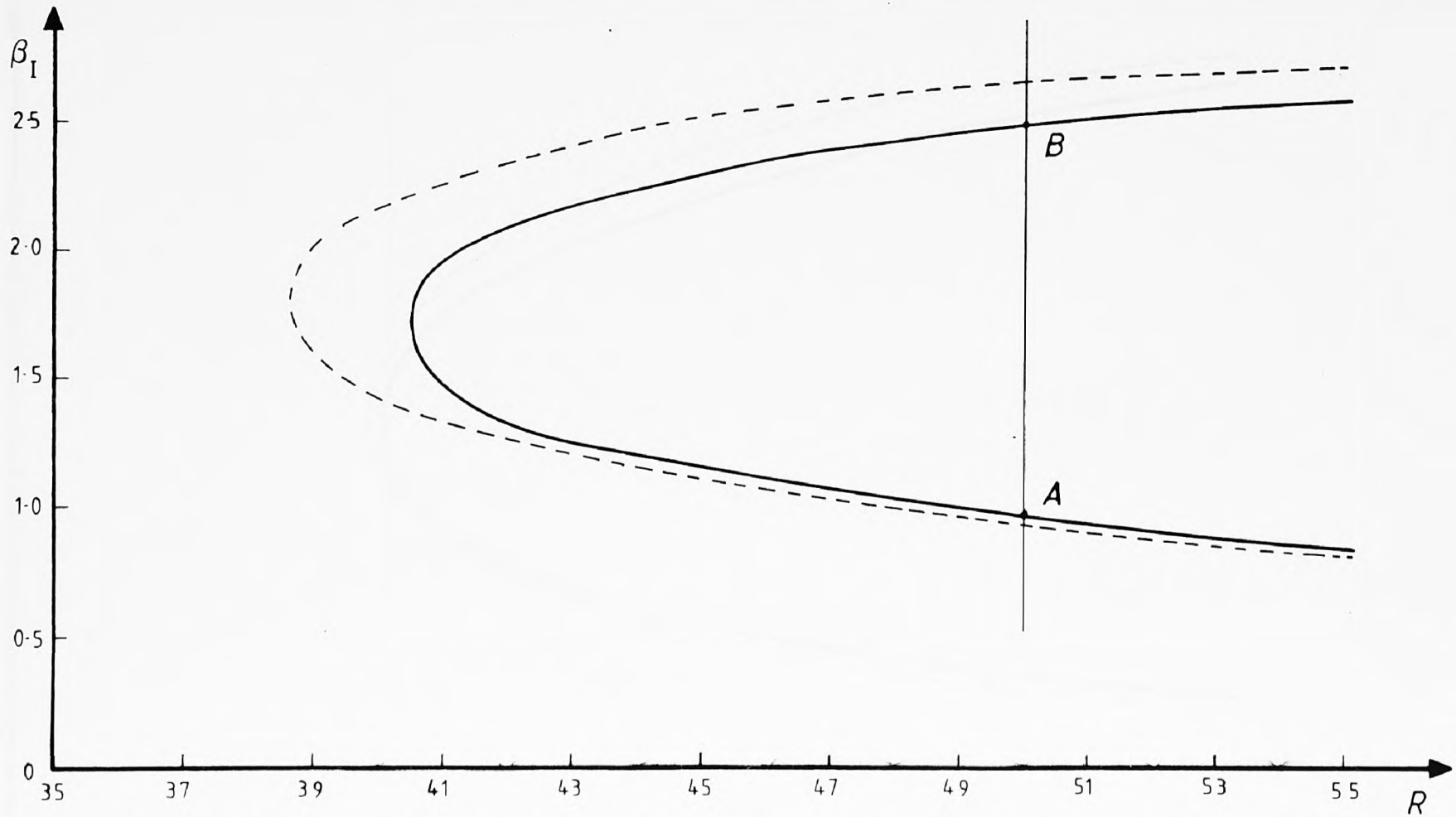

Neutral stability curves at different orders for the straight walled channel with $v = 3{\cdot}572$.

_____ *E & W* ; _____ $O(\varepsilon)$ *correction.*

FIG -16

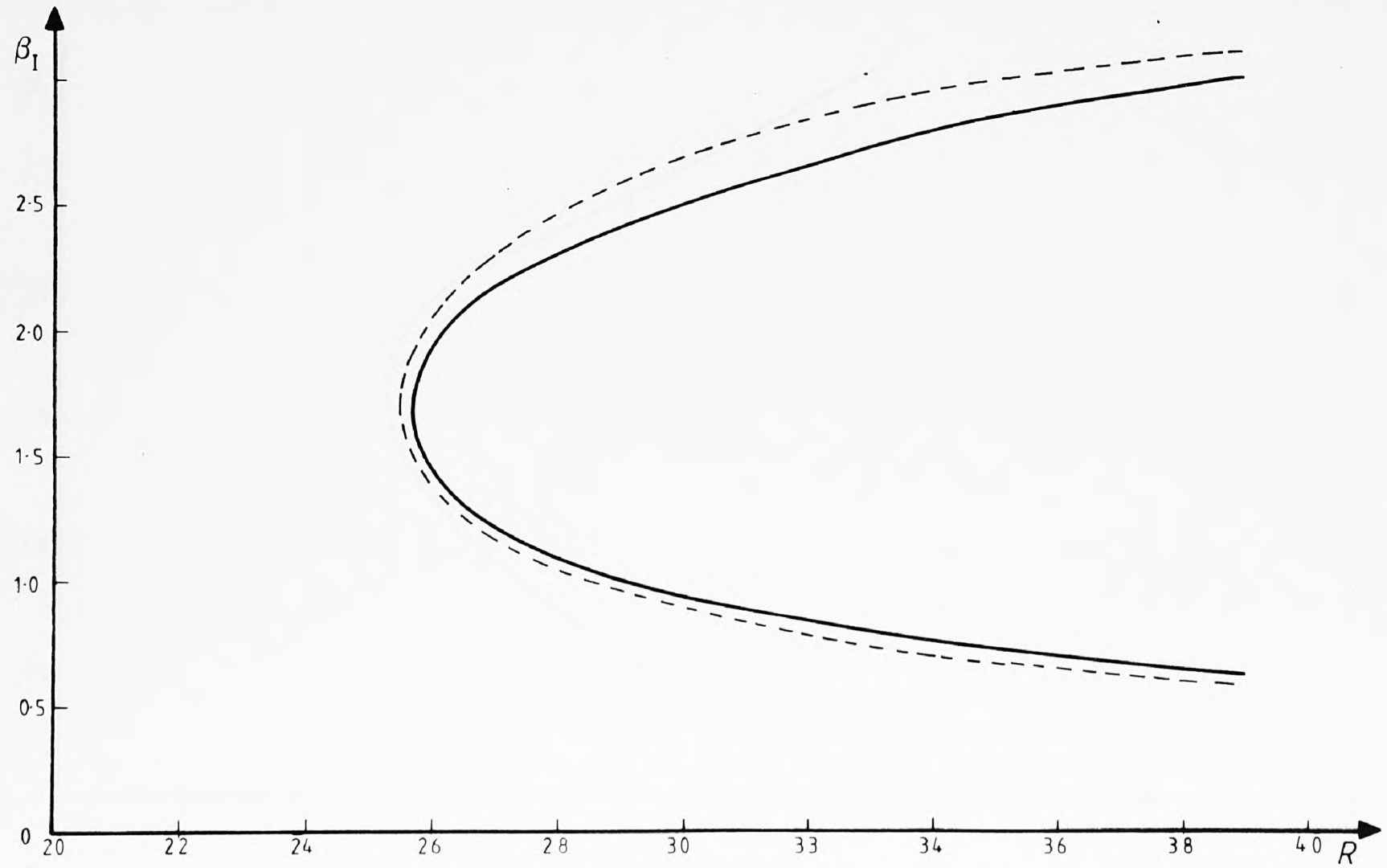

Neutral stability curves at different orders for the straight walled channel with v = 4·093.
----- *E & W* ——— *O(ε) correction.*

FIG-17

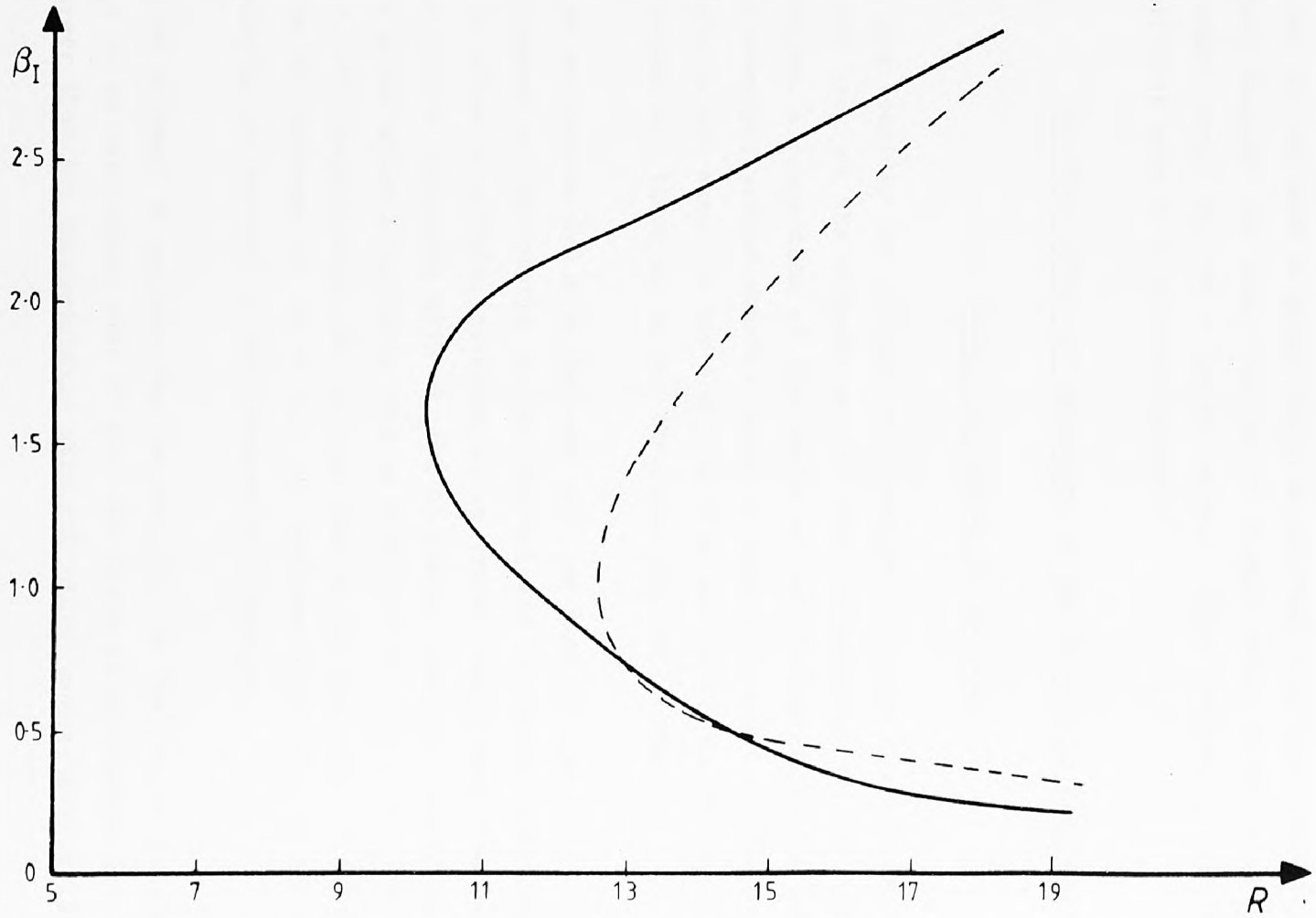

Neutral stability curves at different orders for the straight walled channel with v=4·71.
----- E & W ; ——— O(ε) correction.

FIG-18

The feature of the higher order terms exemplified in TABLE 6 or FIG-19, could have been anticipated when we consider FIG-12 and FIG-13. These results suggest that some critical v exists (v-crit) about which the addition of higher order terms stabilizes the flow (v < v-crit) or destabilizes the flow (v > v-crit).

Allmen's (1980) direct numerical attack on the straight walled channel is briefly considered here. In fact Allmen did not provide a graph of R vs. v, but such a graph could be plotted from his results, and it would suggest the same feature of higher order corrections as the present ones, but to a lesser extent. This feature is not really noticable when R is plotted against $\varepsilon^{1/2}$.

6.2 The Effect of Curvature in the Stability Problem.

6.2.1 The Steady State Case.

We now consider the effects of curvature through the m term. We shall first look at the effects on Ω and subsequently on the stability problem. A comparison of the curved walled channel (for various m) and the straight walled channel (m=0) is made at a position where the local angle is the same. In our analysis this was chosen to be at $\sigma_1 = 0$. Both problems are taken up to and including the $O(\varepsilon)$ term.

When we compare m=0 with the case m=1, we find that at $\sigma_1 = 0$, $\frac{\partial \Omega}{\partial \eta}$ is decreased at the centre of the channel and increased near the walls. This state of affairs reverses as we travel downstream. The velocity at the centre increases with σ_1 and decreases near the walls. Two graphs are given which illustrate this in FIGS-20 & 21, for v = 4.093, and v = 4.71 respectively. We can see that in the case of v = 4.71 reversed flow is observed at $\sigma_1 = 1.2$, in contrast with m=0, in which the velocity is constant in the streamwise direction.

In an attempt to explain why the velocity at the centre is smaller at $\sigma_1 = 0$, we can reason that if m>0, the angle of divergence for $\sigma_1 > 0$ is larger than the corresponding straight walled angle. Similarly if m>0,

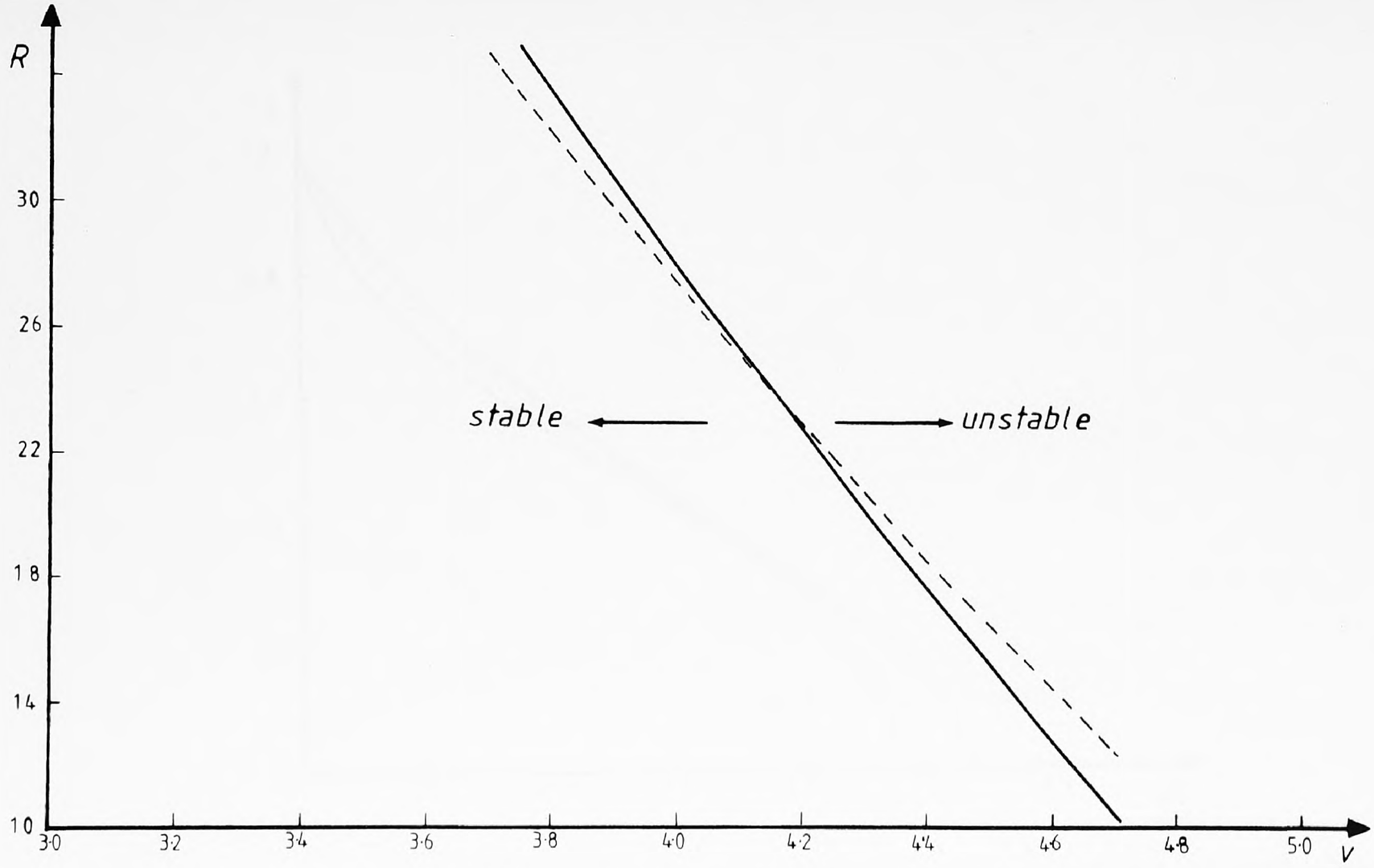

Boundary curves separating stable and unstable flow at different orders for the straight walled channel. ----- E & W , ——— O(ε) correction.

FIG-19

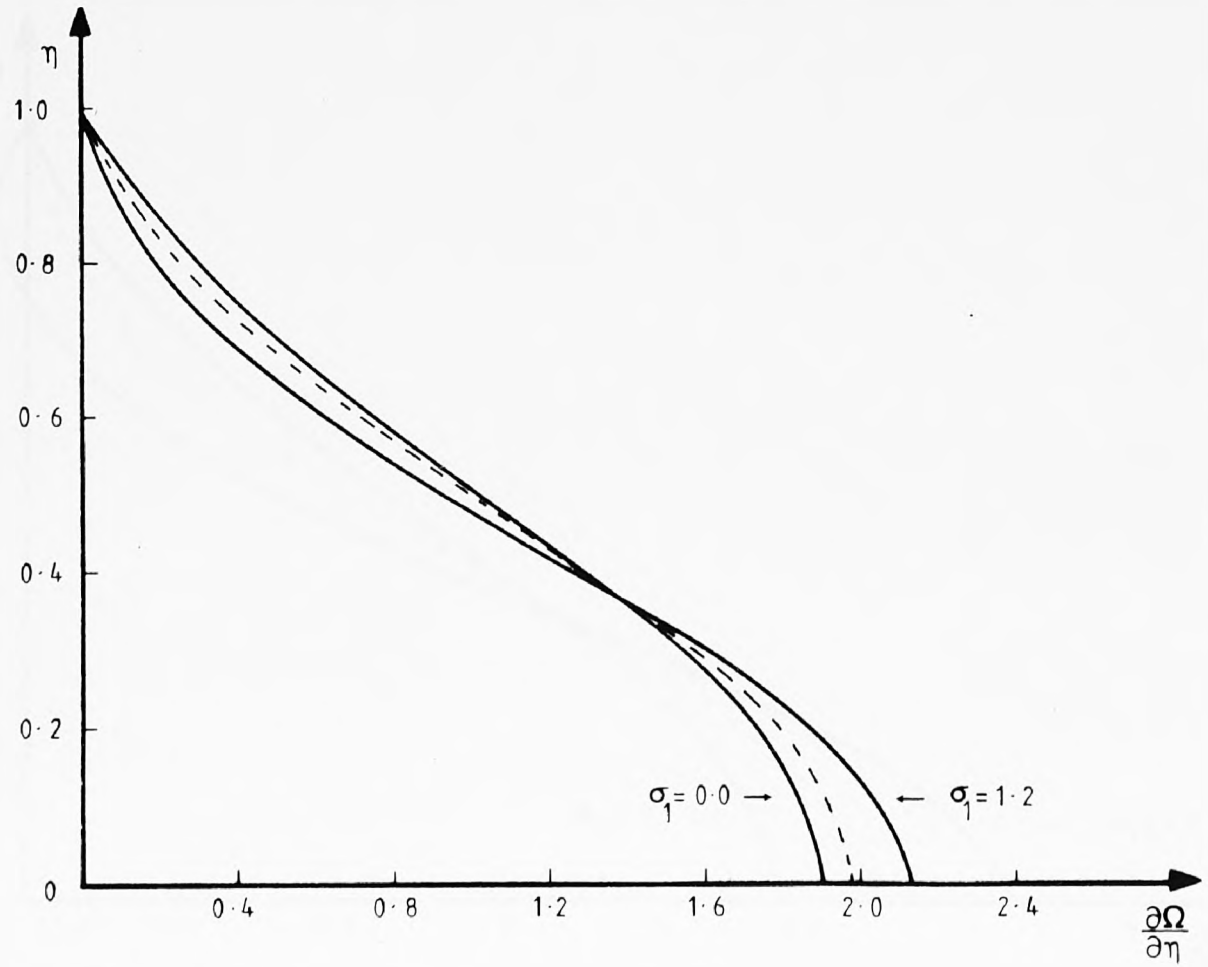

The transverse behaviour of the steady state profile for the curved and straight walled channel, at different positions downstream, with $v = 4{\cdot}093$ *and* $R = 30$.

---- *straight walled* ($m = 0$) ——— *positive curvature* ($m = 1$)

FIG - 20

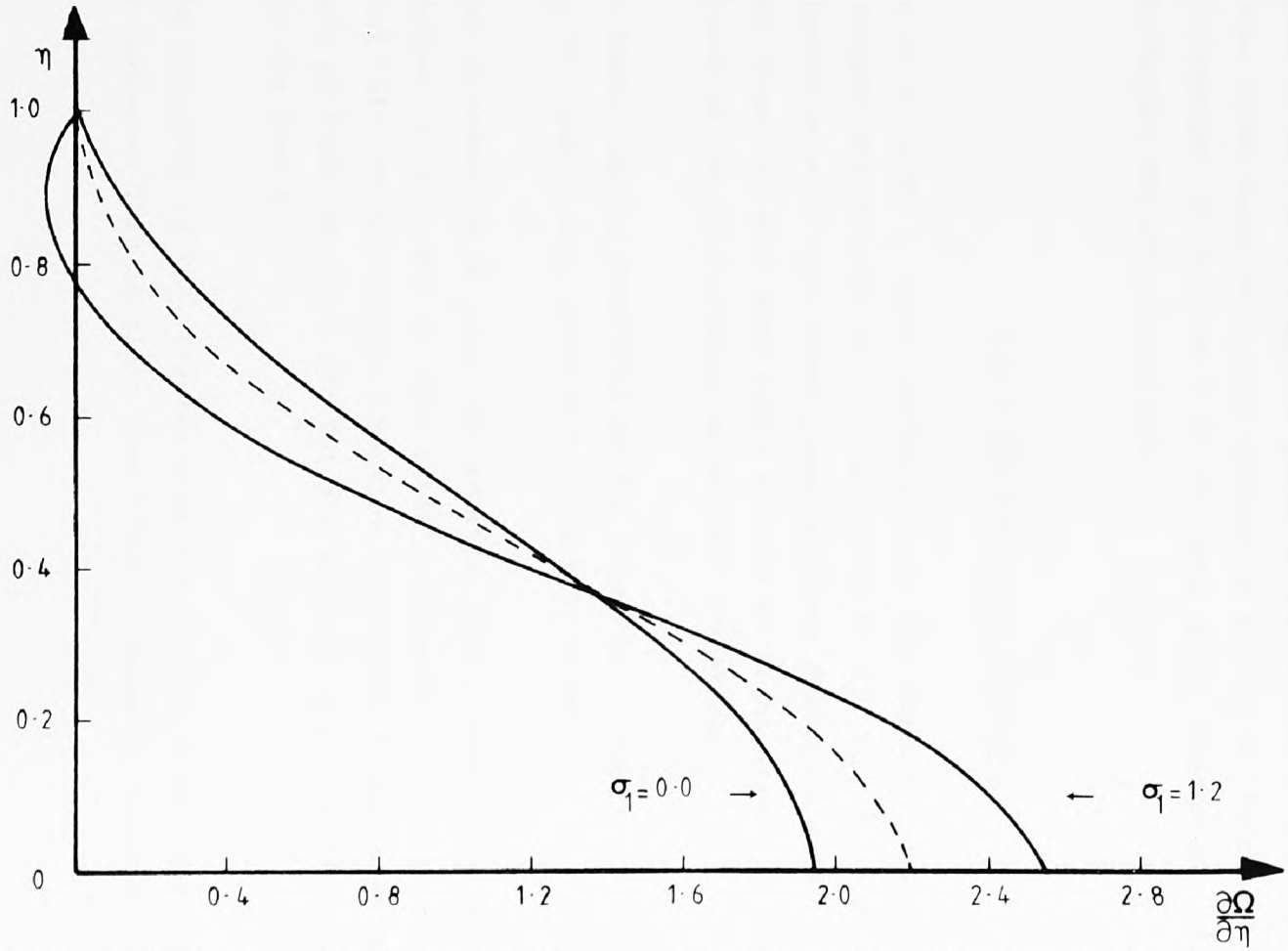

The transverse behaviour of the steady state profile for the curved and straight walled channel, at different positions downstream, with v = 4·71 and R = 30.

---- *straight walled (m = 0)* —— *positive curvature (m = 1)*

FIG - 21

then the angle of divergence for $\sigma_1 < 0$ is smaller than the corresponding straight walled angle. The steady state velocity profile might then be expected to be smaller at the centre of the channel for $\sigma_1 < 0$, and because of the upstream influence this may persist to $\sigma_1 = 0$. If this was the case, then we might expect the reverse to happen at $\sigma_1 = 0$ for a value of $m < 0$. A graph is given in FIG-22 for m=-1 to substantiate this. Other cases were also considered and as $|m|$ increased the effects illustrated in FIGS-20,21,& 22 were more pronounced, and the σ_1 dependence was more noticable.

6.2.2 The Stability Problem.

We will offer a brief discussion on the combined curvature and non-parallel effects to the functions k, f_0, A_0, A_1, and f_1. This discussion will show comparisons of these functions with the equivalent m=0 cases and will shed light on what we might expect to happen to the growth of the disturbances as we move downstream.

On examining the equations of the above functions it is clear that only A_0, A_1, anf f_1 are directly dependent on curvature.

The introduction of positive curvature (m=1) tends to decrease $|A_0|$ and $|A_1|$ near $\sigma_1 = 0$, and in many cases considered, this decrease persisted well into the streamwise direction ($\sigma_1 = 1.0$). Comparisons with m=0 are made in FIGS-23a,23b,& 23c for the case of A_0 and in FIGS 24a,24b,& 24c for the case A_1.

The behaviour of $|f_1|$ however does not exhibit a decrease near $\sigma_1 = 0$ but an increase. This is clear from FIG-25a, where f_1 compared with the

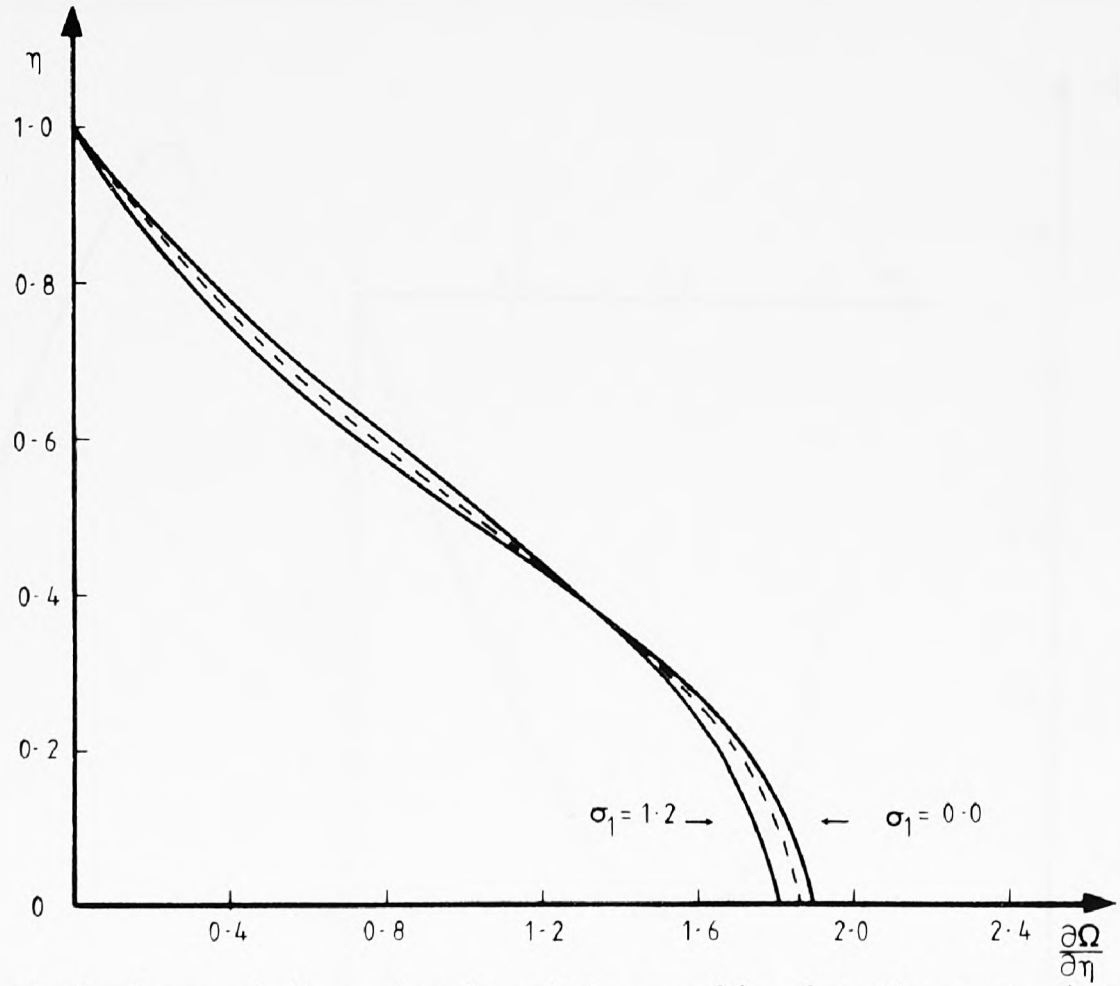

The transverse behaviour of the steady state profile for the curved and straight walled channel, at different positions downstream, with $v = 3{\cdot}572$ *and* $R = 30$.

----- *straight walled* ($m = 0$)

—— *negative curvature* ($m = -1$)

FIG -22

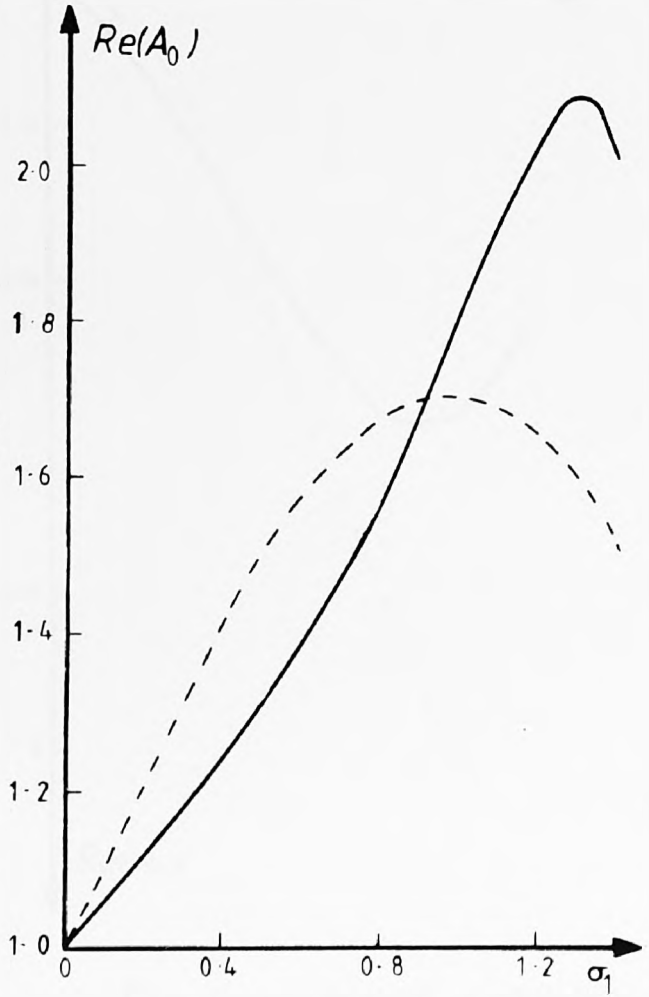

FIG-23a

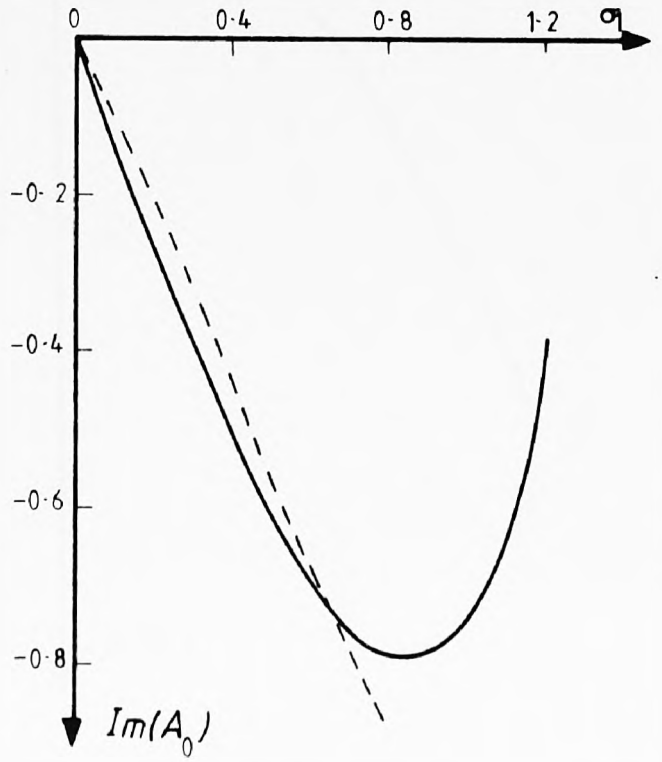

FIG-23b

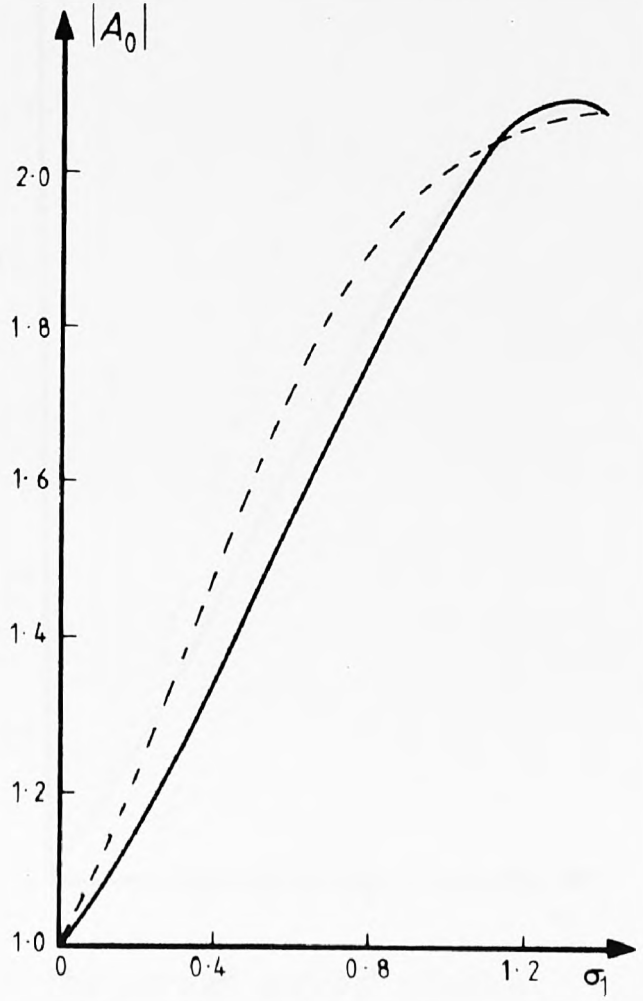

FIG-23c

The downstream development of the amplitude function A_0 for the curved walled channel, with $v = 4{\cdot}093$, $R=30$ and $\beta = 0{\cdot}2$. ----- straight walled (m=0), —— positive curvature (m=1).

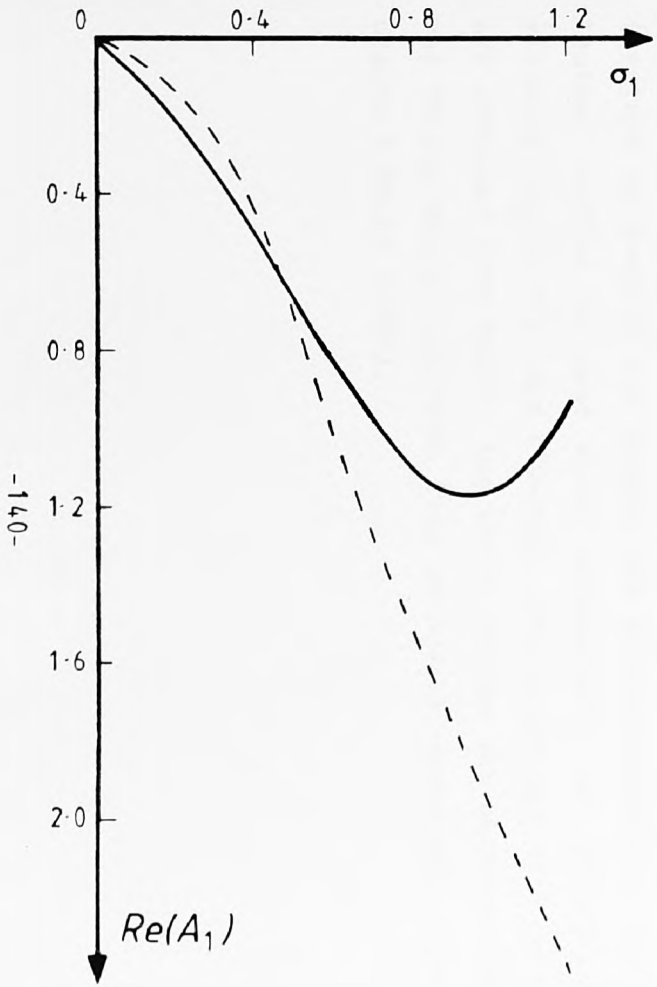

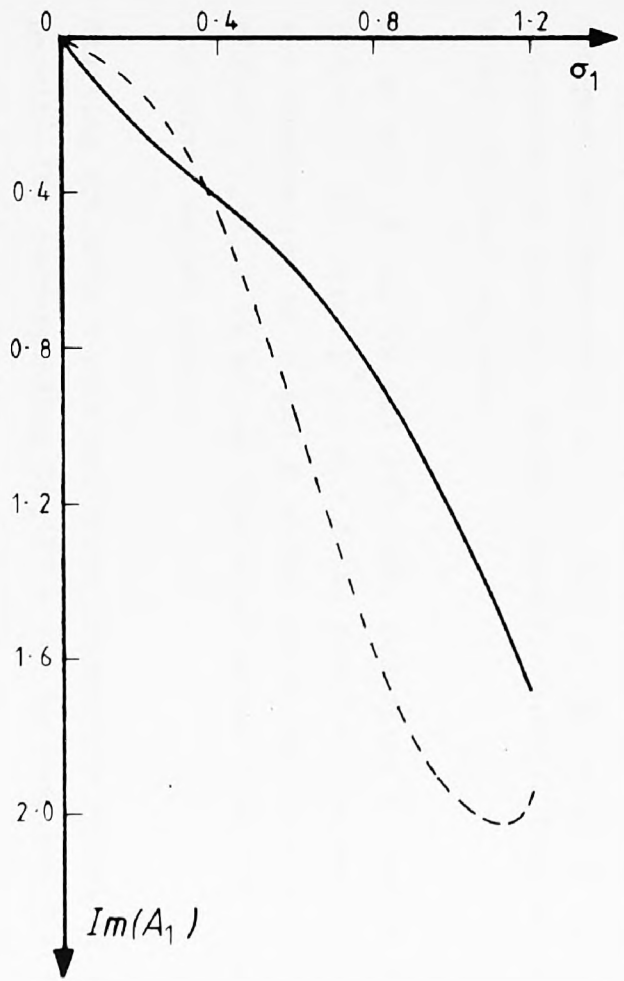

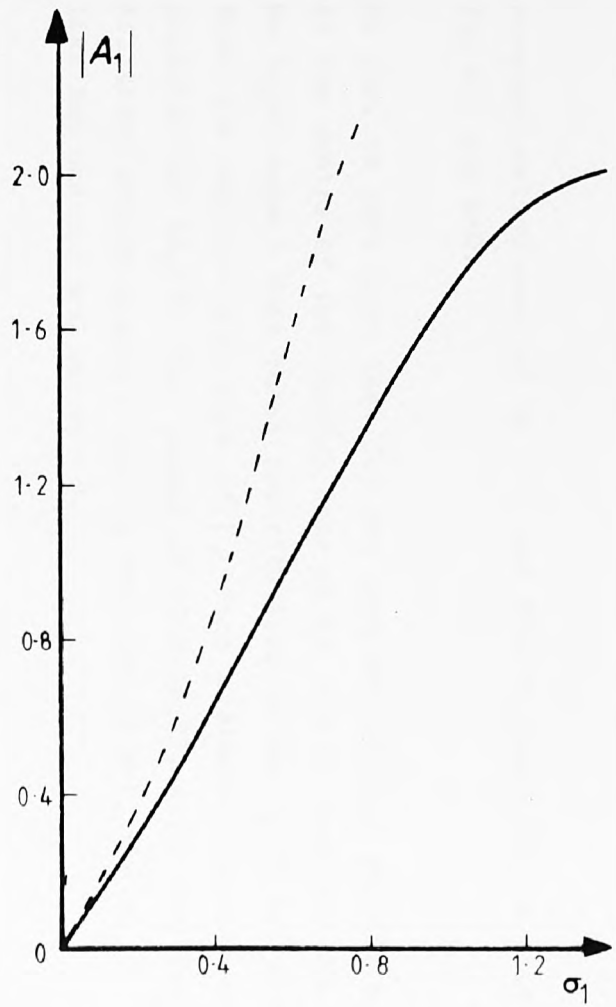

The downstream development of the amplitude function A_1 for the curved walled channel, with $v = 4{\cdot}093$, $R = 30$ and $\beta = 0{\cdot}2$. ----- straight walled ($m=0$), —— positive curvature ($m=1$).

FIG-24a

FIG-24b

FIG-24c

straight walled case at $\sigma_1 = 0$, and FIG-25b, where $|f_1|$ is plotted against σ_1 for m=1 and m=0.

So far, we have seen that for the case m=1, Ω, $|A_0|$ and $|A_1|$ are smaller at the centre of the channel near or at $\sigma_1 = 0$, than for the case m=0. We might expect that these contributions to the $G_\xi(\hat{E})$ are more dominant than the contribution from $|f_1|$, thus a similar feature could be expected for $GR_\xi(\hat{E})$. The graphs of FIGS-26,27, & 28 show this clearly. All these graphs suggest that in the case of m=1, the $GR_\xi(\hat{E})$ is smaller than the case of m=0 at $\sigma_1 = 0$.

To obtain a measure of which of the two cases (m=0, m=1) is more stable at $\sigma_1 = 0$, we compare R-crits. However, in the curved walled channel the non-parallel dependence is not just in β_I, since β and σ_1 appear independently ((4.35), (4.38), (4.40), (4.43)). Thus we can only obtain R-crit for each σ_1 plane.

If we plot β vs. $GR_\xi(\hat{E})$ (FIG-29a) for fixed R, and R vs. $GR_\xi(\hat{E})$ (FIG-29b) for fixed β at $\sigma_1 = 0$ the behaviour becomes clear. We require the combination of R and β which yields $GR_\xi(\hat{E}) = 0$. Thus, using FIGS-16,17,18, & 19 we can obtain estimates of R-crit, (and β-crit) for the curved walled case.

Starting off with R-crit and three consecutive values of β (centred on β-crit) the corresponding $GR_\xi(\hat{E})$'s can be computed for fixed v. A routine which interpolates a β giving the minimum $GR_\xi(\hat{E})$ is obtained (see FIG-19a). With this new β-crit, three consecutive values of R (centred on R-crit) are chosen and the corresponding $GR_\xi(\hat{E})$ computed. Another routine is used which interpolates (or extrapolates) an R yielding $GR_\xi(\hat{E}) = 0$ (see FIG-29b). Thus a new set of R-crit, and β-crit are obtained from which the whole process can be repeated. Convergence was fairly easily achieved. This method is essentially that also used by Eagles & Smith (1980).

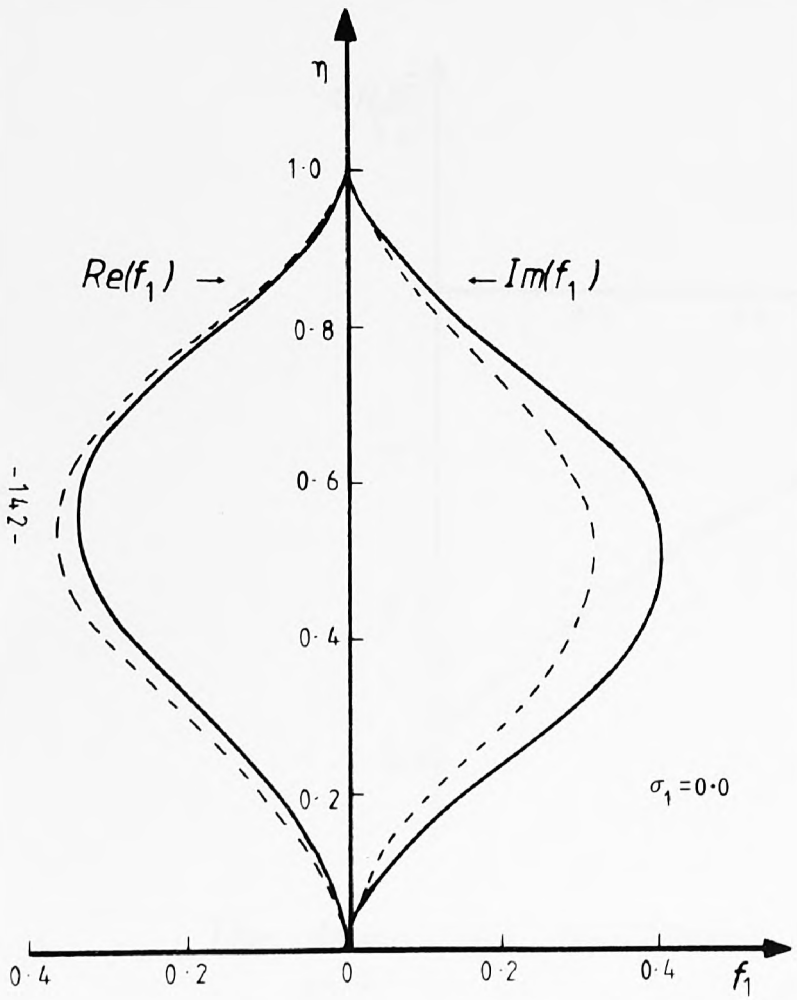

FIG-25a

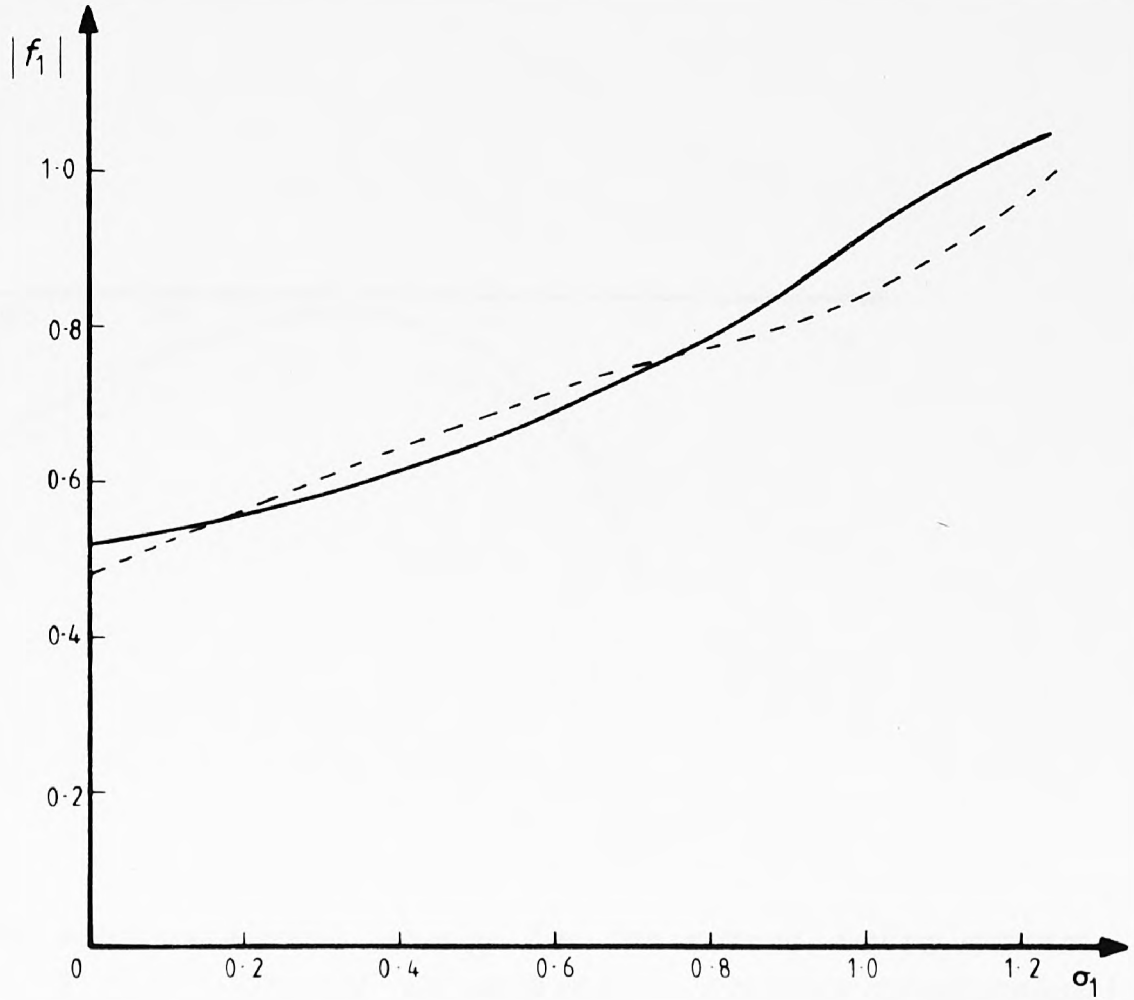

FIG-25b

The downstream development of f_1 with fixed η ($\eta = 0{\cdot}5$) for the curved walled channel with $v = 3{\cdot}572$ $R = 30$ and $\beta = 0{\cdot}2$. ---- straight walled ($m=0$), —— positive curvature ($m=1$).

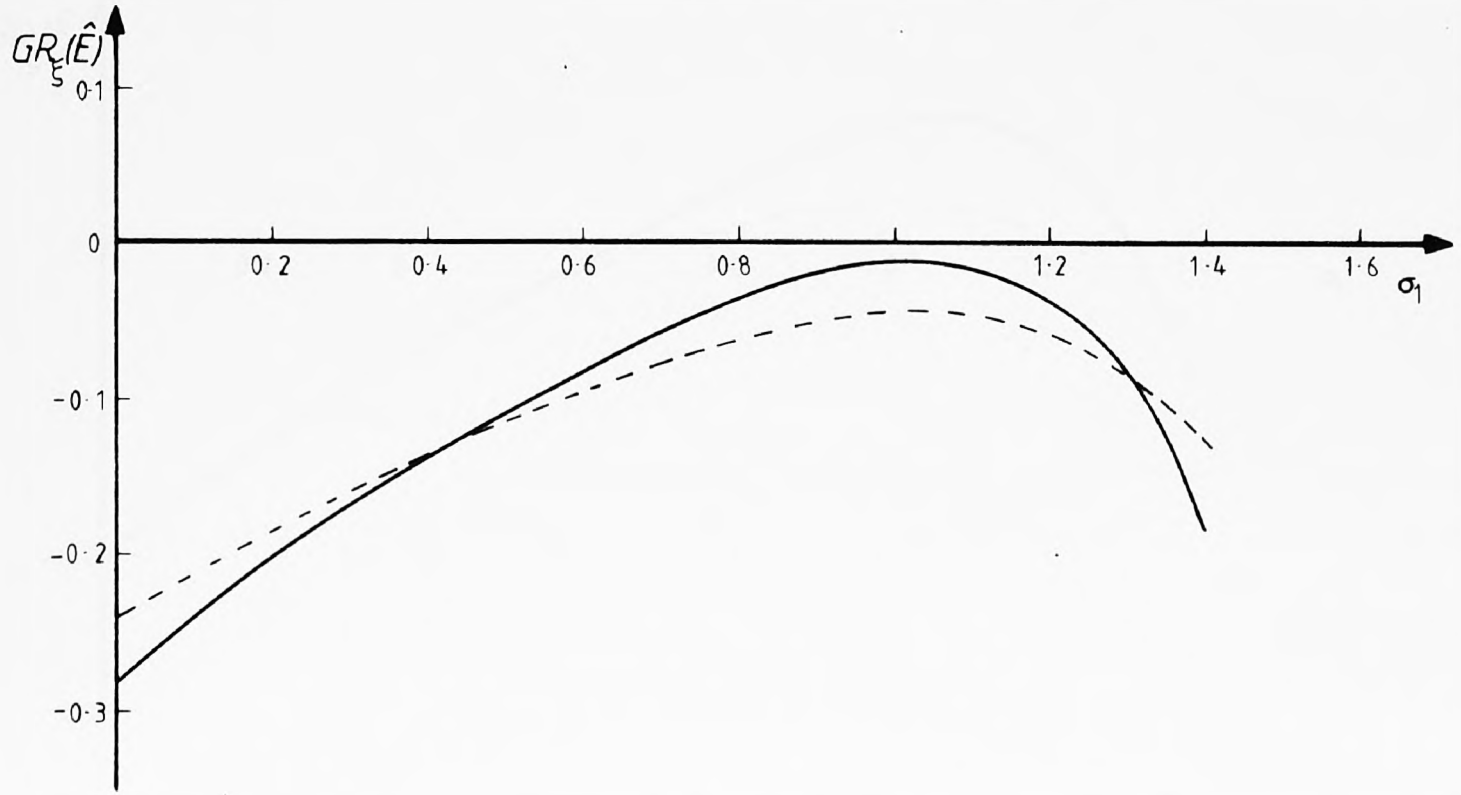

The downstream development of the relative kinetic energy for the curved walled channel, with $v = 3{\cdot}572$, $R = 30$ and $\beta = 0{\cdot}2$. ---- straight walled (m=0) —— positive curvature (m=1).

FIG-26

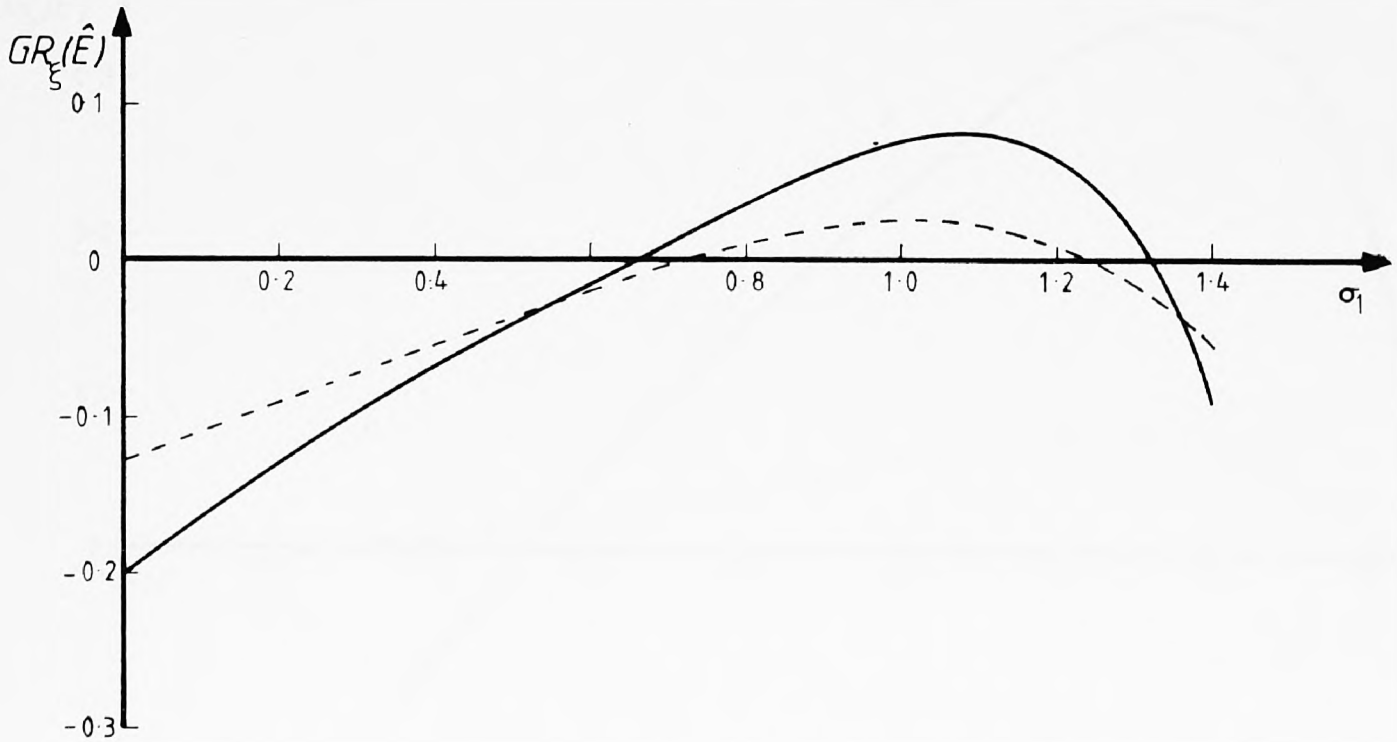

The downstream development of the relative kinetic energy for the curved walled channel, with $v = 4{\cdot}093$, $R = 30$, $\beta = 0{\cdot}2$. ---- *straight walled* $(m = 0)$ —— *positive curvature* $(m = 1)$.

FIG -27

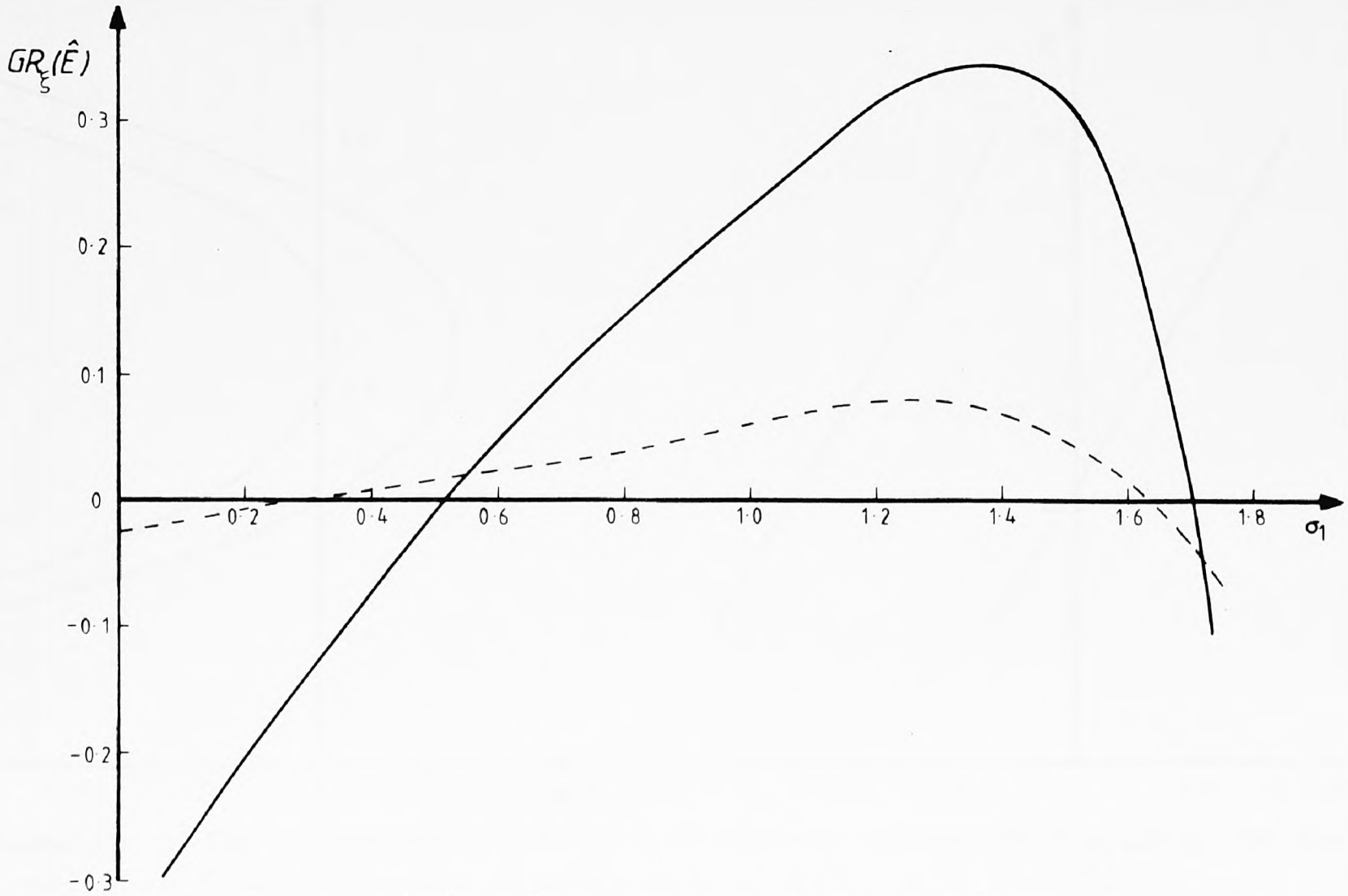

The downstream development of the relative kinetic energy for the curved walled channel, with $v = 4{\cdot}71$, $R = 20$ *and* $\beta = 0{\cdot}12$. ----- *straight walled (m=0)* —— *positive curvature (m=1).*

FIG -28

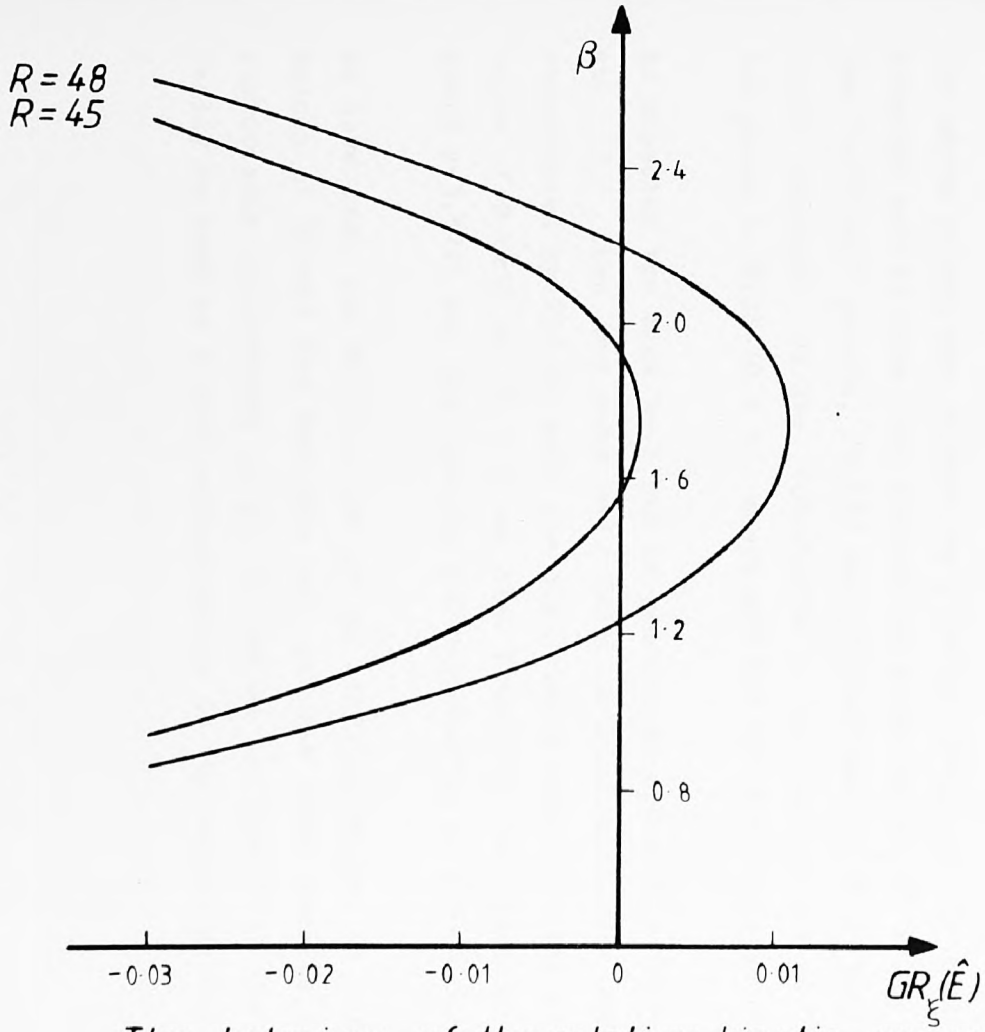

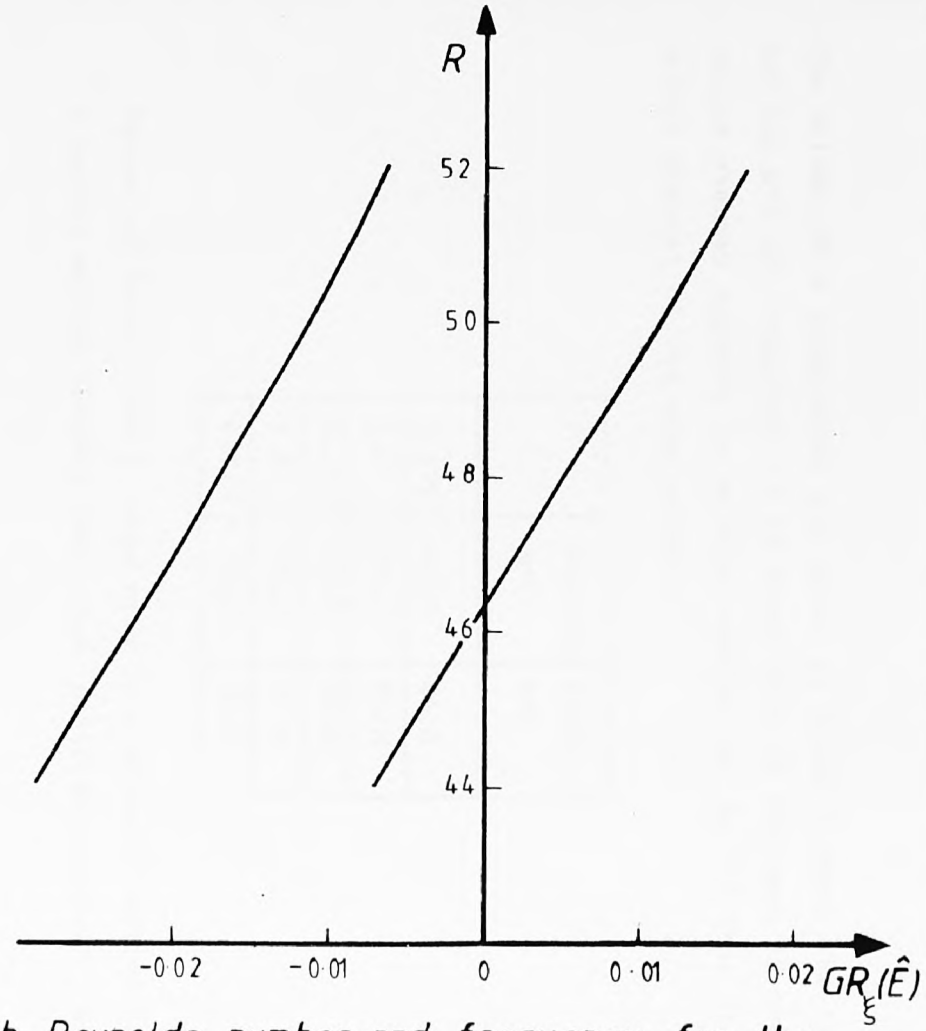

The behaviour of the relative kinetic energy with Reynolds number and frequency, for the curved walled channel (positive curvature m=1), at $\sigma_1 = 0$ with $v = 3{\cdot}572$.

FIG -29a

FIG -29b

The values of v considered are given in TABLE 7 where the two cases of m=0 and m=1 are compared. It is clear that in the case of m=1 the curved walled channel appears to be more stable at $\sigma_1 = 0$ than the straight walled channel of the same angle.

v	R-crit; m=0	R-crit; m=1
3.572	40.5	44.6
3.8	33.4	38.8
4.093	25.5	33.8
4.5	15.2	30.4
4.71	10.2	30.3

Values of R-crit for a range of v in a straight walled (m=0) and a curved walled channel (m=1, i.e. positive curvature) at $\sigma_1 = 0$.

TABLE 7.

The above scheme was checked by a method identical to that used in the straight walled case, but instead of plotting $GR_\xi(\hat{E})$ vs. β_I to establish the "critical" points, $GR_\xi(\hat{E})$ was plotted against β in the plane $\sigma_1 = 0$. These "critical" points contribute to the neutral curves. Two of these are given in FIGS-30 & 31, where m=0 and m=1 are compared at $\sigma_1 = 0$.

As expected the case m=-1 had in general an opposite effect on $|A_0|$, $|A_1|$ and $|f_1|$ than the case m=1. This, coupled with the effect on Ω represented by FIG-22, made the disturbance more unstable at $\sigma_1 = 0$. The value of R-crit at $\sigma_1 = 0$ was also found for the cases m=-1, and m=2 where v=3.572, and the results are represented in FIG-32.

We have used the R-crits for m=0 as starting values to obtain correct values of R-crit for the case m=1, but the final results for m=1 show appreciable differences at $\sigma_1 = 0$, and we conclude that the wedge cannot really be used as a good approximation to the curved walled channel.

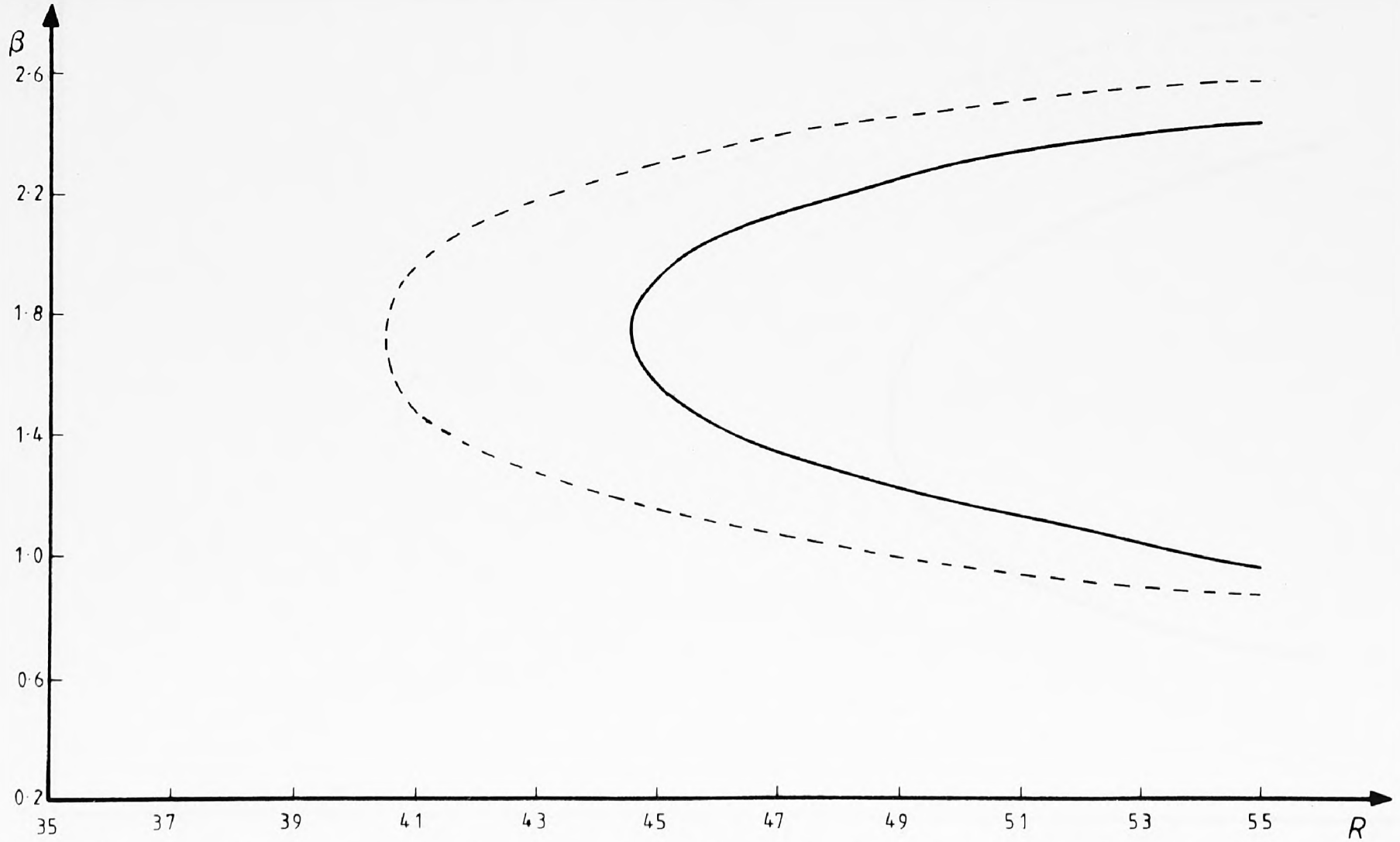

A neutral stability curve for the curved walled channel at $\sigma_1 = 0$ for the case $v = 3 \cdot 572$.
----- straight walled (m=0) *—— positive curvature (m=1)*

FIG-30

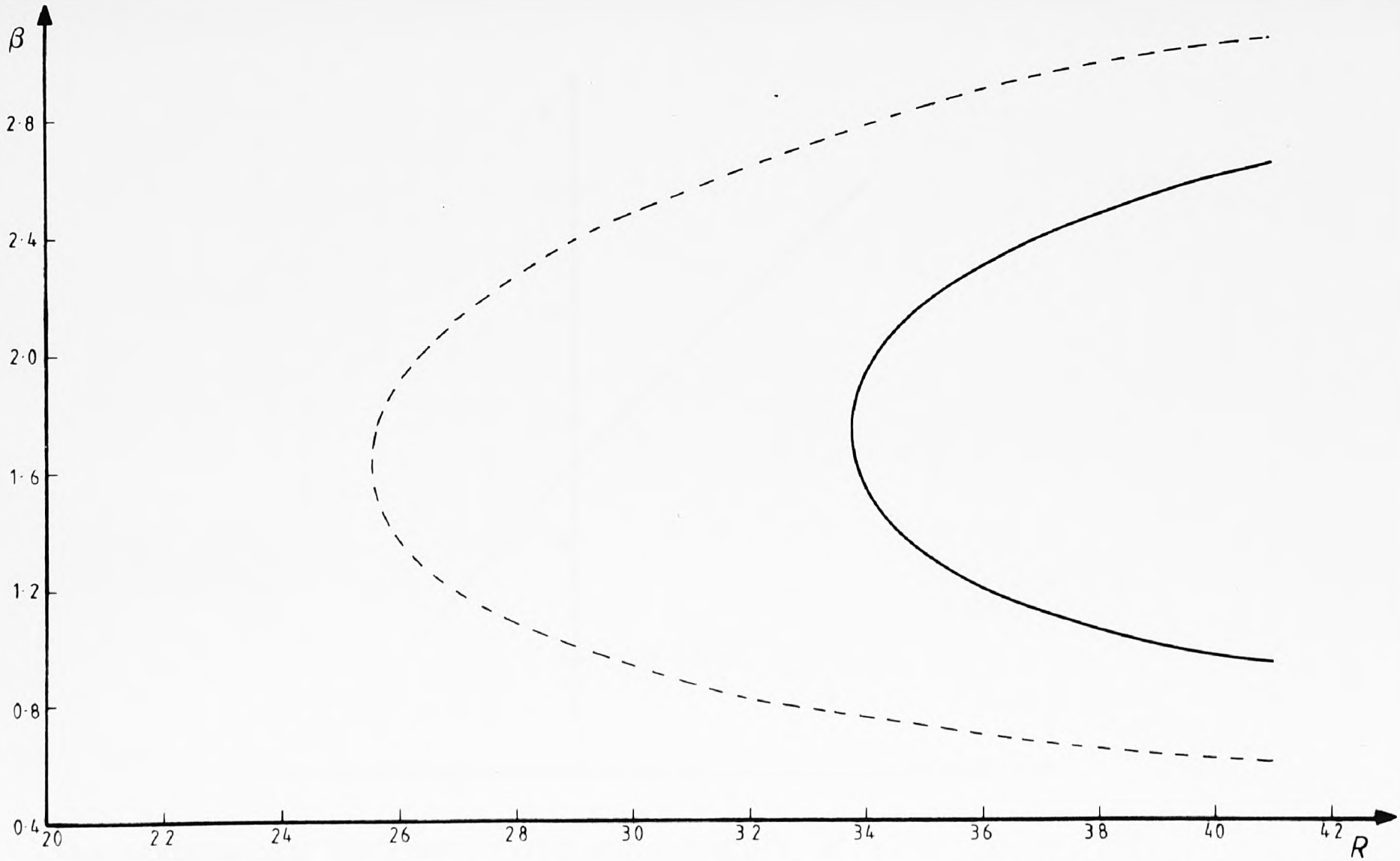

A neutral stability curve for the curve walled channel at $\sigma_1 = 0$ for the case $v = 4{\cdot}093$.
----- straight walled ($m = 0$) FIG-31 —— positive curvature ($m = 1$)

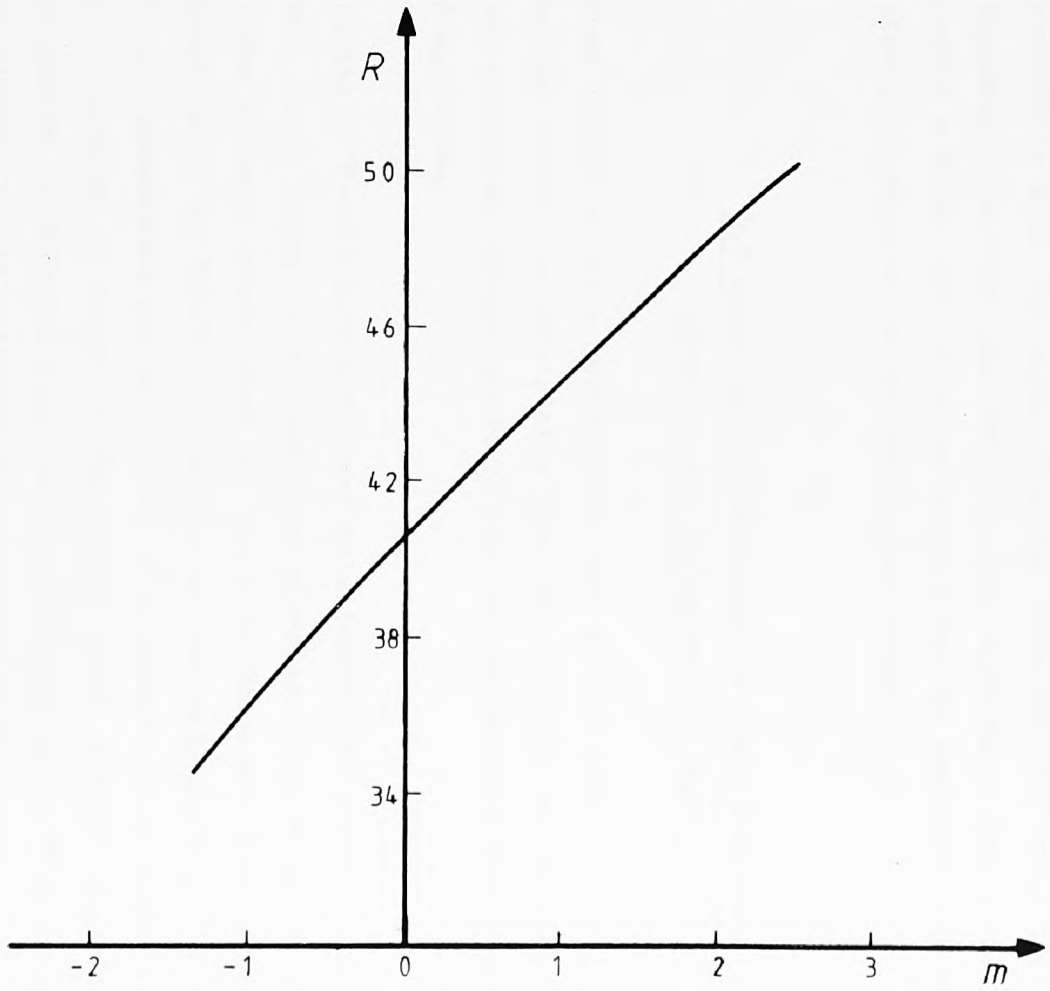

The relationship between R-crit and curvature at $\sigma_1 = 0$ for $v = 3{\cdot}572$.

FIG-32

It is interesting to see what, if anything, predominantly accounts for the shifts in R-crit represented by FIGS-30 & 31. In the case of m=0, a smaller velocity profile along the centre of the channel is clearly associated with a higher R-crit. We could ask "since the velocity profile at $\sigma_1 = 0$ for the case m=1 is smaller than for the case m=0, does this account for most of the increase in R-crit at $\sigma_1 = 0$? To answer this question we could examine what would happen to R-crit in a straight walled channel if the Ω based on m=1 replaced the Ω in m=0, keeping everything else the same. This was done for the cases available and typically, for the case v=3.572, the shift went from R-crit = 40.5 to R-crit = 45.3. this is close to 44.6 and we conclude that the shift is strongly dominated by the particular change in Ω.

6.3 Development Downstream of Fixed Frequency Waves in the Curved Walled Channel.

Even though we have established that in the case of m=1, the curved walled channel is more stable than the straight walled channel at $\sigma_1 = 0$, the situation changes as we follow the disturbance downstream for fixed frequencies.

Values of R-crit have also been established for various σ_1 in the case of m=1, for a range of v. These are given in TABLE 8 for $\sigma_1 = 0.4$ with those already established at $\sigma_1 = 0$. They are also represented graphically in FIG-33. It became increasingly difficult to establish R-crit downstream for all values of v considered in TABLE 8. At $\sigma_1 = 0.8$ for instance, a study of the steady state profile shows it to be excessive in reversed flow for higher values of v. This makes the scheme of finding R-crit untrustworthy for such cases.

v	R-crit; $\sigma_1 = 0$	R-crit; $\sigma_1 = 0{\cdot}4$
3.572	44.6	40.6
3.8	38.8	34.4
4.093	33.8	28.2
4.5	30.4	21.0
4.71	30.3	17.9

Values of R-crit for a range of v at σ_1=0.0 and σ_1=0.4 for the curved walled channel (m=1, i.e positive curvature).

TABLE 8.

Referring to FIG-33 we can see that in the case of v = 4.0 and R = 32 (A) we cannot find frequencies which correspond to the disturbance growing at $\sigma_1 = 0$. However, frequencies exist in which the disturbance grows at $\sigma_1 = 0.4$.

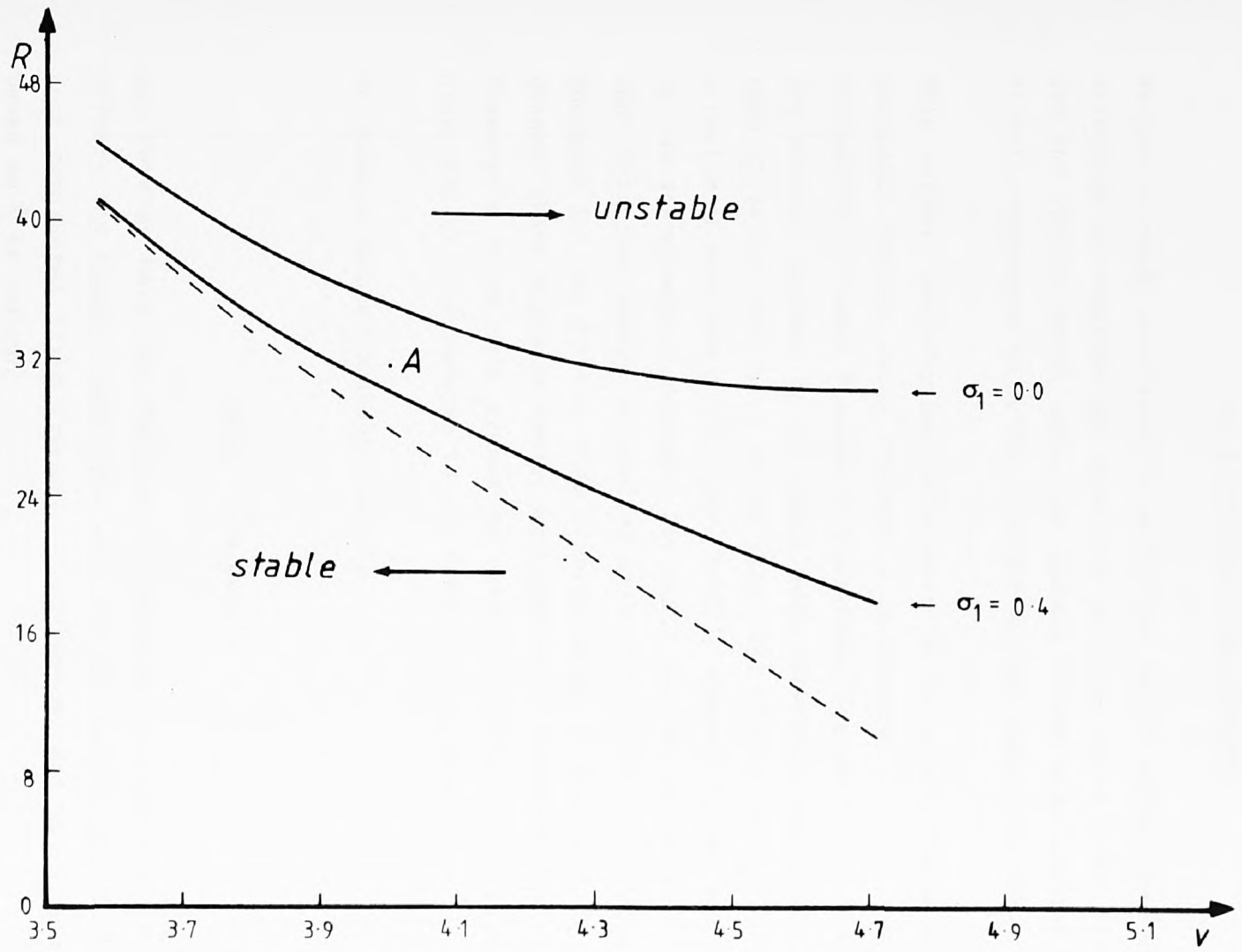

Boundary curves separating stable and unstable flow for the curved walled channel, at different σ_1 planes. ----- straight walled (m=0), ——— positive curvature (m=1).

FIG-33

7. A Fraenkel-Type Channel.

We have already considered a particular curved walled channel, and have attempted to describe the stability of flows whose first approximations are the Jeffery-Hamel ones. The channel chosen also enabled us to make direct comparisons with the straight walled channel of E&W.

This current analysis was undertaken in an attempt to study a more realistic channel using Fraenkel's coordinate system. One difficulty in using Fraenkel's coordinate system is the dimensions of the channel implied by the small wall curvature assumption (Fraenkel 1963 II p411). The ratio of the final and initial throat width contains a factor of $\exp(\tanh\sigma/\varepsilon^{1/2})$ (see (7.43)), where σ is defined by (7.7) and is the downstream coordinate. For small typical values of $\varepsilon^{1/2}$ (say 0.1), such that the theory is applied with confidence, the ratio becomes 'enormous' for say $\sigma = 1.0$. This problem makes it difficult to construct a channel which might be tested experimentally. Nevertheless, we have used Fraenkel's coordinate system to obtain quantitative results of the stability of disturbances to the steady state flow.

We chose a channel characterised by

$$\alpha(\tau) = \varepsilon^{1/2} m_1 \operatorname{sech}^2\tau \qquad ,(7.1)$$

and here we have the facility of choosing any position in which to perturb the steady state flow with our new definition of σ (7.7). We have considered fixed frequency disturbances and established R-crits based on $\hat{E}$ as before.

We note that the channels defined by (7.1) satisfy the conditions required by Fraenkel (1963 II p.403). That is $\alpha(\tau) \rightarrow$ real constant values as $\sigma \rightarrow \pm \infty$ and $\alpha(\tau)$ is real on $\eta = 0$. We refer to this channel as a Fraenkel-type channel.

All the equations and results have been taken up to and including the $O(\varepsilon)$ terms. We have finally compared R-crits predicted by including the $O(\varepsilon)$ terms with those predicted by including only the $O(\varepsilon^{1/2})$ terms.

For the sake of simplicity, we have used the same notation as before, but we bear in mind that the functions are not the same.

7. The Steady State Equations.

We use (2.18a) as before and substitute (4.4) into it. This form of $\alpha(\tau)$ gives us

$$\kappa = \varepsilon^{1/2} m_1 \operatorname{sech}^2\sigma \, (1 + O(\varepsilon^2)) \qquad ,(7.2)$$

and

$$\lambda = \varepsilon^{1/2} 2m_1 \operatorname{sech}^2\sigma \tanh\sigma \, (1 + O(\varepsilon^2)) \qquad ,(7.3)$$

The resulting equations for Ω_0, Ω_1 and Ω_2 are as follows :

$O(1)$

$$\frac{\partial^4\Omega_0}{\partial\eta^4} + 2vm_1\operatorname{sech}^2\sigma\left(\frac{\partial\Omega_0}{\partial\eta}\frac{\partial^2\Omega_0}{\partial\eta^2}\right) = 0 \qquad ,(7.4)$$

$O(\varepsilon^{1/2})$

$$\frac{\partial^4\Omega_1}{\partial\eta^4} + 2vm_1\operatorname{sech}^2\sigma\,\frac{\partial}{\partial\eta}\left(\frac{\partial\Omega_0}{\partial\eta}\frac{\partial\Omega_1}{\partial\eta}\right) = v\left(\frac{\partial\Omega_0}{\partial\eta}\frac{\partial^2\Omega_0}{\partial\eta^2} - \frac{\partial\Omega_0}{\partial\eta}\frac{\partial^3\Omega_0}{\partial\eta^3}\right) \qquad ,(7.5)$$

$O(\varepsilon)$

$$\frac{\partial^4\Omega_2}{\partial\eta^4} + 2vm_1\,\mathrm{sech}^2\sigma\,\frac{\partial}{\partial\eta}\left(\frac{\partial\Omega_0}{\partial\eta}\frac{\partial\Omega_2}{\partial\eta}\right) = v\left(\frac{\partial\Omega_0}{\partial\eta}\frac{\partial^3\Omega_1}{\partial\sigma\partial\eta^2} + \frac{\partial\Omega_1}{\partial\eta}\frac{\partial^3\Omega_0}{\partial\eta^3} - \frac{\partial\Omega_0}{\partial\sigma}\frac{\partial^3\Omega_1}{\partial\eta^3}\right.$$

$$\left. - \frac{\partial\Omega_1}{\partial\sigma}\frac{\partial^3\Omega_0}{\partial\eta^3} - 2m_1\,\mathrm{sech}^2\sigma\,\frac{\partial\Omega_1}{\partial\eta}\frac{\partial^2\Omega_1}{\partial\eta^2}\right)$$

$$- 4m_1^2\,\mathrm{sech}^2\sigma\,\frac{\partial^2\Omega_0}{\partial\eta^2} \qquad .(7.6)$$

The boundary conditions are identical to (4.5b)-(4.7b).

The similarity here with (4.5a)-(4.7a) is not surprising when one considers that the terms previously containing $(1+m\sigma)$ now contain $m_1\,\mathrm{sech}^2\sigma$. These terms arise directly from the $\alpha(\tau)$ chosen.

The steady state equations are valid for all σ. We introduce two new parameters now, σ_0 and σ_1, defined by

$$\sigma = \sigma_0 + \varepsilon^{1/2}\sigma_1 \qquad ,(7.7)$$

where σ_0 is a constant and we emphasize that the slow variable σ_1 is not the same as the previous σ_1, here it is defined explicitly by (7.7). From our previous work we know it was necessary to introduce the other slow variable σ_1 in order to ensure boundedness of h in the time perturbation analysis. With this new definition we shall be expanding Ω_0, Ω_1 and Ω_2 about $\sigma = \sigma_0$ and not about $\sigma = 0$. There was no virtue in doing this for the previous constantly (signed curvature channel, as changing $\varepsilon^{1/2}$ effectively achieved the same thing, that is, increasing or decreasing the angle of divergence at $\sigma_1 = 0$. Here however, the "bottle-neck" characteristic of this Fraenkel-type channel (FIG-34) makes it ideal

for this approach. We can choose any starting position in which to perturb the steady state flow.

One important result from (7.7) is that

$$\frac{\partial}{\partial \xi} = \varepsilon^{1/2} \frac{\partial}{\partial \sigma_1} \qquad ,(7.8)$$

which is the same as before.

Using a Taylor series expansion of Ω_0, Ω_1, and Ω_2 about $\sigma = \sigma_0$, and expanding $\mathrm{sech}^2\sigma$ in powers of $\varepsilon^{1/2}$ we can obtain equations for the functions G_0, G_1, G_2, F_0, F_1, and H_0 as before (i.e. (4.9)-(4.11)). All the boundary conditions are the same and we quote these equations for the purpose of comparing with the previous analysis. They are

$$\frac{d^4G_0}{d\eta^4} + 2vm_1\,\mathrm{sech}^2\sigma_0 \; \frac{dG_0}{d\eta}\frac{d^2G_0}{d\eta^2} = 0 \qquad ,(7.9)$$

$$\frac{d^4G_1}{d\eta^4} + 2vm_1\,\mathrm{sech}^2\sigma_0 \frac{d}{d\eta}\left(\frac{dG_0}{d\eta}\frac{dG_1}{d\eta}\right) = v4m_1\,\mathrm{sech}^2\sigma_0\,\mathrm{Tanh}\sigma_0 \frac{dG_0}{d\eta}\frac{d^2G_0}{d\eta^2} \qquad ,(7.10)$$

$$\begin{aligned}\frac{d^4G_2}{d\eta^4} + 2vm_1\,\mathrm{sech}^2\sigma_0 \frac{d}{d\eta}\left(\frac{dG_0}{d\eta}\frac{dG_2}{d\eta}\right) &= -2vm_1\,\mathrm{sech}^2\sigma_0 \cdot \frac{dG_1}{d\eta}\frac{d^2G_1}{d\eta^2} \\ &+ v4m_1\,\mathrm{sech}^2\sigma_0\,\mathrm{Tanh}\sigma_0 \frac{dG_0}{d\eta}\frac{d^2G_1}{d\eta^2} \\ &+ v4m_1\,\mathrm{sech}^2\sigma_0\,\mathrm{Tanh}\sigma_0 \frac{dG_1}{d\eta}\frac{d^2G_0}{d\eta^2} \\ &- 2vm_1\,\mathrm{sech}^2\sigma_0\,(3\mathrm{Tanh}^2\sigma_0 - 1)\frac{dG_0}{d\eta}\frac{d^2G_0}{d\eta^2} \qquad ,(7.11)\end{aligned}$$

$$\frac{d^4F_0}{d\eta^4} + 2vm_1\,\mathrm{sech}^2\sigma_0\frac{d}{d\eta}\left(\frac{dG_0}{d\eta}\frac{dF_0}{d\eta}\right) = v\left(\frac{dG_0}{d\eta}\frac{d^2G_1}{d\eta^2} - G_1\frac{d^3G_0}{d\eta^3}\right) \quad ,(7.12)$$

$$\begin{aligned}\frac{d^4F_1}{d\eta^4} + 2vm_1\,\mathrm{sech}^2\sigma_0\frac{d}{d\eta}\left(\frac{dG_0}{d\eta}\frac{dF_1}{d\eta}\right) &= v\left(2\frac{dG_0}{d\eta}\frac{d^2G_2}{d\eta^2} + \frac{dG_1}{d\eta}\frac{d^2G_1}{d\eta^2} - G_1\frac{d^3G_1}{d\eta^3}\right.\\ &\quad - 2G_2\frac{d^3G_0}{d\eta^3} - 2m_1\mathrm{sech}^2\sigma_0\frac{dF_0}{d\eta}\frac{d^2G_1}{d\eta^2}\\ &\quad - 2m_1\mathrm{sech}^2\sigma_0\frac{dG_1}{d\eta}\frac{d^2F_0}{d\eta^2}\\ &\quad + 4m_1\mathrm{sech}^2\sigma_0\,\mathrm{Tanh}\sigma_0\frac{dG_0}{d\eta}\frac{d^2F_0}{d\eta^2}\\ &\quad \left. + 4m_1\,\mathrm{sech}^2\sigma_0\,\mathrm{Tanh}\sigma_0\frac{dF_0}{d\eta}\frac{d^2G_0}{d\eta^2}\right) \quad ,(7.13)\end{aligned}$$

$$\begin{aligned}\frac{d^4H_0}{d\eta^4} + 2vm_1\,\mathrm{sech}^2\sigma_0\frac{d}{d\eta}\left(\frac{dG_0}{d\eta}\frac{dH_0}{d\eta}\right) &= v\left(\frac{dG_0}{d\eta}\frac{d^2F_1}{d\eta^2} + \frac{dF_0}{d\eta}\frac{d^2G_1}{d\eta^2} - G_1\frac{d^3F_0}{d\eta^3}\right.\\ &\quad \left. - F_1\frac{d^3G_0}{d\eta^3} - 2m_1\,\mathrm{sech}^2\sigma_0\frac{dF_0}{d\eta}\frac{d^2F_0}{d\eta^2}\right)\\ &\quad - 4m_1\,\mathrm{sech}^4\sigma_0\frac{d^2G_0}{d\eta^2} \quad .(7.14)\end{aligned}$$

An interesting consistency can be observed between (7.9)-(7.14) and the equations (4.13a)-(4.18a). The equation for G_2 contains an additional term $-2vm_1\mathrm{sech}^2\sigma_0(3\tanh^2\sigma_0 - 1)\frac{dG_0}{d\eta}\frac{d^2G_0}{d\eta^2}$, this extra term can be shown to come from the fact that the curvature is varying (more generally here, and in this case directly from the $O(\varepsilon)$ term in the expansion of $\mathrm{sech}^2\sigma$ in ascending powers of $\varepsilon^{1/2}$. This consistency is explicitly realized when (3.7) is modified to

$$\alpha(\tau) = 1\varepsilon^{1/2} + \varepsilon^{1/2}m\tau \quad .(7.15)$$

The parameter 1 was always taken to be unity in the previous analysis. Here, it can be used as a transformation parameter.From an algebraic and hence computational point of view, the choice of

$$1 = m_1 \operatorname{sech}^2 \sigma_0 \qquad ,(7.16)$$

and

$$m = -2m_1 \operatorname{sech}^2 \sigma_0 \tanh \sigma_0 \qquad ,(7.17)$$

makes the two systems equivalent with the exeption of the additional term arising from curvature in G_2 .

7.2 The Time-dependent Equations.

The overall scheme is the same as before, but the resulting form of h (7.38) makes it necessary to define Φ in a slightly different way. The term $h^2 \frac{\partial}{\partial t}(D^2\Phi)$in (2.19a) will now only be bounded if we choose Φ in the following way,

$$\Phi(\xi,\eta,t) = \Phi(\sigma_1,\eta;\sigma_0)\exp\left[i\left\{\Theta(\xi) - \beta\exp(-2m_1 \tanh \sigma_0/\varepsilon^{1/2})t\right\}\right] + \text{c.c} \qquad .(7.18)$$

The factor $\exp(-2m_1 \tanh \sigma_0/\varepsilon^{1/2})$ can be removed by introducing a new time variable t' (which is different for each σ_0) where

$$t' = \exp(-2m_1 \tanh \sigma_0/\varepsilon^{1/2})t \qquad ,(7.18a)$$

and is the dimensionless time, scaled on the channel half width at σ_0. Thus β in (7.18) is a "locally non-dimensionalized" frequency.

Proceeding as before we obtain

$O(1)$

$$L\Phi_0 = 0 \qquad ,(7.19)$$

$$L \equiv \frac{1}{R}(D_1^2 - k^2) + i\left(\beta_I - k\frac{dG_0}{d\eta}\right)(D_1^2 - k^2) + ik\frac{d^3G_0}{d\eta^3} \qquad ,(7.20)$$

where

$$\beta_I = \beta \exp(2m_1\sigma_1 \operatorname{sech}^2\sigma_1) \qquad .(7.21)$$

$O(\varepsilon^{1/2})$

$$L\Phi_1 = L_1\frac{\partial\Phi_0}{\partial\eta} + \frac{dk}{d\sigma_1}L_2\Phi_0 + (L_3 + L_4)\Phi_0 \qquad ,(7.22)$$

where

$$L_1 \equiv \frac{-4ik}{R}(D_1^2 - k^2) + 2k\beta_I + \frac{dG_0}{d\eta}(D_1^2 - 3k^2) - \frac{d^3G_0}{d\eta^3} \qquad ,(7.23)$$

$$L_2 \equiv \frac{-2i}{R}(D_1^2 - 3k^2) + \beta_I - 3k\frac{dG_0}{d\eta} \qquad ,(7.24)$$

$$L_3 \equiv m_1 \operatorname{sech}^2\sigma_0\left\{\frac{4ik}{R}(D_1^2 - k^2) - \left[\frac{2dG_0}{d\eta} - 2i\beta_I\sigma_1^2\tanh\sigma_0\right](D_1^2 - k^2) - 2\frac{d^2G_0}{d\eta^2}D_1\right\}, \qquad (7.25)$$

$$L_4 \equiv ik\left\{\frac{dF_0}{d\eta} + \sigma_1\frac{dG_1}{d\eta}\right\}(D_1^2 - k^2) - ik\left\{\frac{d^3F_0}{d\eta^3} + \sigma_1\frac{d^3G_1}{d\eta^3}\right\} \qquad .(7.26)$$

$O(\varepsilon)$

$$L\Phi_2 = L_1\frac{\partial\Phi_1}{\partial\sigma_1} + \frac{dk}{d\sigma_1}L_2\Phi_1 + (L_3 + L_4)\Phi_1$$

$$+(M_1 + M_2)\frac{\partial\Phi_0}{\partial\sigma_1} + \frac{dk}{d\sigma_1}(M_3 + M_4)\Phi_0 + \frac{dk}{d\sigma_1}M_5\frac{\partial\Phi_0}{\partial\sigma_1}$$

$$+\left(M_6 + M_7 + M_8 + \frac{d^2k}{d\sigma_1^2}\left(\frac{4k}{R} + i\frac{dG_0}{d\eta}\right) + \frac{3}{R}\left[\frac{dk}{d\sigma_1}\right]^2\right) - iL_2\frac{\partial^2\Phi_0}{\partial\sigma_1^2} \qquad ,(7.27)$$

where

$$M_1 \equiv \frac{4m_1 \operatorname{sech}^2\sigma_0}{R}(D_1^2-3k^2) - 4m_1 \operatorname{sech}^2\sigma_0\left[ik\frac{dG_0}{d\eta} + \beta_I k\sigma_1 \tanh\sigma_0\right] \quad ,(7.28)$$

$$M_2 \equiv \left[\frac{dF_0}{d\eta} + \sigma_1\frac{dG_1}{d\eta}\right](D_1^2-3k^2) - \left[\frac{d^3F_0}{d\eta^3} + \sigma_1\frac{d^3G_1}{d\eta^3}\right] \quad ,(7.29)$$

$$M_3 \equiv -m_1 \operatorname{sech}^2\sigma_0\left[\frac{12k}{R} + 2i\frac{dG_0}{d\eta} + 2\sigma_1^2\tanh\sigma_0\right]\beta_I \quad ,(7.30)$$

$$M_4 \equiv -3k\left[\frac{dF_0}{d\eta} + \sigma_1\frac{dG_1}{d\eta}\right] \quad ,(7.31)$$

$$M \equiv \frac{12k}{R} + 3i\frac{dG_0}{d\eta} \quad ,(7.32)$$

$$\begin{aligned} M_6 \equiv\ & 4m_1\operatorname{sech}^2\sigma_0\left[\sigma_1\frac{dG_0}{d\eta}\tanh\sigma_0 - \frac{m_1}{R}\operatorname{sech}^2\sigma_0 - \frac{2\sigma_1}{R}\tanh\sigma_0 ik\right](D_1^2-k^2) \\ & - i\beta_I m_1\left[\frac{2\sigma_1^3}{3}(1+2\tanh^2\sigma_0) + 2m_1\sigma_1^4\tanh^2\sigma_0\operatorname{sech}^4\sigma_0\right](D_1^2-k^2) \\ & + 4m_1\sigma_1\operatorname{sech}\sigma_0\tanh\sigma_0\frac{d^2G_0}{d\eta^2}D_1 \end{aligned} \quad ,(7.33)$$

$$\begin{aligned} M_7 \equiv\ & -\left[2m_1\operatorname{sech}^2\sigma_0\left\{\frac{dF_0}{d\eta} + \sigma_1\frac{dG_1}{d\eta}\right\} + G_1D_1\right](D_1^2-k^2) \\ & + \left[\frac{d^2G_1}{d\eta} - 2m_1\operatorname{sech}^2\sigma_0\left\{\frac{d^2F_0}{d\eta} + \sigma_1\frac{d^2G_0}{d\eta}\right\}\right]D_1 \end{aligned} \quad ,(7.34)$$

$$M_8 \equiv ik\left[\frac{dH_0}{d\eta} + \sigma_1\frac{dF_1}{d\eta} + \sigma_1^2\frac{dG_2}{d\eta}\right](D_1^2-k^2) - ik\left[\frac{d^3H_0}{d\eta^3} + \sigma_1\frac{d^3F_1}{d\eta^3} + \sigma_1^2\frac{d^3G_2}{d\eta^3}\right] \quad .(7.35)$$

If the previous time-dependent analysis was carried out using the modified form of $\alpha(\tau)$, (7.15), then the transformations given by (7.16) and (7.17) make the equations (4.38)-(4.45) equivalent to (7.28)-(7.35), with the exception of the additional term in M_6, that is $-i\beta_I m_1(\frac{2\sigma_1^3}{3}(1+2\tanh^2\sigma_0))(D_1^2-k^2)$ which naturally arises from the extra term already discused in G_2 (7.11).

Thus the two transformations (7.16) and (7.17) made it convenient to modify the existing computer program from the previous analysis, to study the stability of this Fraenkel-type channel.

7.3 The Channel.

We can obtain semi-analytic expressions for the coordinates of the channel by recalling (2.8) and using (7.1) for $\alpha(\tau)$. On integrating (2.8) and using (2.7) we obtain

$$h = K_1 \exp(m_1 \tanh\sigma/\varepsilon^{1/2})(1+0(\varepsilon^{3/2})) \qquad ,(7.36)$$

$$\vartheta = \eta\,\alpha(\sigma)\ (1+0(\varepsilon^{5/2})) \qquad .(7.37)$$

The interpretation of h and ϑ have already been discussed in an earlier chapter. The necessary asymptotic expansion of h in ascending powers of can be obtained by expanding $\tanh\sigma$ in terms of σ_0 and σ_1. It is quoted here as it determines the form of Φ already given in (7.18).

$$h = K_1 \exp(m_1 \tanh\sigma_0/\varepsilon^{1/2})\ \exp(m_1\sigma_1 \operatorname{sech}^2\sigma_0)\left[1-\varepsilon^{1/2}m_1\sigma_1^2 \tanh\sigma_0 \operatorname{sech}^2\sigma_0\right.$$
$$\left.+\varepsilon\left[\frac{m_1\sigma_1^3}{3}(1+2\tanh^2\sigma_0) + \frac{m_1^2\sigma_1^4}{2}(\tanh^2\sigma_0\operatorname{sech}^4\sigma_0)\right]\right] \qquad .(7.38)$$

Continuing and integrating (2.8) once more we obtain the expression for z,

$$z = \frac{K_1}{\varepsilon}\int_{\sigma_0}^{\tau} \exp(m_1 \tanh s/\varepsilon^{1/2})\ ds \ + K_2 \qquad .(7.39)$$

The constants K_1 and K_2 are real and again correspond to different z scales and choice of origin respectively.

We can reduce (7.39) to an integral of a complex function along a real path and show that, if we choose some starting position $S(\sigma_0,0)$ along the centre of the channel, and if $P(\sigma_p,0)$ and $Q(\sigma_p,\eta)$ are two points corresponding to $(x_p,0)$ and (x_Q,y_Q) then

$$x_Q - x_p = \frac{K_1 \exp(m_1 \tanh\sigma_p/\varepsilon^{1/2})}{\alpha(\sigma_p)}\left[\cos(\alpha(\sigma_p)\eta)-1\right]\left[1+0(\varepsilon^{3/2})\right] \quad ,(7.40)$$

$$y_Q = \frac{K_1 \exp(m_1 \tanh\sigma_p/\varepsilon^{1/2})}{\alpha(\sigma_p)}\left[\sin(\alpha(\sigma_p)\eta)\right]\left[(1+0(\varepsilon^{3/2})\right] \quad ,(7.41)$$

where $$x_p = \frac{K_1}{\varepsilon}\int_{\sigma_0}^{\sigma_p} \exp(m_1 \tanh s_1/\varepsilon^{1/2})\, ds_1 + K_2 \quad .(7.42)$$

The difficulty mentioned earlier in using Fraenkel's coordinate system is exemplified by (7.41). If the initial throat width W_I is at $(\sigma_0,1)$ and the final throat width W_F is at $(\sigma,1)$, then the ratio of W_F to W_I is given by

$$\frac{W_F}{W_I} = \frac{\exp(m_1(\tanh\sigma - \tanh\sigma_0)/\varepsilon^{1/2})\, \sin(\varepsilon^{1/2} m_1 \operatorname{sech}^2\sigma_0)\operatorname{sech}^2\sigma_0}{\sin(\varepsilon^{1/2} m_1 \operatorname{sech}^2\sigma_0)\operatorname{sech}^2\sigma_0} \quad ,(7.43)$$

and we can see that it is independent of K_1. For very large values of σ_0, $\sigma_0 \sim \sigma$ and (7.43) is close to the value 1, in fact we are in a region where the walls are nearly parallel, and this is to be expected. However, for a choice of $\varepsilon^{1/2} = 0.1$, $m_1 = 1$, $\sigma_0 = -0.2$ and $\sigma = 1.08$, a case in which more interesting phenomena (such as separation) is more likely

to occur, since we pass through the region where the angle of divergence assumes its maximum value at $\sigma_0 = 0$, this ratio is of the order of 20,000.

$$x_Q(\sigma_0, 0) = 0 \qquad ,(7.44a)$$

and

$$y_Q(\sigma_0, 0) = 0 \qquad ,(7.44b)$$

we obtain

$$K_2 = 0 \qquad ,(7.45)$$

and without loss of generality if we define W_I by

$$W_I = \frac{\exp(m_1 \tanh\sigma_0/\varepsilon^{1/2}) \sin(\varepsilon^{1/2} m_1 \operatorname{sech}^2\sigma_0)}{\varepsilon^{1/2} m_1 \operatorname{sech}^2\sigma_0} \qquad ,(7.46)$$

then

$$K_1 = 1 \qquad .(7.47)$$

The physical coordinates of a variety of such channels were computed using Simpson's rule applied to integrals along complex paths. The results were checked using the approximate expressions (7.40)-(7.42).

For a particular choice of parameters, $\varepsilon^{1/2}=0.4$ and $m_1 = 1$, this Fraenkel-type channel is given in FIG-34.

7.4 The Results.

The overall scheme here was to consider fixed values of v and establish the R-crits based on $GR_\xi(\hat{E})$ at various σ stations. From these results

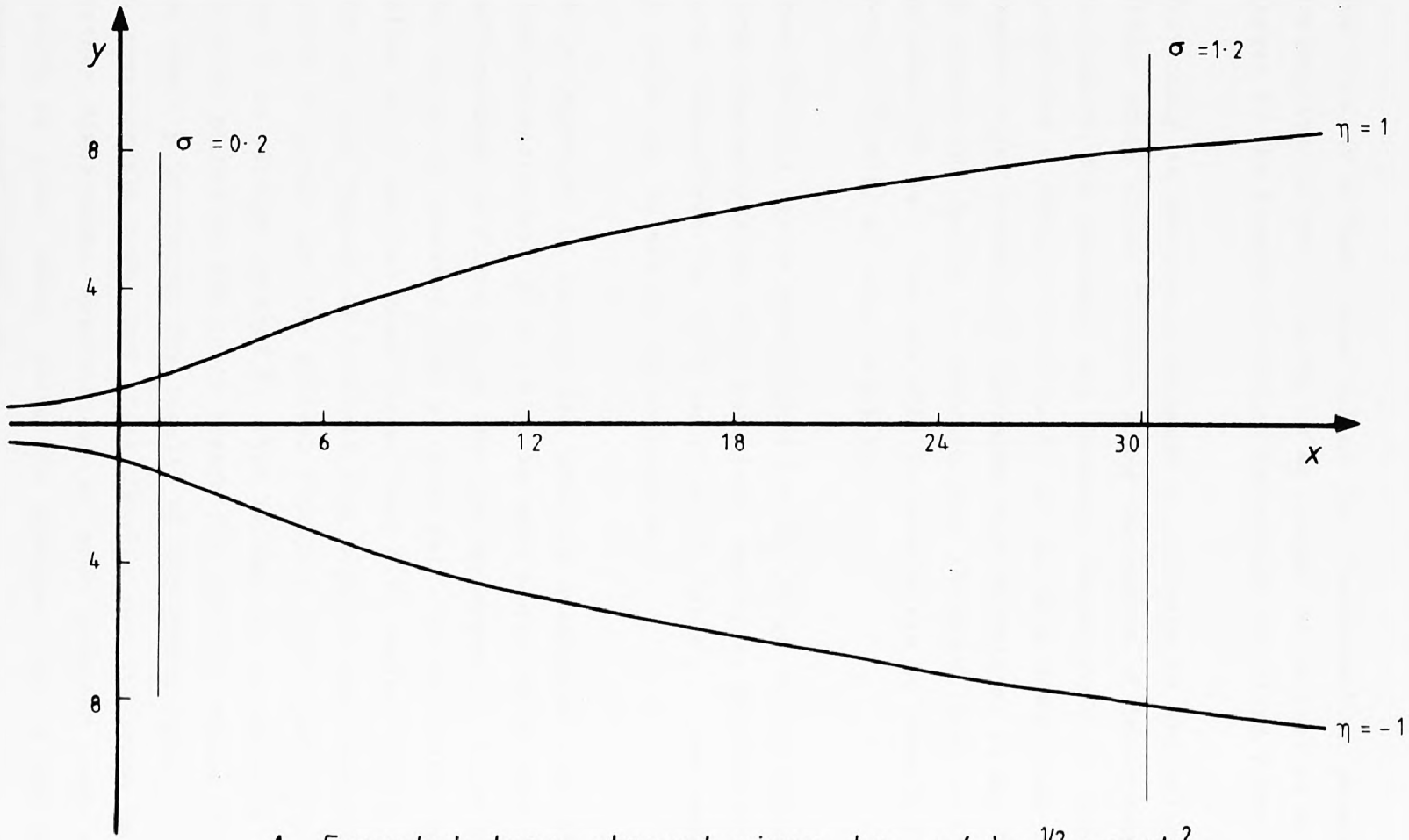

A Fraenkel-type channel given by $\alpha(\tau) = \varepsilon^{1/2} m_1 \operatorname{sech}^2 \tau$
with $\varepsilon^{1/2} = 0 \cdot 4$ *and* $m_1 = 1$.

FIG-34

a minimum R-crit is obtainable for each v.

The role of m here (now called the transformation parameter) is instructive in that it gives us an insight as to what we might expect to happen to the R-crits in moving downstream for fixed v and m_1.

Previously we saw how a decrease or increase in the velocity of the steady state stream function along the centre of the channel, strongly influenced the increase and decrease respectively of R-crit at a particular σ station (Ch.6.2.2). As we move downstream for this Fraenkel-type channel, $\frac{\partial \Omega}{\partial \eta}$ increases then decreases, it may be reasonable to expect the R-crit to decrease then increase. This is in fact what happens. For each v we are able to interpolate an overall minimum R-crit (R^*-crit) at some σ station.

These R^*-crits can be established for $GR_\xi(\hat{E})$ up to and including the $O(\varepsilon)$ terms (henceforth the $O(\varepsilon)$ solution), and up to and including the $O(\varepsilon^{1/2})$ terms (henceforth the $O(\varepsilon^{1/2})$ solution). A table of these results is given in TABLES 9a, 9b and 10 for comparison.

It is important to realize the problems associated with steady state flows characterized by $v \geq 4.7$. We have mentioned already that for the Jeffery-Hamel profiles to be the simpler symmetric types with at most one region of reversed flow at each wall, we must limit ourselves to values which are not much bigger than 4.7. Eagles (1966), showed that when we have regions of reversed flow negative wave velocities are more likely to occur, and the neutral stability curve goes below the R axis when R is plotted against β. Thus it may not be possible to achieve critical points on the lower branch for positive values of β no matter how small β is chosen. The results of the growth rates for $v > 4.7$ may be questionable here, and these results may influence the results further downstream. Nevertheless we have produced some consistent results in these cases, where the reversed flow is not too severe (Eagles & Smith (1980) p10).

v	$O(\varepsilon^{1/2})$		$O(\varepsilon)$		σ
	R-crit	β	R-crit	β	
3.0	99.12	1.48	101.67	1.46	-0.4
	71.24	1.64	73.85	1.60	-0.2
	62.92	1.68	65.42	1.65	0.0
	69.50	1.65	71.97	1.62	0.2
	95.99	1.50	98.37	1.48	0.4
3.5	65.59	1.67	68.31	1.63	-0.4
	46.93	1.78	49.31	1.72	-0.2
	40.76	1.80	42.78	1.74	0.0
	44.32	1.79	46.32	1.73	0.2
	60.87	1.67	63.20	1.66	0.4
4.0	46.81	1.78	49.38	1.72	-0.4
	33.06	1.79	34.88	1.73	-0.2
	27.32	1.75	28.49	1.69	0.0
	28.58	1.76	29.83	1.70	0.2
	40.13	1.80	41.67	1.73	0.4

v	$O(\varepsilon^{1/2})$		$O(\varepsilon)$		σ
	R-crit	β	R-crit	β	
4.5	35.94	1.81	38.15	1.74	-0.4
	24.68	1.69	25.89	1.66	-0.2
	17.21	1.37	17.46	1.48	0.0
	15.91	1.23	14.77	1.44	0.2
	25.70	1.71	25.56	1.64	0.4
4.7	33.12	1.80	35.16	1.74	-0.4
	22.16	1.64	23.52	1.61	-0.2
	12.80	0.98	13.24	1.44	0.0
	20.33	1.54	18.58	1.49	0.4
	40.06	1.80	41.13	1.73	0.6
4.8	32.01	1.79	33.95	1.73	-0.4
	22.03	1.61	22.65	1.59	-0.2
	9.62	0.82	11.12	1.48	0.0
	17.30	1.34	13.63	1.41	0.4
	37.00	1.80	37.76	1.72	0.6

R-crits for a range of v, at various σ planes including and excluding the $O(\varepsilon)$ correction

TABLE 9a. TABLE 9b.

v	$O(\varepsilon^{1/2})$		$O(\varepsilon)$		σ
	R^*-crit	β	R^*-crit	β	
3.0	62.88	1.68	65.39	1.65	0.013
3.5	40.67	1.80	42.67	1.74	0.030
4.0	27.02	1.74	28.08	1.68	0.065
4.5	15.10	1.23	14.16	1.43	0.140
4.7	10.58	0.96	9.01	1.41	0.160
4.8	7.42	0.85	6.36	1.39	0.178

The overall R-crit (R^*-crit) for a range of v, including and excluding the $O(\varepsilon)$ correction

TABLE 10

We include the results for v = 4.8 in TABLES 9a,9b and 10, and note that at σ = 0.2 the R-crit was not achieved for both v = 4.7 and 4.8 by the scheme already described (Eagles & Smith 1980). Reverse flow is observed at σ = 0.0 for both these values, and the downstream influence was apparently too severe to achieve an R-crit no matter how small β was chosen. The values in TABLE 10 were interpolated from TABLE 9. The behaviour of R-crit vs. σ for the $O(\varepsilon)$ solution is given in FIG-35a for the various v's considered. A graphical representation of the $O(\varepsilon^{1/2})$ and the $O(\varepsilon)$ solutions is given in FIG-35b. The inclusion of the $O(\varepsilon)$ terms stabilizes the disturbance to the steady state flow at all σ stations for certain values of v. On the other hand a v exists above which the $O(\varepsilon)$ solution is more unstable than the $O(\varepsilon^{1/2})$ solution. A similar result has already been discussed in Ch.6.1.1 and was illustrated by FIG-19.

Finally, a plot of R-crit vs. v (FIG-36), which goes across σ planes can be used to answer the following question, "what is the overall R-crit for a particular channel ?"

To define an infinite channel uniquely, we can see by (7.40) and (7.41) that $\varepsilon^{1/2}$, and m_1 do this for $\eta = \pm 1$. We can imagine this channel with some fixed $\varepsilon^{1/2}$, and m_1, and by gradually increasing R, we see that a point (R,v) in FIG-36 would move along one of the typical straight lines (dotted). In the particular case of $\varepsilon^{1/2} = 0.4$ (corresponding to FIG-34) we

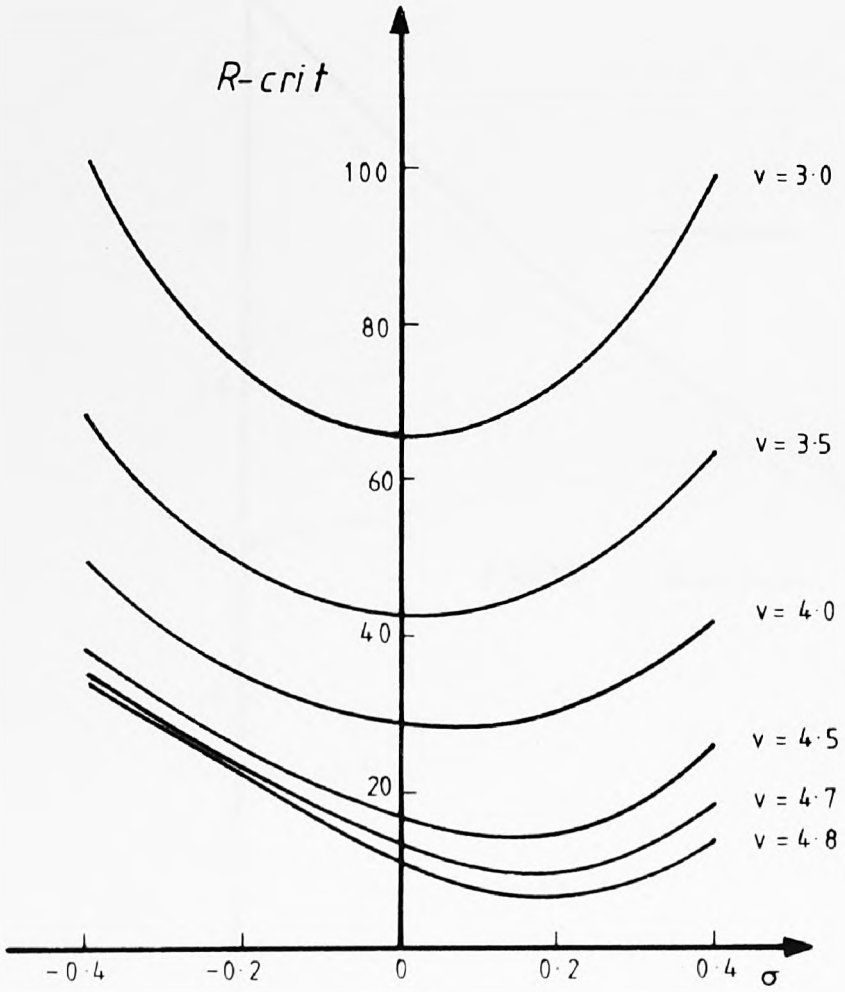

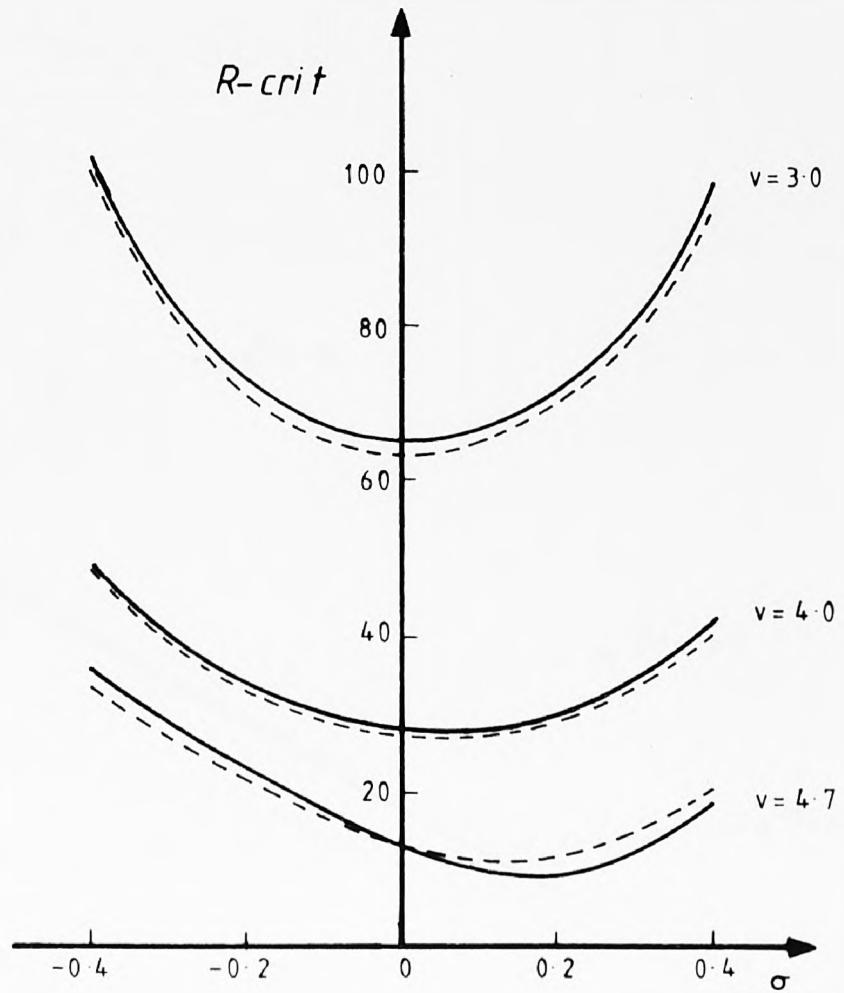

The downstream development of R-crit in a Fraenkel-type channel channel (m_1=1), for different v's at different orders. ----- $O(\varepsilon^{1/2})$ solution, _____ $O(\varepsilon)$ solution.

FIG-35a

FIG-35b

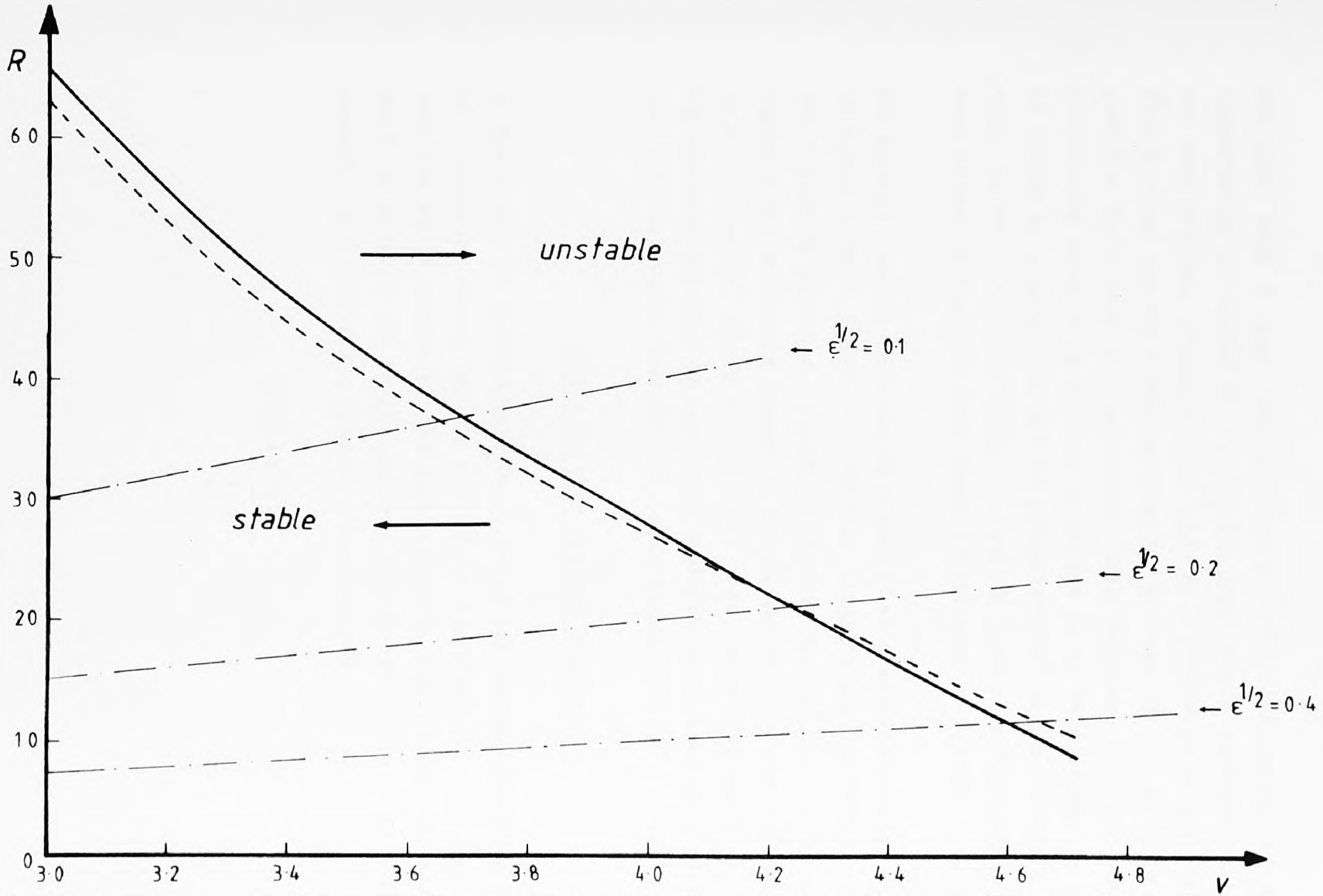

Boundary curves separating stable and unstable flow for a Fraenkel-type channel, at different orders. —·— $R = v/\varepsilon^{1/2}$, ----- $O(\varepsilon^{1/2})$ *solution*, ——— $O(\varepsilon)$ *solution.*

FIG-36

see that when R just reaches R^*-crit (=13), the growth of the disturbances characterised by $GR_\xi(\hat{E})$, just become positive at $\sigma = 0.15$ for some critical frequency $\beta = 1.42$. As R continues to increase beyond R^*-crit, then the disturbances grows for a range of σ , and this will be possible for a band of frequencies. Both the range of σ and the band of frequencies widen with further increases in R. Thus it may be possible to choose an appropriate set of parameters $(\varepsilon^{1/2}, m_1)$ to define a channel which is not "enormous" (FIG-34), and by gradually increasing R, the results may be compared with those illustrated by FIG-36.

Our general results here can be compared in a qualitative way with those of Eagles & Smith (1980). In addition Allmen's more accurate solution of their problem exhibits a similar feature as our $O(\varepsilon)$ solution. The higher order solutions appear to stabilize the flow for values of v up to a critical v (about 4.2 in this case) at all σ stations, but destabilizes the flow in only some σ planes for values of v greater than this critical value (see FIG-35b, also Allmen 1980).

7.5 A Further Channel Problem.

In the light of the previous problems we can see how Fraenkel's small wall curvature theory may be applied to any class of such channels. In fact the whole scheme of the solution both theoretical and numerical could be generalised to include any appropriate $\alpha(\tau)$. As a further example, lets consider a channel characterised by

$$\alpha(\tau) = \frac{\varepsilon^{1/2} m_2 \tau}{1+\tau^2} \qquad ,(7.48)$$

where m_2 is a curvature parameter like m_1. This channel also satisfies the conditions $\alpha(\tau) \rightarrow$ real constant values as $\sigma \rightarrow \pm\infty$, $\alpha(\tau)$ is real on $\eta = 0$, where σ is still defined by (7.7). We can obtain expressions for h and ϑ in the usual way, and we can show that

$$h = P_1(1+\sigma^2)^{\frac{m_2}{2\varepsilon^{1/2}}}(1+0(\varepsilon^2)) \qquad ,(7.49)$$

and

$$\vartheta = \eta\alpha(\sigma)\ (1+0(\varepsilon^2)) \qquad .(7.50)$$

Continuing by integrating (2.8) once more we obtain

$$z = P_1 \int_{\sigma_0}^{\tau} (1+s^2)^{\frac{m_2}{2\varepsilon^{1/2}}}\, ds + P_2 \qquad ,(7.51)$$

where P_1 and P_2 represent real constants of integration corresponding to different z scales and choice of origin respectively. The appropriate disturbance function Φ would be given by

$$\Phi(\xi,\eta,t) = \Phi(\sigma,\eta;\sigma_0)\ \exp\left[i\left[\Theta(\xi) - \beta e^{-\frac{m_2}{\varepsilon^{1/2}}}\, t\right]\right] \qquad ,(7.52)$$

to ensure that the term $h^2\frac{\partial}{\partial t}\left[D^2\Phi\right]$ in (2.19a) is bounded. A schematic representation is given of this channel in FIG-37.

The stability problem could be considered in the same manner as before by obtaining the corresponding transformations ((7.16) and (7.17)).

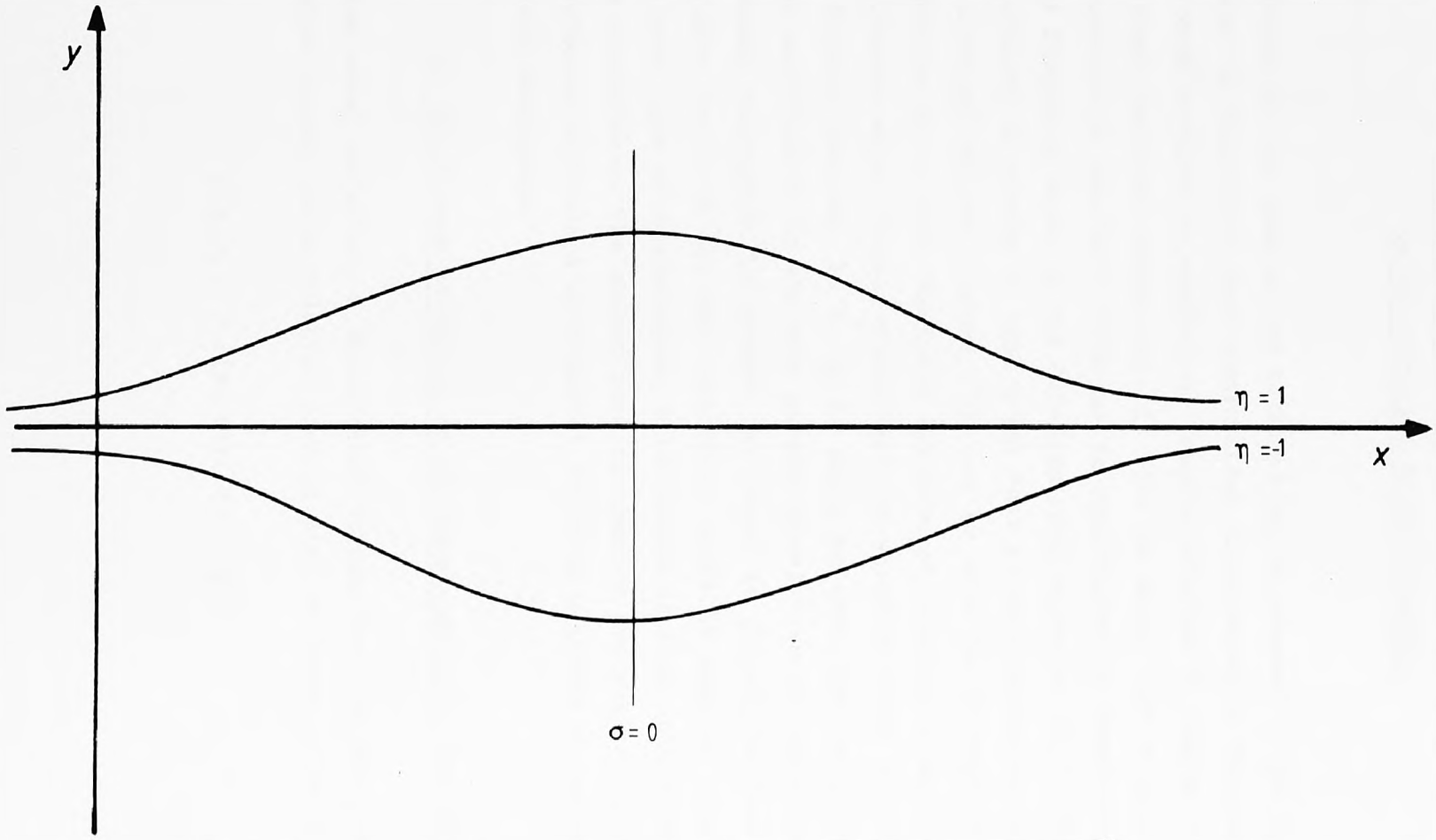

Another Fraenkel-type channel, given by $\alpha(\tau) = \varepsilon^{1/2} m_2 \tau / (1+\tau^2)$.

FIG-37

8. Superposition of Fixed Frequency Modes in the Straight Walled Channel.

We return to the case of the straight walled channel of E&W here in an attempt to consider a more generalized disturbance to the basic flow. This work is based on analytical results obtained by Eagles (1979) using the quasi-parallel assumption. It will be shown that a more general disturbance to the basic flow can be constructed by summing up suitable fixed frequency modes of the Orr-Sommerfeld equation (8.2). This general disturbance is chosen in such a way that at some convenient position in the straight walled channel, it can be made to correspond to a δ-function in t. This impulsive disturbance produces a wave packet type disturbance which travels downstream and which is shown to grow if R > R-crit. However, it is by no means an easy task to extend these ideas analytically to the more general slowly-varying approximation, but it seems reasonable to assume at least in principle, that fixed frequency modes of the E&W type (8.8) could be used to construct an impulsive type of disturbance, which would develop into a wave packet type disturbance. The object here is then to see whether this isolated disturbance produces a wave packet which is unstable in any sense as it travels downstream.

8.1 The Theory According to the Quasi-parallel Assumption.

In the usual notation, a disturbance stream function $\psi(x,y,t)$ to the parallel steady state velocity profile w(y) is taken to be of the form

$$\psi(x,y,t) = f(y)\exp(i\alpha x - i\beta t) \qquad .(8.1)$$

Here, x and y are the usual cartesian coordinates, t is the time, β is specified as the real frequency, and f(y) is the symmetric eigenvector normalized by

$$f(0) = 1 \qquad ,(8.2)$$

and satisfying the Orr-Sommerfeld equation

$$(D_2^2-\alpha^2)\, f = i\alpha R\left\{\left[w(y)-\frac{\beta}{\alpha}\right](D_2^2-\alpha^2)f - w''(y)f\right\} \qquad ,(8.3)$$

$$f(1) = f'(1) = 0 \qquad ,(8.3a)$$

and

$$f'(0) = f'''(0) = 0 \qquad ,(8.3b)$$

where $D_2 = d/dy$.

The problem is to specify β (real) and search for the complex eigenvalue α such that α_i is just negative for the minimum value of R (R-crit). In fact, as far as quasi-parallel theory is concerned the same R-crit is found by specifying real α and searching for the eigenvalue β such that β_i is just positive (see Allmen (1980) pp22-24). The former procedure is more convenient to use for non-parallel flows than the latter. In principle however, α and β could both be complex in (8.3) and their real parts α_r and β_r would then correspond to the wavenumber and frequency respectively, while their imaginary parts α_i and β_i would correspond to the "spatial" and "temporal" growth rates respectively.

Neutral curves for "spatially growing" and "temporally growing" waves are illustrated in FIGS-38a,38b. In this analysis we are particularly interested in the mapping of $\alpha=\alpha(\beta)$, which can be extrapolated from FIGS-38a,38b. In fact by taking the complex conjugate of (8.3) we can show that $\alpha(-\bar{\beta}) = \overline{-\alpha(\beta)}$ (where the bar indicates the complex conjugate), and hence the mapping of $\alpha=\alpha(\beta)$ can be drawn over the whole complex domain of β (see FIG-38c). The mapping of $\beta=\beta(\alpha)$ can be extrapolated in the same way.

Suppose now, β is specified as real, and α (complex) is that eigenvalue giving the greatest growth in the x-direction (for the solution $\exp(i\alpha x-i\beta t)f(y)$ of the Navier-Stokes equations). In order to obtain the behaviour of a more general type of disturbance than (8.1), we may consider

$$\psi_g(x,y,t) = \int_{-\infty}^{\infty} \exp(i\alpha(\beta)x - i\beta t)f(y;\alpha(\beta),\beta)\ Q(\beta)d\beta \qquad ,(8.4)$$

to be another solution to the disturbance equations, provided the integral converges for real β . The function $Q(\beta)$ is real and by specifying it we can construct a suitable disturbance at x=0,y=0 as a function of time. By using the normalisation given by (8.2), we can formally show using Fourier transforms (Lighthill (1959)), that if $\psi_g(0,0,t)$ is modelled by a step function (i.e. $\psi_g(t)=0$ $t<1$; $\psi_g(t)=A$ $-1<t<1$; and $\psi_g(t)=0$ $t>1$, with $A\rightarrow\infty$ as $1\rightarrow 0$ and $A1=1$) $Q(\beta)$ has to be a constant. Without loss of generality we take $Q(\beta)$ as unity. It is worth noting that whereas the choice of $Q(\beta)$ reduces (8.4) to a δ-function in t at x=0,y=0, it is not a δ-function in x at t=0, y=0.

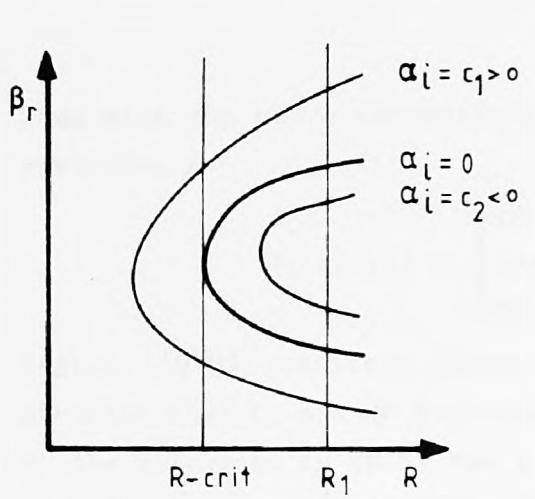

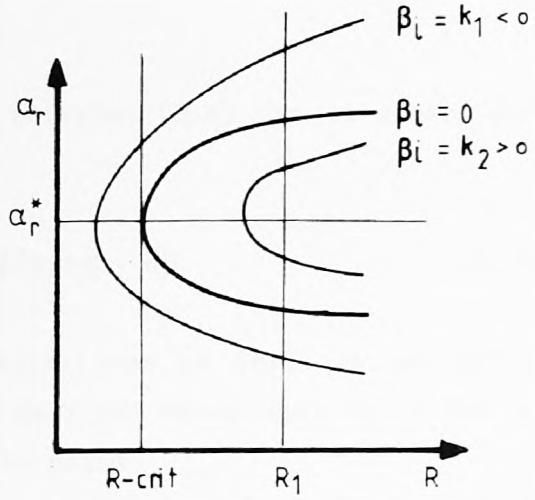

Neutral stability curves for 'temporally growing' and 'spatially growing' waves respectively.

FIG-38a

FIG-38b

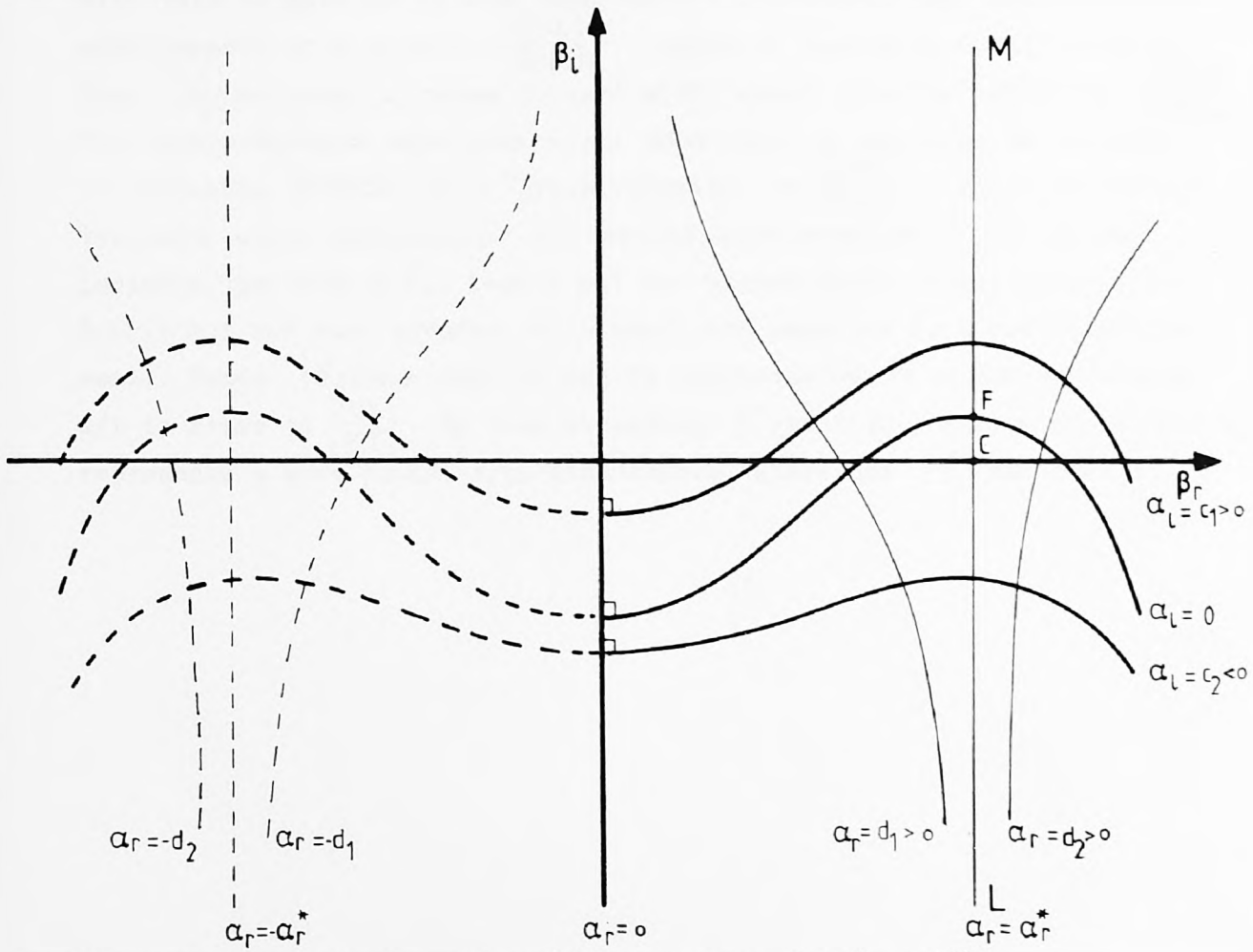

The complex mapping of α (the wavenumber) with β (the frequency).

FIG-38c

Thus with the above assumptions the integral (8.4) can be conveniently rewritten as

$$\psi_g(x,0,t) = \int_{-\infty}^{\infty} \exp(i\alpha(\beta)x - i\beta t)\, d\beta \qquad .(8.5)$$

Eagles (1979) considers three approximations to (8.5) by generally assuming that α, and β are complex. He first shows that for fixed x and t, the integrand in (8.5) has a saddle point at $\beta = \beta^*$ when $\frac{d}{d\beta}\left[\mathrm{Re}(i\alpha(\beta)x - i\beta t)\right] = 0$, and that it lies on the line LM at $\alpha = \alpha_r^*$ in FIG-38c, and since $\alpha(-\bar{\beta}) = \overline{-\alpha(\beta)}$ there is another along $\alpha = -\alpha_r^*$. His first approximation considers an expansion of the integrand about $\beta = \beta^*$ where he neglects the terms $O((\beta-\beta^*)^2$ and higher. With this he goes on to show that as x/t increases, $|\psi_g|$ has a maximum with respect to x at $x/t = 1\Big/\left[\frac{\partial\alpha_r}{\partial\beta_r}\right]_F$ (where F lies on $\alpha_i = 0$ in FIG-38c). Thus $|\psi_g|$(max over x) moves forward with "group velocity" given by $1\Big/\left[\frac{\partial\alpha_r}{\partial\beta_r}\right]_F$. The Cauchy-Riemann equations would show that by assuming an inverse relationship $\beta = \beta(\alpha)$ this "group velocity" is $\left[\frac{\partial\beta_r}{\partial\alpha_r}\right]_F$, which is perhaps the more usual definition. The second approximation to (8.5) now includes the $O((\beta-\beta^*)^2)$ term (but not higher order terms), and if R > R-crit but not much greater, α_i is small and negative at C and CF is also small. Hence $|\psi_g|$(max over x) can be approximated by values of x such x/t is close to $\left[\frac{\partial\beta_r}{\partial\alpha_r}\right]_C$. By then expanding β^* about β_C, Eagles shows that ψ_g represents a wave packet type disturbance, where now $|\psi_g|$(max over x)

occurs when $x/t = \left[\frac{\partial \beta_r}{\partial \alpha_r}\right]_C$. He also shows that this result is a good estimate of the previous result (that $|\psi_g|$(max over x) occurs when $x/t = \left[\frac{\partial \beta_r}{\partial \alpha_r}\right]_F$), when α_i is small at C. The third and best approximation to (8.5) comes from the method of steepest descent (Jeffries & Jeffries (1950) pp 501-505, Morse & Feshback (1953)), where the approximation is based on the point C. Here $\alpha(\beta^*)$ is complex ($\alpha_{rc}+i\alpha_{ic}$ represents α at C) and β^* is real (β_c). Thus (8.5) can be approximately written as

$$\psi_g \sim \left[\exp(-\alpha_{ic}x)\ \exp(i\,\Xi_1)\right]\Xi_2 \qquad .(8.6)$$

Here, Ξ_1 and Ξ_2 are real functions dependent on α, β, x and t. The second approximation bears a close resemblance to (8.6), which shows ψ_g again to be a wave packet type disturbance. Thus if R > R-crit, the wave packet will grow downstream (since $\alpha_{ic}<0$), if R = R-crit, the wave packet will travel with a constant height downstream (since $\alpha_{ic}=0$), and if R < R-crit then the wave packet will decay downstream (since $\alpha_{ic}>0$).

It is not easy to generalize, or be as precise analytically when applying the ideas already discussed to the case of fixed frequency disturbances of the type considered by E&W (also Ch.4 of this thesis). Nevertheless, if we assume the ideas extend to this case, then in the present notation, we can generalize a fixed frequency disturbance which is given by

$$\phi(\sigma_1,\eta)\ \exp(i(\Theta(\xi)-\beta t)) \qquad ,(8.7)$$

to become

$$\phi_g(\sigma_1,\eta,t) = \int_{-\infty}^{\infty} \exp(i(\Theta(\xi;\beta)-\beta t))\, \phi(\sigma_1,\eta;\beta)\, Q(\beta)\, d\beta \qquad .(8.8)$$

We recall that ϕ could be written in the form

$$\phi(\sigma_1,\eta) = A_0(\sigma_1)f_0(\sigma_1,\eta) + \varepsilon^{1/2}(f_1(\sigma_1,\eta)+A_1(\sigma_1)f_0(\sigma_1,\eta)) + \varepsilon\,(f_2(\sigma_1,\eta)+A_2(\sigma_1)f_0(\sigma_1,\eta)) \quad .. \quad .(8.9)$$

Also, since we shall be analysing the disturbance at the centre of the channel (η=0), then we need to recall the normalisations of $f_0(\sigma_1,0)$, $f_1(\sigma_1,0)$ and $f_2(\sigma_1,0)$, implied by (4,61). Hence

$$\phi(\sigma_1,0) = A_0(\sigma_1) + \varepsilon^{1/2}A_1(\sigma_1) + \varepsilon A_2(\sigma_1) + \ldots \qquad .(8.10)$$

In the original stability problem the amplitude function A_2 was never computed as it was not required in the stability analysis. It would have also meant going to the $O(\varepsilon^{3/2})$ disturbance equation. It is not even felt that the term $\varepsilon^{1/2}A_1$ will make much contribution to this analysis in the light of earlier work on the straight walled channel, but we includeit for completeness. The more general disturbance given by (8.8) was not in fact considered for separate contributions of the different orders. We recall that

$$A_0(0) = 1 \qquad ,(8.11a)$$

and

$$A_1(0) = 0 \qquad ,(8.11b)$$

for consistency with (4.61). Hence by choosing $Q(\beta) = 1$ again,and posing

$$\Theta(0) = 0 \qquad ,(8.12)$$

then (8.8) reduces to

$$\phi_g(0,0,t) = \int_{-\infty}^{\infty} \exp(-\beta t)\, d\beta \qquad ,(8.13)$$

which is a δ-function in t at $\sigma_1 = 0$. At this stage we can rewrite the integral (8.8) as

$$\phi_g(\sigma_1,0,t) = \int_{-\infty}^{\infty} \exp\left[i(\Theta(\xi;\beta)-\beta t)\right](A_0(\sigma_1;\beta)+\varepsilon^{1/2}A_1(\sigma_1;\beta))d\beta \qquad .(8.14)$$

This integral will be evaluated numerically, though some discussion on its analytical approximation will be given later.

8.2 Numerical Techniques and Checks.

The approximation of (8.5) by the method of steepest descent, can be shown to be real, if the contribution from the other saddle point (along $\alpha = -\alpha_r^*$) is included. We can show that (8.5) aswell as (8.14) can be rewritten in a more convenient form for numerical evaluation. In fact (8.14) can be expressed by

$$\phi_g(\sigma_1,0,t) = \int_{0}^{\infty} \exp\left[i(\Theta(\xi;\beta)-\beta t)\right](A_0(\sigma_1;\beta)+\varepsilon^{1/2}A_1(\sigma_1;\beta))d\beta + \text{c.c.} \qquad ,(8.15)$$

where c.c. is the complex conjugate of the preceeding integral. Thus we need only consider positive values of β .

The first problem then was to compute $\Theta(\xi)$ for some fixed β . We can recall (4.25) which originally defined the phase function Θ .

In terms of σ_1 (4.25) becomes

$$\Theta(\sigma_1) = \frac{1}{\varepsilon^{1/2}} \int_0^{\sigma_1} k(s)\, ds \qquad (8.16)$$

The integration was carried out using Simpson's rule after defining $\Theta(0) = 0$, and evaluating $\Theta(1)$ using an extrapolation formula already used for $A_0(\sigma_1)$ and $A_1(\sigma_1)$ (see (5.8)). The values of $\Theta(\sigma_1)$ were checked by evaluating $\frac{d\Theta}{d\xi}$ using fourth order central difference formulae. These checked with known values of $k(\sigma_1)$ to 5 significant figures.

In all previous numerical work, the disturbance stream function ϕ was considered for a single, real, fixed frequency β. Now however, we need to compute several of these disturbances (for each β) and store them. For this purpose, we need an automatic scheme to solve the eigenvalue problem for every value of β considered. The original routine (see Ch.4 pp74-77) which gave a starting value to the eigenvalue problem, worked well for values of β up to about 1.4. The scheme did not work for values of $\beta > 1.4$, but converged to the wrong eigenvalue. This problem was overcome by using the original routine for $\beta < 1$, and then switching over for $\beta > 1$ using starting values given by the previous correct k's ($\beta = 1$). From the numerous test cases, this worked if the β increments ($\delta\beta$) were small enough (i.e $\delta\beta \leq 0.05$). It was found necessary to have a combination of these two schemes, to be assured of correct eigenvalues for small and large values of β.

We must bear in mind that (8.14) need only be evaluated for a relatively small range of β. Referring to FIG-39, (the neutral curve based on $GR_\xi(\phi)$ at the centre of the channel) we can see that for $R = 60 >$ R-crit, we would expect ϕ to grow at the centre of the channel

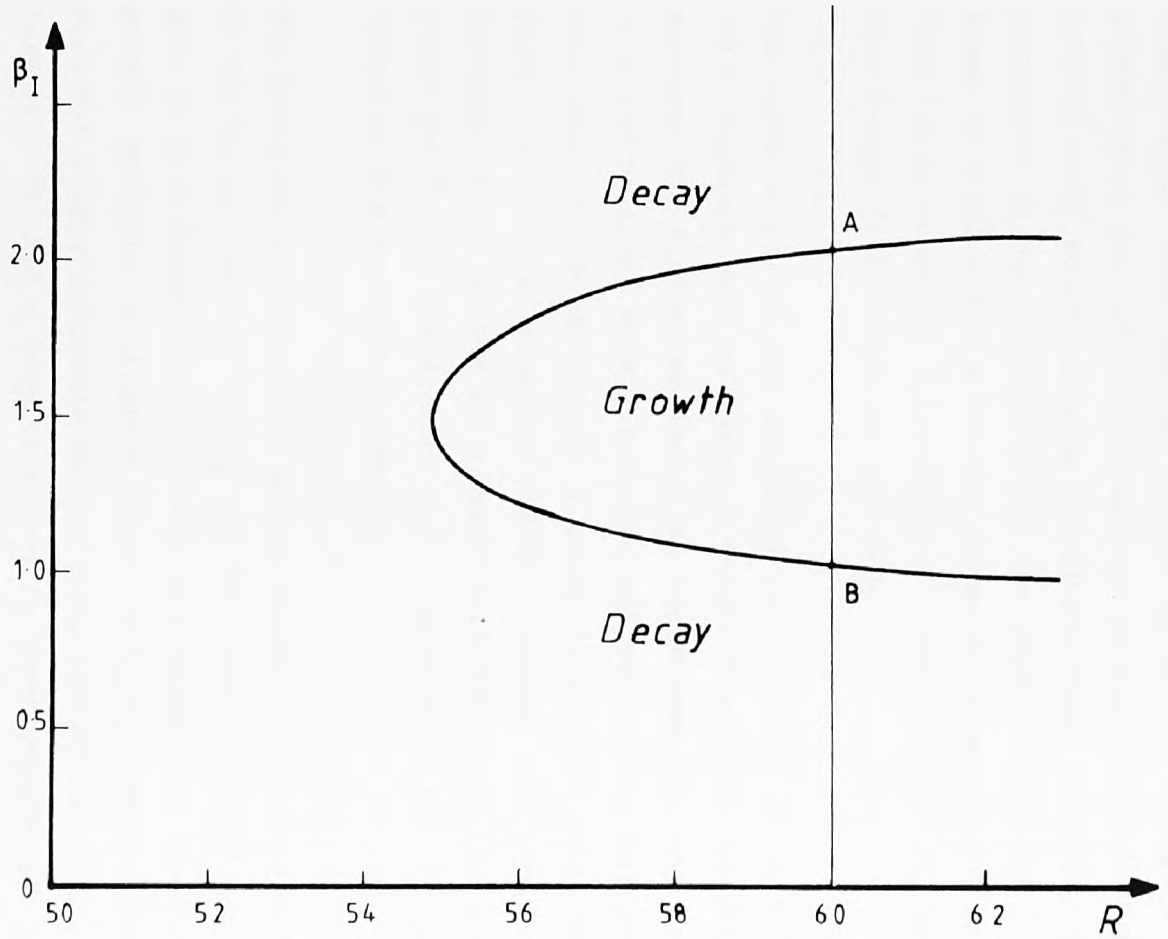

The neutral stability curve for the disturbance function Φ at the centre of the straight walled channel, with v = 3·572.

FIG-39

for a given σ_1 value and a range of β between A and B. The widest range of β being at $\sigma_1 = 0$. As we move in the σ_1 direction, the band of frequencies which we would expect growth in ϕ narrows because of the exponential factor in β_I.

The major contribution to the integral (8.14) for some fixed σ_1, comes from the β range implied by the β_I values between A and B. The contribution outside this range can be neglected. A study of any such neutral curve would indicate the finite range necessary to obtain a good approximation to (8.14). In all the cases considered (a range of v given by $3.572 \leqslant v \leqslant 4.71$) the range of β was taken to be 0 to 2.5. This finite range of β however, will now imply (8.14) only approximates to a δ-type disturbance at $\sigma_1 = 0.0$.

The integral (8.14) was evaluated for a range of σ_1's ($0 \leqslant \sigma_1 \leqslant 1.56$) using Simpson's rule at every σ_1 value. Numerical instabilities always appeared the further we travelled downstream. It took several computer runs before these were pinpointed and reasonably eliminated. We should also note that summing over β using finite $\delta\beta$ makes the results of (8.14) periodic with period $2\pi/\delta\beta$ (through the term $\exp(i\delta\beta t)$). An increase in the number of β steps will naturally increase this period, where the δ-type disturbance will appear again at $\sigma_1 = 0.0$ for $t = 2n\pi/\delta\beta$ (where n is a positive integer).

The numerical instabilities always became more acute with larger values of the parameters R, β, and α_1, and the function $H(\sigma_1)$ was the first to be seen to grow dramatically at some σ_1 station (see (4.66a). This dramatic growth gradually manifested itself in $A_0(\sigma_1)$ aswell. These large values were not always noticable in the final evaluation of (8.14) because the term $\exp(-\Theta_i)$ had a damping effect in these regions of σ_1.

It is worth pointing out that initially, it was not clear whether this dramatic growth was due to numerical instabilities, or whether the disturbance was truly growing. It was unfortunate that the R value about which this dramatic growth was observed, roughly coincided with the R-crit for this curve (R-crit $\simeq$ 54.8 in FIG-39). It was not until a detailed study of the values $C_1(\sigma_1)$,$C_2(\sigma_1)$, $C_3(\sigma_1)$, and $C_4(\sigma_1)$ defining $H(\sigma_1)$ ($C_5(\sigma_1)$=0 for the straight walled channel), revealed that more steps were required to accurately evaluate the integrals defining these C's ((4.67a)-(4.67d)). In fact, this only partially removed the numerical errors, and it was not until a much greater number of β steps were taken aswell, that all the instabilities disappeared. This is illustrated by FIGS-40a & 40b. The case of ϕ corresponding to 50 βsteps took roughly 92 CDC(7600) units, and the case of 100 β steps took 191 CDC(7600) units.

Our original aim was to construct an impulsive type disturbance and see whether it grew or decayed as it travelled downstream. The illustration in FIG-41 demonstrates the behaviour of a typical wave packet (for 100 β steps) at different values of t. This graph tends to indicate that the wave packet decays, even though R = 70 > R-crit. We shall look at this graph again in more detail when discussing the results.

Even when all these problems of numerical instability have been ironed out, there was another and possibly more crucial problem inherent in integrals of the type

$$J(z) = \int_C \exp(zf(t))\, dt \qquad ,(8.17)$$

where $|z| \to \infty$. In these integrals, large values of $|z|$ will usually

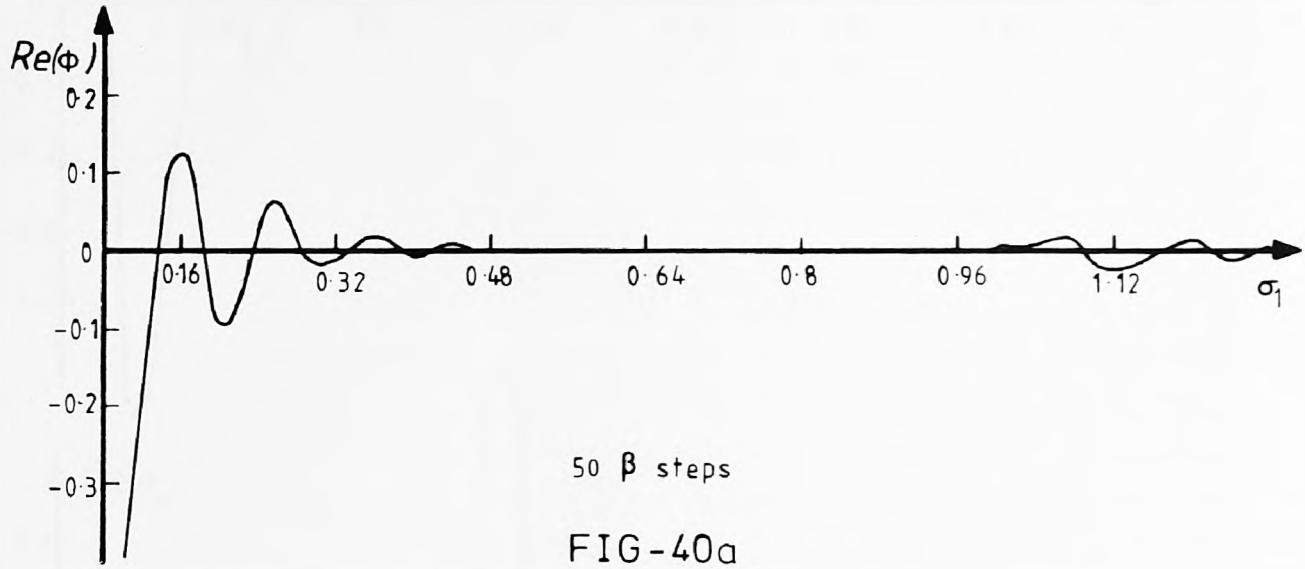

50 β steps

FIG-40a

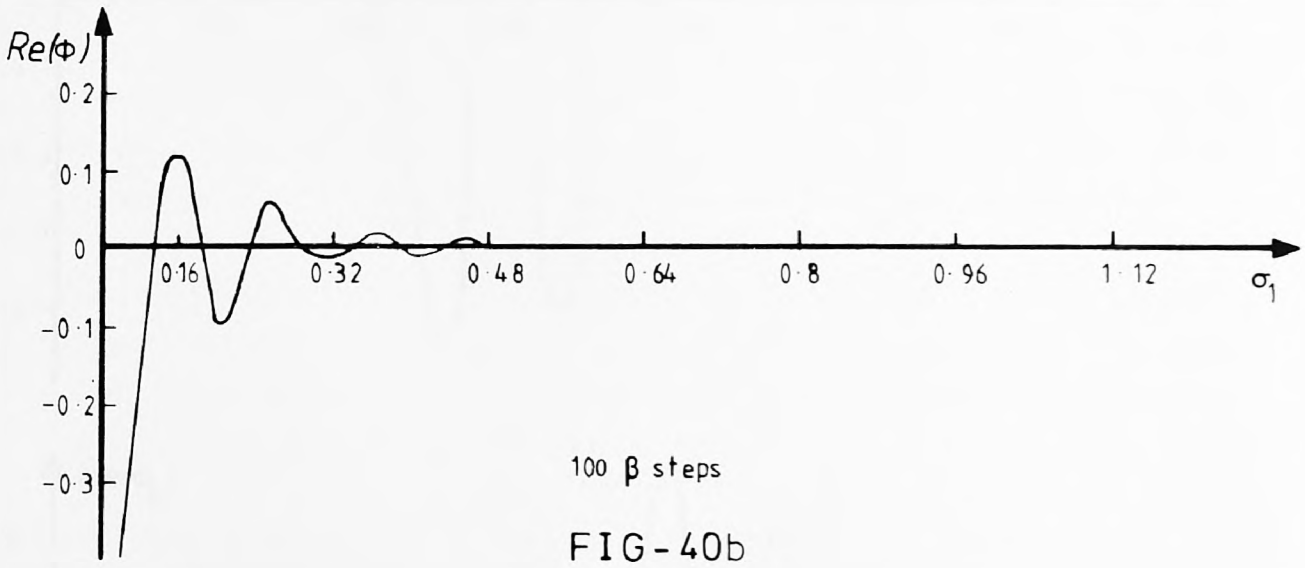

100 β steps

FIG-40b

The behaviour of the generalized disturbance downstream at time t=0 evaluated with different incremental steps of the frequency β, where v=3·572 and R=70.

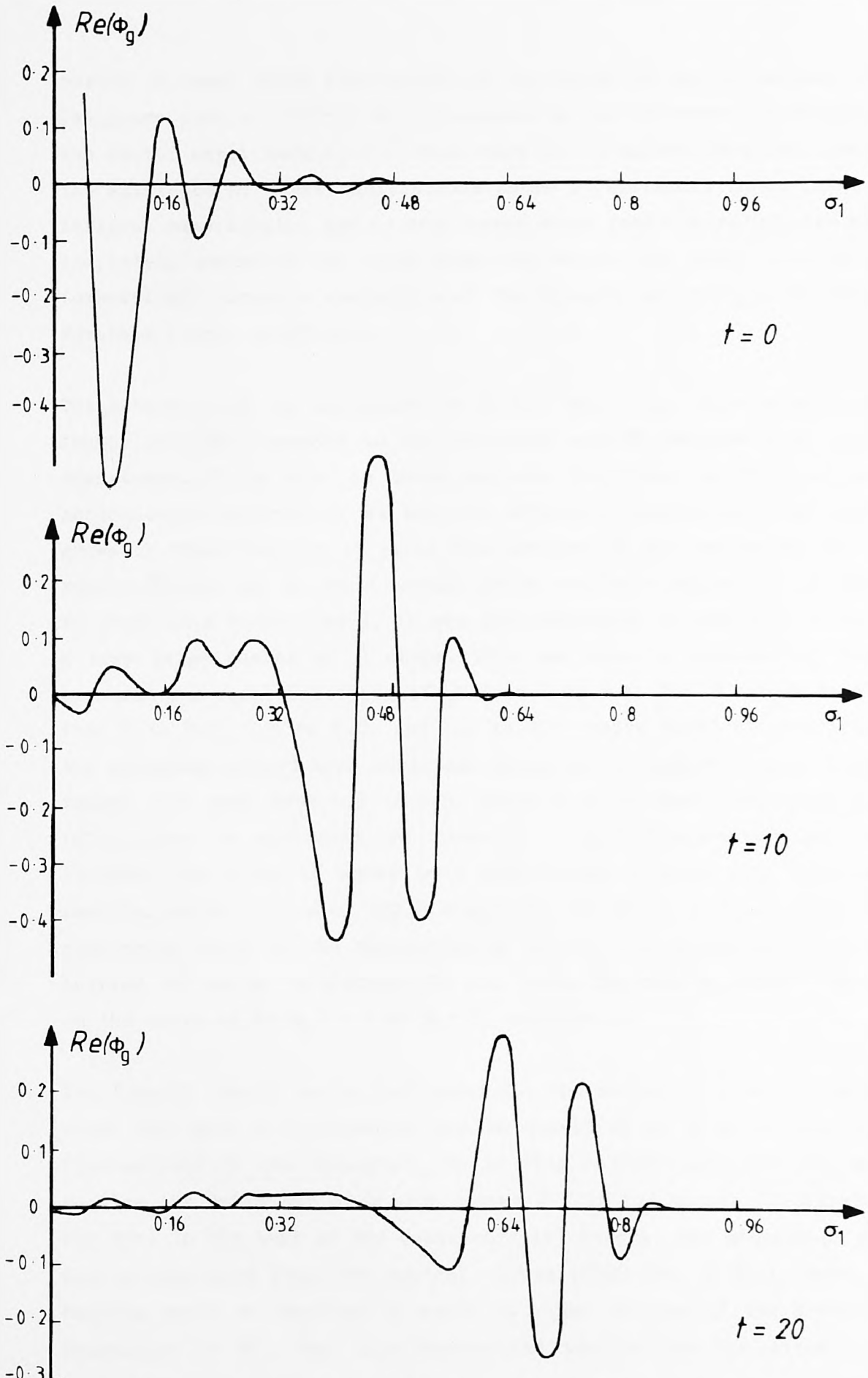

The travelling wave packet at different times with $v = 3{\cdot}572$ and $R = 70$.

FIG-41

result in some rapid fluctuation of the value of the integrand. The imaginary part of z(f(t)) will increase as $|z|$ increases, consequently the factor exp(i Im(z(f(t)))) will make the integrand oscillate rapidly. The existence of these oscillations makes it difficult to evaluate the integral numerically, and in many cases large positive values are almost completely cancelled by large negative values. We might require a forbiddingly accurate evaluation of the integral at every point (Morse & Feshback (1953) pp437-440).

The behaviour of the integrand in (8.14) falls into this category as a factor $\exp(i\Theta_r)$ appears in the integrand and Θ_r becomes very large downstream. It is also in these regions downstream in which we are particularly interested. We want to determine whether the disturbance grows in these regions of rapid fluctuations of the integrand. For this reason $\delta\beta$ may not be small enough for an accurate evaluation of (8.14). To check this convincingly, it was felt necessary to evaluate (8.14) for a very large number of β steps. This was done by considering five separate and equal intervals of β from 0 to 2.5. The β ranges that went from 0 to 0.5, 0.5 to 1.0, and 1.0 to 1.5 (where rapid fluctuations of the integrand occur) were evaluated using 250 β steps for each case. The ranges that went from 1.5 to 2.0, and 2.0 to 2.5 were evaluated using 100 β steps in each case, as there is rapid fluctuation here. The integral was found to agree to 5 significant figures with previous results, which only used 100 β steps for the whole σ_1 range. With this convincing check on the evaluation of (8.14), all subsequent runs were carried out using 100 β steps. In all cases the results were normalised on the basis of $Re(\phi_g) = 1$ at $\sigma_1 = 0$, and $t = 0$.

The form of (8.14) is in fact ideal for the method of steepest descent, where the path of integration may be chosen so as to avoid the rapid fluctuations of the integrand. To do this convincingly however, would require the behaviour of Θ with complex β in the manner illustrated by FIG-38c. In the case of the quasi-parallel theory, the mapping of α with β was extrapolated from the neutral curves (FIGS-38a, & 38b). Here, the mapping would be required at every σ_1 plane because of the downstream dependence of Θ, but this theoretical problem was not attempted.

8.3 The Results.

If we refer back to FIG-41, we see what appears to be a decaying wave packet type disturbance, even though R > R-crit here. However, if the disturbance ($Re(\phi_g)$) was plotted for the time interval given by $0 < t < 2$, we would in fact see some growth, but this growth is small and only extends into a small σ_1 range ($0 < \sigma_1 < 0.08$). To illustrate these results clearly we have considered more extreme cases, by taking $v = 4.093$ and $v = 4.71$. These results are shown in FIGS-41 & 42 respectively. The growth is more visible here and the pattern suggested by these results is that an increase in v is associated with the wave packet travelling with a larger "head" extending into wider regions downstream, and prevailing for larger time intervals. Nevertheless, if we go far enough downstream, the wavepacket eventually decays irrespective of whether R > R-crit or R < R-crit.

With hindsight one may even argue that this behaviour of the wave packet was to be expected since we were summing different fixed frequency modes which all eventually decayed. This reasoning of course is not completely clear in regions where collections of these fixed frequency modes are growing.

The results presented here do not agree with the quasi-parallel prediction (that when R > R-crit the wave packet will grow indefinately in the streamwise direction), but they are in agreement with the former analysis (fixed frequency disturbance) where the disturbance to the steady flow was seen to grow for limited regions downstream at some instant.

For the cases illustrated, the value of R is appreciably larger than the R-crit. Many other cases were also considered in which R was not as large (but still > R-crit), and time intervals were always found in which the wave packet grew, but for typically smaller downstream regions.

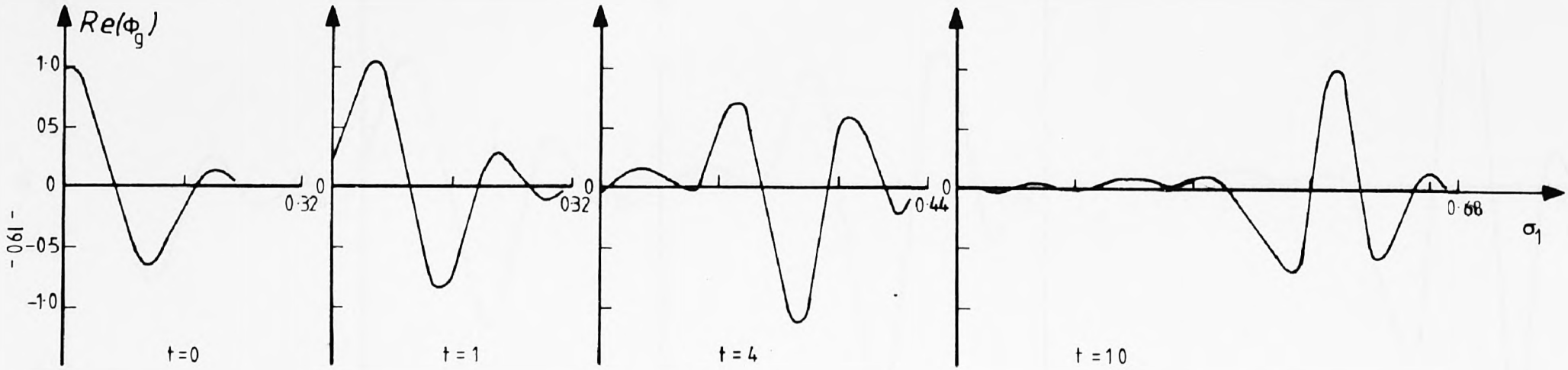

The travelling wave packet at different times with v=4·093 and R=70.

FIG-42

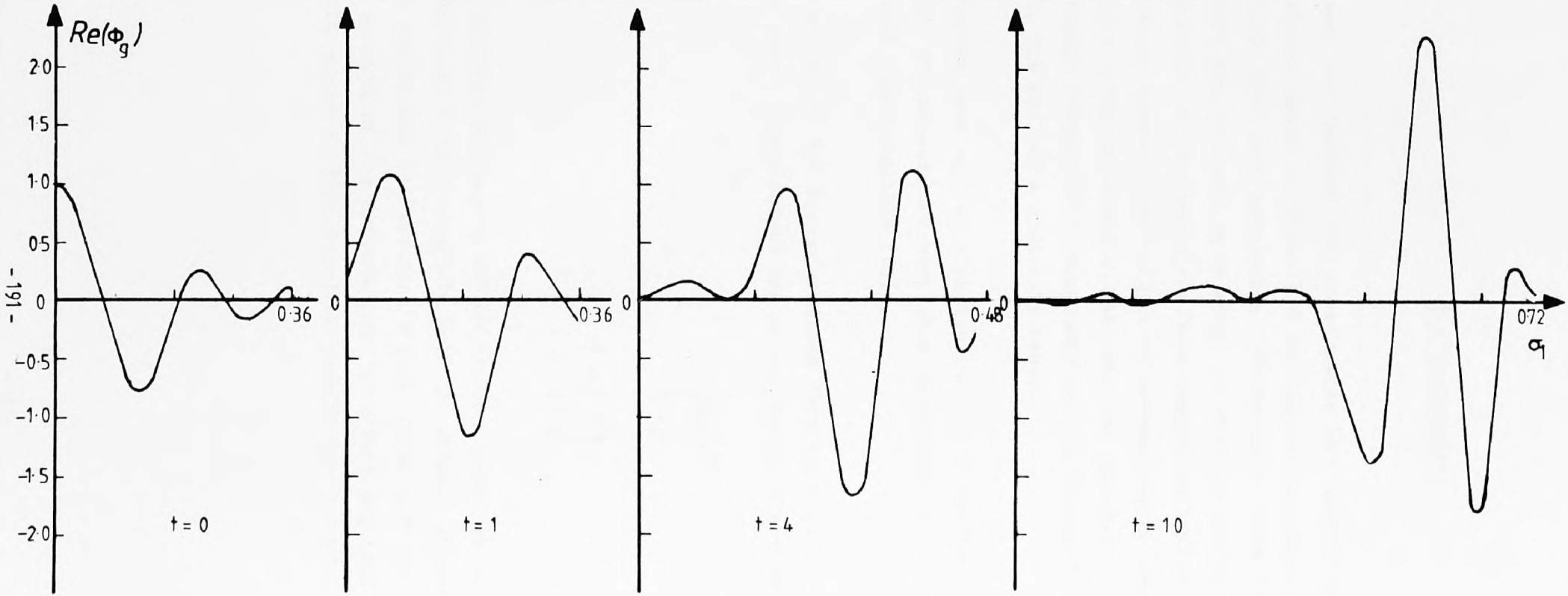

The travelling wave packet at different times with v = 4·71 and R = 70.

FIG-43

8.4 Discussion.

We may ask whether the time scales and length scales exhibiting growth,as shown in FIGS-42 & 43, are within experimental limits and whether they are measurable. Patterson's (1934,1935) experimental channel may be used as a model to help us appreciate the physical dimensions of the space and time variables implied by σ_1 and t. We emphasize however that we are not attempting to compare our theoretical results with Patterson's, as the two channels are intrinsically different (Patterson's experiment was on Blasius's exponential channel) also, his was not a stability study.

Patterson used air as a medium (ν = 0.15 cm^2/sec at 20° C, Goldstein (1938) p7),because at very slow velocities air can be likened to a viscous incompressible fluid.

Let us recall the dimensionalised form of r (the polar distance) and T (the time). A convenient way of expressing these are

$$r = \left(\frac{bR}{\nu}\right)e^{\sigma_1} \qquad ,(8.18)$$

and

$$T = \left(\frac{b^2}{R\,\nu}\right)t \qquad .(8.19)$$

The physical dimensions of our channel could be likened to Patterson's by choosing b (approximately half the channel throat width at $\sigma_1 = 0$, and here equivalent to Patterson's w/2) to be 0.25 cm. If we then consider the results of the extreme case in FIG-43 and take as an example that growth occurs in the downstream region for $0 < \sigma_1 < 0.7$ and for a time

interval $0 < t < 10$, the parameters then imply that r is about 8 cm. and the time T about 0.1 secs. These do not seem very large on the face of it, but the length of our channel under analysis ($0 \leqslant \sigma_1 \leqslant 1.56$) would correspond to about 18 cm.. The initial throat width is 0.5 cm. and the final throat width in this σ_1 region would be about 2.4 cm.. In fact the results of this extreme case (and others) extend further into the streamwise direction and for larger time intervals than the ones illustrated. Such lengths, time scales, and parameters seem within Patterson's experimental observations and so should be measurable (Patterson (1934) pp770-773).

CONCLUSION.

If we consider the steady state problem for the straight walled divergent channel we find that the higher order corrections are directly responsible for the increase in the steady state velocity at the centre of the channel, and the decrease near the walls. This effect is small in general but in some extreme cases (for larger v) can cause reversed flow near the walls (see FIG-5).

In the stability problem, the higher order corrections do produce shifts in the neutral stability curves, but once again these are small even for comparitively large values of $\varepsilon^{1/2}$(see FIG-19). They nevertheless exhibit a distinct stabilizing effect for values of v up to some critical value (say 4.15 in this case), and a destabilizing effect for values of v larger than this critical v. This destabilizing effect for larger v is consistent with the reversed flow effect (and hence more unstable flow) described above.

The comparison of flows in curved walled channels (positive or negative curvature), with divergent straight walled channels at positions where the angle of divergence is the same (at $\sigma_1 = 0$), shows that positive curvature has an appreciable stabilizing effect, and negative curvature an appreciable destabilizing effect. As we move further downstream, we find perhaps the more natural result, that the channel with positive curvature is more unstable , and the one with negative curvature more stable. The major contributor to these effects has been shown to be the change in Ω associated with curvature, rather than general non-parallel and curvature terms in the disturbance equation. Physically speaking, we can argue that for this comparison at $\sigma_1 = 0$, the channel with positive curvature has a greater angle of divergence for $\sigma_1 > 0$, and a smaller angle of divergence for $\sigma_1 < 0$ than the divergent straight walled channel. Thus, if $\sigma_1 < 0$ we expect the overall flow properties to produce a more stable flow, and because of the upstream influences, this persists till $\sigma_1 = 0$. Subsequently, we expect the flow to become more unstable as the angle of divergence increases. A similar argument is consistent with the results for a channel with negative curvature.

The Fraenkel-type channel which might be constructed for experimentation is shown to be naturally more stable far upstream and downstream than near the viscinity of $\sigma = 0$, where the angle of divergence is maximum. The most unstable region being $0.0 < \sigma < 0.2$.
A comparison of the "$0(\varepsilon^{1/2})$ solution" and the "$0(\varepsilon)$ solution" in the case of the Fraenkel-type channel (FIG-36), validates the asymptotic development, and the effect of including higher order terms here is consistent with the straight walled divergent case (FIG-19). The value of the critical v for this Fraenkel-type channel is about 4.2.

The construction of an impulsive type disturbance for the straight walled channel (based on the superposition of slowly varying fixed frequency modes), was shown to produce a wave packet type disturbance. The results can be illustrated clearly when R is appreciably larger than R-crit (FIGS-41 & 42). Even though these results do not support the quasi-parallel prediction (that the wave packet will grow indefinately in the streamwise direction if R > R-crit), they exhibit they same type of behaviour as the former case for fixed frequency modes, where the disturbance grew in a limited region downstream for some instant in time.

Fraenkel's pioneering work on symmetric curved walled channels paved the way for studying the stability of the Jeffery-Hamel profiles. His orthogonal coordinates and the fact that the non-linear profiles enter the algebra appear to have discouraged most investigators from applying Fraenkel's theory explicitly. In this respect this present investigation is a positive contribution to the theory of stability of two dimensional channels with small wall curvature. It could be extended to deal (both theoretically and numerically) with a general class of symmetric channels which have physically interesting features (FIGS-34 & 37).

There is an overwhelming need for experimentation in this field in order to test the theory realistically. The problem of setting up the Jeffery-Hamel profiles should be easier with channels similar to those illustrated by FIGS-34 & 37 where the flow is initially like plane Poiseuille flow.

REFERENCES.

ABRAMOWITZ,M (1949)
On backflow of a viscous fluid in a divergent channel.
J.Maths.Phys. 28 : 1

ALLMEN,M (1980)
Ph.d. Thesis : The City University, Department of Mathematics.

BENNEY,D.J., & ROSENBLAT,S. (1964)
Stability of Spatially Varying and Time-Dependent Flows.
Phys. of Fluids, 7 : 1385

BLASIUS,H (1910)
Laminare Stromung in Kanälen Wechselnder Breite.
Z.Maths.Phys. 58 : 225

BOUTHIER,M (1972)
Stabilité linéare des écoulments presque parallèles.
J.Méchanique 11 : 599

BOUTHIER,M (1973)
Stabilité linéare des écoulments presque parallèles.
J.Méchanique 12 : 75

BRIGGS,R.J (1964)
Electron-Stream Interaction with Plasmas.
M.I.T. Press, Research Monograph No. 29 chapter 2

BRILLOUIN,L (1926)
Compt.Rend. 183 : 24

BROWN,S.N. & STEWARTSON,K (1969)
Laminar Separation.
Annual Review of Fluid Mechanics, Vol 1

COLES,D (1958)
Motion Picture of Circular Couette Flow.
Nat.Sci.Foundation (Under Grant G-3494)

CROLL,J.G.A
Personal Communication.

DAVIES,S.J. & WHITE,C.M (1928)
An experimental study of flow of water in pipes of rectangular section.
Proc.Roy.Soc. A, 119 : 92

DEAN,W.R (1950)
Note on the motion of a liquid near a position of separation.
Proc.Camb.phil.Soc. 46 : 293

DI PRIMA,R.C & STUART,J.T (1972)
Non-local effects in the stability of flow between eccentric rotating cylinders.
J.Fluid Mech. 54 : 393

DRAZIN,P.G (1974)
On a model of instability of a slowly varying flow.
Qaurt.J.Mech.Appl.Math 27 : 69

EAGLES,P.M (1966)
The stability of a family of Jeffery-Hamel solutions for divergent channel flow.
J.Fluid Mech. 24 : 191

EAGLES,P.M (1973)
Supercritical flow in a divergent channel.
J.Fluid Mech. 57 : 149

EAGLES,P.M (1977)
On the stability of slowly varying flow between concentric cylinders.
Proc.Roy.Soc.Lond. A, 355 : 209

EAGLES,P.M (1978)
Personal communication

EAGLES,P.M (1979)
Personal communication

EAGLES,P.M & WEISSMAN,M.A (1975)
On the stability of slowly varying flow : the divergent channel.
J.Fluid Mech. 69 : 241

EAGLES,P.M & SMITH,F.T (1980)
On the steady flow and its stability in certain channels with slowly varying width.
J.Eng.Maths. 14(3) : 219

FALES,E.N (1955)
A new laboratory technique for investigation of the origin of fluid turbulence.
J.Franklin Inst. 259 : 491

FRAENKEL,L.E (1962)
Laminar flow in symmetric channels with slightly curved walls I. On the Jeffery-Hamel solutions for flow between plane walls.
Proc.Roy.Soc. A, 267 : 119

FRAENKEL,L.E (1963)
Laminar flow in symmetric channels with slightly curved walls II. An asymptotic series for the stream function.
Proc.Roy.Soc. A. 272 : 406

GASTER,M (1962)
A note on the relation between temporally-increasing and spatially-increasing disturbances in hydrodynamic stability.
J.Fluid Mech. 14 : 222

GASTER,M (1965)
On the generation of spatially growing waves in a boundary layer.
J.Fluid Mech. 22 (3) : 433

GASTER,M (1974)
On the effects of boundary layer growth on flow stability.
J.Fluid Mech. 66 : 465

GOLDSTEIN,S (Editor) (1938)
Modern Developments in Fluid Dynamics.
Clarendon Press, Oxford

GOLDSTEIN,S (1948b)
On laminar boundary-layer flow near a position of separation.
Quart.J.Mech. 1 : 43

HALL,P & PARKER K.H. (1976)
The stability of decaying flow in a suddenly blocked channel.
Adv.App.Mech. 14 : 241

HAMEL,G (1917)
Spiralförmige Bewegungen zäher Flüssigkeiten.
Jber.dtsch.Matver. 25 :279

HARTREE,D.R (1939a)
A solution for the laminar-boundary equation for retarded flow.
Rep.Memor.aero.Res.Coun.,Lond. No. 2426 (Spec.Vol.I)

HELMHOLTZ,H.Von (1868)
Über discontinuierliche Flüssigkeitsbewegungen.
Mber.K.Akad.Wiss.Berlin 23 : 215 (see also Phil.Mag. 36 : 337-346)

HEIS ENBERG,W (1924)
Über Stabilität und Turbulenz von Flüssigkeitsströmen.
Ann.Phys.,Lpz. 74 (4) : 577
Translated as "On the stability and turbulence of fluid flows"
Tech.Memor.nat.adv.Comm.Aero., Wash. No. 1291

INCE,E.L (1956)
Ordinary Differential Equations.
Dover Publications.

JEFFERY,G.B (1915)
The two-dimensional steady motion of a viscous fluid.
Phil.Mag. 29 (6) : 455

JEFFREYS,H (1923)
Proc.London Math.Soc. 23 (2) : 428

JEFFREYS,H & JEFFREYS, (1950)
Methods of Mathematical Physics.
Cambridge University Press

JOSEPH,D.D (1974)
Response curves for plane Poisseuille flow.
Adv.App.Mech. 14 : 241

KÁRMÁN,Th.V & LIN,C.C (1955)
Theoretical comments on the paper of Mr E.N.Fales
J.Franklin Inst. 259 : 517

KRAMERS,H.A (1926)
Z.Physik 39 : 828

LANDAU,L.D (1944b)
On the problem of turbulence.
Dokl.Ak.Nauk S.S.S.R 44 : 311

LANCHON,H & ECKHAUS,W (1964)
Sur l'analyse de la stabilité des écoulments faiblement divergents.
J.de Méchanique 3 : 445

LIGHTHILL,M.J (1959)
Introduction to Fourier analysis and generalised functions.
Cambridge University Press

LIN,C.C (1945 I)
On the stability of two dimensional parallel flows.
Quart.appl.Math. 3 : 117

LIN,C.C (1945 II)
On the stability of two dimensional parallel flows.
Quart.appl.Math. 3 : 218

LIN,C.C (1951)
A Critical Discussion of Similarity Concepts in Isotropic Turbulence.
Proc.Symp.Appl.Math. 4 : 19

LIN,C.C (1955)
The Theory of Hydrodynamic Stability.
Cambridge University Press

LIOUVILLE,J (1837)
J.de Math. 2 : 16

LING,C.H & REYNOLDS,W.C (1973)
Non-parallel flow corrections for the stability of shear flows.
J.Fluid Mech. 59 : 571

LOCK,R.C (1954)
Hydrodynamic stability of the flow in the boundary layer between parallel streams.
Proc.Camb.phil.Soc. 50 : 105

LORENTZ,H.A (1896b)
On the resistance experienced by a flow of liquid in a cylindrical tube.
Collected papers, 4 : 15 (Martinus Nijhoff, The Hague (1937))

LUCAS,R.D (1972)
Ph.d. Thesis : Stanford University

MATTINGLY,G.E & CRIMINALE,W.O (1972)
The stability of an incompressible two-dimensional wake.
J.Fluid Mech. 51 : 233

MEKSYN,D (1946a)
Fluid motion between parallel planes. Dynamical Stability.
Proc.Roy.Soc. A 186 : 391

MEKSYN,D & STUART,J.T (1951)
Stability of viscous motion between parallel planes for finite disturbances.
Proc.Roy.Soc. A 208 : 517

MEKSYN,D (1956)
Integration of the boundary layer equation.
Proc.Roy.Soc. A 237 : 543

MORSE,P.M & FESHBACK,H (1953)
Methods of Theoretical Physics.
McGraw-Hill Inc.

MULLER,D.E (1956)
A method for solving algebraic equations using an automatic computer.
MTAC. 10 : 208

NAYFEH,A.H, MOOK,D.T, & SARIC,W.S (1974)
Stability of non-parallel flows.
Arch.Mech. 26 : 409

ORR,W.M.F (1907)
The stability or instability of the steady motions of a liquid.
Proc.R.Irish Acac. A 27 : 9,69

OSTROWSKI,A,M (1960)
Solutions of equations and systems of equations.
Academic Press Inc. New York

PATTERSON,G.N (1934)
Flow forms in a channel of small exponential divergence.
Canadian J.Res. 11 : 770

PATTERSON,G.N (1935)
Viscosity effects in a channel of small exponential divergence.
Canadian J.Res. 12 : 676

PRANDTL,L (1904)
Über Flüssigkeitsbewegung bei sehr kleiner Reibung.
Verh. III int.Math.Kongr.,Heidelberg : 484

PRANDTL,L (1922)
Phys.Zeit. 23 : 19

RALSTON,A (1965)
A first course in Numerical Analysis
Mcgraw-Hill

RAYLEIGH,Lord (1880)
On the stability or instability of certain fluid motions.
I.Scientific papers 1 : 474

RAYLEIGH,Lord (1912)
Proc.Roy.Soc.(London) A 86 : 207

REYNOLDS,O (1883)
An experimental investigation of the circumstances which determines whether the motion of water shall be direct or sinuous, and of the law of resistance in parallel channels.
Phil.Trans. 174 : 935

REYNOLDS,O (1895)
Scientific papers.
Cambridge University Press, Cambridge Vol. 2 : 535

ROSENBLAT,S & HERBERT,D.M (1970)
Low frequency modulation of thermal instability.
J.Fluid Mech. 43 : 385

ROSENHEAD,L (1940)
The steady two-dimensional radial flow of a viscous fluid between two inclined plane walls.
Proc.Roy.Soc. A 175 : 436

ROSENHEAD,L (Editor) (1963)
Laminar Boundary Layers.
Oxford

ROSS,J.A, BARNES,F.H, BURNS,J.G, & ROSS,M.A.S (1970)
The flat plate boundary layer Part 3. Comparison of theory with experiment.
J.Fluid Mech. 43 : 819

SARIC,W.S & NAYFEH,A.H (1975)
Non-parallel stability of boundary-layer flows.
Phys.Fluids 18 : 945

SCOTTI,R.S & CORCOS,G.M (1972)
An experiment on the stability of small disturbances in a stratified free shear layer.
J.Fluid Mech. 52 : 499

SCHLICHTING,H (1933)
Zur Entstehung der Turbulenz bei der Plattenströmung.
Nachr.Ges.Wiss.Göttingen, Math.Phys. Klasse, no. 181-208

SHEN,S.F (1954)
Calculated amplified oscillations in plane Poisseuille and Blasius flows.
J.aero.Sci. 21 : 62

SHEN,S.F (1961)
Some considerations on the laminar stability of time-dependent basic flows.
J.aero.Space Sci. 28 : 397

SCHUBAUER,G.B & SKRAMSTAD,H.K (1947)
Laminar boundary layer oscillations and transition on a flat plate.
Rep.nat.adv.Comm.Aero.Wash. No. 909

SMITH,F.T (1979)
On the non-parallel flow stability of the Blasius boundary layer.
Proc.Roy. Soc. Lond. A.336 : 91-109

SOMMERFELD,A (1908)
Proc. 4th. Int. Congress Math. Rome : 16

STEWARTSON,K (1958)
On Goldstein's theory of laminar separation.
Quart.J.Mech. 11 : 399

STEWARTSON,K & STUART,J.T (1971)
A non-linear stability theory for a wave system in plane Poisseuille flow.
J.Fluid Mech. 48 (3) : 529

STUART,J.T (1951)
Ph.d. Thesis : Imperial College of Science and Technology.

STUART,J.T (1960)
On the non-linear mechanics of wave disturbances in stable and unstable parallel flows : Part 1. The basic behaviour in plane Poisseuille flow.
J.Fluid Mech. 9 : 353

TAYLOR,G.I (1938)
Proc. 5th. Int.Congress Appl.Mech. Cambridge,Mass. U.S.A

TERRILL,R.M (1960)
Laminar boundary-layer flow near separation with and without suction.
Phil.Trans. A 253 : 55

THOMAS,L.H (1953)
The stability of plane Poisseuille flow.
Phys.Rev. 91 (2) : 780

TIETJENS,O.G (1925)
Beiträge zur Entstehung der Turbulenz.
Z.angew.Math.Mech. 5 : 200

TOLLMIEN,W (1929)
Über die Entstehung der Terbulenz.
Nachr.Ges.Wiss. Göttingen : 21

TOLLMIEN,W (1935)
Ein allgemeinnes Kriterium der Instabilität laminarer Geschwindigkeitsverteilungen.
Nachr.Ges.Wiss.Fachruppe, Göttingen 1 : 79

TRAUB,J.F (1964)
Iterative methods for the solution of equations.
Prentice-Hall Inc.

WATSON,J (1960)
On the non-linear mechanics of wave disturbances in parallel flows : Part 2. The development of a solution for plane Poisseuille flow and for plane Couette flow.
J.Fluid Mech. 9 : 371

WATSON,J (1962)
On spatially-growing finite disturbances in plane Poisseuille flow.
J.Fluid Mech. 14 : 211

WENTZEL,G (1926)
Z.Physic 38 : 518

ZOLLARS,R.L & KRANTZ,W.B (1976)
Laminar film flow down a right circular cone.
Ind.Engng.Chem. Fundamentals 15 : 91

ZOLLARS,R.L & KRANTZ,W.B (1980)
Non-parallel flow effects on the stability of film flow down a right circular cone.
J.Fluid Mech. 96 (3) : 585